Spectral Photovoltaic Energy Collection & Transmission to Earth

Final Report V1.00
Spring DSE 2018 Group 9

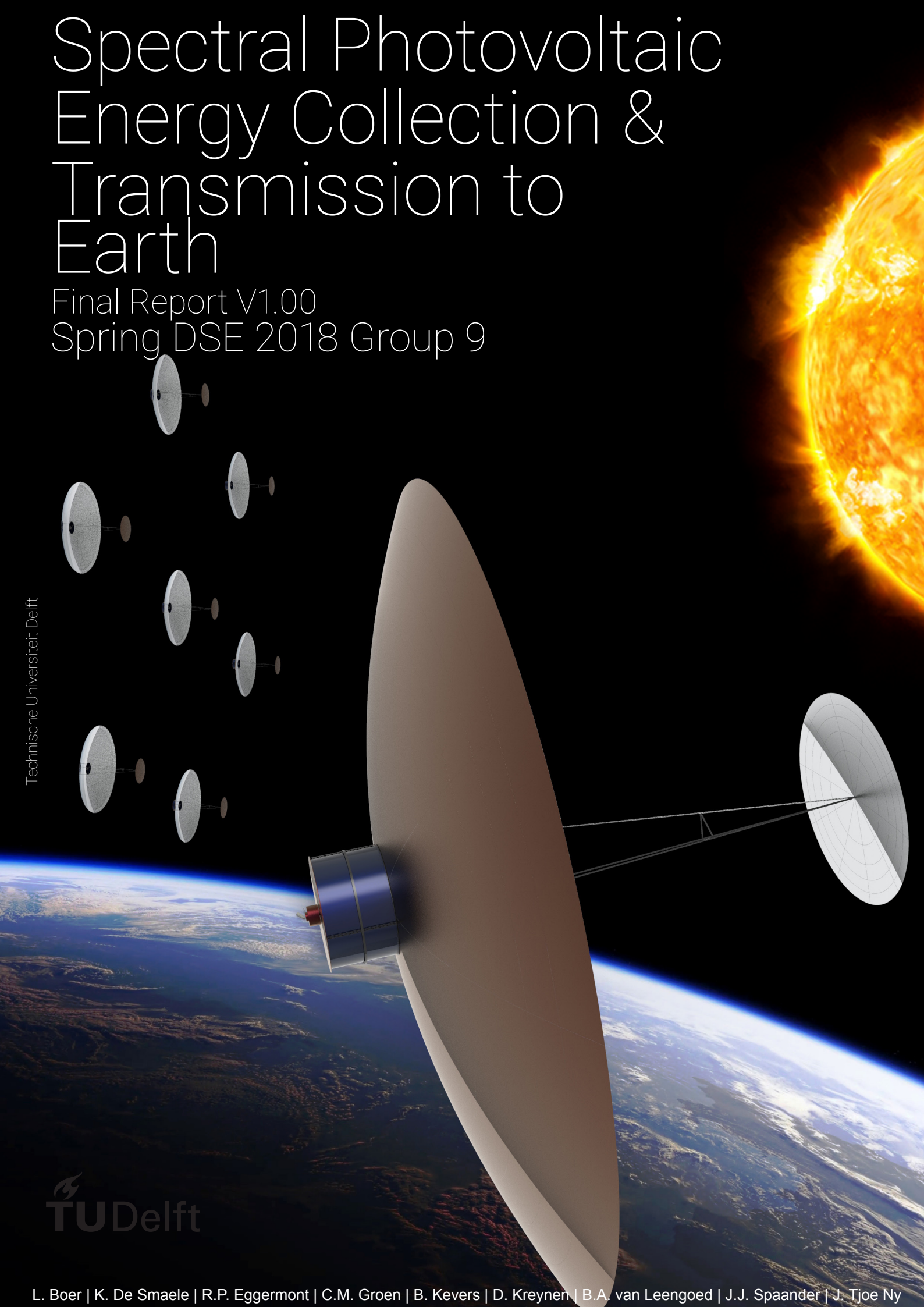

Technische Universiteit Delft

TU Delft

L. Boer | K. De Smaele | R.P. Eggermont | C.M. Groen | B. Kevers | D. Kreynen | B.A. van Leengoed | J.J. Spaander | J. Tjoe Ny

This page is intentionally left blank

Spectral Photovoltaic Energy Collection & Transmission to Earth

Final Report V1.00

by

Spring DSE 2018 Group 9

Supervisor:	Dr. ir. J. Guo	
Coaches:	Dr. J.A. Poulis	
	C. Hur, MSc.	
Authors:	Lars Boer	4287827
	Kasper De Smaele	4482433
	Rik Eggermont	4013727
	Chris Groen	4442806
	Bart Kevers	4436423
	Dylan Kreynen	4176669
	Berend van Leengoed	4439147
	Joshua Spaander	4430468
	Jamie Tjoe Ny	4400356

Preface

The final report is the fourth and concluding progress report of DSE Group 09, a team consisting of 9 BSc Aerospace Engineering students tutored by Dr. Guo. This technical report can be read stand-alone and gives an overview of the complete conceptual design of a space-based solar power system. The results are to be presented during the 2018 DSE Symposium at the TU Delft Faculty of Aerospace Engineering and will be summarised on a poster. After 11 weeks of hard work, the project ends here for the group, but we hope that the findings can serve as a baseline for further research. Recommendations for post-DSE activities can be found at the end of this document.

The team wants to express their gratitude to Prof. Arno Smets, Dr. Florian Bociort, Dr. Zian Qin and Dr. Thiago Batisto Soeiro of TU Delft as well as Dr. Ugo Lafont and Michel van Pelt of the European Space Agency (ESA) for their contributions. A special thank you goes out to our team of tireless coaches, with our ever-supportive and always enthusiastic tutor, Dr. Jian Guo, supported by Dr. Hans Poulis and Chihoon Hur.

Spring DSE 2018 Group 9
Delft, June 2018

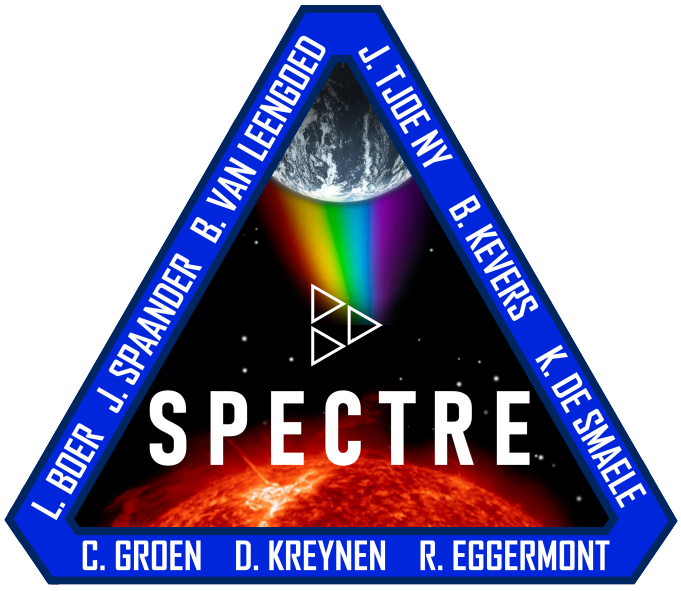

The Task Distribution of Group 9 has been submitted separately with this report.

Version	Purpose/Change	Author	Date
0.01	First draft	Group	22-06-2018
0.02	Official draft	Group	27-06-2018
1.00	Final version	Group	03-07-2018

Executive Summary

With depleting fossil fuel supplies and a continuous increase in demand for energy, humanities search for renewable energy sources is only growing. Over the past decades extensive research has already been performed on the subject, with the main focus on wind and solar energy. The main issue with solar energy on Earth is that it is not always available. The day-night cycle means that solar energy is available less than half of the time, while atmospheric attenuation and low solar cell efficiencies further decrease the power output. To tackle all these problems at once, a conceptual design for a space-based solar power system has been made in this report. This is the concept of a spacecraft that collects solar power and somehow transmits it to Earth for use on the ground, preferably at greater quantities and efficiencies than on Earth.

This summary will be structured as follows: first the mission need statement and project objectives are discussed to give an idea of the goal of this design study. Next, the key requirements which must be met will be shown, after which the market analysis is briefly presented to ensure that there is indeed a market for this type of power supply. This is followed by a short overview of the initial design process steps to explain the choices made before the final design was achieved. Since this concerns a renewable energy source, sustainability is also very important to the project. That is why the section that follows will analyse the sustainability. To discover additional requirements and envision the design in a practical matter, the logistics and operations aspect of the project are also discussed. The most important information is of course the actual design itself, which is revealed in two parts. The power collection system is elaborated on first, after which the overall spacecraft design is presented. Since this design requires in-orbit production, a production plan is also summarised, after which this design is verified and validated. Finally, the activities and schedule required after this conceptual design phase are shortly presented.

Project Goals
The mission need statement for this project was identified to be:

"Collect solar power in space on a Gigawatt scale and make it commercially available on Earth".

In the context of the project, this lead to the project objective statement:

"Develop a concept with 9 students and within 11 weeks for a solar energy collecting system that can generate Gigawatt-range power in orbit by 2030 within the budget of one and a half billion Euros"

To achieve this objective, there have been four different phases: project planning, baseline, midterm and final design. This report is the fourth and final report of these phases and includes a full conceptual design with low level design of the technical aspects as well as the well-documented systems engineering approach that was used in this project.

Driving Requirements
The design was mainly driven by a couple of stakeholder requirements, these will be shortly discussed below. Many more requirements have been given or discovered during the project, but the key requirements were the ones that had the largest impact on the design and are also the ones shown below:

- **M-ST-S-ECON-000** - The total cost of constructing such a system shall be less than 1.5 billion Euros (FY2018), including manufacturing, launching and assembling adjusted for inflation.
- **M-ST-S-ECON-001** - The system shall be operational before 2030.
- **D-ST-S-ECON-002** - The break-even point will occur before the end of 30 years in service, adjusted for inflation.
- **M-SY-S-ECON-000** - The system shall be operational for at least 30 years in space.
- **D-SY-S-ECON-000** - The mass of the space segment should be no more than 1000 tonnes.
- **M-SY-P-POCO-000** - The space-based solar collection system shall produce at least 1 Gigawatt of electrical power at end of life.

The main conclusion of these requirements is that from 2030 until 2060, the system should produce more than 1 Gigawatt of electrical power. This system should not weigh more than 1000 tonnes and should be profitable.

Market
Firstly, to ensure a profitable system, a market needs to be identified. Since the renewable energy market in the world is still relatively small (6.3% of total energy production) and considering the fact that this system would consistently provide at least 150 MW at the ground, it is found that the market share is large enough to ensure a viable economic project. This 150 MW is found assuming the power can be transmitted to the ground at 15% efficiency.

Using current energy costs of €60 to €84 per MWh, the profit of this project over 30 years is estimated to be between €48M and €908M, with the break-even point occurring 18 years into operation with the best case scenario or 28 years with the worst case. However, the gain of knowledge in space exploration and sustainable energy would be unprecedented.

Initial Design Process
To start this design study, first literature studies were conducted into various subjects. Once sufficient knowledge was gathered on the subject, all possible top-level designs were considered. These ranged from a monolithic PV system to an algae pool using photosynthesis to collect power. Eventually, the weak and infeasible solutions were removed, after which a trade-off was performed between the survivors. This trade-off was conducted carefully using specifically chosen criteria such as mass, cost, reliability and production complexity. Studies where performed to dedicate weights to these criteria and a rubric was produced to ensure objective grading of these survivors. The result was found to be a cluster of 20 spacecraft which uses spectral splitting to increase photovoltaic cell efficiency. This design was given the name "SPECTRE", which stands for Spectral Photovoltaic Energy Collection & Transmission to Earth. Any use of the term SPECTRE relates to the complete space segment, where a SPECTRE spacecraft is one spacecraft of the whole cluster.

Technical Risk Assessment
Considering the large scale of this project, it is crucial to conduct an in-depth risk analysis into the system. Therefore, as many risks as possible related to every subsystem had to be identified. This was mainly done using a fault analysis to ensure that the relation of every risk on other risks was also defined.

From this fault analysis, 121 risks were identified. Every risk was then given the most applicable likelihood of occurrence and severity of impact. It was determined that the most critical risks were related to the accurate design of the subsystems and components, as well as sufficient redundancy for the in-orbit production machines. However, the most likely risks were delay risks due to launching or production delays.

Based on the likelihood of occurrence and severity of impact, a risk map could be created to visualise the high and low risks. The high and medium-high risks were then mitigated, and a new risk map was created to show the mitigated risks. As expected, this risk analysis mitigated all of the high risks, and only low to medium risks remained. The risk mitigation was further improved by applying passive risk mitigation techniques, which include contractual risk transfer and system separation. Nevertheless, additional risk contingency plans were also identified to contain the impacts of the risks in case they do occur.

Sustainability
Since this project is based on being a renewable and thus an environmentally sustainable source of energy, the sustainability of this project should be analysed in detail. There are three fundamental pillars to sustainability: social, environmental and economical. The social sustainability is based on minimising detriment and maximising benefit to communities and society as a whole. This was mainly related to the requirement that dictates that the system should not harm any other human beings, in accordance with the International Bill of Human Rights established by the United Nations. The second pillar is environmental sustainability, which is mainly focused on not harming any objects or life on Earth or in orbit, as well as ensuring the net energy consumption and CO_2 output of this project is minimised. Also, since this project is in direct competition with alternative energy sources, environmental sustainability is considered to be of very high importance. The third pillar is the economical sustainability which, in short, is aimed at making the project economically viable. The economic sustainability will ensure wide adoption and investment into the further development of this project, and is hence vital for the realisation of this system. These three pillars have been satisfied in three different aspects, as discussed below.

The first aspect is the launcher selection. The launcher will bring the components of SPECTRE into orbit, for which large amounts of energy are required. To provide this energy, different launchers have different engines as well as different payload capacities and launch costs. The aim is to identify the most economically, but also environmentally sustainable launcher to launch the system. An elaborate analysis showed that the SpaceX Big Falcon Rocket was the optimal launcher for this task, and was thus selected.

The second aspect is the material choice. The materials chosen have a large influence on environmental sustainability. High grade aerospace materials used for space applications are interesting due to light weights, large strength, temperature resistance or other specifications. However, these materials often come at a cost of higher energy consumption to obtain and manufacture, higher toxicity or higher CO_2 emissions. That is why the material choices will always be made keeping environmental sustainability in mind.

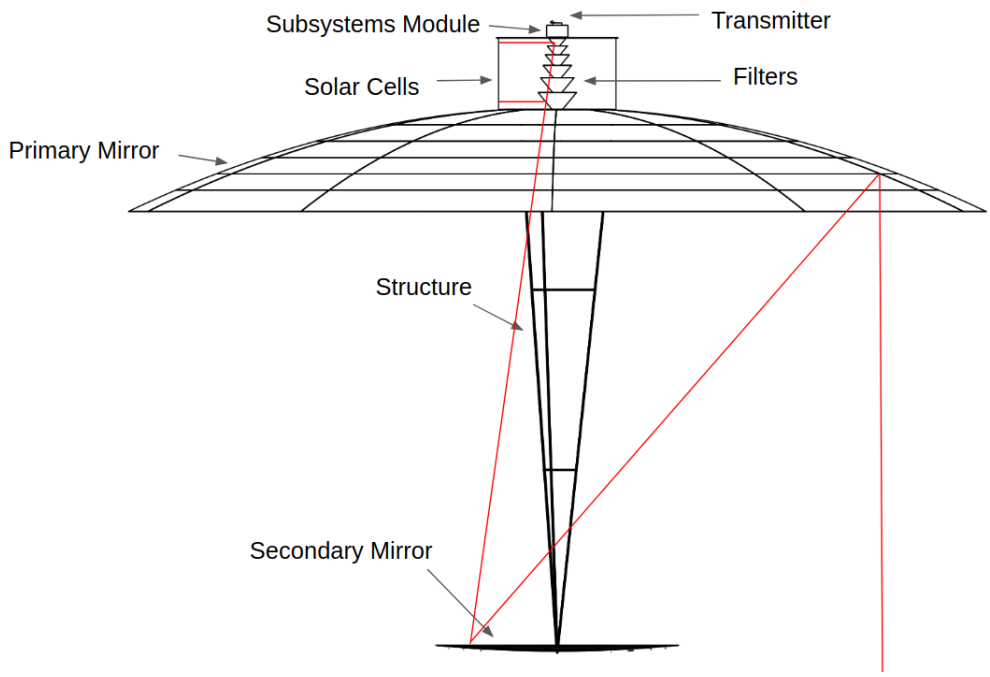

Figure 1: Schematic of Power Collection System

The third aspect is the integration of sustainability in the design. This means that for every subsystem the design choices will also be considered from an environmentally sustainable point of view. This will ensure the sustainability of the SPECTRE system.

Operations & Logistics
The operations & logistics of SPECTRE mainly describes the use of the system. This can again be divided into seven aspects: pre-launch, on-Earth production, maintenance, storage logistics, communications, power transmission and safe mode. These will shortly be discussed below. Note that the discussion of in-orbit production was discarded in this section since it required a lot of design and innovation. Therefore, in-orbit production was discussed separately, after the design of the system.

The pre-launch logistics include the production and storage of the SPECTRE components, as well as obtaining launch certificates. The components will have to be validated through testing and be certified according to international regulations.

The second aspect relates to the terrestrial production of the components. This will be done both in-house and by third parties, after which they will be brought together in an integration facility and put together to maximise the amount of components per launch.

The third aspect is the maintenance of the SPECTRE system. This could entail mirror repairs during the operational lifetime as well as repairs to the subsystem module. Next, the storage logistics in orbit also need to be considered. To conduct maintenance it is not unusual to require spare parts. This needs to be taken into account in the design.

As the SPECTRE system is in operation, ground contact is required to monitor the situation, detect and solve problems and give commands. This will also require a live video feed during in-orbit production. The power transmission of the spacecraft is required to wirelessly deliver power to a power-receiving ground station. Lastly, different safe modes will be required to safely operate the system. An innovative safe mode will be required to deactivate the power collection and shortly switch off solar cells such that the electrical power system cannot be damaged by high current surges.

Having discussed the market, risk, sustainability, and logistics & operations, a few additional constraints and requirements have now become clear. These will be taken into account during the design, which will now be discussed.

Power Collection
The technical design of SPECTRE has been the main focus of this design phase and is based on the previously discussed requirements and constraints. The Power Collection System per SPECTRE spacecraft consists of two mirrors, six thin film filters, six solar arrays and the structural support of the whole system. The layout of this design and the sunlight path is illustrated in Figure 1.

The goal of both mirrors is to concentrate the incoming sunlight in order to minimises the required surface area (and therefor mass and costs) of the solar cells and filters. They obtain a final concentration factor 384 on the filters and 17 on the solar cells (expressed in sols). To achieve this they are parabolically shaped with radii of the primary and secondary mirror respectively 180.8 m and 51.15 m.

The concentrated sunlight is focused on a cascade of 6 thin film filters which reflect and transmit the light onto 6 different solar arrays, each one optimally tuned to fit a specific bandgap. The filters reflect radially, decreasing the sunlight concentration factor to 17 in order to keep the solar cells within their operational temperature limits.

The bandgaps of the solar panels are determined in such a way that it results in maximum power output. The solar cell materials that fit these bandgaps consist mainly of Indium Gallium Nitride and Indium Gallium Arsenide alloys. Using the spectral splitting allows the solar arrays reach a total efficiency of 70%.

The generated electric power is transmitted to Earth via multiple lasers attached to each spacecraft.

Spacecraft Design

To maximise illumination time and make power transmission stations on Earth more practical, geostationary orbit was selected. This means it will always stay above the same point on Earth, which is yet to be determined based on the chosen market. To get the spacecraft there, the Big Falcon Rocket will boost 45,000 kg of payload up each time, 15 times over 2 years. To keep the cluster here over the 30 years of operations, each spacecraft was fitted with 5 ion thrusters, mounted radially to provide control in all directions. These thrusters also have the capability to desaturate the control moment gyroscopes used by the attitude determination & control system. Each spacecraft has nine of these control moment gyroscopes to provide enough momentum storage and redundancy as well as a sun-pointing accuracy of one degree.

Without any thermal control, several elements would have severe thermal problems. First of all, the solar arrays, subsystems module and filters reach equilibrium temperatures well above their limit. In addition, the extreme temperature, reaching almost 800 K, of the secondary mirror can result in thermal problems. Additionally, during eclipse periods the temperatures drop significantly and temperature gradients are considerably steep.

The indicated issues are solved by implementing heat pipes and thermal energy storage into the spacecraft. The heat pipes run throughout all parts of the system and spread the generated heat out over a large radiator surface formed by the backside of the primary mirror. The thermal energy storage is connected to the system during eclipses to keep the spacecraft from cooling down too much and too quick. The temperature gradients induced by entering and leaving eclipses are also solved by gradually decreasing and increasing the concentration of light. This is achieved by adjusting the guy-wires of the mirrors. The additional weight of this passive thermal control system is approximately 3000 kg per spacecraft. Due to the fact that this is a passive system, no significant amounts of electric power are needed.

Since each spacecraft will be dealing with more than 50 MW of electric power on board, a heavy duty electrical power system has been developed. This consists of a combination of the best of AC and DC, using a custom design for a DC to AC inverter coupled to an extremely efficient high frequency transformer with a full bridge noise reduced AC to DC rectifier. This has a very high power density with respect to mass, with very high losses.

For monitoring and control, the command and data handling system has been designed, with a robust on-board CPU and connections to all subsystems in the spacecraft. One of these subsystems is the telemetry, tracking & command, which is responsible for communication between the spacecraft and the ground station. To livestream video during operational life the downlink uses X-Band to communicate at 70 Mbps, whereas uplink commands are less heavy and use S-Band at 7.5 kbps.

The structure of the spacecraft will support the system and consists of the trusses connecting the primary and secondary mirror, the mirrors themselves, the filter/photovoltaic complex and the connection to the subsystems module. These have been designed to be lightweight, weighing in at around 900 kg per spacecraft.

To fit all these subsystems on the spacecraft efficiently and maintain optimum conditions, a dedicated subsystems module was designed, which is located behind the power collection unit.

To summarise this design, the mass breakdown is shown in Table 1, showing a total mass per spacecraft of 14.5 tonnes and an overall mass of 289 tonnes the SPECTRE, well within the 1000 tonnes required.

Production

Due to mass and volume limits associated with launching a payload to operational orbit, in-orbit production was identified as an integral and design-driving aspect of the project. Apart from the higher packing efficiency, a structure produced in space can be much lighter (or larger) than one produced on Earth as the former does not have to survive launch loads.

Table 1: Spectral Photovoltaic Energy Collection & TRansmission to Earth (SPECTRE) Mass Breakdown in Tonnes

Subsystem	Total SPECTRE Mass Breakdown [tonnes]	Mass Breakdown per Spacecraft [tonnes]	Mass Breakdown (%)
Propulsion	35	1.8	12.11
ADCS	49	2.4	16.96
Thermal Control	60	3.0	20.76
Telemetry, Tracking and Command (TT&C)	0.3	0.01	0.10
Power Collection	64	3.2	22.15
Power Storage	8	0.4	2.77
EPSY	26	1.3	9.00
Maintenance	20	1.0	6.92
Structure	26	1.3	9.00
Total	**289**	**14.4**	**100.0**

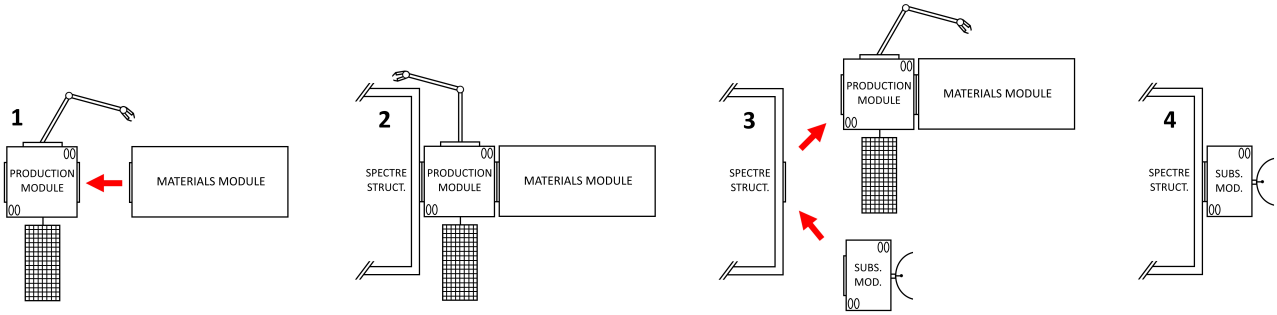

Figure 2: Modular production sequence. 1. Production module berths materials module; 2. This combination produces the SPECTRE structure; 3. The production and materials module detach (and go on to produce the next structure) and the subsystems module docks with its structure; 4. The operational combination ready for spin up.

The SPECTRE system will be launched as three types of modules: five production modules, ten materials modules and twenty subsystems modules. The modular sequence is illustrated in Figure 2. The production module houses all the tools required for production, which consist of a robotic system for assembly based on the robotics present on the ISS and so-called trusselators which use a combination of pultrusion and 3D printing to spit out continuous lengths of PEEK/carbon fibre composite trusses. Once the structure is complete and all the functional elements from the materials module have been integrated, the SPECTRE configuration including the subsystems module is spun up in order to centrifugally deploy a space web on which web crawling robots use a novel Chemical Vapour Deposition process to produce and attach a reflective aluminium thin film. The same robots and process will be used to periodically maintain the surface of the created concentrators.

Verification and Validation

Verification and validation is a very important aspect of any engineering project. This is done by proving that the design has met the requirements. All requirements were met, with the exception of one: **D-SY-THER-003** - All materials in the Thermal Control System shall be non-toxic to life on Earth. Due to the high demands placed on the thermal control system, the only feasible option was to use a toxic substance for thermal storage, however this was a desirable requirement so the design is still considered to be compliant.

The models used in the design (numerical and analytical) need to be verified using inspection, analytical calculations and tests. Once the manufacturing and testing starts, the verification of the product can be done using inspection, analysis or test. Each subsystem and component requires a different method, and extensive testing plans have been created. To validate the product experience, analysis or comparison can be used.

Conclusion

To conclude, a cluster of 20 spacecraft in geostationary orbit has been designed to provide more than one Gigawatt of electric power using only solar energy. To collect this power efficiently, two parabolic concentrating mirrors are used, combined with a spectral splitting method and photovoltaic cells. To produce these large spacecraft, advanced in-orbit techniques have been applied. SPECTRE will take two years to be built in orbit, after which it will operate for 30 years consistently producing more than one Gigawatt for almost 24 hours per day all year round. This power will be distributed on the ground and leads to profits of up to €1.2 billion. The main design challenges at this point are the thin film filters, the innovative production techniques, the thermal control system and the high-power, low mass electronic power system.

Contents

Acronyms

AC Alternating Current

ADCS Attitude Determination and Control System

AIT Assembly, Integration and Test

AITP Assembly, Integration and Test Plan

AR Acceptance Review

BER Bit Error Rate

BFR Big Falcon Rocket

BOL Beginning of Operational Life

BPSK Binary Phase Shift Keying

C&SM Collector and Subsystems Module

CBS Cost Breakdown Structure

CDHS Command & Data Handling System

CDR Critical Design Review

CMG Control Moment Gyroscope

CVD Chemical Vapour Deposition

DC Direct Current

DOT Design Option Tree

DSE Design Synthesis Exercise

ECSS European Cooperation for Space Standardisation

EOL End of Operational Life

EPS Electrical Power System

FEM Finite Element Method

FFF Fused Filament Fabrication

GEO Geostationary Orbit

GSP Power Receiving Ground Station

GTO Geostationary Transfer Orbit

HEO High Earth Orbit

HV High Voltage

IADC Inter-Agency Space Debris Coordination Committee

IDSS International Docking System Standard

IGBT Insulated-Gate Bipolar Transistor

ISS International Space Station

ITU International Telecommunications Union

LEO Low Earth Orbit

LHP Loop Heat Pipe

LV Low Voltage

MAI Manufacturing, Assembly and Integration

MEO Medium Earth Orbit

MEOP Maximum Expected Operating Pressure

MPPT Max Power Point Tracker

MRU Motion Reference Unit

OBC On-Board Computer

PCM Phase Change Material

PDR Preliminary Design Review

QFD Quality Function Deployment

QR Qualification Review

RAMS Reliability, Availability, Maintainability, Safety

SNR Signal-to-Noise Ratio

SPECTRE Spectral Photovoltaic Energy Collection & TRansmission to Earth

SSPS Space-based Solar Power System

TCS Thermal Control System

TPM Technical Performance Measure

TRL Technology Readiness Level

TT&C Telemetry, Tracking and Command

TUI Tethers Unlimited, Inc.

Symbols

Symbol	Description	Unit
A_c	Nominal contact area of two surfaces	m^2
A_r	Radiative surface area	m^2
A_s	Frontal area of the spacecraft	m^2
B_λ	Spectral radiance per unit wavelength	$W \cdot sr^{-1} \cdot m^{-3}$
B	Bandwidth	Hz
C_R	Solar Radiation Pressure Coefficient	–
C_c	Channel capacity/Bitrate	$bit \cdot s^{-1}$
C_{GJmax}	Maximum price of solar power per GJ in 2030	EUR$\cdot GJ^{-1}$
C_{GJmin}	Minimum price of solar power per GJ in 2030	EUR$\cdot GJ^{-1}$
D_m	Spacecraft residual dipole moment	$A \cdot m^2$
F_T	Thrust	N
F_r	View factor	–
H_c	Heat capacity	$J \cdot K^{-1}$
H_e	Minimum Hardness of two contacting materials	MPa
I_{sp}	Specific impulse	s
I_{trans}	Electrical transmission current	A
I	Mass moment of inertia	$kg \cdot m^2$
L_{MOM}	Momentum storage	$N \cdot m \cdot s$
L_{Slew}	Stored angular momentum	$N \cdot m \cdot s$
M_m	Product of Earth magnetic moment and magnetic constant	$T \cdot m^3$
$M_{\max}$	Maximum control torque around spin axis	$N \cdot m$
M	Torque around spin axis	$N \cdot m$
P_c	Contact pressure between two contacting surfaces	MPa
P_{trans}	Electrical transmission power	W
$P_{wireloss}$	Electrical power loss in a wire	W
P	Orbital period	s
Q_c	Heat transfer due to conduction	W
Q_r	Heat transfer due to radiation	W
Q_{in}	Incoming heat flow from the sunlight	W
Q	Total heat flow	W
R_e	Earth's radius	km
R_{GEO}	Geostationary orbital radius	km
R_{max}	Maximum yearly revenues	EUR
R_{min}	Minimum yearly revenues	EUR
R_{wire}	Electrical resistance of a wire	Ω
R	Distance from the spacecraft to Earth's centre	m
T_D	Total disturbance torque	$N \cdot m$
T_m	Disturbance torque due to the magnetic field	$N \cdot m$
T_s	Disturbance torque per spacecraft due to solar radiation	$N \cdot m$
T	Temperature	K
$U_{operational}$	Percentage of time that the solar collector system is operational	–
V_{GEO}	Velocity in geostationary orbit	$m \cdot s^{-1}$
$V_{GTO,a}$	Apogee velocity in geotransfer orbit	$m \cdot s^{-1}$
V_{trans}	Electrical transmission voltage	V
V	Orbital Velocity	$m \cdot s^{-1}$
ΔH	Altitude increase	km
ΔT	Temperature difference between two components	K
ΔV	Change in velocity	$m \cdot s^{-1}$
Δi	Inclination change	°

Symbol	Description	Unit
$\dot{\theta}$	Required maximum slew rate	$\circ \cdot s^{-1}$
$\dot{m}$	Fuel mass flow	$kg \cdot s^{-1}$
Φ	Solar constant at 1366 $W \cdot m^{-2}$	$W \cdot m^{-2}$
α	Angle of slope of parabola at a given point	–
ϵ	Surface emissivity	–
$\eta_{transmission}$	Transmission efficiency	–
λ_m	Function of the magnetic latitude	–
λ	Wavelength	m
μ	Standard gravitational parameter	$m^3 \cdot s^{-2}$
ω_h	Angular velocity of the hub	$Rad \cdot s^{-1}$
ω_{h0}	Initial angular velocity of the hub	$Rad \cdot s^{-1}$
ϕ	Incidence angle of sunlight	$\circ$
σ_e	Effective surface roughness of two contacting materials	MPa
σ_s	Stefan-Boltzmann constant	$W \cdot m^2 \cdot K^{-4}$
θ_a	Allowable angular motion	$\circ$
θ_e	Effective surface angle of two contacting materials	Rad
θ_v	Angle of the view factor	Rad
a	Semi-major axis	m
c_m	Centre of mass	m
$c_{p,s}$	Solar radiation centre of pressure	m
c	Speed of light	$m \cdot s^{-1}$
g_0	Standard gravity	$m \cdot s^{-2}$
h_c	Thermal contact conductance coefficient	$W \cdot m^{-2} \cdot K^{-1}$
h_g	Thermal gap conductance coefficient	$W \cdot m^{-2} \cdot K^{-1}$
h_r	Thermal radiative conductance coefficient	$W \cdot m^{-2} \cdot K^{-1}$
h_t	Total thermal conductance coefficient	$W \cdot m^{-2} \cdot K^{-1}$
h	Planck constant	$J \cdot s$
k_e	Effective thermal conductivity of two contacting materials	$W \cdot m^{-1} \cdot K^{-1}$
k_B	Boltzmann constant	$J \cdot K^{-1}$
m_{dry}	Dry mass of the spacecraft	kg
m_{final}	Wet mass of the spacecraft	kg
m_{prop}	Propellant mass	kg
m	Spacecraft mass	kg
q	Reflectivity of the spacecraft	–
r	Distance between two orbiting bodies	m
t_b	Burn time	s
t_{year}	Amount of seconds in a year in order to find the yearly revenue	s
t	Time	s
v_e	Exhaust velocity	$m \cdot s^{-1}$

1

Introduction

For decades humankind has been investigating energy collection from sustainable energy sources, among which is the collection of solar energy. Solar energy collection has been around for a significant amount of time in terms of terrestrial solar panels and its accompanying technology. However, the major drawbacks of terrestrial solar energy collection are the attenuation of solar intensity on Earth's surface due to the atmosphere and the limited availability of sunlight over the course of a day. The solution to these problems would be to collect solar energy in space and transmit it wirelessly to Earth. To accommodate to this solution, DSE Group 9 has designed a space solar energy collecting system that comprises of optimal sustainability and state-of-the-art technology, while maintaining economic feasibility.

The project objective of DSE Group 9 is stated as follows:

"Develop a concept with 9 students and within 11 weeks for a solar energy collecting system that can generate Gigawatt-range power in orbit by 2030 within the budget of 1.5 billion Euros"

This project objective has been achieved after 4 design phases. First, the initial planning of the design process has been set up, this is reflected in the Project Plan [21]. Afterwards, multiple concepts have been identified and potential solutions to the project objective have been established, as described in the Baseline Review [19]. The feasibility of those solutions is analysed, and a final solution for in-depth design has been selected in the Midterm Report [20].
The purpose of this report is to present the final phase in the conceptual design process of a space solar energy collecting system. This encompasses the detailed technical and non-technical design of the chosen solution in the Midterm Report called: Spectral Photovoltaic Energy Collection & TRansmission to Earth (SPECTRE).

SPECTRE is a cluster of spacecraft where each spacecraft makes use of two mirrors to concentrate light onto a cascade of thin film long-pass filters, which reflect portions of the solar spectrum onto optimally bandgap-tuned solar cells. Subsequently, the generated energy is transmitted to a ground station on Earth for consumption.
This report holds the details of above mentioned power collecting system in terms of its technical design, functions, production process, costs, Reliability, Availability, Maintainability, Safety (RAMS), sustainability, and operations & logistics.

The outline of this report is as follows: first an overview of the mission background and the selected solution from the Midterm Report is presented. Subsequently, in chapter 3 the project requirements are listed, after which the resource allocation and the budget breakdown are discussed in chapter 4. Next, the functional description of the system is given in chapter 5, followed by the cost breakdown structure and market analysis in chapter 6. The technical risk assessment is discussed in chapter 7, which includes a fault tree analysis, risk maps and mitigation plans. Since this project revolves around sustainable energy, it is only logical that the development should be sustainable as well, this is why a sustainable development strategy was developed in chapter 8. The project operations and logistics have been documented in chapter 9.

Subsequently, the power collection and system design are presented in chapter 10 and chapter 11, respectively. The system design includes the astrodynamics, subsystem designs such as Attitude Determination and Control System (ADCS), propulsion, Telemetry, Tracking and Command (TT&C), Thermal Control System (TCS) and the Electrical Power System (EPS). Due to the scale of this system, not all production can be done on Earth. This is why in-orbit production will also be performed, as described in the production plan in chapter 13. To verify all used models and designs, meticulous verification and validation was conducted, which is described in chapter 14.

This report presents a conceptual design, which, depending on its feasibility, is taken into the next stage. Chapter 15 shows the activities that would take place after the conclusion of the conceptual design phase and the planning of these activities. Finally, the conclusion and recommendations are presented in chapter 16.

2

Mission Background and Overview

This chapter is included to provide explanation and context to this report, to give a general overview of all the activities performed and choices made previous to this report, and to summarise the overall project before the time of writing this report.

2.1. Mission Background

This report is the result of 11 weeks of work by 9 TU Delft Aerospace Engineering students for their final Bachelor project called the Design Synthesis Exercise (DSE). The DSE requires 4 reports to be produced; the Project Plan, the Baseline report, the Midterm report and the Final report. This is the final report, and it builds on the results obtained in the previous 3 reports.

The Project Plan was used to create and explain a functional road map for the progression of the DSE, and to schedule the required tasks. This is where the approach to trade-offs, reviews and other project aspects were decided upon. This report also includes the first Gantt charts, Work Breakdown Structure, Organogram and other organisational documents, and it laid the foundation for the rest of the project.

In the Baseline report, the project requirements were derived. It produced top-level user requirements, system requirements and a mission flow down [19]. Preliminary resource allocations and budget breakdowns were presented in this report as well, which were updated and developed throughout the next 2 reports. The final allocations can be found in chapter 4, and the resulting breakdowns are discussed in chapter 6. A sustainable development strategy was also introduced and developed, with the idea of using indicators such as CO_2, energy consumption, profit margins and other parameters to base the sustainability of the project on. The main purpose of the Baseline report was to present a wide variety of developed concepts for the final system. The concept ranged from monolithic, traditional photovoltaic systems, produced and assembled in space, to algae pools and solar wind turbines. The concepts that where considered for further study are shown in Table 2.1.

The Midterm Report had the goal to analyse the concepts discussed in the Baseline report and, using the requirements found for the system [20], to perform a trade-off on those concepts. Further in-depth analysis and iterations of the designs and their masses was performed. This was still done at a high design level however.

With the performed trade-off, the final concentrated spectral splitting concept (Solution 2 in Table 2.1 was chosen. This was mainly due to its relatively low mass, high sustainability and its economic potential. Especially its mass performance was far superior over the other concepts.

The basis for the sustainability analysis was also performed in accordance with what was discussed in the Baseline report. This was done through analysing the European energy balance and production output in order to evaluate where the most CO_2 and energy was consumed. The sustainability of possible production materials was found and the detailed design phase discussed in this report was in large part based on that analysis. This was further more expanded and improved in chapter 8. The material choice influenced the concept selection [20]. The choice of launcher resulted in the Big Falcon Rocket (BFR) offered by SpaceX. This was mainly due to its superior payload carrying capabilities, very low cost and recycling capabilities.

Table 2.1: List of Considered Design Solutions

Solution #	Solar Collection Method	Orbital Configuration
Solution 1	Solar Pumped Laser	Cluster
Solution 2	Concentrated with Spectral Splitting	Cluster
Solution 3	Concentrated Photovoltaic	Cluster
Solution 4	Concentrated Photovoltaic	Monolithic
Solution 5	Photovoltaic	Cluster
Solution 6	Photovoltaic	Monolithic
Solution 7	Photovoltaic with Thermal Improvements	Cluster
Solution 8	Photovoltaic with Thermal Improvements	Monolithic

The orbit of the system was chosen to be Geostationary Orbit (GEO) in this report after a trade-off on all feasible orbit options. It was chosen in order to meet visibility and availability requirements. Due to the low cost and low mass relative to the other concepts, it was also economically possible to utilise this orbit.

Also investigated was the TCS. Here it was found that the TCS is a very critical aspect of the system, and the need for active thermal control could not yet be discounted. Furthermore, the ADCS design criteria and preliminary sizing was performed based on the disturbances present in GEO and attitude sensors and actuators were chosen for the system. Ion propulsion using xenon propellant was chosen for station keeping. It was also decided to use multiple busses for the EPS for reliability reasons as well as using as high as possible voltages. For the production, web crawlers were chosen in order to produce and maintain the mirrors through the method of Chemical Vapour Deposition (CVD). Furthermore, a data budget was sized for the communication subsystem. All these conclusions formed the basis for the their respective sections in this report.

2.2. SPECTRE System Overview

Some readers of this report might have a hard time finding their bearings around the complex SPECTRE system, so this section should give a simple overview which can be used to place concepts and descriptions in context. SPECTRE is a backronym for Spectral Photovoltaic Energy Collection and TRansmission to Earth. The name already suggests much of its inner workings. The system consists of a solar energy collector in the form of a concentrator array consisting of two mirrors, the primary mirror and the secondary mirror. The primary mirror is a parabolic mirror which reflects and concentrates the incident solar light on to the secondary mirror. The secondary mirror then reflects the light and concentrates it even further.

These mirrors both consist of a thin film aluminium layer supported by a structure referred to as a 'space web' in this report, named for its resemblance of a big spider web. In order to save weight on the structure, the space web is kept in shape by a spinning motion of the spacecraft, utilising the centripetal force to keep it deployed. Guy-wires are then used to acquire the required parabolic shape.

The secondary mirror reflects and concentrates the light onto optical or thin film filters which reflect light above a certain frequency and pass all other frequencies. These frequencies are specifically tailored to be optimal for each solar cell material. The reflected light is radially dispersed to a lower concentration onto the solar cells. The materials of the solar cells are chosen in such a way as to maximise the efficiency of the system as a whole. The combination of the filter array and the solar array will be referred to as the "knikkerbaan" in this report.

After the solar cells use the solar energy to generate electricity, the power is transferred to the EPS. The solar cells are placed in series, with each string emitting 600V. The system converts the low 600V voltage electricity from the solar cells and steps it up to high 100,000V and transfers this to the power transmitter.

The power transmitter consists of one or a collection of high-power laser(s) which emits light at a frequency which attenuates least in the atmosphere, is invisible, and is non-ionising or harmful to life on Earth.

Subsystem power is delivered through a 600V cable from the solar cells. These subsystems are supplied by a battery during eclipse on the same network. The TT&C subsystem will transmit and receive data from a ground station on Earth, at a high enough data rate as to support video streaming and other required data.

The ADCS consists of 9 Control Moment Gyroscope (CMG)s, which apply torques through actuators to the spacecraft in order to keep pointing accuracy.

The propulsion system consists of five ion engines that are used to maintain the orbit. These are fuelled by xenon stored in a high pressure tank.

The TCS is fully passive, relying on heat pipes to cool down the solar cells and using coatings to radiate the heat to space. It also stores heat energy in a thermal energy storage container, which, when the system is in eclipse, keeps the system warm in order to prevent large temperature fluctuations and too low temperatures.

Finally, the structural system shall support and provide rigidity to the spacecraft, allowing for accurate pointing and transfer of loads from the guy-wires, ADCS and propulsion to the rest of the system. It consists of a beam structure surrounding and shaping the thin and flexible solar cells by acting as a mould, while the centripetal force shapes them. It supports the secondary mirror through a triangular truss structure between he primary and secondary mirror. There are some triangular stiffening members in order to reduce flexing and deformations.

An illustration of all these components is depicted in Figure 2.1.

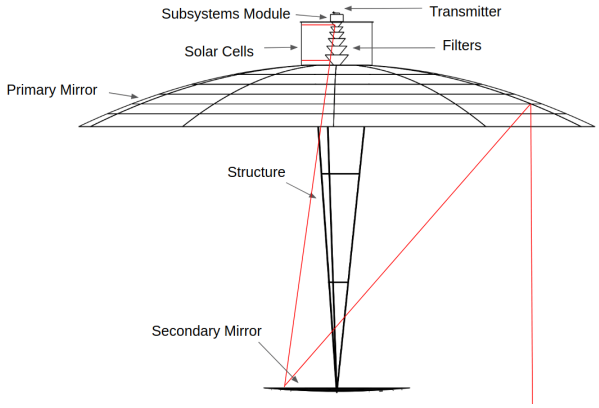

Figure 2.1: A labelled overview of the major components of SPECTRE

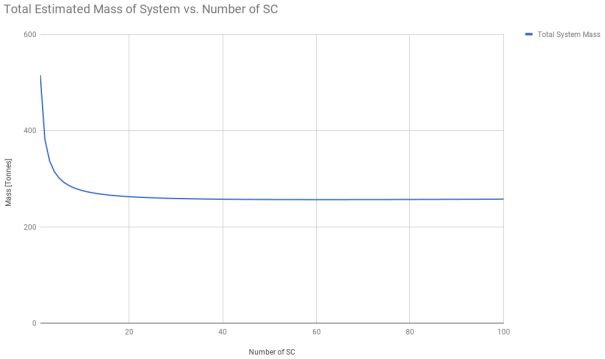

Figure 2.2: Estimated mass of the total system vs the number of spacecraft

2.3. Number of Spacecraft

In order to determine the number of spacecraft that would be optimal for this design, an estimation was made for the scaling dynamics of different subsystems. It was assumed that the structure and maintenance would scale quadratically with increasing radius, because the in-orbit production will reduce the need for heavy structural supports. Hence the mass contribution of this subsystem to the total system would decrease with the increased number of satellites. In contrast, the telecommunications system is based purely on the distance between the Earth and the spacecraft, assuming the data rate does not increase. Hence this increased linearly with the number of spacecraft.

The ADCS system will increase cubically however, since the total rotational inertia of an increased radius increases in higher order values. For this system this was assumed to be cubically.

The propulsion system would increase steadily as well. The mass of the thruster might have to increase, however this increase would be much smaller compared to the fuel mass gain. The fuel mass increase is given by the rocket (or Tsiolkovsky) equation presented in Equation 2.1. Hence the propulsion system will increase linearly with any increased weight.

$$m_f = m_0 e^{-\frac{\Delta V}{V_e}} \tag{2.1}$$

Finally, the total power or efficiency does not change with the number of spacecraft. Hence the EPS and power collection system do not contribute more mass with increasing number of spacecraft. The resulting estimations for the system is illustrated in Figure 2.2.

As seen in Figure 2.2, the mass for a monolithic solution is very high and then drops steeply. At around 20 spacecraft, the mass decrease is negligible and after about 60 spacecraft it starts increasing again. The reason for this is that the structural mass is the majority mass, due to quadratic relation. However, when this decreases, the second most heavy subsystem, the power collection subsystem, starts to dominate. This system does not vary with the number of spacecraft. Hence it stays steady after 20 spacecraft.

On the scale of this system the difference between 20 and 60 spacecraft for all intents and purposes is negligible. Therefore, for practical reasons concerning the number of launches, number of slots in GEO, production simplicity and others, 20 spacecraft where chosen. This number shall be used for the remainder of the report.

3
Requirements

This chapter discusses the requirements that the Space-based Solar Power System (SSPS) design must meet. The chapter starts off with sustainability requirements, which are divided in stakeholder and system requirements. They are further split up into environmental, economic and social sustainability. The performance and logistics/life requirements are based on findings throughout the engineering analysis of the system. The performance requirements are split up into each subsystem: propulsion, ADCS, TCS, TT&C, power collection, EPS, power transmission, power storage, maintenance and structures. The last section is logistics/life requirements. The subsections of this section are: production, maintenance, operational life and disposal.

During the engineering design process, it was found that some requirements were deemed unnecessary or should be stated differently. As a consequence it might appear that some indexes are missing, this is because the indexes of deleted requirements were not reused to preserve the traceability of the requirements.

3.1. Sustainability Requirements

Stakeholder Sustainability Requirements

Stakeholder Requirements: Environmental Sustainability

M-ST-S-ENVI-000 - The system shall not harm any objects or life on Earth or in Earth orbits.
Rationale: The system must not harm life or damage property due to falling debris after re-entry or through the transmission of power. Either of these contingencies is both morally and legally unacceptable. Hence it is a mandatory requirement.

M-ST-S-ENVI-001 - The system shall be able to be removed from the operational orbit without space debris issues.
Rationale: The Kessler syndrome should not be worsened because of debris emanated from the destruction of the station, neither should new space missions be affected by this. Hindrance and damage to other craft in orbit can also not be tolerated. Hence it is considered mandatory as a requirement.

D-ST-S-ENVI-003 - The net energy put into the manufacture, construction and operation of the system should be less than the produced net useful electrical energy available for consumers on Earth in accordance with the sustainability analyses.
Rationale: The production, construction and operation of the system costs energy. The environmental impacts, such as CO_2 emissions, as well as social and economical repercussions are directly related to this. The solar power system must make more energy available than it took to produce, meaning it is a net energy contributor to the energy supply. This would also prove its social, environmental and economic sustainability. This should not come at the expense of the mandatory requirements however.

D-ST-S-ENVI-004 - Any failed component of the collection system should be recycled.
Rationale: Space hardware is expensive economically, socially and environmentally. Hence recycling is more sustainable.

Stakeholder Requirements: Economic Sustainability

M-ST-S-ECON-000 - The total cost of constructing such a system shall be less than 1.5 billion Euros (FY2018), including manufacturing, launching and assembling, adjusted for inflation.
Rationale: This is the budget given to us by our "customer". Since the budget of the project is most likely funded by public institutions such as governments, this money will be largely sourced from taxation. The resulting budget shall be capped and minimise social costs. Space missions depend predominantly on the available money. Hence it is considered an essential requirement. The previous budget was 1 billion, this was raised to 1.5 billion after consultation with the costumer.

M-ST-S-ECON-001 - The system shall be operational before 2030.
Rationale: The system must not take more than 12 years to produce in order to make it economically viable as well

as ensuring the pace by which the technology develops stays adequate. This also has social implications, ensuring that the project does not fall out of the social eye before it is built.

D-ST-S-ECON-002 - The break-even point should occur before the end of 30 years in service, adjusted for inflation.
Rationale: The driver of this mission should not only be the technological advancements, but also prove whether space solar power systems are viable and sustainable economically. The technology is still in its infancy and hence it must primarily prove viability and potential. Hence it is considered to be a desirable requirement but not mandatory.

O-ST-S-ECON-000 - The system should preferably produce useful electrical energy available into the grid at competitive rates when compared with similar capacity terrestrial solar power stations.
Rationale: The station can still be profitable even when producing above the market price. However, in order for wide implementation of this energy generation method it should be competitive with other generation methods such as ground based solar power stations of similar capacity.

Stakeholder Requirements: Social Sustainability

M-ST-S-SOCI-000 - The system shall not be in violation of the International Bill of Human Rights established by the UN.
Rationale: If during the production worker safety is not taken into account, or the materials are sourced from unethical sources encouraging the violation of human rights elsewhere, or any other activity is performed that is in conflict with the human rights, it would be a failure of sustainable social policy and would be immoral and bad for all the stakeholders involved. Hence this is considered to be a mandatory requirement.

O-ST-S-SOCI-000 - The station should preferably be accessible for future missions.
Rationale: Future missions might benefit from such a facility, hence it should be considered for long term use. This could for example be done by including universal adapters or have the adapter plans public.

System Sustainability Requirements

System Requirements: Environmental Sustainability

D-SY-S-ENVI-000 - The production in orbit should not exceed 1% scrap (in terms of weight) from the initial material.
Rationale: This requirement was made to ensure sustainability by not wasting material which was paid for to be launched into space in both economic terms as well as environmental terms.

O-SY-S-ENVI-001 - The system should preferably produce electrical energy available for the grid at a lower net CO_2 output than the grid average.
Rationale: This project is meant to develop in part a new sustainable electrical energy generation method. This would imply that the CO_2 output would have to be lower than the current non-renewable energy generation methods, and even go as far as to produce similar CO_2 footprints as terrestrial renewable energy generation methods.

System Requirements: Economic Sustainability

M-SY-S-ECON-000 - The system shall be operational for at least 30 years in space.
Rationale: This is a driving requirement for the system, to prove this technology can be a reliable long term investment for this type of power generation. Hence it is considered as a driving requirement.

D-SY-S-ECON-000 - The mass of the space segment should be no more than 1000 tonnes.
Rationale: This is in order to minimise launch costs. Should these costs be within the budget, then this can feasibly be exceeded. However, this should done as little as possible. It is therefore classified as a desired requirement.

D-SY-S-ECON-002 - The system should not be unavailable for more than 7 days per year, during its operational life time.
Rationale: This is the preferable unavailability of the system in order to minimise disruption and maximise use, which could be lower than the **M-ST-L-OPER-000**. In this case it is comparable to the unavailability of solar power stations on Earth [84]. This however could result in more expense than there is budget. As a result, this is a desired requirement.

3.2. Performance Requirements

This section presents the performance requirements that the system shall comply to.

Propulsion System

M-SY-P-PROP-001 - The propulsion system shall provide a ΔV of at least 47 $\frac{m}{s}$ per spacecraft each year after target orbit insertion for station-keeping.
Rationale: This is to make sure that the propulsion system can maintain orbital station keeping.

M-SY-P-PROP-003 - The propulsion system efflux shall not damage other subsystems.
Rationale: This is to ensure that the subsystems are not damaged by leaking propellants.

M-SY-P-PROP-004 - The propulsion system shall provide a ΔV of at least 186 $\frac{m}{s}$ per spacecraft at End of Operational Life (EOL) needed for removal from the operational orbit.
Rationale: This is to ensure that the system can be removed from the operational orbit to meet **M-ST-S-ENVI-001**.

M-SY-P-PROP-005 - The propulsion system shall have a lifetime of at least 33 years.
Rationale: This is to comply with the lifetime stated in **M-SY-S-ECON-000** and includes the production time.

M-SY-P-PROP-006 - The pressure of the propellant storage tanks shall not exceed 250 bar.
Rationale: - The tanks that will be used are designed for Maximum Expected Operating Pressure (MEOP) of around 250 bar, so this value can not be exceeded.

D-SY-P-PROP-000 - The dry mass of the propulsion system should not exceed 50 kg per spacecraft.
Rationale: This is to ensure the mass of the total collection system will not violate requirement **D-SY-S-ECON-000**.

D-SY-P-PROP-001 - The mass of the propellants should not exceed 1500 kg per spacecraft.
Rationale: This is to ensure the mass of the total collection system will not violate requirement **D-SY-S-ECON-000**.

D-ST-P-PROP-000 - The propulsion system should make use of green propellants [100].
Rationale: This is in order to reduce the environmental impact as stated in **D-ST-S-ENVI-003**.

Attitude Determination and Control System

M-SY-P-ADCS-000 - The ADCS shall allow for a slew rate of the spacecraft of 0.1 °/s.
Rationale: This is to ensure the potentially very large space segment will be able to point its solar collection system at the sun during the entire operation without putting too high stresses on the structure.

M-SY-P-ADCS-001 - The ADCS shall limit the drift rate of the spacecraft to 0.03 °/s.
Rationale: This is to ensure pointing deviations will stay manageable during the mission duration.

M-SY-P-ADCS-002 - The ADCS shall have a lifetime of at least 33 years.
Rationale: This is to comply with the lifetime stated in **M-SY-S-ECON-001** and includes the production time.

M-SY-P-ADCS-003 - The ADCS shall limit the drift of the solar collection system to 0.05 degrees.
Rationale: This is to ensure pointing deviations will stay manageable during the mission duration.

M-SY-P-ADCS-004 - The ADCS shall keep a sun pointing accuracy of no more than 1 degree during solar collection.
Rationale: This is to ensure that the solar collection system produces the maximum power output possible, maximising the revenue and use of the collection system.

M-SY-P-ADCS-005 - The ADCS shall keep an Earth pointing accuracy of no more than 1 degree for the transmission system.
Rationale: This is important for transmitting power to Earth efficiently as well as for the communication with the ground station.

M-SY-P-ADCS-006 - The ADCS shall have a pointing knowledge of 10 arcsec.
Rationale: This is to ensure that pointing deviations are known in time.

M-SY-P-ADCS-007 - The ADCS shall allow for a transient response decay to less than 0.1 degrees in 60 seconds.
Rationale: - The slew rate should slow down sufficiently so the system does not overshoot its intended attitude by more than 10%.

M-SY-P-ADCS-008 - The ADCS shall limit the jitter of the transmission system and communication antennas to 5 arcsec/s.
Rationale: The transmission system as well as the antennas should point accurately in order to receive power and data consistently on Earth.

M-SY-P-ADCS-009 - The ADCS shall have control of all attitudes within the range of 30 degrees of Nadir.
Rationale: It is unnecessary to control the spacecraft beyond this range.

M-SY-P-ADCS-010 - The ADCS shall have control of the spacecraft up to a maximum rotation of 2 rad/s.
Rationale: When the spacecraft rotates faster than this, it is considered uncontrollable. This should be avoided at all cost.

D-SY-P-ADCS-000 - The mass of the ADCS should not exceed 3000 kg per spacecraft.
Rationale: This is to ensure the mass of the total collection system will not violate requirement **D-SY-S-ECON-000**.

D-SY-P-ADCS-001 - The average power usage of the ADCS should not exceed 2500 Watts per spacecraft.
Rationale: This to ensure at least 1 GW of power remains for transmission to Earth to meet **M-SY-P-OPER-000**.

D-SY-P-ADCS-002 - The peak power usage of the ADCS should not exceed 3000 Watts per spacecraft.
Rationale: This to ensure at least 1 GW of power remains for transmission to Earth to meet **M-SY-P-OPER-000**.

Thermal Control System

M-SY-P-THER-000 - The Thermal Control Subsystem shall maintain all components of the propulsion system within their survival temperature limits for the entire mission duration.
Rationale: This is to ensure no components get damaged by thermal effects.

M-SY-P-THER-001 - The Thermal Control Subsystem shall maintain all components of the ADCS within their survival temperature limits for the entire mission duration.
Rationale: This is to ensure no components get damaged by thermal effects.

M-SY-P-THER-002 - The Thermal Control Subsystem shall maintain all components of the TT&C system within their survival temperature limits for the entire mission duration.
Rationale: This is to ensure no components get damaged by thermal effects.

M-SY-P-THER-003 - The Thermal Control Subsystem shall maintain all components of the Power Collection system within their survival temperature limits for the entire mission duration.
Rationale: This is to ensure no components get damaged by thermal effects.

M-SY-P-THER-004 - The Thermal Control Subsystem shall maintain all components of the Power Transmission system within their survival temperature limits for the entire mission duration.
Rationale: This is to ensure no components get damaged by thermal effects.

M-SY-P-THER-005 - The Thermal Control Subsystem shall maintain all components of the EPS within their survival temperature limits for the entire mission duration.
Rationale: This is to ensure no components get damaged by thermal effects.

M-SY-P-THER-006 - The Thermal Control Subsystem shall maintain all components of the Power storage system within their survival temperature limits for the entire mission duration.
Rationale: This is to ensure no components get damaged by thermal effects.

M-SY-P-THER-007 - The Thermal Control Subsystem shall maintain all components of the propulsion system within their operational temperature limits during system operation.
Rationale: This is to ensure normal operation of all components.

M-SY-P-THER-008 - The Thermal Control Subsystem shall maintain all components of the ADCS within their operational temperature limits during system operation.
Rationale: This is to ensure normal operation of all components.

M-SY-P-THER-009 - The Thermal Control Subsystem shall maintain all components of the TT&C system within their operational temperature limits during system operation.
Rationale: This is to ensure normal operation of all components.

M-SY-P-THER-010 - The Thermal Control Subsystem shall maintain all components of the Power Collection system within their operational temperature limits during system operation.
Rationale: This is to ensure normal operation of all components.

M-SY-P-THER-011 - The Thermal Control Subsystem shall maintain all components of the Power Transmission system within their operational temperature limits during system operation.
Rationale: This is to ensure normal operation of all components.

M-SY-P-THER-012 - The Thermal Control Subsystem shall maintain all components of the EPS within their operational temperature limits during system operation.
Rationale: This is to ensure normal operation of all components.

M-SY-P-THER-013 - The Thermal Control Subsystem shall maintain all components of the Power storage system within their operational temperature limits during system operation.
Rationale: This is to ensure normal operation of all components.

M-SY-P-THER-014 - The Thermal Control Subsystem shall have a lifetime of at least 33 years.
Rationale: This is to comply with the lifetime stated in **M-SY-S-ECON-000** and includes the production time.

D-SY-P-THER-000 - The mass of the Thermal Control System should not exceed 8000 kg per spacecraft.
Rationale: This is to ensure the mass of the total collection system will not violate requirement **D-SY-S-ECON-000**.

D-SY-P-THER-001 - The average power usage of the Thermal Control System should be 0 Watts.
Rationale: This to ensure at least 1 Gigawatt of power remains for transmission to Earth according to requirement **M-SY-P-POCO-000.** It is preferred that all power is used for useful applications. The thermal control system preferably does not use power at all times.

D-SY-P-THER-002 - The peak power usage of the Thermal Control System should not exceed 10 Watts.
Rationale: This is to ensure at least 1 Gigawatt of power remains for transmission to Earth according to requirement **M-SY-P-POCO-000**. The only time the thermal control system uses power is when actuators change the connection of the heat sink to a heat source during eclipse.

D-SY-P-THER-003 - All materials in the Thermal Control System should be non-toxic to life on Earth.
Rationale: The materials used in manufacturing the Thermal Control System could include substances like heat pipe working fluids that can have adverse health effects on the production workers.

Telemetry, Tracking and Command System

M-SY-P-TT&C-000 - The TT&C system shall be able to communicate with the ground up to a distance of 40,000.0 km.
Rationale: This is to ensure communication is possible with the space segment in orbit.

M-SY-P-TT&C-001 - The TT&C system shall have an uplink data rate of 7.5 kbps.
Rationale: This is to ensure the required data can be received by the space segment during ground contact.

M-SY-P-TT&C-002 - The TT&C uplink shall be only in the X-Band or S-Band.
Rationale: This is to ensure communications between the ground and space comply with frequency standards.

M-SY-P-TT&C-003 - The TT&C downlink shall be only in the X-Band or S-Band.
Rationale: This is to ensure communications between the ground and space comply with frequency standards.

M-SY-P-TT&C-004 - The uplink bit error rate shall not exceed 10^{-5} bits per second.
Rationale: This is to ensure the required data can be received by the space segment in an accurate fashion during ground contact.

M-SY-P-TT&C-005 - The TT&C system shall have a lifetime of at least 33 years.
Rationale: This is to comply with the lifetime stated in **M-SY-S-ECON-001** and includes the production time.

M-SY-P-TT&C-006 - The TT&C system shall have an downlink data rate of at least 70 Mbps.
Rationale: This is to ensure the required data and live video can be transmitted by the space segment during ground contact.

M-SY-P-TT&C-007 - The downlink bit error rate shall not exceed 10^{-5} bits per second.
Rationale: This is to ensure the required data can be received by the ground station in an accurate fashion during ground contact.

D-SY-P-TT&C-000 - The mass of the TT&C system should not exceed 20 kg per spacecraft.
Rationale: This is to ensure the mass of the total collection system will not violate requirement **D-SY-S-ECON-000**.

D-SY-P-TT&C-001 - The average power usage of the TT&C system should not exceed 150 Watts per spacecraft.
Rationale: This to ensure at least 1 GW of power remains for transmission to meet requirement **M-SY-P-POCO-000**.

D-SY-P-TT&C-002 - The peak power usage of the TT&C should not exceed 200 Watts per spacecraft.
Rationale: This to ensure at least 1 GW of power remains for transmission to meet requirement **M-SY-P-POCO-000**.

D-SY-P-TT&C-003 - The TT&C system should be accessible for maintenance.
Rationale: This is to ensure the system can be easily maintained/repaired regarding to requirements **D-ST-P-MAIN-000** and **D-ST-P-MAIN-001**.

D-SY-P-TT&C-004 - The TT&C system should have a link availability of 99%.
Rationale: This is to ensure a near-continuous connection between ground station and spacecraft in order to maintain a constant data flow.

Power Collection

M-SY-P-POCO-000 - The SSPS shall produce at least 1 Gigawatt of electrical power at EOL.
Rationale: The system is expected to produce power in the order of 1 Gigawatt, hence at least 1 Gigawatt is required. This is the driving requirement from the customer, to prove that large scale space based solar power collection is possible. Hence it is considered to be a mandatory requirement.

M-SY-P-POCO-001 - The power collection system shall produce the required electrical power for at least 90% of its lifetime.
Rationale: This is a driving requirement for the collection system, to prove that the generation method can return investment with a high degree of certainty. Hence it is considered as a driving requirement.

M-SY-P-POCO-002 - The power collection system shall have a lifetime of at least 33 years.
Rationale: This is to comply with the lifetime stated in **M-SY-S-ECON-000** and includes the production time.

D-SY-P-POCO-000 - The mass of the power collection system should not exceed 3500 kg per spacecraft.
Rationale: This is to ensure the mass of the total system will not violate requirement **D-SY-S-ECON-000**.

D-SY-P-POCO-001 - The power collection system should be accessible for maintenance.
Rationale: This is to ensure the system can be easily maintained/repaired regarding to requirements **D-ST-P-MAIN-000** and **D-ST-P-MAIN-001.**

Electrical Power System

M-SY-P-EPSY-000 - The EPS shall provide all subsystems with their required amount of power.
Rationale: This is to ensure all subsystems are able to operate according to their requirements.

M-SY-P-EPSY-001 - The EPS shall provide all subsystems with the required voltage and/or current of each subsystem.
Rationale: This is to ensure all subsystems are able to operate according to their requirements.

M-SY-P-EPSY-002 - The EPS transients shall not persist for longer than 0.1 second.
Rationale: This is to ensure unwanted transients do not negatively affect the performance of the system.

M-SY-P-EPSY-003 - The EPS voltage ripple in the subsystem power supplies shall be smaller than 0.1% of the steady Voltage.
Rationale: - This is to ensure a too large voltage does not negatively affect the performance of the system.

M-SY-P-EPSY-004 - The EPS current ripple in the subsystem power supplies shall be smaller than rated for the subsystem.
Rationale: - This is to ensure a too large current ripple does not negatively affect the performance of the system.

M-SY-P-EPSY-005 - The EPS shall have a lifetime of at least 33 years.
Rationale: This is to comply with the lifetime stated in **M-SY-S-ECON-000** and includes the production time.

M-SY-P-EPSY-006 - Electrical power shall be compatible between systems in terms of voltage, current, power and type (for AC including phase(s)).
Rationale: This is to prevent outages, burnouts or other problems with the electrical power supply incompatibilities.

D-SY-P-EPSY-000 - The mass of the EPS should not exceed 55% of the total system mass.
Rationale: This is to ensure the mass of the total collection system will not violate requirement **D-SY-S-ECON-000** and from studies it seems feasible to size it to about 55% of the final weight.

D-SY-P-EPSY-001 - The average power usage of the EPS should not exceed 6% the total power generated.
Rationale: This to ensure at least 1 Gigawatt of power remains for transmission to Earth according to requirement **M-SY-P-OPER-000**.

D-SY-P-EPSY-002 - The peak power usage of the EPS should not exceed 1% above the power allocated in **D-SY-P-EPSY-001**.
Rationale: This to ensure at least 1 Gigawatt of power remains for transmission to Earth according to requirement **M-SY-P-OPER-000**.

D-SY-P-EPSY-003 - The EPS should have a maximum power loss of 93% from the power source to each load.
Rationale: This is to ensure not too much power is lost and more power can be used for transmission.

Power Transmission System

M-SY-P-POTR-000 - The power transmission system shall not harm life on Earth.
Rationale: As part of **M-ST-S-ENVI-000**, the transmission of power should not be harmful to life on Earth.

M-SY-P-POTR-002 - The power transmission system shall transmit power for 90% of the time.
Rationale: This is to ensure all useful collected power can be transmitted to the ground segment.

M-SY-P-POTR-003 - The power transmission system shall be able to transmit a minimum of 150 MW of power at EOL to Earth.
Rationale: This is to ensure the transmission system can transmit all useful collected power to the ground segment for the entire mission duration. The value corresponds to a minimum transmission efficiency of 15%.

M-SY-P-POTR-005 - The power transmission system shall have a lifetime of at least 33 years.
Rationale: This is to comply with the lifetime stated in **M-SY-S-ECON-001** and includes the production time.

D-SY-P-POTR-001 - The power transmission system should be accessible for maintenance.
Rationale: This to ensure the system can be easily maintained/repaired regarding to requirements **D-ST-P-MAIN-000** and **D-ST-P-MAIN-001**.

Power Storage System

M-SY-P-POST-000 - The power storage system shall have a lifetime of at least 33 years.
Rationale: This is to comply with the lifetime stated in **M-SY-S-ECON-001** and includes the production time.

M-SY-P-POST-001 - The power storage system shall be able to store a minimum of 24 kWh at EOL.
Rationale: The ADCS, TT&C and Propulsion system will need to stay operative during emergencies. From a depth of discharge of 15% it should let ADCS and TT&C stay active for 12 hours and give essential thruster power of 1 hour.

D-SY-P-POST-000 - The mass of the power storage system should not exceed 500 kg per spacecraft.
Rationale: This is to ensure the mass of the total collection system will not violate requirement **D-SY-S-ECON-000**.

D-SY-P-POST-001 - The power storage system should be accessible for maintenance.
Rationale: This to ensure the system can be easily maintained/repaired regarding to requirements **D-ST-P-MAIN-000** and **D-ST-P-MAIN-001**.

O-SY-P-POST-001 - The power storage system should preferably be able to charge to full capacity in 1368 minutes at EOL.
Rationale: The power storage system should be able to store enough energy in the time between eclipses.

O-SY-P-POST-002 - The power storage system should preferably be able to discharge its full capacity in 72 minutes at EOL.
Rationale: The power storage system should be able to discharge its full capacity during the longest eclipse.

Maintenance

D-ST-P-MAIN-000 - The system should allow self in-orbit repairing / replacement of components.
Rationale: Due to the size and scale of the collection system, there are many components that can potentially fail and would hence require repair in orbit. This requirement is to ensure that expensive repair missions for regular repair and replacement do not have to be implemented in order to keep the station running. However, this is not as important as the above mandatory requirements and should hence not compromise them. This is thus a desired requirement.

D-ST-P-MAIN-001 - The system should allow self-maintenance.
Rationale: This requirement was implemented with the idea of minimising the reliance on and costs of hiring in-orbit service providers. This however cannot come at the cost of a mandatory requirement. Hence it is deemed to be a desired requirement.

D-ST-P-MAIN-002 - Third parties should not be involved with in-orbit assembly.
Rationale: This will cut down costs of hiring third parties, maintain in house knowledge, and guarantee self-maintenance. This should keep down costs, making it economically viable. However this should not come at the cost of mandatory requirements.

O-ST-P-MAIN-003 - The system should preferably allow for future upgrades to be implemented into the system.
Rationale: This can be done in order to extend the life and increase the overall efficiency and profitability.

Structures

M-SY-P-STRU-000 - All components shall be able to survive maximum transport loads with a 1.5 safety factor.
Rationale: This is in order to ensure that the parts are not unnecessarily damaged or compromised during transit.

D-SY-P-STRU-001 - The total deflection of the collection area should not exceed 0.04 degrees.
Rationale: This is to ensure the angle of incidence of sunlight will stay within limits over the entire collection area, as specified in **D-SY-P-ADCS-003**.

D-SY-P-STRU-002 - The maximum stress in the structure should be at most one-third of the ultimate stress.
Rationale: Untested structures should have spacious safety margins, therefore a factor of safety of three is taken into consideration during the structural design.

D-SY-P-STRU-003 - The spacing between space web elements should not be bigger than one metre.
Rationale: In order to produce the thin film mirror, the web crawler needs to be able to move itself on the space web structure. To be able to do this, the spacing cannot be bigger than one metre.

D-SY-P-STRU-004 - The mass of the structures should not exceed 1500 kg per spacecraft.
Rationale: This is to ensure the mass of the total collection system will not violate requirement **D-SY-S-ECON-000**.

3.3. Logistics/Life Requirements

Production

M-ST-L-PROD-000 - Materials and parts in orbit shall be manipulatable by the machines available.
Rationale: This is to ensure that the parts can be assembled and produced from materials available in space by the available machines. Should this material be unmanipulatable then parts cannot be made. Should the parts be unmanipulatable, then the system cannot be assembled.

M-ST-L-PROD-001 - Launch payload shall be certified and qualified for the launcher and local regulations.
Rationale: This is to cover legal basis and to be allowed to launch the payload. The insurance will also require this.

M-ST-L-PROD-002 - The components in the system shall be fail safe.
Rationale: This is to ensure that the loss of a single component or subsystem will not result in the loss of the entire station and its operations. This could for example allow the consumers, who could be in remote locations without other means of power, to rely completely on the power station. Hence is considered as a mandatory requirement.

D-SY-L-PROD-000 - The construction of the system should be completed within 2 years from the first launch.
Rationale: This is to ensure a timely delivery and start of operation to ensure the components can maximise their lifetime and supply the market demand. The technology and methods used for construction cannot guarantee the time allocation, but are still required for the success of the mission. Hence this requirement can only be considered to be desired and not mandatory.

D-SY-L-PROD-001 - All products produced on Earth should have a backup.
Rational: In case of launch failure, which leads to destruction of the payload, backups can be kept for timely launch.

O-ST-L-PROD-000 - Every component in the system should preferably be fully redundant.
Rationale: The production of spare parts and intensive repair jobs are costly, however the increase in weight is also costly. Hence it should only be done should the above requirements be met adequately.

Operational Life

M-ST-L-OPER-000 - The system unavailability due to maintenance shall be less than 14 days per year during its operational life time.
Rationale: This is to ensure that failures occur as little as possible to ensure a similar unavailability of a regular terrestrial solar power station. Due to the extreme conditions of space, twice the regular value of 98% was taken [84]. This is to ensure trust in the generation method and is therefore of utmost importance for the future the space generation industry. Hence it is considered as a mandatory requirement.

D-ST-L-OPER-000 - The system should not rely on external parties to make and implement decisions.
Rationale: This is to ensure minimum input from the ground, saving costs, as well as ensuring minimal intervention from external parties. The infrastructure can be implemented in a way that the system is not self-reliant, if this would allow the mandatory requirements to be met. Hence it is considered to be a desired requirement.

D-ST-L-OPER-001 - The system should be able to operate autonomously for all nominally scheduled procedures that relate to inspection, receiver pointing, orbital maintenance, searching for contact with the ground, maximising energy output and avoidance of debris.
Rationale: This is to ensure that the system is not lost when contact is lost or when it is out of range. The system could also go into a waiting state, stopping power production operations and hence stop making money. However,

with a larger chance of recovery and contingencies not going wrong. As a result, it cannot be considered mandatory and is therefore deemed desirable.

D-ST-L-OPER-002 - The system should be in view of receivers for at least 10% of its operational orbital period.
Rationale: This is to ensure that every receiver on the ground obtains their fair share of power beamed back. Should the inclinations of the stations be such that this is impossible, then it should not stop the mission from occurring. Hence this is considered desirable. Because the chosen orbit is geostationary, this requirement is met with ease.

D-ST-L-OPER-003 - Station keeping should not negatively affect the solar collecting capabilities.
Rationale: The use of certain propellants can reduce the efficiency and degrade of solar cells during the lifetime of the system, requiring a larger collection area. This would increase costs and waste usefulness of the system.

Disposal

O-ST-L-DISP-000 - The system should preferably be recoverable.
Rationale: Space hardware is expensive and one might want to reuse it for future missions, research, novelty key chains, cool museum pieces and memorabilia for space geeks. This adds to economic and environmental sustainability but especially to social sustainability.

4

Preliminary Resource Allocation & Budget Breakdown

This chapter provides an overview of the preliminary mass, power, and time budget, as well as the Technical Performance Measure (TPM) parameters tracked during the design phases.

4.1. Tracking of TPM Parameters

Since the second design phase, the TPM parameters of the system have been continuously considered with the contingencies in mind. The most critical parameter, mass, has been tracked in order to analyse how the system's mass develops over time, and how volatile the design of the system is. The volatility of the design has aided us in determining the proper design risks. Below, one may find a table that presents the development of mass throughout the design phases.

4.2. Mass Allocation

The mass allocation is a guideline during the design which is produced at the start of the detailed design phase. This is done in order to prevent subsystems from being over-designed during the design phase. The state of the mass budget after the midterm report is depicted in Table 4.1 [20].

This mass budget however does not reflect the state of the design at the start of the detailed design phase. Not only have the names of the subsystems changed slightly, the mass allocation has undergone large and unpredictable fluctuations in mass since the start of the concept selection phase due to new-found insights. Hence a baseline of 400 tonnes and an updated mass budget should be used. The system can be updated using the help of the New SMAD [83]. On page 422 of the New SMAD is a mass breakdown, however this is only applicable for conventional spacecraft. Hence the values have to be edited in order to ensure these become applicable for the scale of the SPECTRE system.

The spacecraft has to produce and handle such large amounts of power, it can be assumed that the subsystems directly related to this will be the heaviest, as is the case in Table 4.1. Hence it is assumed that the power collection and the thermal systems will contain the lion's share of the mass, in order to be able to achieve the requirements. However, due to the flexible, thin film mirror concept and some concentrator and solar sail feasibility studies, it is found that this could be reduced significantly. It was chosen to allocate 20% to the power collection system and 12% to the TCS. The EPS was given the largest share, since for terrestrial applications this can weigh many hundreds of tonnes for similar power applications. Hence this was given 55% of the mass. These subsystems hence will be allowed to take up 87% of the mass. The system also does not contain any payload, hence this was reduced to 0%.

The production/maintenance could include the production module as well as potential robotics. The TT&C is similar to conventional spacecraft. However, conventional spacecraft weigh much less than 400 tonnes, so it is assumed to not be relevant to the mass and is given an allocation of 0% (note that it still exists, it is however too small to discuss). ADCS and propulsion are related to the size and mass of the spacecraft and therefore form a relatively bigger part of the mass compared to a conventional spacecraft. The allocations are summarised in Table 4.2.

4.3. Power Allocation

The power budgets are made at the start of the detailed phase and exist in order to guide the design, in a similar fashion as the mass allocation. This was produced with the following rationale.

Table 4.1: Mass distribution of the system at the end of the midterm report

Subsystem	Power	Thermal Control	Structures	TT&C	On-Board Comp.	ADCS	Propulsion	Other	Total
Mass [tonne]	579	50.6	21.7	3.6	3.6	28.9	14.5	21.7	723

Table 4.2: Preliminary Mass Budget Allocation

Subsystem:	Payload	Structure	Thermal	Power Collection	EPS	TT&C	ADCS	Propulsion	Total
Mass Budget [%]	0	3	12	20	55	0	4	5.5	100
Mass Budget [Tonnes]	0	12	48	80	220	0	16	22	400

Table 4.3: Preliminary Power Budget Detailed Design Phase

Subsystem:	Transmitter	EPS	ADCS	TT&C	Propulsion	Thermal	Total
Power [W]:	1,000,000,000	75,260,000	38,500	470	70,000	10,000	1,075,378,970
Power [%]:	93	7	0	0	0	0	100

The goal of the mission is to produce at least 1 Gigawatt of power for transmission to Earth, in accordance with **M-SY-P-POCO-000**. Due to the scale and importance of this requirement, the majority of the power budget is allocated to this. From **D-SY-P-EPSY-003**, it can be determined (should the output power be 1 GW from the electrical system) that the EPS should consume/dissipate a maximum of 7% of the total power budget.

The data and link budget does not differ much from a regular geostationary spacecraft. This being said, it should be possible to stream videos. From Table A-9 on page 953 in the New SMAD [83], concerning high Earth satellites, the highest power and percentage were taken: 1621 W and 29% from the TDRS-7 respectively. The power required for communications and data handling should be in the order of 470 W. Hence this was chosen.

The ADCS was taken from the same mission and scaled from the TDRS-7 mass given in Table A-8 to 400 tonnes. Hence the power budget for the ADCS system would be of the order of 35,000 W. Adding a safety factor of 1.1 should include any potential unexpected contingencies due to the early stages of the design and would result in 38,500 W.

Furthermore, electric propulsion is used, which has a high power consumption. However, it should only be designed to be used for station keeping purposes. Due to the high electrical power density of the system, and the small orbital disturbances, this should only be a very small percentage. Hence the power of a regular ion-propelled spacecraft scaled to the size of this system would not give an accurate representation. Knowing this, it is assumed to be twice as large as the ADCS, which results in 70,000 W.

From the preliminary analysis, it was uncertain if only passive thermal control would suffice, or active thermal control would be needed. This power should be kept at a minimum however. Hence the power allocation will be placed in the order of 10,000 W. Passive subsystems such as the structural subsystem are given no power budget, since these can be expected to use no power. There is also no payload for this mission. Hence this was also discarded. The power budget is summarised in Table 4.3. As will be discussed later in subsection 11.5.6, the subsystems turned out to be more efficient and less power intensive. This indicates that the design has achieved staying within the guidelines.

4.4. Time Allocation

The time budget allocation is mostly determined by **M-SY-S-ECON-000** and **M-ST-S-ECON-001**. This means that from now (at the time this was written in 2018) until 2028, all further design and production on Earth must be performed. The last 2 years are required for launch and production in space in order to comply with **D-SY-L-PROD-000**. Once the operation has started, it is expected to operate for at least for 30 years in accordance with **M-SY-S-ECON-000**. Finally there is the disposal period at the end of 2060, or the program is extended or modified. It is estimated however, that reaching a designated disposal orbit should take about 1 month. It was estimated that the production on Earth would take the same amount of time as in space, this results in the time line that is illustrated in Figure 4.1.

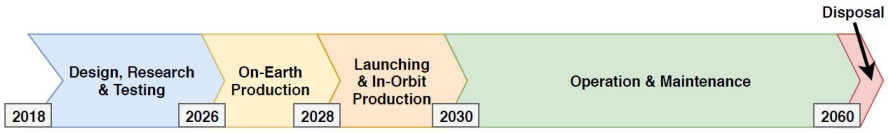

Figure 4.1: Time Allocation

5
Functional Description

In order to assess the required system functions, a brief investigation will be performed in this chapter. This investigation will aim to produce a functional description of the SPECTRE system. Additionally a functional flow diagram, and a functional breakdown diagram are developed to aid the later design phase. In section 5.1 the functional flow diagram is discussed, and in section 5.2 the functional breakdown diagram is presented.

5.1. Functional Flow Diagram

The functional flow diagram is used to identify and present all the functions the SPECTRE system will have to perform. An initial breakdown in functions is made on a high level, this is presented in flow diagram in Figure 5.1. As presented in the flow diagram, the high level function is split up into four functions, based mainly on the different parts of the lifetime of the system. Starting with all on-Earth production, assembly and launch preparation, followed by the in-orbit production and assembly, after which the operational phase is presented and finally the retirement of the system is considered.

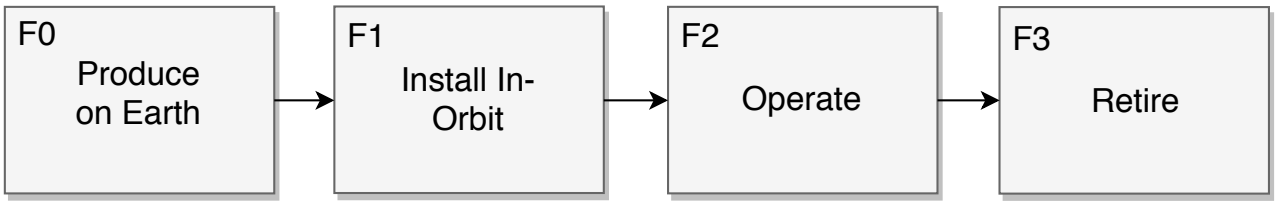

Figure 5.1: High Level Functional Flow Diagram

The functional flow of the system is further broken down in lower levels in Figure A.1 in the appendix. Each of the high level functions is broken down into two levels of subdivided functions. Each level goes into more depth describing the system. The breakdown of the first high level function, on-Earth production, describes all the steps that are required to get all the materials and systems ready for launch. This includes the production and assembly of necessary components but also the qualification procedures and contact with third parties. The next high level function describes all the functions that occur in orbit before the operational phase of the system. This starts off with the launch to orbit and the necessary steps to perform the launch. This is followed by all the in-orbit activities required to make the system ready for operation. When this has been completed the system will enter its 30 year operational phase, which will start with the testing and validation of the system. The nominal operation of the system provides the technical functions of converting the solar light into electrical energy. Additional functions that are described under operation are maintenance and transmission. Finally the retirement of the system is described in the last lower level breakdown as three possible options linked with an OR function. As this decision will be made after the end of the operational phase, and only then an evaluation can be made towards the retirement, all the possible options are given. These options include de-orbiting the system, extend the operational lifetime or recycling and recovering parts of the system.

5.2. Functional Breakdown Diagram

In the functional breakdown diagram the functions described in the functional flow diagram are broken down one level further. This diagram is ordered hierarchically based on the level of depth of each function. The lower level functions that are added describe each of the lowest level functions from the functional flow diagram in detail, ensuring that the full scope of the function is covered in depth. A high level breakdown is given in Figure 5.2 whereas the full depth breakdown is presented in Figure A.2 in the appendix.

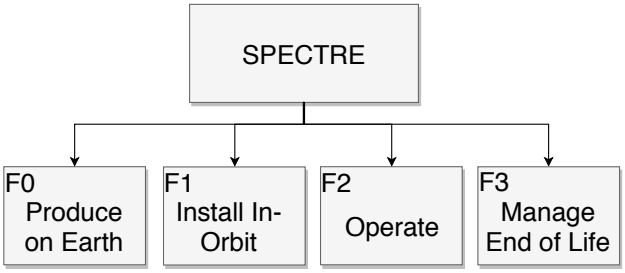

Figure 5.2: High Level Functional Breakdown Diagram

With the functional description clearly defined in the functional flow and breakdown diagrams this description can be used in the coming chapters. These descriptions can provide a solid understanding of the system's functionality during designing and analysising the remainder of the system.

6

Cost Breakdown & Market Analysis

In this chapter, the cost breakdown structure of SPECTRE will be shown, including all significant cost that would be incurred after this DSE, if the project would be continued. After this, a market analysis will be performed in order to analyse the optimal markets for power distribution and perform a financial analysis of the concept.

6.1. Cost Breakdown Structure

The Cost Breakdown Structure (CBS) of a system is an AND tree and is used to show all costs included in the production and development of a product [69]. In this case, the costs during operational lifetime are also shown although they are not included in the budget. This is very useful to predict costs at the start of a project and to ensure that the design complies with the budget.

The CBS is also a very powerful tool in cost saving, as it structurally breaks down where money flows to and thus also where money can be saved. The CBS for SPECTRE is shown in Figure 6.1. There are two major divisions: direct and indirect costs. The direct costs relate to the money that actually goes into the product, such as costs to purchase parts, salary and so on. The indirect costs are the costs that are not directly related to building this system but more related to the general operation of the company, such as factory security, cleaning services etc. They do not directly contribute to the product but they are used to keep the company going.

Most costs were estimated statistically, with some contingency included. To ensure some margin for error, 10% of the budget, or 150 million euros was set aside as a risk budget in case some estimations were too optimistic or unexpected costs were incurred during the design and production. This 10% was derived previously in the beginning of this project [19].

6.1.1. Direct Costs

The direct costs are divided into five big categories: design, launch, production, testing and direct materials. They will each be discussed below.

Design Costs
Design costs are related to the costs of the design phase, which is dominated by salaries of engineers and design employees. The assumed average salary of an employee was taken to be around €55,000 per year for 400 employees [109]. Other contributions include supporting staff, office space and R&D costs. Here, office space was calculated based on the number of employees, where around 25m^2 per employee was accounted for, including offices, walkways, sanitary, break rooms, meeting rooms and so on. This led to a total area of 10,000 m^2 with the office space cost around €200 per m^2 per year [132]. This will be rented for 12 years (2018 until 2030). With further research and development costs taken into account, the direct design cost turned out to be around €344M.

Launch Costs
Launch costs are given by the launcher, the BFR, and the launch insurance which is around 4% of the spacecraft worth [66]. Projected launch costs for the BFR are €7M, however, due to the fact that this is unproven, the cost breakdown will assume €15M per launch, with 15 launches used in total. The total spacecraft worth is based on the actual materials in the spacecraft, not including the design costs. This means insurance at 4% is €11.6M for all 15 launches.

Production Costs
Production relates to the production of the system on the ground (do not confuse this with the in-orbit production). This entails the costs of building a factory, a storage, a clean room, labour cost and tooling. The facilities such as the factory were estimated at 50,000 m^2 at €500 per m^2 to build it [131]. Specialised transport and storage are estimated at €5M [131]. Adding onto this a clean room of 3600m^2 at €2000 per m^2, facilities in total add up to €37.2M [131].

Tooling for production is a very important cost since this tooling is very specific and tailored to the design of SPECTRE. That is why costs for tooling will be fairly large, with the tooling for web production, subsystem modules, the in-orbit production system and general production were estimated to cost €5M each. The filter production process is highly innovative and already expensive on a small scale, so €30M was budgeted for the production of the thin film filters. This leaves tooling at €50M. Labour for manufacturing is estimated using 800 workers at €40,000 per year for 4 years (2026 until 2030) [103]. Total production costs are thus found to be €215.2M.

Testing
Testing spacecraft systems is a crucial part of development, since trial and error is very expensive for these applications and there are no reference projects comparable to SPECTRE. Testing will consist of five categories. Vibration testing is to ensure all systems survive the launch. This is readily available as vibration beds have been in use for a long period of time. A cost of €10M was reserved for the vibration testing.

Vacuum testing (in combination with thermal testing) is to ensure that the system works in the space environment. For SPECTRE, this can be done only for separate components. Since it relies on microgravity to deploy, it can never be self-supporting on Earth. This is why thermal testing in combination with a lot of analyses will need to be done, leading to €80M being budgeted for thermal testing and vacuum testing. Production testing will also have very high costs due to the low Technology Readiness Level (TRL), and was estimated to cost around €60M in combination with the Assembly, Integration and Test (AIT). AIT is to test all systems and modules to see if if they fit and interfaces work as expected. This means a testing cost of €150M was foreseen, although this is a very rough estimate due to the low TRL of SPECTRE.

Direct Material Costs
The direct material costs relate to the actual purchased hardware for the system. These are considered for all subsystems, both raw materials and off-the-shelf parts, as well as for production. This direct material cost was estimated for the power collection system, TCS, ADCS, propulsion, TT&C and EPS systems.

The power collection system, being the main focus of this design, was also estimated to be the most expensive at €142.82M. This includes raw material costs for the structure, estimated at €250K. Mirror material for in-orbit production was found using aluminium standard prices at about €2 per kg, using about 12 tonnes overall which leads to €24K [80]. The largest cost in the power collection system is the thin film filters, estimated to cost around €7K per m^2 and using 19300m^2, which means €135M is required [106]. The photovoltaic cells are also quite expensive, estimated to be €94 per m^2, coming in at 77,525.9m^2 which leads to a price of €7.29M [56]. Lastly, the mirror behind the filters is estimated to cost another €400K, which is relatively low for a space mirror. This is because the required accuracy of this mirror is not very high, such that readily available mirror technology can be used.

For the TCS, the cost of the phase change material of the thermal energy storage container (lithium chlorate trihydrate) costs around €150 per kg (assuming bulk discounts of around 25%), where 2,000.0 kg is present in each spacecraft [124]. This means the total cost is around €6M. Other costs include the heat pipes and other costs, weighing in at €3M and €5M respectively. These are relatively coarse estimations since no comparable systems exist and it is all highly experimental. It is for costs like these that the contingency budget of €150M is present.

As for the ADCS, there are 60 sun sensors present in total, at €12k per sensor leading to €720K [48]. For safe modes and redundancy, there are 20 coarse sun sensors for €2k per sensor, so €40k overall and there are 120 horizon sensors at €15k per sensor which is a total of €1.8M [48]. There are also 80 star trackers present in total, estimated to cost €50k per sensor which is a total cost of €6M [48]. The actuation of the ADCS is done using 9 L3 Control Moment Gyroscopes, estimated to cost €200K per piece. This is a very rough estimation again since price information is not readily available for these Control Moment Gyroscopes. This price means a total cost of €36M for the actuators, and a grand total for the ADCS of €44.56M.

In the propulsion system there is about 30,000.0kg of xenon on board as propellant, which costs around €850 per kg [6]. This means the total propellant cost is €25.5M. Next to this, there are also five Busek BIT-7 ion thrusters present per spacecraft, costing around €8000 per piece based on an inquiry at Busek. The total cost is then €8M for the thrusters. The feed system for this system would include many expensive feed lines and valves as well as sensors, so €1M has been set aside for this due to the lack of better estimations. The xenon tanks were chosen to be the MT Aerospace S-XTA-60 high pressure xenon tanks, costing around €120k each based on an inquiry. This leads to €2.4M for the tanks and thus €11.4M for the overall propulsion system.

The TT&C requires a 1m diameter transmitting antenna on board each spacecraft, estimated to be around €60k. The high speed X-Band transmitter is bought from Meisei Electric, and from an inquiry was found to cost €50K a piece. For SPECTRE, which uses 80 transmitters, this leads to a cost of €4M. The S-Band receiver, which is very common and thus much lower in cost, is estimated at €5k per piece, or €400k in total. The amplifiers were assumed to have a similar cost and are thus another €400k. This leads to a TT&C of €4.86M.

For the EPS, bus wires were estimated to be €0.5 per meter and each spacecraft uses around 270m of wires [26]. This means the wires would be €2.7k. To have the ability to shut down parts of the EPS, 100 solar switches were installed per spacecraft, estimated to be around €2.5k each, leading to €5M in total [67]. The capacitors required for the EPS have around €5M allocated to them since the cost estimations for these capacitors will depend heavily on the type used. Same goes for the inductors, for which another €5M is reserved. The 60,000 diodes, 800 transistors, the fuses and controllers were estimated to cost €63.3k together. [47] [62].

The power transmission system should also be included in this CBS, however due to the focus of this DSE being on the power collection, an accurate cost estimation cannot be made. However, it is reasonable to assume that this cost will be in the order of at least €100M due to the low TRL and highly specific needs. Again, this CBS can be seen graphically in Figure 6.1.

6.1.2. Indirect Costs

The indirect costs that play a major role in this CBS are overhead costs, such as engineering, maintenance and legal support, as well as variable costs and general & administration costs. The overhead cost for engineering support is mainly throughout the lifetime and thus not part of the allocated budget, although the maintenance and legal support is already in effect during design & production phases. Facility cleaning, security and maintenance were foreseen to be €2.4M, €4M and €9.5M respectively [23][105][137]. Legal fees were foreseen to be around 0.5% of the total budget, which would be €7.5M. Company insurance is estimated at around 5% of the total budget, hence €75M is allocated to this. Any extra costs that may occur such as events, sponsorships etc. are budgeted for €5M.

Finally, general and administration costs were considered. This includes mainly lifetime costs that are not in the budget, but have been considered in this CBS. This includes ground centre operation and maintenance, administration of the firm during operations, customer service and more. However, these are all part of the operational costs and thus not included in this CBS.

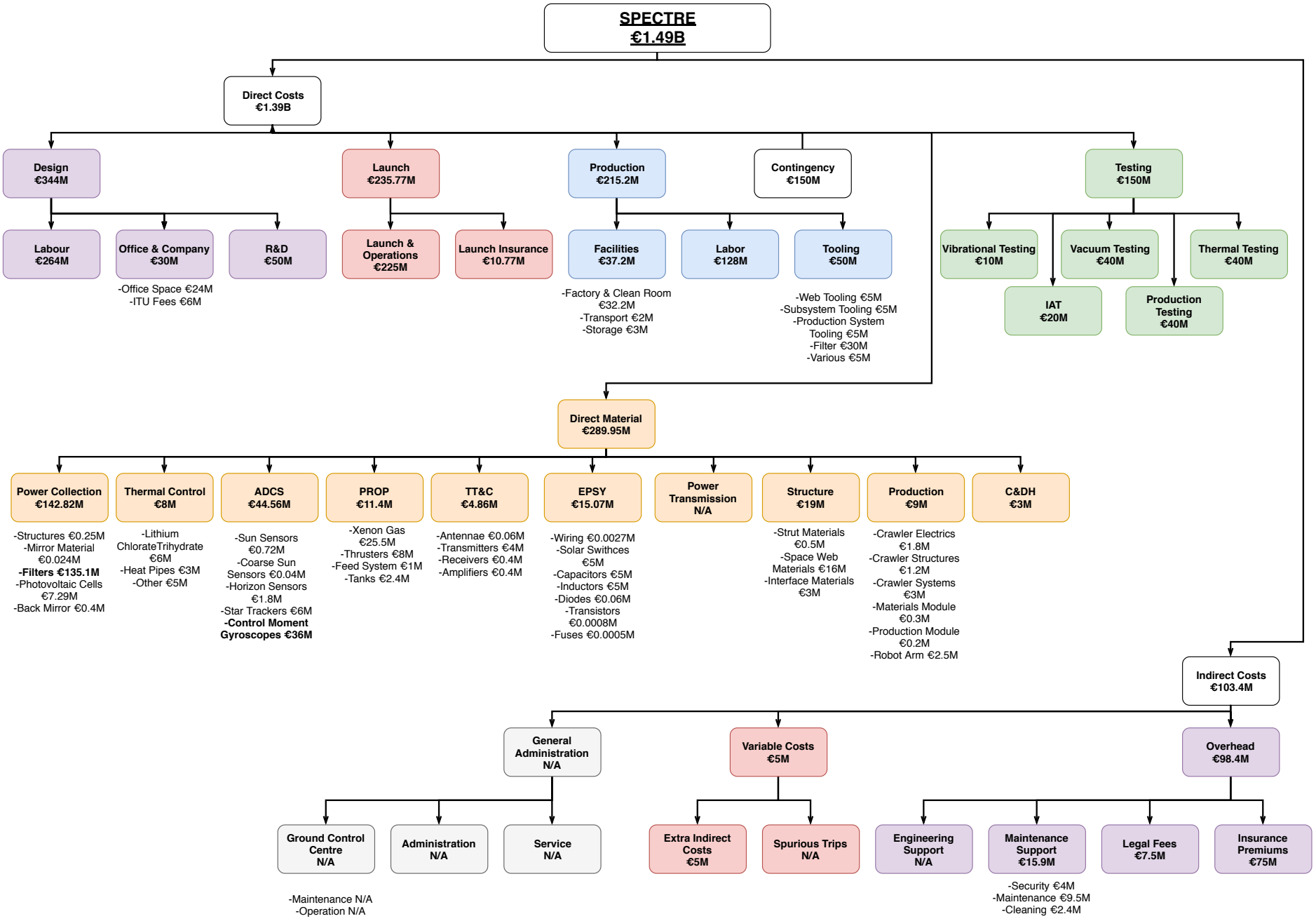

Figure 6.1: SPECTRE Cost Breakdown Structure

6.2. Market Analysis

The first step of developing the SSPS was performing a market analysis to determine the viability of the project. An initial market analysis was developed in the baseline report, where it was determined that the returns would outweigh the budget [19]. This market analysis was redeveloped for the current design phase. In this section, the added value of the system will be evaluated, all of the stakeholders and competitors will be discussed, the consumer locations and marketing strategy will be chosen and finally the revenue estimate will be refined.

6.2.1. Added Value of the System

To perform a feasible market analysis, it is first important to understand what the added value of the product is. This product will generate 1GW of power in space, through solar radiation. Once this 1GW is generated, this power will be transmitted down to Earth with an estimated 15% efficient laser transmitter. Given this, there will be 150MW of available power on Earth, through the virtue of this system. This power can then be distributed and sold to consumers. Of course it is important to understand this value in relative terms, therefore it has to be compared to the worldwide generation of electricity. In 2016, the worldwide generation of electricity resulted in 23,816TWh, with only 6.3% of this originating from renewable sources (1500TWh) [74]. Considering that the product produces 150MW, over a year this translates to 1.314TWh. Therefore, the system would acquire a market share of 0.0876% in electricity generation with renewable sources, and 0.00552% in overall electricity generation. Given these values and the ever-increasing demand for power, the system is at low risk of encountering competition that would make the system obsolete. This is looking at the system through the view point of the system being a power generator, rather than a company that serves as an energy provider. This is desirable since the market of energy providers is extremely competitive, and with an overall market share of 0.00552%, the system could not survive as an energy provider. Therefore, alternative strategies for the sale of the generated power will have to be considered, which will be done below.

6.2.2. SWOT market analysis

In this section a market SWOT analysis will be performed on the system's position in the market. In this SWOT analysis, the strengths, weaknesses, opportunities, and threats to the system's position in the market will be highlighted. This market SWOT analysis will be used to refine the marketing strategy of the system.

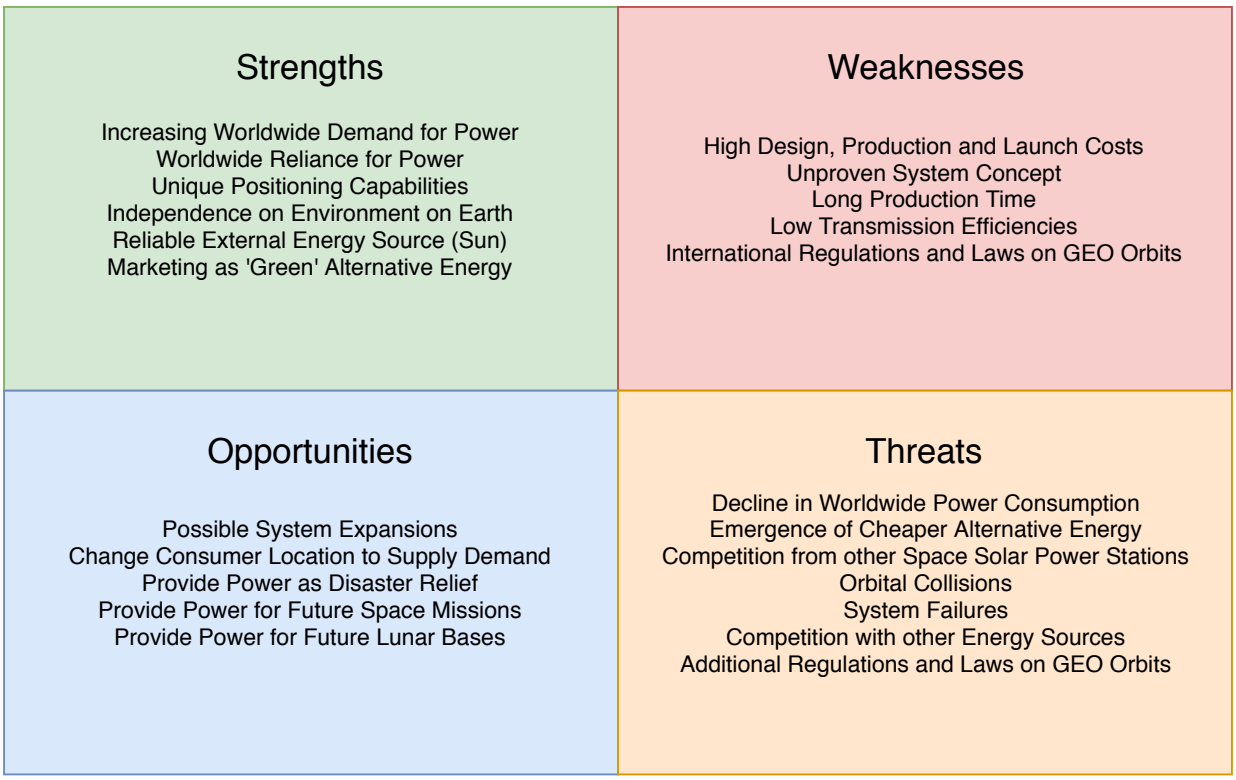

Figure 6.2: SWOT Analysis for the Market

6.2.3. Stakeholder Identification

In this section the stakeholders in the market will be identified, and will be put into subgroups depending on their contribution to the system. The stakeholders will involve all of the third party producers, advisers and operators, the consumers and customers of the product, and the social, public and regulators.

Third Party Identification
Since the scope of this project is similar to that of the International Space Station in terms of mass, but in a commercial market, a large amount of third parties will be required to realise the system. These third parties will include all parties that support the system in one way or another. The first organisations considered are related to production. These will not have all of the resources (facilities and labour) to produce every required element, some of the production will have to be outsourced to more experienced and reliable producers. On-Earth assembly of certain components of subsystems can also be outsourced to third parties. Furthermore, since the team is specialised on designing, the team will require legal, financial and managerial consultancy, as well as possible support during operation from the ground station. Finally, due to the large amount of material and component flow during production, the transport of these materials and components can be supported by third parties.

Consumer Identification
Another stakeholder for this system, and arguably the most important one, is the consumer. The consumer is the person responsible for the purchase and consumption of the product. For this product, the end consumer will be an entity that is reliable and capable of purchasing all of the generated power by the system, or a collection of such entities that would purchase large shares of the power. This is required for two reasons. The first reason is to minimise the operational costs of the system, since the logistics of distributing the power will be more simple. Furthermore, the system is expected to be more competitive when delivering through partnering with energy companies than direct delivery to household consumers as discussed above.

Customer Identification
The customer of this system is the entity responsible for the realisation of this project, as this is the entity who sets the requirements for the system. This is the source of the design requirements for whom the system is being designed, and the source of funding, production and operation of the system.

Social Public and Regulators
Due to the global reach and extent of the system, the social public and regulators, which include governments and non-profit organisations, will also have to be considered. This system is being produced for the development of humanity, and therefore, it should be ensured that the public also views it in that way.

Overview of Stakeholders
Below, an overview of all of the stakeholders involved will be shown and segmented.

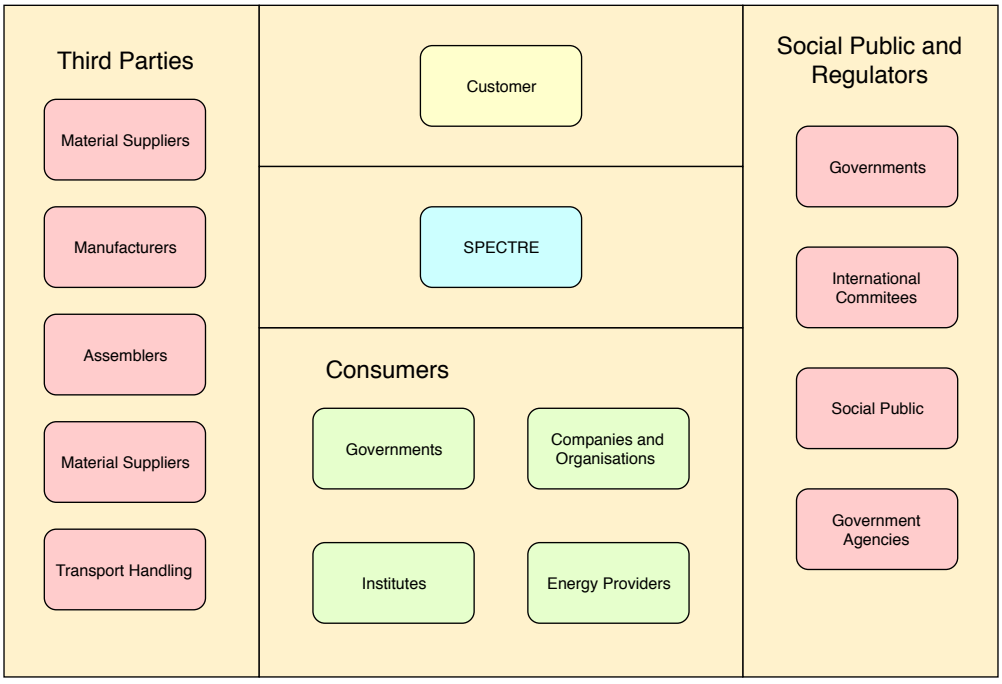

Figure 6.3: Stakeholders Segmented into their own Constituents

6.2.4. Market Segmentation

The end consumers identified in the previous section can be segmented into various types of consumers, depending on the characteristics of those consumers. The consumers can be split into energy providers, institutes, governments and organisations requiring flexible power distribution. These consumers will be discussed in more detailed below.

Energy Providers
The first possible consumers in the market are energy providers. Energy providers could be used as a means to distribute the generated power, as well as purchasing and re-selling or auctioning power. This way, energy providers do not become competitors to the system, but rather they become the customers of the system. Furthermore, since energy providers have come under scrutiny in recent years due to their continued use of fossil fuels. In order to curb this, some energy providers in fact subsidise the generation of renewable energies. Since SPECTRE generates power through renewable energy sources, energy providers could possibly subsidise the operation of SPECTRE, and could therefore be reliable customers.

Institutes
Institutes, especially ones that conduct large amounts of research, require substantial amounts of power to function. Furthermore, research institutes are also usually eager to become involved in new and innovative projects. Given that a system like this is one of a kind, it is inevitable that research institutes would support its operation by becoming consumers or sponsors.

Governments
A variety of large governments, and government agencies, also require large amounts of power for research projects, and general operations. Furthermore, unlike companies (such as energy providers) or institutes, governments are usually more reliable, as their chance of bankruptcy is very low due to strict regulations imposed by central banks as well as large revenue streams. Governments could be interested in the system due to its flexibility, allowing for them to become a lot more flexible in terms of its operations.

Organisations and Companies
Finally, large scale organisations and companies could also become consumers of the power generated by SPECTRE. Organisations and Companies could essentially do this to improve their carbon footprint.

6.2.5. Marketing Strategy & Consumer Locations

In order to maximise the return from the system, some possible locations to which the power should be transmitted must be chosen. These locations must be reliable, implying that the debt is low, has a high GDP, and low chance of internal conflicts. They must also be interested in the system, which means that the location must be in need of alternative energy sources due to geopolitical or environmental issues.

Regarding commercial consumers such as energy providers, companies and organisations, one possible option is New Zealand. Due to the country's remote location, the delivery of natural gas and other fossil fuels is costly. Furthermore, the country is highly developed, has a positive trade balance, and has had no detrimental internal conflicts since its unified formation. Additionally, two of the tiger economies, Singapore and Hong Kong, with a rapidly growing economy and power consumption, could also be considered. Although both of these coastal locations have a high availability of energy sources, Singapore has especially been working towards becoming sustainable, and may therefore be interested in this system.

Alternatively, a possible use for the system could be humanitarian disaster relief. Recent catastrophic natural disasters such as the 2004 Indian Ocean tsunami and 2010 Haiti earthquake - which resulted in large-scale and long-term damage to the electric power infrastructure, greatly hindering humanitarian aid - have put portable power solutions high on the agenda. If the system could cater to such electrical power needs, or be adapted to do so, one can imagine a scenario in which e.g. the United Nations invests some of its resources into its development.

Furthermore, the SSPS can and should be marketed as a renewable and clean form of energy. It is unavoidable that the world's demand for sustainable energy will only increase further over the foreseeable future and with international agreements agreeing on greenhouse gas reduction, countries will be looking for viable solutions to scale-up their renewable energy harvesting. The system should be proposed as a good candidate for investments and subsidies. For an elaboration on the impact of the system's implementation and operation on global sustainability, please refer to section 8. Therefore, with the virtue of producing renewable and clean energy, it is feasible to acquire various financial and institutional sponsorships and partnerships with other various companies, organisations and institutions. Such sponsorships would allow for an increased budget and accelerated development of systems.

6.2.6. Revenue Estimation

Research had to be done in order to estimate the expected revenue, which includes finding the average cost of using solar power on Earth. This will also show that the system can provide electrical energy into the grid at a competitive rate (**O-ST-S-ECON-000**). For this value, an estimate from a UK Government study was taken, which indicated that in 2030, the average price of large-scale solar power will be 52-73 GBP per MWh (Mega-Watt-hour) [49]. Although this range of values is estimated for UK households, it will be used to estimate the revenue as this was the most reliable source for the required information. Dividing this value by 3600 will give the cost per MJ, which results in 0.01444-0.02028 GBP per MJ or rather, 14.44-20.28 GBP per GJ. Since the total budget is given in Euros, the result will be converted to EUR with the current exchange rate, which results in 16.61-23.32 EUR per GJ.

If it is assumed that the system will collect energy for at least 99% of the time, that all generated power is being consumed by paying customers and that the transmission to Earth efficiency is 15%, the following relation can be used to estimate the maximum and minimum revenue. Furthermore, note that the generated power is variable, and degrades over time. This was also integrated into the revenue estimates.

$$R_{max} = C_{GJmax} \cdot \eta_{transmission} \cdot U_{operational} \cdot t_{year} \tag{6.1}$$

$$R_{min} = C_{GJmin} \cdot \eta_{transmission} \cdot U_{operational} \cdot t_{year} \tag{6.2}$$

Where R_{max} and R_{min} are the maximum and minimum yearly revenues respectively, C_{GJmin} and C_{GJmax} are the maximum and minimum price of solar power per GJ in 2030, $\eta_{transmission}$ is the transmission efficiency, $U_{operational}$ is the percentage of time that the solar collector system is operational, and t_{year} is the amount of seconds in a year, in order to find the yearly revenue. These equations result in an estimated yearly revenue of 101.1-142.0 million EUR.

This value is only regarded true for the first year. The UK Government is also estimating an average depreciation of the (monetary) value of solar power by 1% a year [49]. On top of this, it can be assumed that there will be a yearly inflation rate of 1%, depreciating the value of the return. This value was derived from historical data from the chosen locations, with consideration put into the fact that the inflation in those locations has been converging to a value of approximately 1% over the last 10 years [53]. This indicates that at the designed EOL of the system, which is the year 2060, the yearly revenues will drop to 47.3-66.4 million EUR.

Therefore, ceteris paribus, over the 30 year operational time of the system, the revenues will total to approximately 2,128-2,988 million EUR. Now the total costs of designing and producing the solar power collector, the transmitters, ground control, ground power station, and operation of all systems must be considered. First of all, a budget for the transmitter has to be assumed. The direct material costs of the transmitter system will be allocated a budget of €100 million. Based on this value and the ratio between direct material costs and total costs of the collection system described in section 6.1, the total costs of launching, producing, and developing the transmitter will be limited to €458 million.

It is critical to understand the costs involved in acquiring ground facilities, which include a mission control centre and a Power Receiving Ground Station (GSP) in case of the SPECTRE system. A terrestrial solar power plant is estimated to cost €1 per Watt. Therefore one could assume the GSP to which the power is being transmitted would cost €150 million [95]. However, the GSP costs should not be solely based off of terrestrial solar power plants, because the GSP will receive a narrow beam of light at only one specific frequency from the laser transmitter. For this reason, the cost for the GSP is estimated to be €75 million. The upkeep of power stations is estimated to be at €8,000 per MW per year [78]. Considering this information, this cost would be €1.2 million per year, or 36 million in total.

The cost of the ground control centre can be estimated to be 2.6% of the total mission cost [83]. However, this percentage mainly applies to GEO satellites, which have mission costs of up to €200 million. Therefore it is assumed the ground control centre will cost approximately €5.2 million. The upkeep of the satellite and ground control centre is estimated at 8% of the total mission cost. This cost amounts to €166 million [98].

Combining all of these costs together and the cost of the power collection system (€1,340 million) amounts to a total cost of €2,080 million. This indicates a maximum and minimum profit margin of €48-€908 million. Respectively, these correspond to break-even points of 28 and 18 years respectively. This shows compliance with **D-ST-S-ECON-002** as the break-even point will be within 30 years.

However, it is important to note that the value of this system should not only be considered in terms of its monetary value. This system is also the first step to establishing an infrastructure in space for in-orbit production and space-based solar power collection. On top of this, it is also laying down a framework for reliable and sustainable energy, which can redefine the generation of power for the future. Therefore, while its monetary value is described by the returns discussed above, its value to society, the environment, and space exploration is unprecedented.

7

Technical Risk Assessment

In this chapter, the risks related to the design, production and operation of the system will be discussed. For this, the risks will first be identified and discussed, with every risk given a certain rating based on the severity of its occurrence, and probability of occurrence on a risk map. The risks with an unsatisfactory severity or probability will be discussed in further detail and risk mitigation and contingency plans will be discussed for those risks. Finally, the risk mitigation and contingency plans will also be split into passive and active risk mitigation and contingency plans.

7.1. Risk Identification

The identification of the risks of the SPECTRE system starts by re-evaluating the risks identified in the midterm report [20]. These can now be updated or removed where necessary to reflect the latest design iteration of the system. Another method of identifying risks of the system is by looking at each subsystem individually and assessing the risks of these subsystems. This was initiated by setting up a fault tree for the system with respect to each subsystem. The fault tree is presented in the appendix in Figure A.3. The tree was set up for catastrophic and critical system failures. A subsystem failure was classified as either catastrophic or critical, where catastrophic failures indicated a complete mission failure, for example a failure related to power collection and transmission, since this would render the spacecraft useless. A critical failure indicates a failure that can still be repaired or remedied, so this could be a failure or partial failure of any of the supporting subsystems. These failures were translated into risks that can cause these failures.

Combining the risks identified in the midterm report [20] and additional risks identified from the fault tree, a complete set of risks is found, which is shown in Table 7.2. The risks obtained from the midterm report are identified with TRI-X-YY-ZZ, where X indicates on Earth (E) or in Orbit (O) risks, and YY and ZZ are a numerical indicator of the risks. The risks from the fault tree are classified per subsystem as follows: TRI-XXXX-YY, where XXXX indicates the subsystem with its abbreviation, and YY are the numerical indicator of the risks. All the risks are also assigned a severity of occurrence and likelihood of occurrence, combining the levels for these parameters results in the overall risk. The likelihood of occurrence was essentially based off of the TRL level, while the impact of occurrence was based off of the criticality of the failing or malfunctioning component on the system. These parameters are explained with further detail in Table 7.1. With these assigned parameters the risks can also be mapped on a risk map, which is provided in Figure 7.1. On this map the risks are indicated with a shortened identifier.

Table 7.1: Quantification of technical risks

Likelihood of Occurrence	
Likelihood	**Technical Readiness**
High Likelihood	Feasible in theory
	Working laboratory model
	Based on existing non-flight hardware
	Extrapolated from existing flight design
Low Likelihood	Proven flight design

Severity of Occurrence
Catastrophic
Critical
Marginal
Negligible

7.2. Risk Mitigation

The risks identified in the previous section can be assessed on their severity and if necessary mitigating actions should be planned to lower the risks. An assessment of which risks should be mitigated was performed by evaluating the risk map. Any of the risks that were qualified as a high risk, thus located in the red area, or medium to high risk, in the borderline orange area, were chosen to be mitigated. In the remainder of this section the mitigation plan will be presented, which is split up into an active mitigation plan for specific risks and a passive mitigation plan that is more general.

Table 7.2: Technical risks

Identifier	Risk	Identifier	Risk
TRI-E-01-01	Pre-launch launch vehicle failure	TRI-POCO-01	Primary mirror misalignment
TRI-E-01-02	In-flight launch vehicle failure	TRI-POCO-02	Primary mirror film deformation
TRI-E-01-03	In-coast launch vehicle failure	TRI-POCO-03	Primary mirror film detachment
TRI-E-01-04	Payload failure before launch	TRI-POCO-04	Primary mirror film rupture
TRI-E-01-05	Payload failure during ascent	TRI-POCO-05	Secondary mirror misalignment
TRI-E-01-06	Payload failure after separation	TRI-POCO-06	Secondary mirror film deformation
TRI-E-01-07	Payload integration failure before launch	TRI-POCO-07	Secondary mirror film detachment
TRI-E-01-08	Payload integration failure during ascent	TRI-POCO-08	Secondary mirror film rupture
TRI-E-01-09	Payload integration failure during separation	TRI-POCO-09	Filter misalignment
TRI-E-02-01	Launch delays due to launch vehicle production delay	TRI-POCO-10	Filter deformation
TRI-E-02-02	Launch delays due to launch vehicle qualification delay	TRI-POCO-11	Excessive filter surface degradation
TRI-E-02-03	Launch delays due to payload integration delay	TRI-POCO-12	Broken filter
TRI-E-02-04	Launch delays due to payload integration qualification delay	TRI-POCO-13	Solar cells short circuiting
TRI-E-02-05	Launch delays due to on the pad launch vehicle test delays	TRI-POCO-14	Excessive solar cell degradation
TRI-E-02-06	Launch delays due to on the pad launch vehicle test failures	TRI-POCO-15	Solar cells misalignment
TRI-E-02-07	Launch delays due to weather violations	TRI-POTR-01	Transmitter failure
TRI-E-02-08	Launch delays due to launch vehicle no-go of (sub)systems	TRI-POTR-02	Transmitter misalignment
TRI-E-02-09	Launch delays due to payload no-go of (sub)systems	TRI-EPSY-01	Converter failures
TRI-E-03-01	Production delay due to raw material delivery delay	TRI-EPSY-02	Bus failures
TRI-E-03-02	Production delay due to on-Earth manufacturing delay	TRI-EPSY-03	Storage failure
TRI-E-03-03	Production delay due to on-Earth transportation delay	TRI-STRU-01	Ultimate load failure
TRI-E-03-04	Production delay due to on-Earth assembly delay	TRI-STRU-02	Fatigue failure
TRI-E-04-01	Transportation accident due to traffic accident	TRI-STRU-03	Deformation due to insufficient strength
TRI-E-04-02	Transportation accident due to shipping accident	TRI-STRU-04	Deformation due to excessive degradation/fatigue
TRI-E-04-03	Transportation accident due to failed attachment	TRI-THER-01	System overheating due to failed passive cooling
TRI-E-05-01	Production of insufficient quality due to underqualified workforce	TRI-THER-02	System overheating due to unexpected thermal loads
TRI-E-05-02	Production of insufficient quality due to poor quality assurance	TRI-THER-03	System undercooling due to failed thermal storage
TRI-E-07-01	Production workforce strike	TRI-THER-04	System undercooling due to unexpected thermal loads
TRI-E-07-02	Engineering workforce strike	TRI-MAIN-01	Mirror web crawling robot failure
TRI-E-07-03	Operations workforce strike	TRI-MAIN-02	Unavailable resources for mirror repair
TRI-E-08-01	Insufficient total funding	TRI-MAIN-03	Failed mirror repair
TRI-E-08-02	Pull out of funders	TRI-MAIN-04	Repair robot failure
TRI-E-08-03	Wrong funding estimation	TRI-MAIN-05	Unavailable replacements
TRI-O-01-01	Failed orbit insertion due to under-performing launch vehicle	TRI-MAIN-06	Failed replacement
TRI-O-01-02	Failed orbit insertion due to under-performing payload	TRI-PROP-01	Tank burst
TRI-O-03-01	Deployment mechanisms failure	TRI-PROP-02	Tank leak
TRI-O-03-02	Deployment sequencing failure	TRI-PROP-03	Piping disconnection
TRI-O-03-03	Structural failure due to deployment	TRI-PROP-04	Thruster disconnection
TRI-O-04-01	In-Orbit manufacturing delay	TRI-PROP-05	Thruster electrodes failure
TRI-O-04-02	In-Orbit transportation delay	TRI-PROP-06	Thruster feed system failure
TRI-O-04-03	In-Orbit assembly delay	TRI-PROP-07	Thruster neutraliser failure
TRI-O-05-01	In-Orbit manufacturing failure	TRI-PROP-08	Manoeuvre provides insufficient thrust
TRI-O-05-02	In-Orbit assembly failure	TRI-PROP-09	Manoeuvre misfire
TRI-O-06-01	Collision with active spacecraft	TRI-TTC-01	Communications antenna misalignment
TRI-O-06-02	Collision with man made space debris	TRI-TTC-02	Communications antenna pointing actuators failure
TRI-O-06-03	Collision with natural occurring space debris	TRI-TTC-03	Receiver experiences too high on board losses
TRI-O-07-01	Solar flare interference	TRI-TTC-04	Receiver experiences deconstructive interference
TRI-O-07-02	Coronal mass ejection interference	TRI-TTC-05	Receiver has insufficient pointing accuracy
TRI-O-08-01	Delays of scheduled maintenance tasks	TRI-TTC-06	Receiver experiences demodulation losses
TRI-O-08-02	Delays of necessary replacement/repair launches	TRI-TTC-07	Transmitter experiences excessive on board losses
TRI-O-09-01	Inaccurate sun pointing accuracy due to insufficient ADCS precision	TRI-TTC-08	Transmitter experiences deconstructive interference
TRI-O-09-02	Inaccurate sun pointing accuracy due to inaccurate ADCS	TRI-TTC-09	Transmitter has insufficient pointing accuracy
TRI-O-09-03	Inaccurate sun pointing accuracy due to inaccurate optics and collectors	TRI-TTC-10	Transmitter experiences demodulation losses
TRI-O-10-01	Inaccurate transmission pointing accuracy due to insufficient ADCS precision	TRI-TTC-11	Failed encoding
TRI-O-10-02	Inaccurate transmission pointing accuracy due to inaccurate ADCS	TRI-TTC-12	Failed decoding
TRI-O-10-03	Inaccurate transmission pointing accuracy due to insufficient precision of transmitter	TRI-ADCS-01	CMG's failure
TRI-O-13-01	Combustion of flammable materials	TRI-ADCS-02	Sun sensor failure
TRI-O-14-01	Uncorrectable orbital deviation due to collision	TRI-ADCS-03	Earth sensor failure
TRI-O-14-02	Uncorrectable orbital deviation due to unexpected solar wind	TRI-ADCS-04	Star sensor failure
TRI-O-14-03	Uncorrectable orbital deviation due to orbital perturbations		
TRI-O-15-01	Failure to collect required power		
TRI-O-15-02	Failure to meet mission lifetime		

7.2.1. Active Risk Mitigation

The active mitigation plan is only applied to the specific risks that were selected to be mitigated. The mitigations that were designed for these risks are listed below.

- Select launchers or redesign the launcher with the launch provider with a lower weather dependency. (TRI-E-02-07)
- Introduce safety factors in the structural design. (TRI-O-03-03)
- Schedule room for delay in the production plan. (TRI-O-04-03)
- Plan redundancy into the materials and machines used in the manufacturing. (TRI-O-05-01)
- Track space debris, or acquire tracking data, and plan avoidance manoeuvres. (TRI-O-06-03)
- Design components with protection against the specific risk. (TRI-O-07-01, TRI-O-07-02)
- Design the repair and maintenance plan without direct dependencies on supply launches. (TRI-O-08-02)

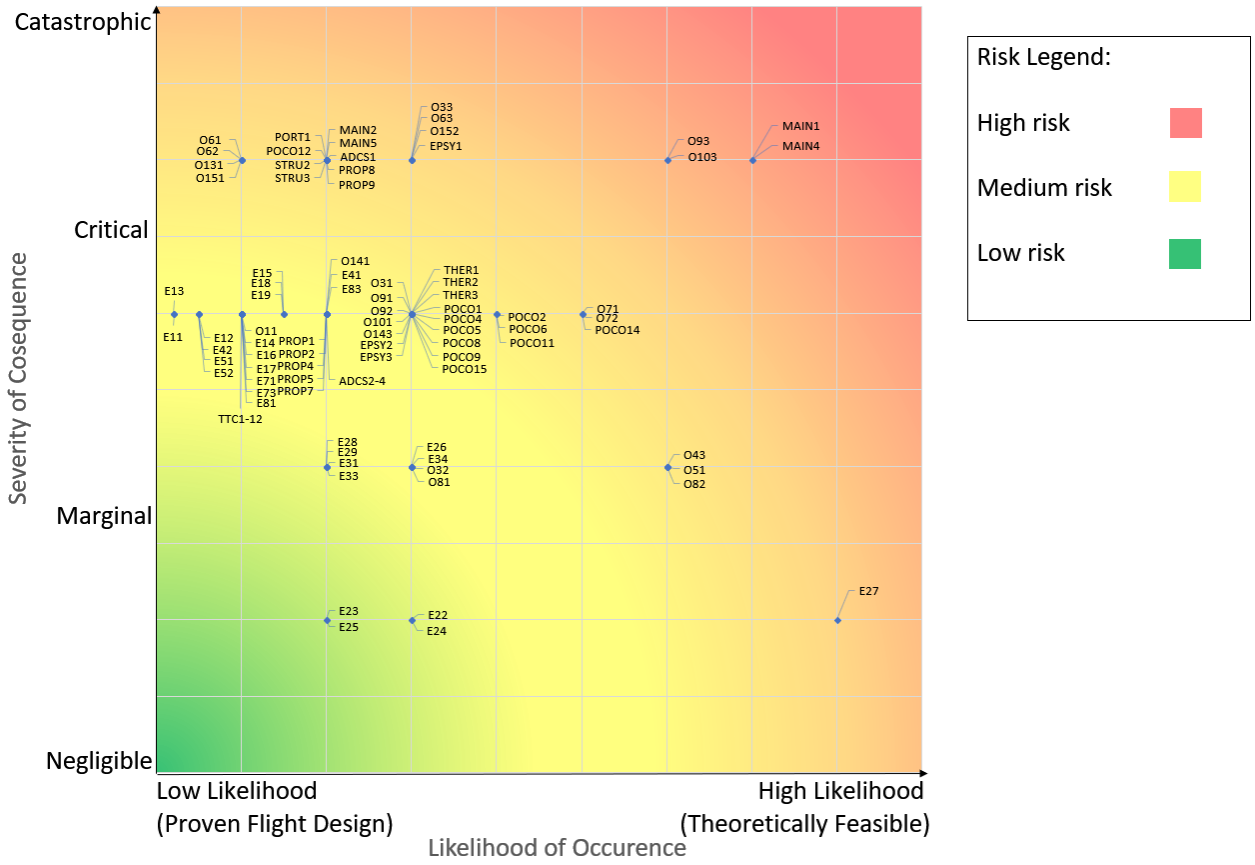

Figure 7.1: Risk map

- Design the subsystem and components with extra accuracy. (TRI-O-09-03, TRI-O-10-03)
- Design the system and maintenance with redundancy in order to meet the lifetime. (TRI-O-15-02)
- Design the solar cells with low degradation. (TRI-POCO-14)
- Design the converters with redundancy. (TRI-EPSY-01)
- Operate redundant web crawling robots. (TRI-MAIN-01)
- Operate redundant maintenance and production modules. (TRI-MAIN-04)

7.2.2. Passive Risk Mitigation

In order to manage risks, some passive techniques have also been applied to the system. Passive techniques are especially useful when mitigating risks since these automatically reduce risks, without the intervention of personnel or other systems. These passive risk mitigation techniques will be mainly related to design choices made now, rather than to the choice of operations being performed in the future.

System Separation

The first form of passive risk mitigation can be described as a separation of systems. Note that this is different to redundancy, as the outcome of this mitigation will still reduce the function of the system. System separation can easily be applied to the design at three points of uncertainty, namely the launches, the solar arrays, and the system itself.

Essentially, the launching of the system would either way require multiple launches, but multiple launches also decrease the risk of launching the system into space. The less launches being used, the larger the portion of the spacecraft there is that may be lost due to a failed launch. However, this will increase the overall probability of a failed launch, but it allows for the overall risk to converge to a more certain value, which will allow for more definitive contingency plans.

Furthermore, through the virtue of spectral splitting, the entire spectrum can be used. This not only increases efficiency, but it also decreases the amount of incoming radiation on each solar cell, and therefore also decreases their degradation. This essentially decreases the risk of excessive degradation.

Also, the system itself is split into 20 separate satellites. This reduces the overall impact of a certain risk, but increases

the occurrence of the risk. Now that 20 satellite are used for the system, if one of them fails, the power generated is only cut by 5%. However, if only one satellite was used and it failed, the power generation would be cut by 100%.

Contractual Risk Transfer
The other form of passive risk mitigation is by outsourcing certain tasks to other companies, and having a signed contract on what the result of their task should be. Therefore, you are not just outsourcing the tasks, but also the risks related to those tasks.

First of all, this can be applied to the launching of the system. The system will be launched by a launcher provided by another company. Therefore, the risk of the launch failing and the launcher and system becoming inoperable is transferred to the launcher provider. This will transfer financial and material setbacks to the launch provider, however will still impact SPECTRE with regards to project scheduling. Similarly, this technique will be applied to the production of certain components.

Furthermore, since the team is only designing the collection system, the transmission system and power receiving ground station will be designed by other teams. Therefore, the risks related to the design, production, and operation of those systems is outsourced, and avoided in this system.

Now that the risk mitigation plan is fully defined the effect of the mitigation can be evaluated by remapping the risks on the risk map. This new risk map is presented in Figure 7.2. On this risk map the risks that were mitigated are shown, the blue indicators depict the risk with the original values, whereas the orange indicators depict the risk with the mitigated values.

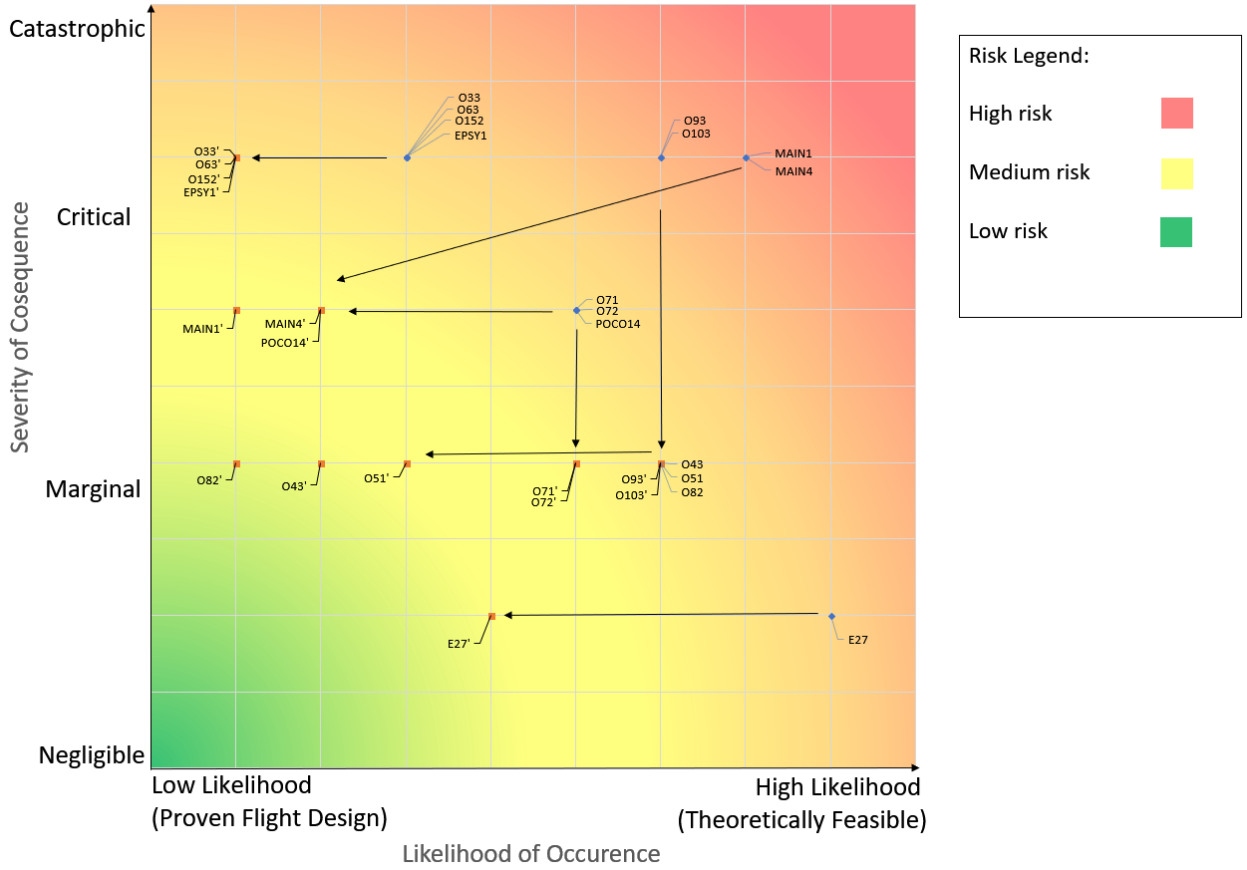

Figure 7.2: Risk map of mitigated risks

7.3. Contingency Plans

In case one of the aforementioned risks occurs, it is vital that there is a contingency plan to minimise the impact of the risk in the long-run, and if possible, short-run. In this section, all of the risks will be grouped based on the required contingency, and these contingencies will be discussed. In this section, there will be discussions of safe modes, which will be described in chapter 12.

Launcher Failure Contingencies - E0101 to E0103, E0107 to E0109, E0201, E0206, E0208, O0101: In case any of these risks occur, the launcher provider must be contacted immediately, and the damage to the payload should be analysed. Afterwards, the need to reproduce the payload should be investigated, as well as the issue with the launcher. If it is required to reproduce the payload, it should be reproduced. Then, it should be explored if a new launcher will be required. If a new launcher will be required, a new launcher provider should be sought after, otherwise the launch should be rescheduled.

Transport Failure Contingencies - E0401 to E0403: For these risks, the transporter must be contacted immediately. Afterwards, the damage to the components and the need to reproduce should be explored. If reproduction is required, the components must be reproduced. Afterwards, the transporter choice should be re-evaluated, and potentially swapped. If swapped, a new transport company should be found, otherwise the transport should be rescheduled.

Payload Failure Contingencies - E0104 to E0106, O0102, O1301: Firstly, the point of failure in the payload should be analysed, and any other unforeseen issues with the payload assembly or production. Afterwards, the payload should be restructured and re-certified by the launcher provider, and the operations should be continued.

Schedule Delay Contingencies - E0202, E0104 to E0105 , E0207, E0301 to E0304, O0401 to O0403, O0801 and O0802: The impact of the delay should be identified, and the future operations should be rescheduled. Depending on this rescheduling, the need for extra personnel or facilities should be explored. If these are required, these should be hired and the operations should continue. If these are not required, the operations should continue anyways.

Harsh Environment and Collisions - O0601 to O0603, O0701 and O0702, O1401 to O1403: In case of a harsh environmental or collision risk, the system should be put into safe mode. In safe mode, all of the systems must be tested to identify the impact of the damage. Depending on the state of the system, it should continue operation, be repaired, or disposed of.

Production and Integration Delays - E0203, E0209, E0501, E0502: In case any of these risks occur, the severity of the delay will have to be identified. Depending on the severity, the production and integration logistics may have to be redeveloped. Furthermore, a larger workforce or more facilities may also be considered to contain this delay. Otherwise, operations will continue.

Improper Design of Systems - O0901 to O0903, O1001 to O1003, THER02, THER04, PROP08, TTC01 to TTC12: Firstly, the system will have to go into a safe mode, and the entire system will have to be analysed to determine the source of the failure. For these risks, the only way to contain their failures is to redesign the systems. This will require the rescheduling of all tasks related to the failed system.

Improper Design or On-Earth Production of Systems - ADCS01 to ADCS04, POCO09 to POCO15, POTR01, POTR02, EPSY01 to EPSY03, THER01, THER03, PROP01 to PROP07, PROP09: Firstly, just like in the previous contingency for an improper design of systems, the system will have to go into a safe mode and the failure will have to be analysed. Afterwards, the on-Earth production methods and reliability will be inspected. If these are deemed to be sufficient, the design will be reviewed and redesigned. In case the deficiency originated from improper production, the production facilities and workforce will be reviewed. In case the deficiency originated from improper design, the system will have to be redesigned.

Improper Design or In-Orbit Production of Systems - POCO01 to POCO08, STRU01 to STRU04: For this risk, the system will also have to go into a safe mode, and the source of the failure will have to be discovered and analysed. Similarly to the previous contingency, the in-orbit production methods and reliability will be inspected. If these are deemed to be sufficient, the design will be reviewed and redesigned. In case the deficiency originated from improper production, the production machines will be reviewed. In case the deficiency originated from improper design, the system will have to be redesigned.

Unsatisfied Investors or Workforce - E0701 to E0703, E0801 to E0803: When these risks occur, the team will have to increase its public relations efforts to contain the lack of funding or workforce. After the containment, more efforts will have to be put into regaining the funding or workforce from other sources.

In-Orbit Production Failure - O0301 to O0303, O0501, O0502: When this failure occurs, the impact of the failure will have to be analysed. Depending on its severity, new in-orbit production methods may have to be designed or considered. If the failure is deemed to be a one-time occurrence, operations may simply continue.

Maintenance Failures - MAIN01, MAIN03, MAIN04, MAIN06: In order to contain maintenance failures, the system will have to go into a safe mode, and the error will have to be found and analysed. Afterwards, depending on the outcome, the maintenance system will have to be redesigned, and everything related to maintenance will have to be rescheduled.

Maintenance Resupply Failure - MAIN02, MAIN05: If these risks occur, the systems that require maintenance, but have no supply for it, will have to enter safe mode. The logistics of maintaining the systems will have to be re-evaluated and applied as soon as possible.

Stakeholder Requirement Failures - O1501, O1502: In case of these risks, the stakeholders will have to be notified as soon as possible. The team will then have to meet with the stakeholders, and discuss what the next steps should be.

With the risks of the system clearly defined and a thorough mitigation and contingency plans set up, the design phase can be started. The critical risks should be kept in consideration during the design as well as the mitigation plans that were set up. These can be presented in the design in order to lower the risks.

8

Sustainable Development Strategy

Sustainability is one of the key components of the design of the system. The sustainability of the project will be crucial for the success of the project, as discussed and demanded in the requirements. It is important that the system is economically, environmentally and socially sustainable. Therefore, a sustainable development strategy was implemented during the design in order to ensure a sustainable and efficient design.

In short, the major guidelines for the sustainability strategy are to reduce mass and to use the most optimal materials with low energy consumption, toxicity, and CO_2 emissions. It was found during the design phase that the materials could often be optimised much more than initially anticipated. Hence the use per kWh and per tonne CO_2 for the system is very high. This section is a continuation from the previously written sustainable development strategy in the midterm report [20].

8.1. Launcher Selection

From a sustainability perspective, the largest risks are the cost, toxicity and amount of fuel burned. The launchers most applicable for this project with launch capabilities of over 10 tonnes were collected. These can be seen in [128]. The most relevant ones are summarised in Table 8.1. [104][115][116][117][118][119][120][121][130][129][149]

Table 8.1: Launcher sustainability data

	Payload to LEO [kg]	Cost total [mil EUR]	Cost per kg [EUR/kg]	Reusability	Toxic Elements	Availability	Reliability	Burn time thrust adjusted [s]	Derived Prop mass per payload [kg/kg]
BFR	150000	7	46.67	Fully	CH4	Not Developed	-	-	19
Falcon Heavy	63800	76.5	1199.06	First Stage	RP-1	Developed	1	162	21
Falcon 9	22800	52.7	2311.40	First Stage	RP-1	Developed	0.97	162	21
Ariane 5 ES(V)	19300	178	9222.80	None	none	Developed	0.89	179	37
Angara A5/KVRB	24500	105	4285.71	None	potentially RP-1-UDMH -N2O4	Developed	0.67	236	6

In order to justify the values in the table above, a short explanation will be given. The derived propellant mass was found as follows:

$$F_T = \dot{m} v_e = \frac{m_{prop} I_{sp} g_0}{t_b} \rightarrow m_{prop} = \frac{F_T t_b}{I_{sp} g_0} \tag{8.1}$$

Weighting the I_{sp} and burn time in accordance with the thrust from the different rocket engines, the fuel mass can be approximated. The fuel per kilogram is an indicator for the environmental sustainability and the economic cost.

The majority of the costs include launch costs, as discussed in the baseline report [19]. Hence the cost per kg of payload is very crucial for economic sustainability. Requirement **M-ST-S-ECON-000** is a mandatory requirement most at risk of violation. The developed option most applicable is the Falcon Heavy launch vehicle, which costs 1199.06 EUR/kg. However the BFR promises a much lower price of 46.67 Euro/kg.

The best specific values most applicable to environmental sustainability (for reusability) are not necessarily dominated by SpaceX. Ariane 5 has the cleanest fuel but also is very costly, and the least amount of fuel per kg of payload is burned by the Angara 5, which is however very toxic. However, due to the economic, social and environmental constrains being in violation of several requirements purely due to the launch costs and pollution, the launch services provided by SpaceX's Falcon Heavy or BFR have to be chosen. This option is also fairly sustainable, since RP-1 and CH_4 are less toxic than some of the other hypergolic and exotic equivalents posed by its competitors. It is also noted that the reusablity allows them to be one of the few providers with a large enough launch capacity due to the short

turnaround time as well as added sustainability due to recycling. Hence the sustainability strategy should push for the utilisation of one of these launch systems.

The choice thus falls on the BFR, mainly due to its economic sustainability. Hence the launch costs amount to about 46.67 Euro/kg payload. When comparing the price of, for example, copper per kilogram costs, it amounts to roughly 5-6 euros per kg. Hence it is still the majority cost of the system with the potential exception of expensive optics and robotics discussed later.

The sustainability risks are hence based of the payload mass, which influences the amount of fuel burned. The policy implemented during design was to reduce the mass of the system as much as possible.

8.2. Material

As previously discussed, the majority of the per kilogram costs are the launch costs and the eventual production costs, with the raw material costs being an order of magnitude smaller. Hence the sustainability of the material will purely be based on the environmental sustainability indicators explained above. The material used should have the lowest energy consumption and CO_2 emissions as well as toxicity.

To estimate the CO_2 and the energy required for different materials, a method of energy balancing was used. It was assumed that the materials were produced in Europe. Hence the energy balance from the European Union statistics obtained from Eurostat can be used [61]. From this the total energy consumed by such industries as the steel and metals industry as well as transportation industries can be found. The data was further processed and reduced on a Google sheets document [128]. The results are summarised in Table 8.2.

The different energy sources were allocated general CO_2 output coefficients in order to find the relevant CO_2 production [101][125]. This gives an indication of the CO_2 production of all industrial activities based on the energy consumption related to the production of said materials. The production of electricity and heat produces pollution, conversion consumption and waste, which is taken into account in the electricity consumption by the relevant industries. This hence is a true all-encompassing method.

The steel production is assumed to be represented fairly accurately by the iron and steel industries. In this case plastic is included in the chemical and petrochemical industry, but weighted in accordance with the total plastic production [31][110]. This was done in order to include the most general chemical and petrochemical applications for the final design. Non-ferrous metals are described by the EU to contain mostly aluminium, copper, zinc, lead and a few other more minor metals [27][68][77][79][114]. Hence these where subdivided using their respective energy consumption per tonne from the non-ferrous metal category.

The total energy consumption per tonne of composites was found through research and used to weigh the total tonnage of European glass reinforced plastics industry [102]. The CO_2 output was deemed to be similar to that of plastics per kWh. Finally, non-ferrous minerals were much harder to divide on a European level. Hence it was assumed that the share of production is proportional to the employment numbers in the respective industries [45][60][63].

Table 8.2: Sustainability of materials at the time of the writing of this report, assuming a life of the SSPS to be 30 years

Material:	kWh/tonne	CO_2tonne/tonne	CO_2tonne/tonne/year	kWh/m³	CO_2tonne/m³
Steel	2713	4629	154	21784	37173
Non-ferrous metals	29199	59665	1989	133736	273272
Aluminium	4632	9465	316	12243	25017
Copper	4632	9465	316	41254	84297
Composites (CFRP based)	15278	32660	1089	35139	75118
Plastics	2706	5785	193	6224	13306
Non-ferrous minerals	1386	3490	116	3866	9733
Cement and lime	1386	3490	116	3881	9771
Ceramics	1386	3490	116	2953	7433
Quartz assumed same as glass	1386	3490	116	3881	9771

Considering other sources for the so-called "embodied energy" of different materials, very different values can be found. Different production methods of the same material can influence the energy and hence CO_2 output significantly. This is easily seen when comparing the findings in Table 8.2 and those found in other approximations. It is however hereby chosen to account for all industrial processes using this method. Due to the shear number and variation of different concepts discussed during this midterm report, no estimations of different production methods of components have been performed.

The limitations of this method are the assumptions made and reliance on accurate and specific data applying to the EU as a whole. This gets complex to obtain when going into deeper levels. Predicting the pollution from material sourced outside the EU is also limited. Even more difficulty is met when considering other risks such as worker safety. The benefit however is a completely unbiased and all-accounting measure of the energy consumption of different

Table 8.3: Emission and energy sustainability coefficients. Density and structural sustainability coefficients also shown.

Material:	kWh/tonne coeff	CO2tonne/tonne Coeff	kWh/m³ Coef	CO2tonne/m³ Coef	Density [kg/m³]	Density Coef	Youngs Modulus [GPa]	Youngs Modulus Coef
Steel	2.39	2.93	1.22	1.47	8030	0.60	200	1.71
Non-ferrous metals	0.22	0.23	0.20	0.20	4580	1.05	93	0.79
Aluminium	1.40	1.43	2.16	2.18	2643	1.82	82	0.70
Copper	1.40	1.43	0.64	0.65	8906	0.54	148	1.27
Composites (CFRP based)	0.42	0.42	0.75	0.73	2220	2.17	150	1.29
Plastics	2.39	2.34	4.26	4.09	2300	2.09	2	0.02
Non-ferrous minerals	4.67	3.89	6.85	5.60	2789	1.72	45	0.39
Cement and lime	4.67	3.89	6.83	5.58	2800	1.72	38	0.33
Ceramics	4.67	3.89	8.97	7.33	2130	2.26	460	3.94
Quartz assumed same as glass	4.67	3.89	6.83	5.58	2800	1.72	72	0.62

material choices, in accordance with all industrial and economic activity as well as a easily comparable values and streamlined specifically for design.

The sustainability strategy for material choice should be to consider all facets of the production and processing of materials when it comes to energy usage and CO_2 pollution using Table 8.2, other sources and toxicity, using mass as a general ballpark estimation initially. It is hence essential to minimise the total mass of the chosen material during the designing and during the trade-off. When applying certain types of materials, processes and weighting criteria, then the Table 8.2 should be expanded to include this. The one which minimally impacts sustainability should be chosen. Risks such as toxicity of different processes and materials are harder to quantify with a similar method. These have to be directly compared, qualitatively assessed and/or processed and plans to mitigate the toxicity or any other sustainability risk should be implemented.

Hence the policy implemented in the design phase was based in large part on mass reduction. However, the performance of the material also has to be taken into account as a method of analysing the sustainability. This would be especially true for system material choices such as wire material for the electronic power system and reflectors for the power collection subsystems. This will be discussed later.

8.3. Sustainability Integration into the Design

This section shall discuss the application of different production methods, material and design choices for different subsystems and aspects of the system from a sustainability perspective. In some cases this can be done using the sustainability coefficient. The coefficient is calculated as follows, respectively for a good or bad effect:

$$\text{Coef good} = \frac{\text{Average}}{\text{Material}} \quad \text{Coef bad} = \frac{\text{Material}}{\text{Average}} \tag{8.2}$$

For general coefficients, Table 8.3 can be seen [28][139][147].

Additional coefficients will be used for economic or production feasibility. This would then cover the economic and social sustainability and shows that the system does not violate the International Bill of Human Rights (**D-ST-S-ECON-002**).

Structure
For structural reasons, it is important for the structure to be both light and stiff. It is also important for it to be produced in space with as little scrap as possible, which reduces launch and Earth production hazards, pollution and costs. Hence the coefficients for kWh/m^3, CO_2tonne/m^3 and density were used for the material pollution and launch pollution. For the structural component the Young's modulus was used, see Table 8.3. For the production extra coefficients were introduced after some discussion. The energy required for any material which requires melting was given an appropriately low score, in order to minimise energy consumption and wear on the production machinery. The methods which required subtracted manufacturing where given low scrap scores. Finally, the viability eliminated all materials which can not be produced effectively in space. This resulted in composites being the most sustainable material. See Table 8.4 for the overview.

Table 8.4: Sustainability of different structural materials

Material:	Coefficient	Production Energy Coef	Production Scrap Coef	Production Viability	Final Score
Steel	2	0.2	0.1	1	0.04
Non-ferrous metals	0	0.3	0.1	1	0.00
Aluminium	6	0.4	0.2	1	0.48
Copper	0	0.2	0.1	0.5	0.00
Composites (CFRP based)	2	1	1	1	1.52
Plastics	1	1	1	1	0.62
Non-ferrous minerals	26	1	1	0	0.00
Cement and lime	21	1	0.9	0	0.00
Ceramics	585	0	0.2	0	0.00
Quartz (assumed same as glass)	40	0	0.9	0	0.00

Table 8.5: Sustainability of different mirror material

Material:	Coefficient	Reflective Performance	Final Score
Steel	1.78	0.4	0.71
Aluminium	4.71	1	4.71
Copper	0.42	0.2	0.08

Table 8.6: Sustainability of conductor materials

Material:	Resistivity [Ohm·m]	Loss Adjusted Coef
Steel	0.00000016	0.06
Aluminium	0.000000029	0.34
Copper	0.0000000172	0.58

Power Collection

The power collection system consists of mirrors, filters and solar cells. This configuration saves thousands of tonnes on the final design, hence it is already very sustainable. It is known that solar cells on Earth are sustainable and the practical application of other solar collection methods were proven to be unfeasible. Hence solar cells are the only option. For the filters the only option available with a high enough TRL level was Quartz glass. Similarly, the mirrors will be produced in space, hence volume considerations where taken using kWh/m^3 and $CO_2 tonne/m^3$. It was found that aluminium was the best performing, as shown in Table 8.5.

Propulsion

For propulsion the most efficient option was chosen. In this case that was ion propulsion thrusters. These are electrically driven, and use very little and very light inert propellant gasses. Hence the energy used to propel the spacecraft comes almost entirely from the sun. This is much more sustainable than chemical propulsion due to the large weight reductions, saving costs as well as decreased toxicity and energy consumption per m/s of ΔV, implying it is socially and environmentally sustainable.

Electrical Power System

The primary material considerations for the electrical power systems are conductor materials for both the bus wires as well as the converters and transformers. The majority of the masses for these systems can be attributed to decreasing the resistance of conductors, in order to comply with the power losses requirements set for the electrical power system. Hence only good conductors should be chosen. The efficiency of the conductors where characterised through the resistivity. The power losses in the system, even for small percentage losses, can amount to unacceptable losses in revenue and clean solar energy while making the thermal control system larger as well. This would lead to a snowball effect, making the system unsustainable in all facets. The loss coefficients where based on the order of magnitude difference between a target resistivity of 10^{-8} Ohm·m. Table 8.6 show that the winner of the trade-off was copper.

Power Transmitter

The power transmitter should scale in mass with the transmitter power from the spacecraft. This implies that choosing 20 spacecraft instead of 1 would not result in a system which is 20 times heavier. This is however the case for a microwave transmitter, making this an economically unsustainable design. Hence a laser power transmitter should be used. In order to maximise the social sustainability of the beam it should not be visible for human or animal eyes, allowing for comfortable and undisturbed living near a receiver on the ground. The frequency of the beam should also not affect life and the environment in a negative manner. Hence should have a non-ionising frequency of light which is not instantly absorbed as heat. Hence sub-infrared lasers should be chosen.

Table 8.7: BFR emissions and energy consumption per kg of payload

Launcher: BFR Fuel: Methane					
GEO	31.35	tonne CO_2/tonne payload	LEO	10.45	tonne CO_2/tonne payload
	478.96	kWh/tonne payload		159.6527697	kWh/tonne payload

Table 8.8: Energy consumption and CO_2 emissions of the system by subsystem

	Launch		Material		Total		Production Safety Factor: 2	
Subsystem	kWh	CO2 tonnes	kWh	CO2 tonnes	kWh	CO2 tonnes	kWh	CO2 tonnes
PROP	16764	1097	94955	162015	111719	163112	223437	326225
ADCS	23450	1535	132828	226636	156278	228171	312557	456341
THER	28737	1881	226783	463406	255520	465287	511040	930575
TT&C	160	11	1230	2361	1391	2371	2781	4742
POCO	30797	2016	133849	282989	164646	285005	329293	570010
POST	3919	257	238901	488168	242820	488425	485639	976849
EPSY	12614	826	121989	249272	134603	250098	269207	500196
MAIN	9579	627	54260	92580	63839	93207	127678	186414
STRU	12453	815	397228	849160	409681	849975	819362	1699950
Total	138473	9064	1402024	2816588	1540497	2825652	3080994	5651303

Table 8.9: Environmental sustainability of SPECTRE

Energy Production in Space	286276869803	kWh
Estimated Trans eff	0.15	
Energy Production on Earth	42941530470	kWh
EOL Energy balance	42937540642	kWh
CO2 Emissions	0.000178	Tonne/kWh
CO2 Emissions	0.178	kg/kWh
CO2 Emissions	178	g/kWh
Europe Average	293	g/kWh

8.4. Environmental Sustainability of SPECTRE

The social sustainability has been discussed above and production related sustainability will be discussed later in the production section. Economic sustainability of the system will be discussed in depth later in the report in market analysis. This leaves environmental sustainability to be discussed. The environmental sustainability requirements state that the system should produce more useful electrical energy on Earth than it took to produce the system (**D-ST-S-ENVI-003**) as well as have a lower CO_2 emissions per kWh than the grid average (**O-SY-S-ENVI-001**). In order to verify these requirements have been met, the total energy production and CO_2 production due to the system should be calculated.

Using the values obtained in Table 8.2, it can be calculated (from the major material components). It is assumed that launching payload to GEO requires 2.39 times the amount of ΔV as launching to Low Earth Orbit (LEO), as is the case with the Falcon Heavy [130]. Hence the LEO values where multiplied with 2.39. It was further more assumed that the CH_4 fuel was burned with perfect combustion with O_2. This would imply that for 19 kg of payload/kg of fuel it can be found that 10.45 is emitted as CO_2 with the remaining weight being water. Assuming an energy density of 55.7 MJ/kg for this reaction [144], then summarised in Table 8.7 are the sustainability indicators for BFR as a launch vehicle.

For the subsystems, there was an essay for each subsystem and their majority material(s) by weight. For the propulsion, ADCS and maintenance systems this was assumed to be steel. For the EPS it was taken to be copper due to the electronic components and wiring. The TT&C subsystem was assumed to be composed 50-50 by weight out of steel and copper. The power storage system consists of non-ferrous metals. The structural subsystem is compromised almost fully out of composite materials. Finally, the power collection system consists mostly out of aluminium for the mirrors, quartz glass for the filters and non-ferrous metals to estimate the solar cells. Finally, to include production and production module losses and consumption this was multiplied with 2. The resulting values are summarised in Table 8.8. As can be seen, the majority of the emissions and energy consumption is due to material and production.

When considering a degradation of the system of 0.05% per year, the degradation can be assumed linear. Hence the total energy production can be assumed as follows:

$$E = (P_{EOL} + 0.5(P_{BOL} - P_{EOL})(30)(365)(24)(60)(60)/1000/3600 \quad [kWh] \tag{8.3}$$

This results in an energy production of more than 286 billion kWh during its entire life. It is assumed that the transmission efficiency from space to Earth is 15%. Combining the statistics from the spread sheet [128] and the values determined in Table 8.8, Table 8.9 can be made.

As can be seen, the system produced more electrical energy on Earth than it consumes by a very large margin. Hence it meets requirement **D-ST-S-ENVI-003**. It also emits less than 40% of the CO_2 than the European grid average per kWh. SPECTRE can hence be compared to a gas power plant in terms of environmental sustainability. It should however be noted that major contributions to the CO_2 was due to the consumption of electricity and old/less sustainable processes for the production of raw material. It could be a policy to produce and purchase only using clean energy sources, in the current state of the economy could result in a price hike. However could reduce these indicators by

at most 25%. The majority can be done to limit damage to the environment from material and produce production. It can also be said that these industries will be pressured by market forces, governments, new technologies as well as moral obligations to clean up their processes, which would significantly reduce the damage to the environment. The result can hence be seen as higher than the actual values will be in 2030. One of the major problems with today's renewable energy sources is the fluctuation in energy production during the day and the unpredictability of the weather. This requires base generators based on fossil and nuclear fuels to make up for the lost power quality and add capacity when required. If anything, this analysis and the rest of the report shows that this system offers to be a viable and cleaner alternative to the current base generators in the grid, while being cleaner than the fossil fuel alternatives with less toxicity risk and more controllability than a nuclear power plant. The total EOL efficiency of the system is hence 9%, which makes it a 150 MW generator on Earth. This is comparable to some old combustion, steam and solar generators. [125]

9

Operations and Logistics

In this chapter, the operations and logistics concepts that will be crucial for the success of the mission will be described. The operations and logistics include the interaction between the production and transport of the required system components to the assembly site, pre-launch testing of components, the launching of the system components and their assembly or production in orbit, the communication between the satellites and ground station, the transmission of the power to Earth, and the in-orbit maintenance of the system, which includes the storage of machines and spare materials. Note that the operations that will be conducted for disposal will be described in the astrodynamics discussion in chapter 11, and the in-orbit production operations and logistics will be discussed in the production plan in chapter 13.

9.1. Pre-Launch Operations and Logistics

As the components are being produced, it will be crucial to get the components tested and certified, validate that they are in fact the required components, and that they have sufficient reliability. This will be done gradually throughout the beginning of on-Earth production, until the first launch of payload.

First of all, the company will be required to apply to be allocated a position in GEO. Since there is a given distance that spacecraft must have between each other, there is limited availability in GEO. However, due to the sustainable nature of this system, the acquisition of such positions will be assumed to be possible.

Afterwards, the components must be validated. This will be the first step after production because it both validates that it is the required component being produced, and at the same time, the reliability can be gradually tested over time. The earlier this is started, the more accurate the results on reliability become. This testing should preferably be done at the site of production, to minimise transport in case the component is flawed.

Finally, certifications for the components can be acquired. The main certifications that would have to be acquired are those for launch and for international regulations on spacecraft. These will most probably have to be performed close to the launch site, with cooperation with the launcher provider (SpaceX) and the international regulations community.

Outside of certifying the system, prior to the launch a proper schedule would have to be defined for when the launching will occur.

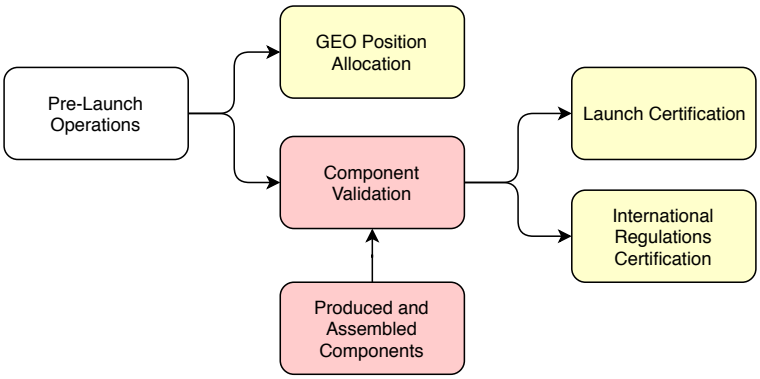

Figure 9.1: A general operations and logistics flow diagram for Pre-Launch activities

9.2. Production Operations and Logistics

The operations and logistics related to the production of the system are denoted in the figure below. As one may see, the system will be dependent on components produced by 3rd parties as well as in-house. The items that would be produced through 3rd parties or in-house are also defined in the figure below. Clearly, novel items such as the filters, trusselator, and the deployable spider web must be produced in-house. Although this will require the team to acquire its own production facilities and labour power, only the team is well aware of the requirements of those components. Therefore, producing those components in-house can reduce risk and cost. On the other hand, TT&C and ADCS components are very standard in spacecraft, and therefore their production can be trusted with 3rd parties.

Of course, when it comes to 3rd parties, some negotiating and contracting with those parties will be required. After the 3rd parties have produced the required parts, it will be beneficial for the in-orbit production phase if those required parts are assembled as much as they can be. This will require transport from the production facilities to the assembly facilities. After assembly, the 3rd party components can be transported to a separate assembly site.

The components produced in-house by the team will also be transported to this separate assembly site. At this site, all of the components will be assembled for launch, such that the volume and mass densities inside the fairings can be maximised for all launches. For the launching of the system, 15 launches will be required, 5 for the production modules, and the remaining 10 for the subsystem and material modules. The launching of the systems will be performed from Boca Chica Village, TX, United States of America.

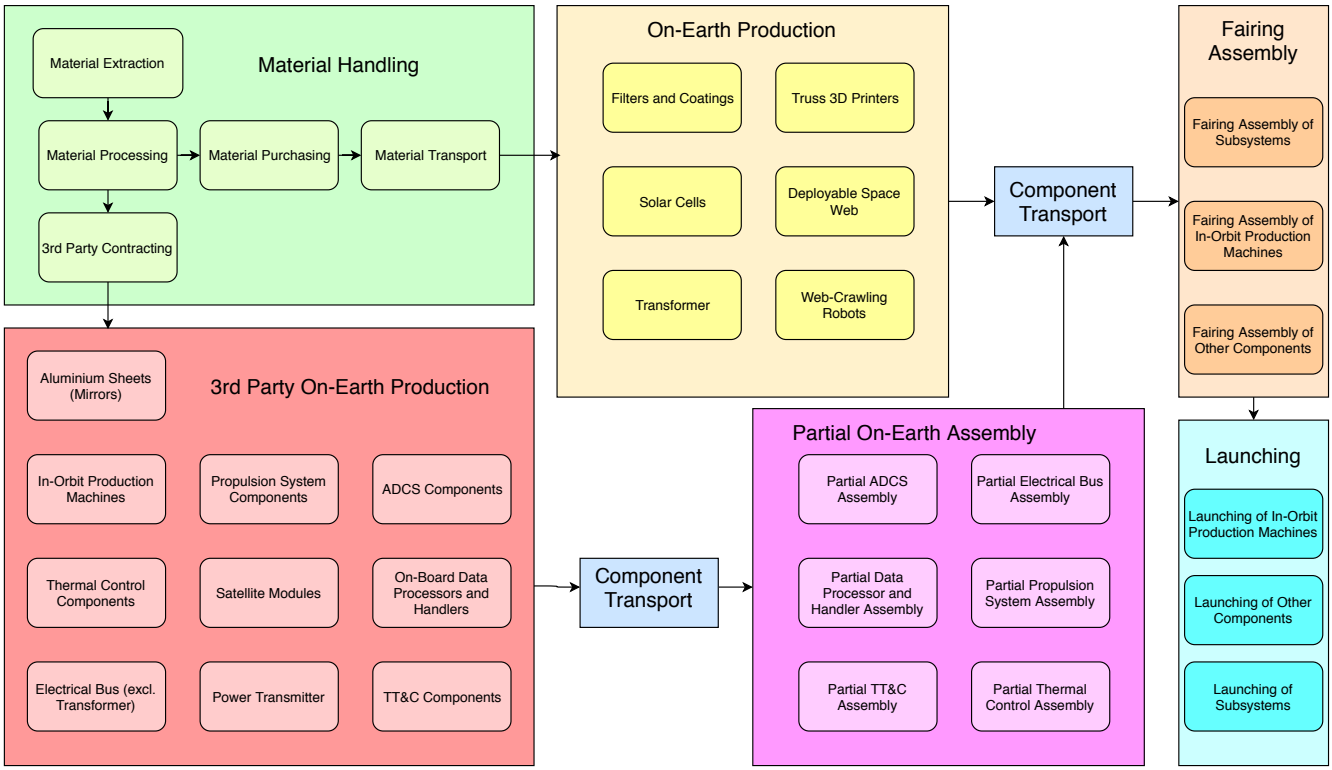

Figure 9.2: Operations and Logistics flow diagram for Production

9.3. Maintenance Operations and Logistics

Due to the extended required lifetime of 30 years, maintenance will be required to upkeep the performance of the system. For logistical reasons, a surplus of components that are prone to failure at some point in the 30 years will be sent up into orbit before 2030. This surplus of components is directly related to the anticipated components that will fail, and other components that are deemed reliable but are crucial for the systems performance.

First of all, due to the effects of debris impacts and high levels of radiation, it was determined that upkeep will be necessary for the mirrors. Therefore, scheduled maintenance will have to be done every 10 years on the mirrors.

Furthermore, maintenance will also have to be conducted on the components of the EPS. In order to maintain the EPS, it will be required that the subsystem module will be decoupled from the power collection system. After this decoupling, the production and maintenance modules must be docked onto the power collection system. Afterwards, through the methods described in chapter 13, the EPS components can be maintained. Although this method is

mainly reserved for the EPS, since all of the production machines will still be present on the production module, other components such as the solar cells can also be maintained, if required. Note that because the power collection system does not consist of TT&C or ADCS subsystems, these docking manoeuvres will have to be performed with the aid of a video feed, and within a time limit. As the spacecraft will continue spinning, it will remain stable and controlled, but to reduce risk, the time limit should be minimal.

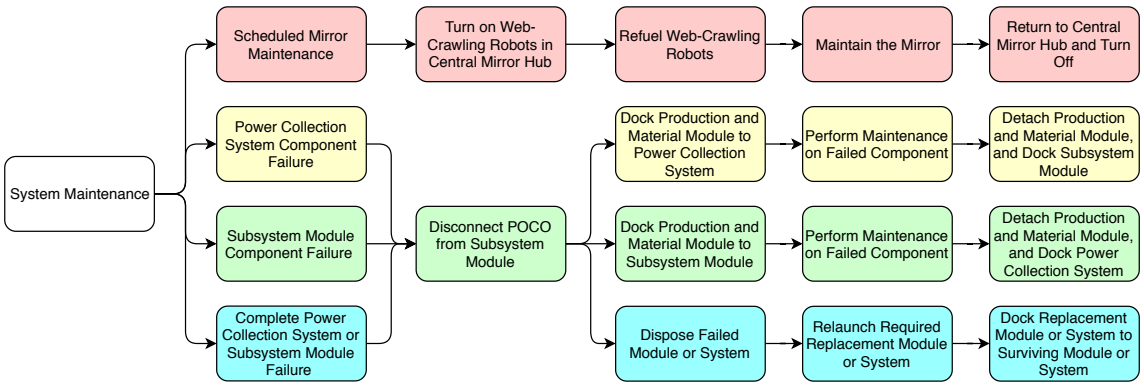

Figure 9.3: Operations and Logistics flow diagram for Maintenance

9.4. Storage Logistics (Production and Maintenance)

For the production and maintenance of the system, the materials and components that will be used must be stored as efficiently as possible. The materials and components must also be easily accessible by machines that can manipulate them.

For on-Earth production, the storage of the materials and components will not be much of an issue. However, in order to decrease costs and increase sustainability, the storage and production of materials should be done locally, close to the launch site. Of course, the storage of the raw materials, processed materials, and various components will vary initially, and will eventually all be brought to a central assembly site for the fairing.

In orbit, the storage logistics do become more complicated and will require planning. For the production and scheduled maintenance of the mirror, the web crawling robots will have to be filled with a 30 year long supply of material directly. The rest of the required production and maintenance will be occurring through the production module. Therefore, the rest of the materials that will be required for production and maintenance can be stored in the materials module, which will be attached to the production module.

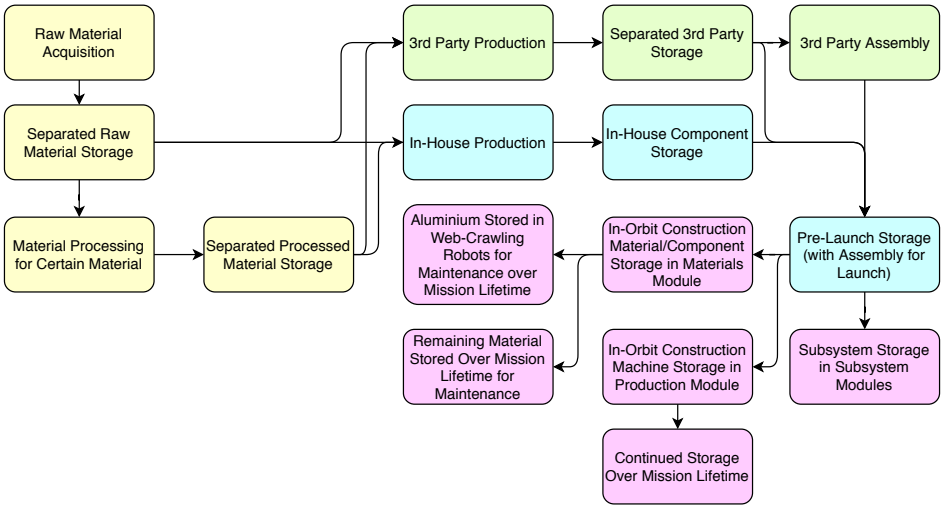

Figure 9.4: Logistics flow diagram for Storage

9.5. Space to Ground Communication Operations

The operations related to the communication between the space segment and the ground segment is visualised in Figure 9.5. As one may see, the communication may be directly between the satellites and the ground communication system, or may also occur through a relay satellite. However due to the GEO orbit, relay satellites will be hardly used, and during production the communication must happen directly through the ground communication system in order to have absolute control over the system, and to not be reliant on relay satellites.

The communication operations will also differ slightly dependent on the phase of the mission. During the in-orbit production of the system, the systems TT&C subsystem will not be functional. Therefore, the attached production and material modules will require individual TT&C subsystems, and the communication with the ground segment will be performed through it. Also, measures must be taken in order to have proper surveillance of the production process. This will include a variety of real-time video streams to ensure there are no discrepancies during production. However after production, while real-time video streams will still be applied to maintenance, these streams will occur less often than during production.

Furthermore, constant communication between the space segment and ground segment will only be required for monitoring the performance of all the systems and the attitude of the system. Therefore, this constant communication will be minimal compared to when a video feed will be required. This means that the TT&C system will have to be flexible in terms of data rates.

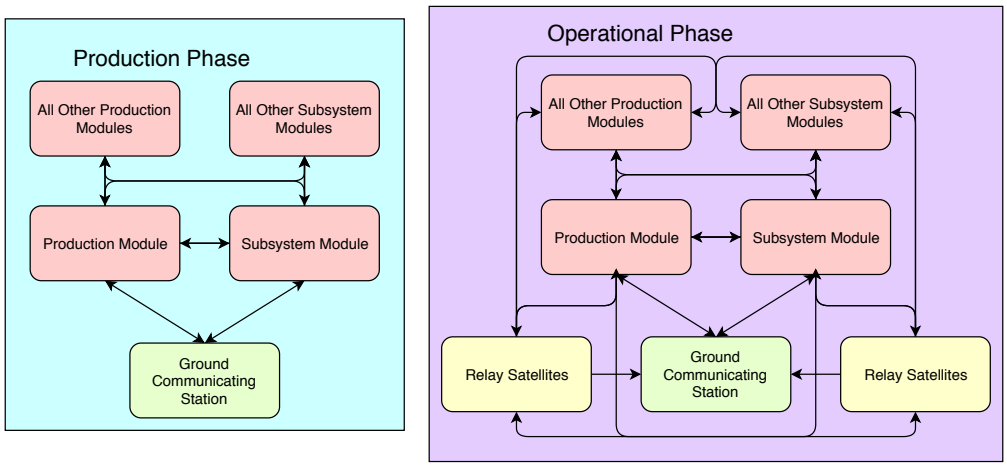

Figure 9.5: Operations flow diagram for the space to ground segment communication

9.6. Power Transmission Logistics

The collection of power will be done by solar cells and this power will of course require to be transmitted to Earth. Therefore, an electrical power subsystem through which the power can be transported was designed. Essentially, the collected power will first be converted to a certain voltage, depending on what the power will be used for. For the subsystems, the voltage can be relatively low, while for the transmission, the voltage will be relatively high. After these conversions, some of the power will be used up by the on-board subsystems, while the rest of it, at least 1 GW, will be transmitted to Earth. The power will be transmitted using lasers, despite their low maximum power transmission. However, using microwave transmission would require very large microwave antennas for all 20 spacecraft, which is deemed unfeasible.

Therefore, the power can be transmitted for every spacecraft by compiling a large amount of lasers together for every spacecraft. Using lasers, and a bearing attachment between the system and the lasers, the lasers can be orientated individually to transmit to a central ground-based power station. From this power station, the power can be distributed to the end customers. Note that the power station will also be used as the ground station for communication.

9.7. Safe Mode Operation

Due to the large amount of systems, and components within the systems, it is inevitable that a component may fail or malfunction. In order to prevent any further failures in the system, safe-modes will have to be used. For this, the power collection system will have to be deactivated, and any other components related to the failure will have to be turned off or heavily monitored. Below, a general flow of operations is depicted into how safe-modes will be handled.

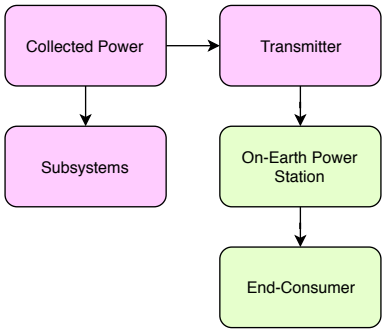

Figure 9.6: Logistics flow diagram for Power Transmission

While safe-modes can be caused by a variety of reasons, one of the most anticipated causes is the need to short circuit the bus, due to a malfunction. If it is not possible to stop the current flow, the bus may get burnt and the entire system would fail. For this, an operation must be performed to stop the current flow through the system. A trade-off on various possibilities was performed for the EPS design in chapter 11. Essentially, the chosen method involves the usage of of individual switches for the solar cells and the unfurling of the space web to flatten out the mirror. Once a failure in the EPS is detected, the current flow must be stopped within a second. For this, the switches on the solar cells will be turned off to stop the flow. However, this will gradually increase the load on the solar cells, and can only be relied on for a couple of seconds. Therefore, at the same time, the space web will be unfurling in order to gradually minimise the load on the solar cells. A more specific operations flow for this safe-mode can be found below.

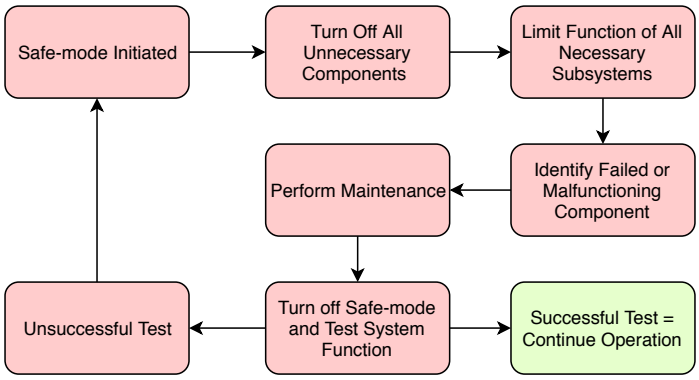

Figure 9.7: A general operations flow diagram for the Safe-Mode

10

Power Collection System Design

Due to the high area mass density of solar cells, it was decided to reduce the solar cell area as much as possible. The first and most straightforward method is to increase the concentration of the light, resulting in a larger power output for a smaller area size. The second method utilises the bandgap nature of semiconductors and spectral splitting to optimise the conversion of light to electrical power. This allows for much more efficient solar cells and hence a vastly reduced area for the solar cells. Throughout this discussion of the design, Figure 10.12 may serve as a visualisation of how the design will be configured, and how the optics will function.

10.1. Bandgap Calculations

Solar cells utilise photons to generate charge carrier pairs by liberating the negative charge carrying electrons from the low energy valence band to the higher energy conduction band, leaving a positive charge carrying holes in the valence band. The energy bandgap, or bandgap, between the conduction and the valence band is what determines the minimum energy/frequency a photon requires to generate electricity. The resulting potential energy of the electrons (voltage) is equal to the bandgap in eV. Photons with energy greater than the bandgap will only release electrons at the bandgap energy, with the access energy converted to heat. Photons with lower energy can still be absorbed, however cannot generate electron hole pairs and hence are completely lost as heat. The resulting bandgap design should maximise the power output of the solar spectrum [22].

The sun can be estimated to be a black-body radiator. The spectral energy density of a black-body radiator can be expressed as follows [91]:

$$B_\lambda(\lambda, T) = \frac{2hc^2}{\lambda^5(e^{\frac{hc}{\lambda k_B T}} - 1)} \tag{10.1}$$

The resulting graph for a temperature of 5778K can be seen in Figure 10.3, depicted in blue. A comparison spectrum for the actual solar radiation both with 0 atmospheres and 1.5 atmospheres is depicted together with a black body radiator at 6000K (note that the model radiator temperature is 5778K)[22], it can be seen that the solar spectrum is fairly close to that of the black body radiator. For the model it was chosen to use a lower temperature, in order to fit just under the actual solar radiation as a safety precaution.

The spectrum was only considered up to a wavelength of 3000nm, as anything longer was assumed to be absorbed by the mirrors and filters. The spectrum is not uniform, and therefore each bandgap should be placed strategically as to maximise the utilisation of the available energy in the solar spectrum. A program was developed, which placed the first bandgap by maximising its power. The resulting utilisation of a single optimised bandgap is depicted in Figure 10.3, the efficiency for this cell would be 38%. Then it placed a second bandgap which in tandem with the first would maximise the combined power. This process could be repeated for any number of bandgaps. The resulting efficiency gain is depicted in Figure 10.4. It was chosen, for mass considerations, to limit the number of bandgaps to 6, resulting in an efficiency of 70%. The spectral utilisation of this array is depicted in Figure 10.2. The power fraction for each bandgap is summarised in Table 10.1.

Table 10.1: Power distribution for different bandgaps

bandgap	1	2	3	4	5	6
Power fraction	0.216	0.243	0.204	0.174	0.106	0.070

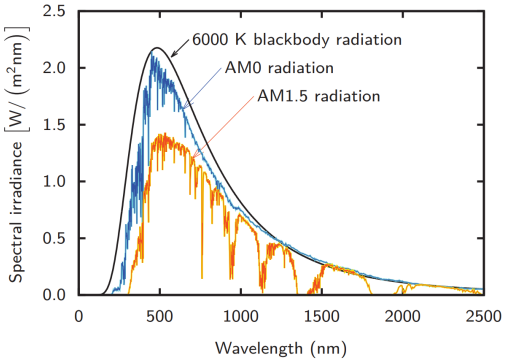

Figure 10.1: Solar spectrum comparisons [22]

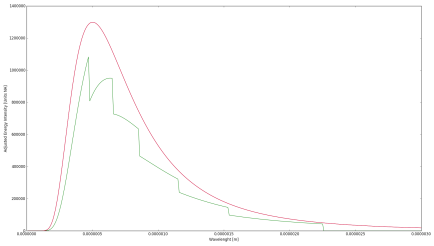

Figure 10.2: Spectral power density utilisation by bandgaps

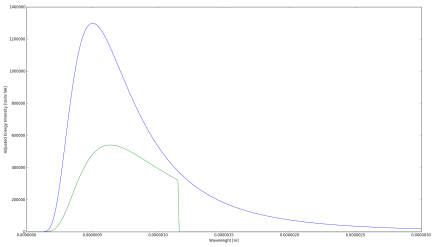

Figure 10.3: Optimum placement of a single bandgap (Note, the y axis was scaled for clarity hence does not have units)

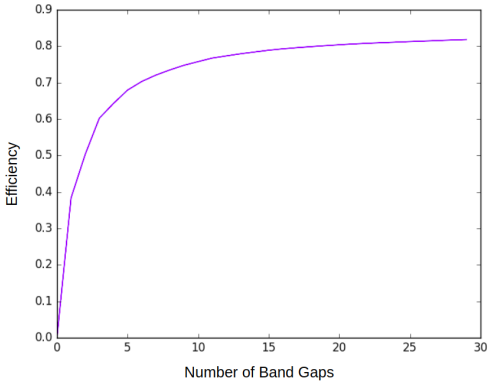

Figure 10.4: Optimum placement of multiple bandgaps vs the efficiency

10.2. Concentrators

The leading design goal was to minimise the mass. For the optical system, limits to the size and concentration factors were the thermal constraints. The spectral splitting method allows for a maximum efficiency of 70% Beginning of Operational Life (BOL) and 61% EOL. In reality the efficiency losses are also due to reflectance and premature electron hole recombination/radiation. As a safety precaution, it is assumed that at BOL 30% is dissipated as heat and 39% at EOL, in order to ensure the TCS can keep the spacecraft at the right temperature with these high thermal loads.

The increased efficiency allows for even higher concentration factors, due to less heat dissipation for the same intensity compared to regular solar cells. For solar cells to operate at higher efficiencies, the temperature was decided to be limited to 300 K, since solar cells become less efficient at higher temperatures. The radiation emitted from a surface to free space is expressed by Equation 10.2. Where Q_r is the heat radiated, ϵ is the emissivity, σ_s the Boltzmann constant, T_s is the temperature of the surface and T_{free} is temperature of free space, assumed to be 4K.

$$Q_r = \sigma_s \cdot \epsilon \cdot A_r \cdot (T_s^4 - T_{free}^4) \tag{10.2}$$

Assuming a perfect absorptivity of the solar cells and using a preliminary thermal analysis based on radiative heat dissipation, it was determined that the maximum allowed concentration of light was 17x regular solar intensity. This results in a solar area of 4566 m^2. The total dimensions are summarised in Table 10.2.

The costs of the thin film/dichroic filters are significant and mostly based on the area of the filters. Should they be constructed on the same scale as the solar cells, would become economically unsustainable. However, due to

Table 10.2: Summary of solar cell dimensions

bandgap	1	2	3	4	5	6
Area [m²]	1086	943	801	678	574	485
Length [m]	7.127	6.190	5.424	4.450	3.767	3.181
Radius [m]	24.25	24.25	24.25	24.25	24.25	24.25

Table 10.3: Primary and secondary mirror dimensions

Dimension	Primary	Secondary
Focal Length [m]	187.42	275.52
X parameter [1/m]	0.001334	0.000907
Y max [m]	37.89	2.37
Radius [m]	180.80	51.15
Frontal Area [m²]	102695	8219
Parabolic Area [m²]	117944	8469
Black Spot Frontal Area [m²]	8219	658
Black Spot parabolic Area [m²]	8584	663
Mirror Frontal Area [m²]	94475	7562
Mirror Parabolic Area [m²]	109360	7806

Table 10.4: Concentration factors for different parts of the optics components

Component	Concentration Factor
Solar Cells	17
Filters	384
Seconndary Mirror	10
Primary Mirror	1

them being made of quartz glass, which can handle very high temperatures [147], combined with a high optical efficiency, allows these to operate at very high concentration factors. From the same thermal analysis it was found that a concentration factor of 384 is possible. The decrease of light intensity would hence have to occur in the space between the filters and the solar cells. The length of the filters determines the length of the solar cells, implying the dispersion should occur radially. This was found to be 24.25 m in radius.

The filters split different frequency ranges, in accordance with the solar cell bandgaps. The reality is however, that the solar spectral intensity is not uniformly distributed across all frequencies of light (see Figure 10.3), and the solar intensity for each bandgap is also not uniform. This means that the thermal loading is not uniform across all filters, resulting in some filters overheating. This will be discussed in the next subsections. However, in effect the concentration angle has to be adjusted such that the thermal loading is within limits for all filters. This effectively sized the filters and its convergence angle. The filters are summarised in Table 10.5.

The filter concentration angle determines the curvature of the secondary mirror, as depicted in Equation 10.3, while the thermal limits and the primary convergence angle determine the area. The secondary mirror does not receive light at a normal incidence. Hence a parabola would have to take this into account. However, for the purposes of this report, this assumption was taken and it was also assumed that the secondary mirror control system will be able to adjust the shape to optimise this. The mirror it self is taken to be 91% efficient. With a maximum acceptable temperature of 700 K, minimum power reflectance, optimised distance from the primary and a convergence angle of 10.52 degrees results in the dimensions given in Table 10.3.

$$y = ax^2 \rightarrow \frac{dy}{dx} = 2ax \rightarrow \alpha = arctan(2ax) = 2\theta \tag{10.3}$$

The primary mirror is similar in construction as the secondary mirror. The primary mirror's objective is to concentrate enough light onto the secondary mirror. This power must include all losses to the transmitter, which sized the total frontal area. This mirror will accept normal incident rays from the sun and concentrate them to a focal point before the secondary mirror in order to fully illuminate it. This convergence angle sized the parabola area from the frontal area. This convergence angle was found to be 52 degrees. Finally, it was found that the primary mirror would have no thermal problems.

Originally, once the black spot was found, effort was put into creating a design that eliminated it. However, the spot was reinstated in order to create space for a central truss beam to connect the filters to the rest of the spacecraft. Finally, the concentration factors are outlined in Table 10.4. It is important to note however, that the area mass density of the mirror is an order of magnitude lower, as discussed in chapter 13. The estimated weight savings through this method are estimated to be around 2600 tonnes or more when considering the iteration mass losses between iterations 1 and 4 as seen in subsection 11.5.5. This allows the mass and sustainability requirements to be met.

10.3. Spectral Splitter

In this section, the method of spectral splitting, and the components used to achieve it will be discussed and designed. Essentially, the method of spectral splitting has been narrowed down to the use of optical filters, specifically thin film filters. Thin film filters have the useful property of reflecting light below or above a certain wavelength, and transmitting the rest of the light at very high efficiencies. This property will allow the system to split the spectrum of light into whatever separated spectra are required [57].

10.3.1. Filter Theory

Before the design of a spectral splitter using optical filters, a solid understanding of optical filters is required. Essentially, optical filters function by applying certain coatings to a substrate, normally fused silica. Fused silica itself has a transmittance of almost 100%, but as the coatings are applied, interference occurs due to the reflection of certain wavelengths of light and transmission of others. Then, the more coatings that are applied, the more interference occurs between the reflection and transmission of light throughout every coating [57].

These coatings are what causes the light to be split up in different wavelengths. The coatings generally alternate between high and low index coatings, with each coating being the quarter of the wavelength you want to reflect in thickness. This reflected wavelength, and the region around it that is also reflected, is known as the stop-band. Therefore, in this design every stop-band of a filter will be the band that is reflected onto the solar array. With every consecutive coating that is applied, the reflection in the stop-band increases and the transition from the transmitted and reflected wavelengths becomes more defined. Nevertheless, the regions outside of the stop-band still have distinct ripples with high variations in transmission and reflection. These ripples can be minimised by applying layers that are not quarter-wavelength thick, and optimising their interface with the other layers [57].

Furthermore, an interesting aspect of filters that will have to be discussed is the effect of altering the incidence angle of light onto the filters. As the incidence angle is changed, the thickness of the layers through which the light must pass through changes, effectively changing the thickness to another quarter-wave thickness which now corresponds to another reflected wavelength. However this is only true for polarised light, as un-polarised light will actually have two wavelengths at which the reflectivity and transmittance drastically changes. Fortunately this will not pose an issue since the incident light in the design will be polarised due to its reflection off of the mirrors [57].

10.3.2. Filter Design

In this section, the design of the filters will be discussed. For the desired dispersive properties of light, the filter will be shaped as a parabola and the solar cells will be placed radially around the filters, allowing for dispersion of light along a plane. Furthermore, the parabola will be modelled based on the dimensions acquired for the reflected light after the secondary mirror. On top of this, other considerations will have to be used as well, including the following.

- The filters might be parabolic, meaning that the angle of incidence of incoming light is different across the entire filter, which will require the application of various coatings along the radial circumference of the filter.
- The light at lower wavelengths is most intense, therefore, to optimise efficiency, the lower wavelengths will be reflected first. This will require long-pass filters.
- Once the lower wavelengths have been reflected onto the solar cells, the transmitting and reflecting qualities of the filter at those wavelengths can be neglected.
- The aforementioned consideration indicates that the ripples will have to be reduced on the long-wavelength side, so the layering structure of the coatings will have to be optimised for the long-wavelength side.
- Since only 6 band gaps will be used, only 5 filters will be required, with the final reflective surface being a mirror.
- The degradation of filters, and the causes of it, must also be considered, as a minimal degradation would be optimal.

Filter Shape Determination

In order to find the parabola, the constraints of the frontal radius of the incoming light, the black spot radius on the filter, and the minimum area to ensure thermal control were considered. Small contingencies were added to these constraints to allow for iterations, in case the given constraints would not result in the optimal design of the filter. For these iterations a program was produced, which will be described below.

The program took into consideration the blackspot radius (due to the secondary mirror), and all other necessary geometrical properties. Essentially a Cartesian plane was taken as a reference, with two straight, opposite slopes defining the divergence of the light, and a parabolic function defining the shape of the filter. Constraints were added

to the program to iterate along applicable values, which were points along the parabola where the slopes of the lines defining the divergence of the light were related to the slope of the parabola with the following relation:

$$\theta_v = 2 \cdot \alpha - \frac{\pi}{2} \tag{10.4}$$

Where θ_v is the angle of the view factor, and α is the slope angle of the parabola at the given point. Then by applying varying coefficients and constants to the equations of the view factor slopes and to the parabola, large variations of applicable parabolic shapes could be found.

However, although it was determined that parabolas could be used to increase the mass-efficiency of the system and to minimise the sizes of the filters, after a large amount of iterations it was determined that the optimal parabolic shape of the filters converged to essentially a conic shape. This was mainly due to the fact that the dispersion of light would be too much, and to size the solar cells optimally, the solar cells would be required to be located within the filters. Therefore, while using parabolic filters would have been optimal to increase the mass-efficiency of the filters, they would have resulted in extremely over-designed solar cells. It was also determined that the application of coatings on a flat surface is relatively cheaper than for a parabolic surface, and that storage of the filters would be much more efficient.

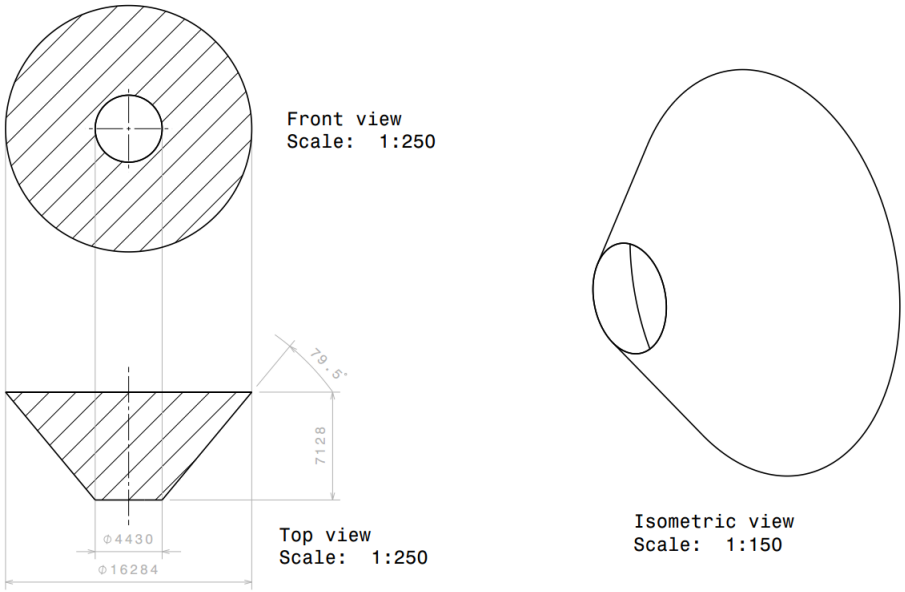

Figure 10.5: Schematics of the first and largest filter.

Filter Sizing

Considering that the filters would now be flat plates when viewed from the side, the light would only be dispersed radially. This radial dispersion of light required that these flat plates would have to be rotated around the axis parallel to the incoming light, resulting in a conical shape, with a portion of the pointed part removed to account for the blackspot and supporting structure. This usage of a flat plate was first applied to the first filter. Afterwards, the calculations were iterated to find the dimensions of the other filters. Depending on the thermal limits of the other filters, and the convergence of light from the secondary mirror, the optimum filter number to base the sizing of the other filters was chosen. Essentially, four iterations were done for this, with the first iteration sizing all filters based off of the first filter, the second iteration considered the second filter, third iteration the third filter, and the final iteration resulted in the second filter being the best filter to base the sizing off on.

Essentially, given the dimensions of the secondary mirror, the convergence of light from it, and the distance of the secondary mirror to the first filter, the sizing could be completed based on the second filter. Essentially the aforementioned information was used to size the second filter based on previous iterations. Afterwards, depending on the orientation of the incoming light, the required orientation of the filters was also found, from which the total areas could be calculated. The dimensions of the first and largest filter are given in Figure 10.5, both from the front and side. The dimensions of all the filters are tabulated in Table 10.5.

Filter Coating

Now that the dimensions of the filters have been determined, it is crucial to study applicable coatings that can be applied. As mentioned in the considerations for the design of the filters, the light at lower wavelengths is a lot more

Table 10.5: Tabulated Dimensions of the Filters

Identifier	Filter 1	Filter 2	Filter 3	Filter 4	Filter 5	Backmirror
Filter + Blackspot Radius (m)	8.142	7.072	6.002	5.084	4.304	3.634
Blackspot Radius (m)	2.216	1.925	1.634	1.384	1.172	0.989
Length (m)	7.127	6.190	5.254	4.450	3.767	3.181
Frontal Surface Areas (m2)	192.8	145.5	104.8	75.2	53.9	38.4
Conical Filter Surface Areas (m2)	303.3	227.6	164.2	118.6	89.7	73.6
Mass (kg)	667.3	500.6	361.2	261.0	197.4	198.7

intense and will therefore be reflected towards the solar cells first, to maximise the total efficiency of the system. Therefore, the long-pass filters will transmit light above the following wavelengths consecutively, first 470 nm, then 650 nm, 850 nm, 1150 nm, and finally 1530 nm. On the following page, some graphs for transmittance and reflectance of commercial filters that are feasible for this application are presented.

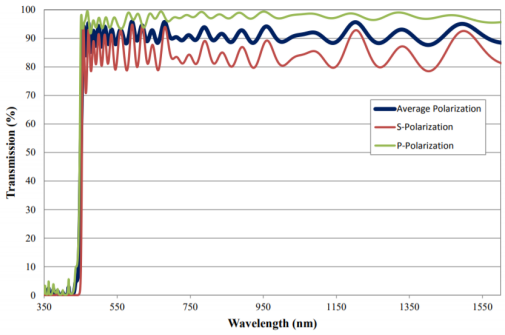

Figure 10.6: Transmission for 450nm Filter [107]

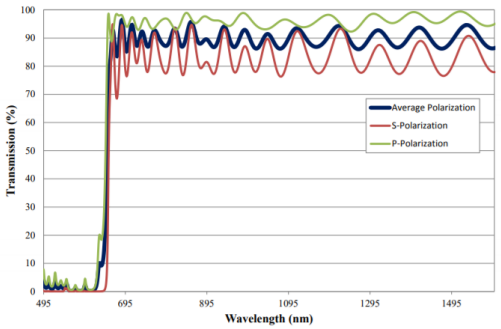

Figure 10.7: Transmission for 650nm Filter [107]

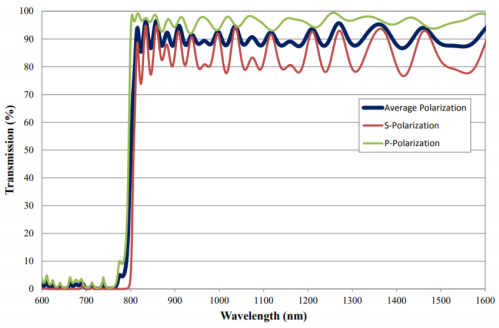

Figure 10.8: Transmission for 800nm Filter [107]

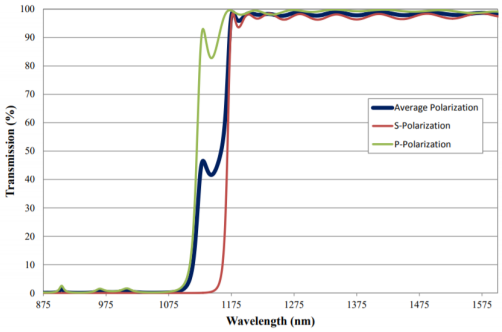

Figure 10.9: Transmission for 1150nm Filter [107]

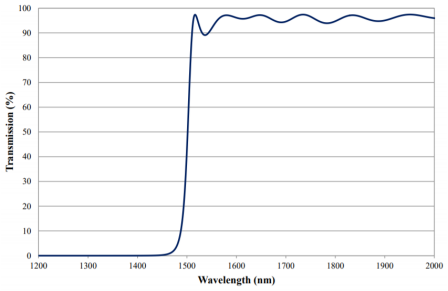

Figure 10.10: Transmission for 1500nm Filter [107]

As one may see from the provided graphs, the filters maintain an efficiency of around 90-99% for both reflectance and transmittance. This indicates an efficiency of approximately 95%, however with technological advancements until launch and with the production of filters specialised for SPECTRE, the efficiency could be increased. Therefore, since in theory these values can reach close to 100%, and filters with continuous efficiencies close to 99% have already been produced (Figure 10.9), it will be assumed that filters of 98% efficiency can be used.

Filter Degradation
Furthermore, research also had to be done into the degradation of filters. It was determined that for hard-coated filters, the degradation due to the environment (excluding temperature) would be negligible. However, filters degrade heavily when they are exposed to rapid temperature fluctuations. This degradation is caused by the sudden and distributed thermal expansion of the various layers, which ruins the interfaces between them. Therefore, to avoid sudden degradation, the filters will have to be hard-coated and temperature fluctuations should be minimised.

10.4. Solar Array

With the solar array bandgaps chosen and the filters modelled appropriately, the arrays were then updated accordingly. The underlying issue with the design of the solar arrays was to ensure that they do not exceed a temperature of 300K. Therefore, as explained previously, the light converged onto the filters would have to be diverged. This is why these solar arrays will be placed around the filters, to allow for the light to be dispersed radially. Since the filters reflect light radially, the light incident on the solar cells is already perpendicular to them, ensuring the optimal orientation of the solar cells.

10.4.1. Solar Cell Efficiency

With reference to section 10.1, the efficiency of the total solar array design will be 70%. As stated in the section, this efficiency was derived by optimising the use of bandgaps.

10.4.2. Solar Cell Degradation

The solar array should withstand the harsh space environment in order to minimise degradation. The main factors typically include space radiation and high temperatures. This degradation had to be taken into account for the design of the power collection system. Essentially, radiation degrades solar cells due to the impact of radiation onto the atoms in the solar cells. Some of these impacts can chip away these atoms in the solar cells, therefore degrading them. High temperatures cause disorder which also deteriorate the bonds between these atoms, which greatly increases the degradation.

Due to the configuration of the spacecraft (refer to subsection 11.5.1), where the solar cells are on the inside of a cylinder, they are already protected significantly from space radiation. Furthermore, the solar panels are not placed in direct sunlight, but only receive partial sunlight which is converted efficiently. This results in minimal heat dissipation, ergo the internal temperature is reduced. Furthermore, through passive thermal control, the temperature is kept below 300K, which is optimal for solar cells. Although the harshness of the space environment has been brought down with respect to the solar arrays, it has not been eliminated, meaning the solar cells need to be space grade. Considering this information, and consultation with solar cell experts, a degradation of 0.5% will be used [1].

10.4.3. Solar Array Sizing

As mentioned before, the solar arrays will be sized and designed according to the design of the filters, with consideration put into the thermal control of the solar cells. Based on the design of the filters, the lengths of the solar array stages would have to be the same as the lengths of the filters. Therefore, the circumference which the solar cells would span would be dependent on thermal control.

Since the thermal model was not complete at this point of the design, preliminary estimates had to be used to incorporate thermal limits into this design. Therefore, only heat flow through radiation was assumed, and a maximum design temperature of 300K without thermal control was set. Of course, since this was only a rough estimate, the final temperatures of the solar cells would be much higher, but this could be dealt with by incorporating thermal control.

From this analysis and iterative process, which was done alongside the design of the filters, the various stages of the solar arrays could be sized. These iterations resulted in a minimum distance from the centre of the filters to the solar cells, at which the solar cells met the 300K limit. This essentially resulted in a radius of 24.25 meters. Taking the filter stage lengths above as well, the entire length of all of the solar array stages would be 29.97 meters.

Furthermore, it should be considered that these solar arrays will have to be flexible, in order to acquire the desired shape of the solar array around the filters. Therefore, it was chosen that thin film solar arrays would be most applicable, both for the application in this system and for launch.

[1] Consultation with Arno Smets

10.4.4. Solar Cell Composition

It is of great importance that the solar cells are tuned to their respective optimal bandgap. An overview of the optimal bandgaps for each solar panel is given in Table 10.6. Given the bandgaps, certain materials for the solar cells have to be chosen, which optimise the conversion of solar radiation into electrical energy with the highest efficiency. For the higher bandgaps, Indium Gallium Nitride is considered. Indium Gallium Nitride has great thermal performance, high radiation resistance and high saturated electron mobility that leads to potentially highly efficient solar cells under concentrated sunlight for space applications [30]. By adjusting the ratio of Indium to Gallium, the solar cell can be optimally tuned for its bandgap. The alloy $In_{0.2}Ga_{0.8}N$ fits perfectly for the 2.64 eV bandgap [50]. Increasing the amount of Indium to $In_{0.42}Ga_{0.58}N$ the bandgap of 1.91 eV is reached.

The third bandgap, 1.45 eV, is well suited for Gallium Arsenide [7], a well-known and widely used solar cell material for space applications. The lower bandgaps are fitted by adding Indium to Gallium Arsenide. The alloys $In_{0.25}Ga_{0.75}As$, $In_{0.45}Ga_{0.55}As$, and $In_{0.75}Ga_{0.25}As$ fit respectively the bandgaps 1.08 eV, 0.81 eV, and 0.55 eV. An overview of all of the materials can also be found below in Table 10.6.

Table 10.6: Solar Array Overview of Stages

Solar Array Stage	1	2	3	4	5	6
Solar Array Stage Length	7.127	6.190	5.254	4.450	3.767	3.181
Radius [m]	24.25					
Area [m^2]	1086.8	943.2	800.5	678.1	574.0	484.6
Bandgap [eV]	2.64	1.91	1.45	1.08	0.81	0.55
Solar Cell Material	$In_{0.2}Ga_{0.8}N$	$In_{0.42}Ga_{0.58}N$	GaAs	$In_{0.25}Ga_{0.75}As$	$In_{0.45}Ga_{0.55}As$	$In_{0.75}Ga_{0.25}As$

This cylindrical collection of solar cells can be visualised in the schematic below. Note that from the front view, the largest radius represents the circumference which the solar arrays span, the intermediate radius represents the frontal radius of the first stage filter, and the smallest radius represents the radius of the first black spot. From the side view, the dimensions at the bottom represent the lengths of the solar array stages (and filter lengths).

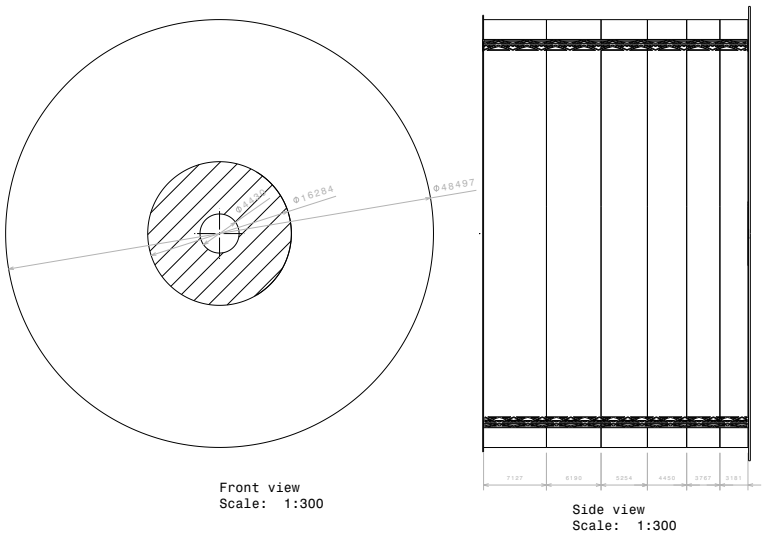

Figure 10.11: Schematic of the Solar Array Design

10.5. Optics of the Power Collection System

In this section, the function of the mirrors and filters will be presented through a schematic diagram. This schematic diagram will show the reflection of light from the primary and secondary mirrors, the reflection and transmission off of the first filter (however note that this happens for every filter, but for clarity only one case is presented), and the reflection of light from the mirror in the final stage.

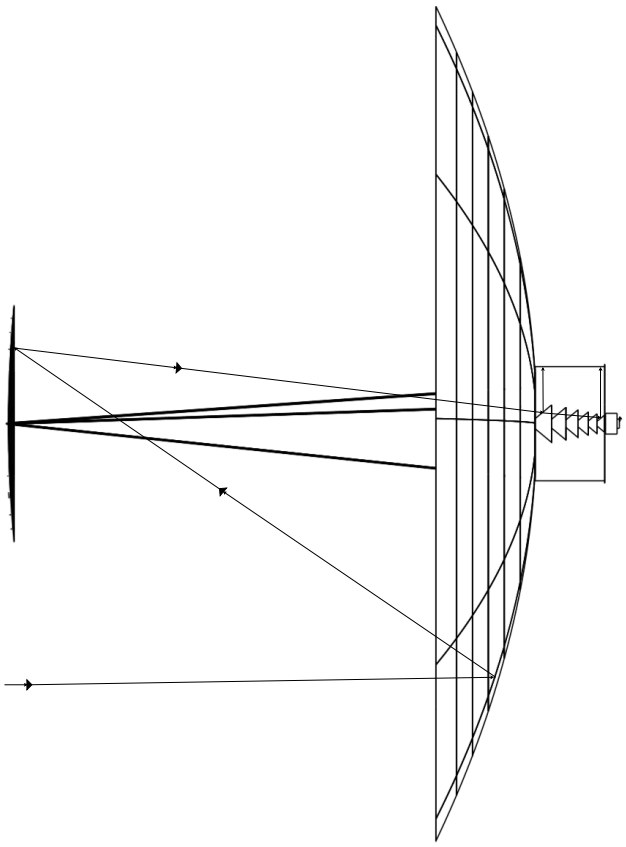

Figure 10.12: Optics of the Power Collection System (not to scale)

10.6. Power Transmission

After successful collection of the solar power through the solar cells it has to be transmitted to Earth for use. There are two main methods of wireless power transmission available: microwave transmission or transmission via laser [133]. However, from [94], it is clear that a microwave transmitter would require a diameter bigger than that of a single SPECTRE satellite, and therefore microwave power transmission was considered infeasible, and a laser power transmitter was chosen. As discussed in chapter 8, the laser should have a non-ionising frequency of light and should not be instantly absorbed as heat, as a result, sub-infrared is chosen as laser medium.

The required transmitted power of 1 GW is split over the 20 SPECTRE spacecraft, resulting in a required laser transmitter capacity of 50 MW for each spacecraft. The current technology of power transmission via laser are still in the low kW range. However recent tests from Lockheed Martin have proven weapon grade laser beams with capacities of over 30 kW [108], with the latest test reportedly providing 58 kW [18]. Extrapolating this increasing laser power and with the use of multiple laser transmitters the 50 MW range can be developed for the SPECTRE transmission system.

Furthermore, due to the choice of the orbit, at some points during the system's operation the transmitters' view of Earth will be obstructed by the primary mirror. Therefore, the most logical solution is to use a large boom to be able to point the transmitters past the primary mirror. This boom could be on a gimbal such that it can be pointed and orientated in any direction. In order to surpass the primary mirror, the length of this boom would have to be a minimum of 181 meters. Of course, there are also other possibilities that could be incorporated, however these would be more experimental and will be discussed in section 16.2. The further integration of the transmission system to SPECTRE can be found in section 11.4.

Currently, no accurate estimate can be put into the amount of laser transmitters required, however, assuming laser technology develops to an input power of 1MW, with an efficiency of 15%, each spacecraft would only require 50 of these laser transmitters. Currently, the masses of laser transmitters are approximately 0.5kg per Watt. However, this would make the system completely infeasible, which is why extra research must be put into laser power transmission, and further recommendations into this will also be discussed in section 16.2.

11

Engineering Design

The major function of the system, the power collection, has been designed. This chapter addresses system parts required to make the system work. This chapter describes the design and design processes for the astrodynamics and subsystems. These include important details on their size as well as interactions/interfaces with the rest of the system. The conclusion shall end with their individual contribution to the system as a whole in terms of mass and power.

11.1. Astrodynamic Characteristics

The orbit which the system will occupy determines how long it can produce power every day. It is hence important to optimise in order to meet requirements **M-ST-L-OPER-000**, **D-ST-L-OPER-002** and **D-SY-S-ECON-002**. To find the optimal orbit for this system, a Design Option Tree (DOT) was made based on the DOT from the Baseline report [19]. This new DOT can be seen in Figure 11.3. Here, only geocentric orbits were considered.

The three big divisions are High Earth Orbit (HEO), Medium Earth Orbit (MEO) and LEO. The subdivisions for LEO were sun-synchronous or not, for MEO there were no subdivisions made and for HEO there was geosynchronous and other HEO's. However, the red options have been eliminated due to infeasibility or being too weak. This is mainly due to large eclipse times or an inconvenient ground track not meeting requirements **M-ST-L-OPER-000**, **D-ST-L-OPER-002** and **D-SY-S-ECON-002**.

11.1.1. Trade-Off

To decide which orbit is most optimal for our system, a trade-off is necessary. The criteria and their weights along with a description can be seen in Table 11.1. The trade-off is then performed using a rubric and yielded the results seen in Table 11.2 which shows that GEO is the best option for this design. This is mainly due to the fact that it is almost continuously illuminated as well as the fact that it is always above the same point which makes power transmission a lot more simple. This is ideal for meeting requirements **M-ST-L-OPER-000**, **D-ST-L-OPER-002** and **D-SY-S-ECON-002**. The illumination of GEO is continuous with the exception of the spring and fall eclipse seasons.

During these periods, the eclipse durations will first get increasingly longer until after around three weeks, at the spring or fall equinox, the maximum eclipse duration of around 72 minutes is reached. After this, the eclipse length gradually decreases again while the Sun travels to one of the Tropics again.

Table 11.1: Trade-Off Criteria

Identifier	Criterion	Weight	Description
CR-OR-01	GSP Availability	0.25	The amount of contact with the GSP and where they are located.
CR-OR-02	Illumination Time	0.3	The amount of illumination per orbit
CR-OR-03	Required Delta V	0.18	Required delta V to achieve this orbit
CR-OR-04	Station Keeping	0.15	How much decay there is in this orbit
CR-OR-05	Environment	0.12	How hostile the environment is in this orbit

Table 11.2: Trade-Off Orbits

Orbit /Criterion	GSP	Illumination	Delta V	Station Keeping	Environment	Total
Sun-Synchronous Polar	2	5	4	3	3	3.53
Other LEO	2	3	5	3	5	3.35
GEO	5	5	2	5	3	4.22

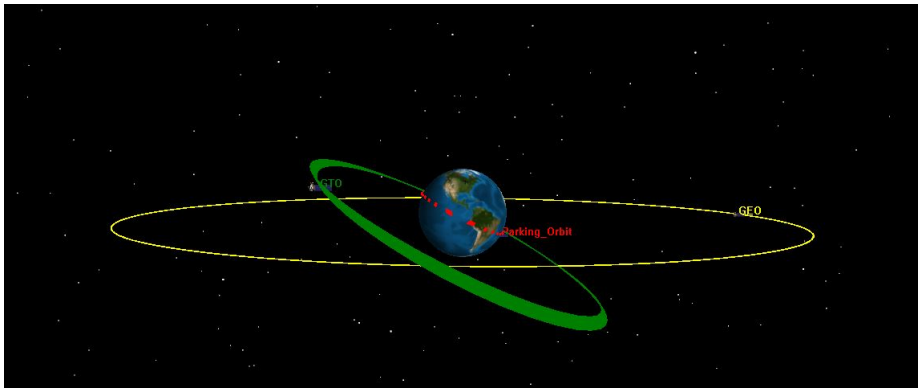

Figure 11.1: Trajectories from parking orbit to Geostationary Transfer Orbit (GTO) and GEO

11.1.2. Launch & Launcher Selection

To get to GEO, a large amount of energy is required. This means a suitable launcher had to be found. After an analysis of launcher costs and a more detailed mass estimation, it was concluded that no existing launcher was capable of providing this service and stay within the given budget. However, SpaceX is designing and building a fully reusable launcher called the BFR which would be capable of lifting 150,000.0 kg to GEO for only $ 7,000,000.0 [145]. This would meet requirement **M-ST-S-ECON-000**. Since this concept is only now being developed and these numbers are mainly used for marketing, the assumed capability was reduced to 45,000.0 kg to GEO and the launch cost increased to $ 15,000,000.0 per launch in fully reusable configuration. Furthermore, the BFR launch system proved also the most sustainable, and a more in depth analysis has been performed in chapter 8.

This launcher is inevitably coupled to the SpaceX launch facility that is being built near Brownsville, Texas [51]. This means the launch will happen at an inclination of around 26°. This is important since an inclination change needs to be done to reach GEO, which is an equatorial orbit.

It is important to keep in mind that it is not guaranteed that the BFR will be ready and fully operational by 2028, nor that it will have the specifications that are listed now. The extra margins used account for that, but in case the BFR is not ready by then the Falcon Heavy could also be used if the budget could be increased to account for around $1,500,000,000.0 launch costs including around 4% insurance (which is mandatory when launching with SpaceX) [66].

11.1.3. Trajectory

The trajectory is the route any launch will follow from the launch site to its final position in the GEO belt. By finding and optimising the trajectory, the amount of energy (and thus propellant) can be optimised as well. The trajectories are described below, and a graphical representation can be found in Figure 11.1.

Launch Trajectory & Parking Orbit
The launch trajectory is the path from the launch pad to the parking orbit. The exact trajectory is determined by SpaceX as they provide the launcher. The circular parking orbit is decided to be at 250 km altitude and launch site inclination (26°). Once this parking orbit is reached, the payload (production module, subsystem module and materials module) has a few orbits to deploy possible power systems and start up systems.

Geotransfer Orbit
After this has been completed, an engine burn is then performed to make the orbit elliptical and increase the parking orbit's apogee to the altitude of GEO (35786.0 km). These burns are also carried out by the BFR cargo spacecraft, and are always done at the perigee to maximise the manoeuvre efficiency.

Geostationary Orbit Insertion
Once the apogee is in the GEO belt, the spacecraft will circularise the orbit and meanwhile change the inclination. This means a combined manoeuvre is performed at apogee changing the semi-major axis to 42,157.0 km and the eccentricity back to 0.0 whereas the inclination now is 0.0° as well. The payload has now reached its operational orbit where it will stay during the mission lifetime of 30 years as well as the two years it takes to do the production.

Disposal
The disposal of the system is a mandatory requirement and should thus be accounted for, in order to meet **M-ST-S-ENVI-001** and **M-ST-S-ENVI-000**. To de-orbit a spacecraft from GEO, additional energy is required. It is therefor custom to place them in a so-called "graveyard orbit", where the spacecraft is passivated [99]. The Inter-Agency

Space Debris Coordination Committee (IADC) determined that the altitude increase of the graveyard orbit should be determined by the following equation:

$$\Delta H = 235 + (1000 \cdot C_R \frac{A_s}{m}) \tag{11.1}$$

Where ΔH is the altitude increase in kilometres, the 235 km is the standard safety margin, C_R is the solar radiation pressure coefficient (assumed to be one), A_s is the frontal area of the spacecraft and m is the spacecraft mass [46]. $\frac{A}{m}$ is also known as the ballistic coefficient. In the case of this system, this means the disposal orbit is around 5611.26 km above the GEO belt. The disposal orbit will be circular and be in the equatorial plane with a semi-major axis of 47768.3 km.

Once in the disposal orbit, the spacecraft will be passivated. This means that all leftover propellant is vented through a normally closed pyrotechnic valve that is implemented for this sole purpose. All electrical energy is dissipated from the spacecraft as heat and all systems are shut down. This is done to prevent high thermal loads from causing explosions and increasing the space debris.

11.1.4. Station Keeping

Station keeping means that the spacecraft should be kept in the same orbit throughout its operational life. Reasons why it could deviate from this orbit consist of, but are not limited to, the following: aerodynamic drag, solar radiation and gravity forces. However, the most significant in GEO are solar radiation and gravitational pull from the sun and moon.

Solar Radiation Pressure

The solar radiation pressure comes from the fact that photons emitted by the sun have momentum, thus when hitting the mirrors of the spacecraft, this momentum is transferred and perturbs the orbit. Since this system is always pointing towards the sun, these accelerations and decelerations will counter-act each other. However, since this will not be exactly true, a safety margin will be added in the ΔV budget.

Solar & Lunar Gravity Pull

For North-South station keeping, the gravitational pull of the Moon and Sun has the biggest effect: the orbit pole is perturbed by 0.85 ° per year [29]. To counteract this, around 45 m/s per year is needed [127]. For East-West station keeping, the effect is an order of magnitude smaller at only around 2 m/s per year [127].

11.1.5. ΔV Budget

This energy that is required to reach orbit, perform manoeuvres and keep station is usually expressed in terms of velocity change, ΔV. To know velocity changes, one needs to know orbital velocities. These can be found using the Vis-Viva Equation:

$$V = \sqrt{\mu \cdot (\frac{2}{r} - \frac{1}{a})} \tag{11.2}$$

Here, μ is the standard gravitational parameter ($3.986004418 \cdot 10^{14} m^3 s^{-2}$), r is the distance between the two orbiting bodies and a is the semi-major axis.

Launch
Upon launch, the velocity is zero, however to escape the Earth and get into orbit, a velocity change is needed which is found by filling in the above equation. It was said that the parking orbit was a circular orbit at 250 km (a = 250 km + 6371 km) at launch inclination, so the Vis-Viva Equation becomes more simple for circular orbits:

$$V = \sqrt{\frac{\mu}{r}} \tag{11.3}$$

Filling in that r equals a, the orbital velocity of 7,759.02 m/s is found, which is the ΔV the launcher needs to provide to get the payload into parking orbit (not accounting for the losses encountered during ascent).

Parking Orbit to Geotransfer Orbit
Once this parking orbit has been achieved and all systems have been checked, the transfer to GTO is also performed by the launcher. To find this velocity change, the velocity at the perigee of the needs to be found. The difference between this velocity and the parking orbit velocity is the required ΔV to change to a GTO.

This velocity change is found again using the Vis-Viva Equation where r is the distance at perigee which is 6621 km. The semi-major axis is then $\frac{250km+2*R_e+R_{GEO}}{2}$ where R_e is the Earth's radius and R_{GEO} is the altitude of GEO, equal to ca. 35786 km. Filling this in, a perigee velocity of 10,201.05 m/s is found, which implies a ΔV of 2442.29 m/s is required. This is most likely spread out over multiple burns around the GTO perigee.

GTO to GEO
To get from GTO into GEO, an engine burn is performed at GTO apogee by the launcher, which changes the inclination to 0.0° and raises the perigee at the same time. This burn will probably also be performed in multiple stages, but for the ΔV this does not change anything. Using the cosine rule, the following relation was obtained:

$$\Delta V^2 = {V_{GTO,a}}^2 + {V_{GEO}}^2 - 2 \cdot V_{GTO,a} \cdot V_{GEO} \cdot cos(\Delta i) \tag{11.4}$$

Here, $V_{GTO,a}$ is the apogee velocity in GTO, V_{GEO} is the velocity in GEO and Δi is the desired inclination change (26°). This yields a result of 1779.31 m/s.

GEO to Disposal
To get into the disposal orbit at 47768 km, the orbital velocity change is found again using the Vis-Viva Equation to find the disposal orbit velocity and is found to be 2888.68 m/s. This means a ΔV of 186.24 m/s is required to achieve this orbit. The ΔV budget is summarised in Table 11.3.

Table 11.3: ΔV budget

Trajectory	ΔV **[m/s]**
Launch	7759.02
GTO	2442.29
GEO	1779.31
Station Keeping	47 · 32 years
Disposal	186.24
Contingency Factor	1.25
Total	17088.58

11.1.6. GEO Regulations

Geostationary orbit is not just defined as a singular orbit but as a "GEO Belt". This belt has some regulations imposed by the International Telecommunications Union (ITU) which ensures that communication frequencies of different missions do not interfere with each other and also dictate that there must be a certain physical separation distance between GEO satellites [38]. Following these relations would ensure no objects in orbit will be harmed (see **M-ST-S-ENVI-000**). This is why the GEO Belt is divided into "slots", which are currently 2° longitude over North-America at this moment, which is the equivalent of around 1470 km [148].

These slots need to be requested, and within this slot the system must be operated within a certain orbital "box". This box is around 0.1 ° of longitude (70 km). For SPECTRE, this will be taken into consideration in the design of the cluster. The license to occupy a slot in GEO will be requested but is not considered to be a problem at this moment since this is 10 years in advance.

11.1.7. Cluster Flying

Since the SPECTRE system will fly in a cluster, this needs to be taken into consideration. The spacecraft will fly in the same plane, which is that perpendicular to the GEO belt. They will have a small offset such that power can be transmitted freely to the ground without interference of other spacecraft in the cluster.

The relative motions of the spacecraft is seen as a rotating circle, due to the small differences in eccentricity and inclination for each of the spacecraft, as seen in Figure 11.2 [111]. This way, the spacecraft will orbit the "centre" of the GEO belt once each day, and are separated from each other by about 1 km such that the production module can easily reach the spacecraft.

The control of these spacecraft is very complex at these close distances, and a subject that needs to be further investigated but is outside of the scope of this conceptual design.

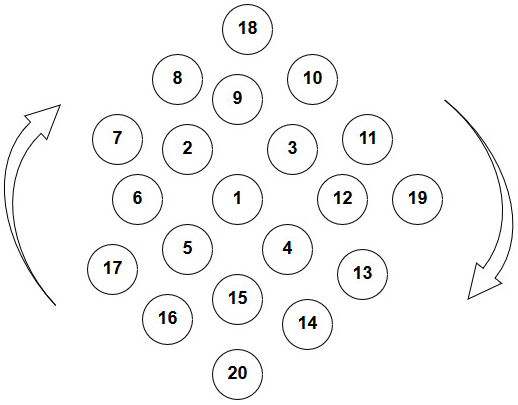

Figure 11.2: Cluster Configuration

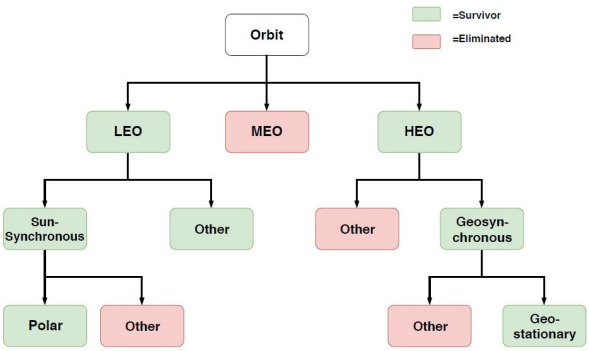

Figure 11.3: DOT Orbits

11.2. Subsystem Design

This section will describe the design approach and the conceptual design for all required subsystems for the SPECTRE system. The propulsion, ADCS, TCS, EPS, Command & Data Handling System (CDHS) and TT&C subsystems are discussed, as well as the spacecraft structure and required maintenance systems.

11.2.1. Propulsion System

From the launch to the GEO orbit insertion, all ΔV is provided by the BFR. However, to perform station keeping in GEO for almost 33 years and then move to a disposal orbit, a dedicated propulsion system must be present in order to meet **M-ST-S-ENVI-000/001** and all the propulsion requirements. As seen in Table 11.3, the propulsion system must provide 2112.8 m/s to each spacecraft. It was decided that the Busek BIT-7 Ion thruster would be used as it has been fully developed, tested and used in space and has accurate data [37].

This thruster has a thrust of 11 mN at a specific impulse of 3300 seconds. It requires 460 W of input power per thruster and the Xenon propellant has a mass flow of 3.5 $\frac{cm^3}{min}$ per thruster [37].

Disposal Orbit Propellant
Knowing the required ΔV, specific impulse and the dry mass of the system (about 18700kg per spacecraft), first the propellant mass to achieve the disposal orbit can be found using the Tsiolkovsky equation:

$$\Delta V = I_{sp} \cdot g_0 \cdot ln\left(\frac{m_{final}}{m_{dry}}\right) \tag{11.5}$$

Which can be rearranged to find the propellant mass as:

$$m_{prop} = m_{dry} \cdot \left(e^{\frac{\Delta V}{I_{sp} \cdot g0}} - 1\right) \tag{11.6}$$

Here, I_{sp} is the specific impulse of the thruster in seconds and g_0 is the gravitational constant of 9.81 m/s^2. Using this relation with the given thruster data, ΔV and dry mass leads to a required propellant mass of 135 kg per spacecraft. This means **D-SY-P-PROP-001** and **D-SY-P-PROP-000** are met.

Station Keeping Propellant
To keep station, 47 m/s is needed every year as mentioned in subsection 11.1.5. To account for unexpected burns, losses and CMG desaturation, a safety factor of 1.25 was used. These burns happen yearly, which means every year a certain amount of propellant is used, which makes the spacecraft mass a bit lighter every year and the required amount of propellant less along with it. It was found that assuming the burns happen in one go every year, 29,029.0 kg of propellant was needed in total, to keep station for almost 33 years. This meets **M-SY-P-RPOP-001**.

Propellant Storage
To store this propellant, high pressure tanks are employed. These tanks use a Titanium liner and a composite shell, such as the MT Aerospace S-XTA-60 Xenon storage tank [24]. These tanks are designed for MEOP of around 250 bar, which means they have been burst tested to 450 bar [24].

When Xenon gas is stored at 250 bar, the density becomes 1440.25 $\frac{kg}{m^3}$ [89] as prescribed in **M-SY-P-PROP-006**. At this density, and using the previously found propellant mass per spacecraft, the required tank volume is found to be

1.01 m^3 for every spacecraft. To size this tank, the shape was approximated by a cylinder with two half spheres as end caps. This leads to a height of 1m and a radius of 1m as well.

Thruster Positioning
Since the spacecraft will be rotating for deployment, the thrusters will rotate as well. It was decided that it is acceptable to fire them within 10 ° of the axis pointing to the center of the Earth. Using 5 thrusters, this means every thruster will be spaced 72 ° apart.

11.2.2. Attitude Determination & Control System

The ADCS is the system that, as the name already reveals, determines and controls the system attitude. This includes sensors, actuators and stabilisation methods. First the operational modes were identified after which the disturbances were quantified and the control mode was selected. To actuate this control mode, actuators were selected and sized and the sensors were also chosen and positioned.

Operational Modes
The operational modes are the different modes the ADCS will be in depending on the phase the system is. These operational modes are shown in Table 11.4 along with their explanation.

Table 11.4: ADCS Operational Modes

Operational Mode	Explanation
Acquisition & Insertion	Decoupling from BFR, positioning into right attitude for production
Production	During production the system is kept pointed at the sun
Normal Operations	The system is still kept pointed at the sun, the transmitter is pointed at the receiver
Slew Mode	Provide slew rate and stabilise during slew
Disposal	Keep orientation for thrusting to disposal orbit
Safe Mode	Keep rough orientation during emergencies & unexpected power losses

Disturbances
The main need for an ADCS comes from the fact that in orbit there are multiple disturbances. These disturbances alter the spacecraft attitude from the initial position and, without further action, can be catastrophic for a mission. These disturbances include, but are not limited to, solar radiation pressure, aerodynamic drag, gravity gradients, magnetic field, outgassing etc. However, these can also come from uncertainties such as thruster misalignment, c.g. uncertainty, thruster output mismatch, liquid slosh, flexible body dynamics and thermal shocks [83].

To quantify these disturbances, first those present in GEO need to be identified. Gravity gradient and aerodynamic drag are very weak to insignificant in GEO, so these will not need to be quantified. Solar radiation pressure and the magnetic field are however very much an influence. To find the solar radiation pressure per spacecraft, the following relation was used [83]:

$$T_s = \frac{\Phi}{c} \cdot A_s \cdot (c_{p,s} - c_m) \cdot (1+q) \cdot cos(\phi) \tag{11.7}$$

Here, T_s is the disturbance torque on each spacecraft due to solar radiation, Φ is the solar constant at $1366 \frac{W}{m^2}$, c is the speed of light (299,792,458 m/s) and A_s is the frontal area of each spacecraft, which is 84169 m^2. $c_{p,s}$ is the solar radiation centre of pressure, and c_m is the centre of mass of the system while q is the reflectivity of the spacecraft, which is 0.9 in this case, and ϕ is the incidence angle which is 0.0° worst case. This leads to a solar radiation disturbance torque of 0.0364 Nm.

To find the magnetic disturbance torque, the following relation was used [83]:

$$T_m = D_m \cdot \frac{M_m}{R^3} \lambda_m \tag{11.8}$$

Here T_m is the disturbance torque due to the magnetic field, $D_m$is the spacecraft residual dipole moment assumed to be $20 A \cdot m^2$ and M_m is the Earth magnetic moment multiplied by the magnetic constant, leading to $7.8 \cdot 10^{15} T \cdot m^3$. The distance from the spacecraft to the centre of the Earth is represented by R at 42157 km and λ_m is a unitless constant which varies from 1 at the equator to 2 at the poles, so equal to 1 in this case. This leads to a magnetic disturbance torque of $2.08 \cdot 10^{-6}$ Nm, which is significantly smaller than the solar radiation pressure torque.

To account for the other smaller disturbances and uncertainties, a safety factor of 1.25 was used on the total disturbance torque, meaning the maximum disturbance torque is found to be 0.04555 Nm.

Control Method Selection

To stabilise this spacecraft and control it, a method should be chosen. As there are many different options, a DOT was created as can be seen in Figure 11.4. Since the gravity field and magnetic field in GEO are not strong enough to use for passive or active stabilisation, these were considered impossible. Momentum bias was considered too weak since it does not provide three-axis control and rate damping is too inaccurate for the requirements (it is however very robust for a safe mode).

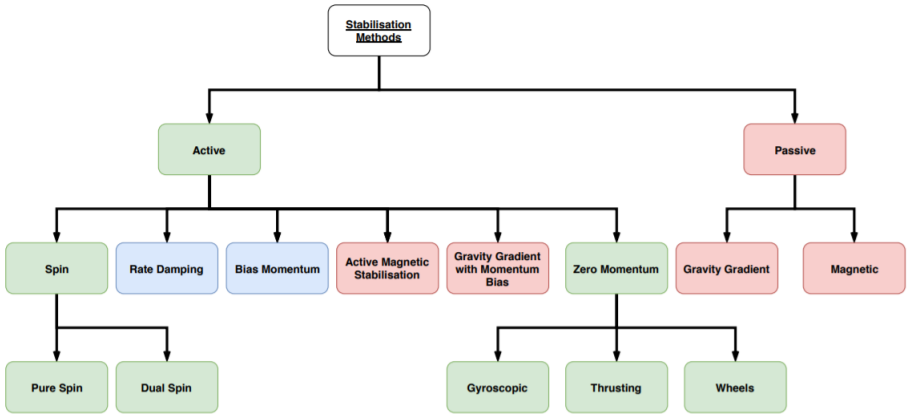

Figure 11.4: Control Method DOT

These survivor concepts again entered a trade-off with criteria and weights as seen in Table 11.5.

The results of the trade-off are shown in Table 11.6. As can be seen, zero momentum control using gyroscopic effects is the best option in this case. This is mainly due to the large amount of momentum storage needed per orbit and the impracticality of spin and dual spin.

Table 11.5: Stabilisation Method Trade-Off Criteria and Weights

Identifier	Criterion	Weight
CR-AD-01	Mass	0,2
CR-AD-02	Accuracy	0,2
CR-AD-03	Reliability	0,2
CR-AD-04	Implementation	0,1
CR-AD-05	Maintainability	0,15
CR-AD-06	Impact of Failure	0,15
	Total	1

Table 11.6: Stabilisation Method Trade-Off

	Mass	Accuracy	Reliability	Ease of Implementation	Maintainability	Impact of Failure	Total
Dual Spin	3	2	1	1	1	1	1,6
Thrusting	1	3	3	2	2	2	2,2
Wheels	1	3	2	2	1	2	1,85
Pure Spin	3	2	2	2	1	1	1,9
CMG	3	3	2	3	2	2	**2,5**

Actuators

To actuate this type of stabilisation, a CMG is used. More specifically, Double Gimbal CMG's with unlimited gimbal freedom about each axis. This is an actuator where a rotor spins at relatively high velocities while the gimbal allows the orientation of the wheel to change and thus tilt the angular momentum and provide torque or momentum storage.

The design of these CMGs is a fairly complex and expensive procedure, so it was decided that existing CMGs would be used. The International Space Station used four L3-Communications CMGs which provide 4760 Nms of momentum storage and can each provide a torque of up to 258 Nm [43]. These provide control in all directions, so the question is only how much momentum needs to be stored. To find this, the momentum storage for the slew rate and the momentum storage in a wheel were taken into account. The momentum storage for the slew rate is determined as follows [83]:

$$L_{Slew} = 4 \cdot \dot{\theta} \cdot I \frac{1}{t^2} \tag{11.9}$$

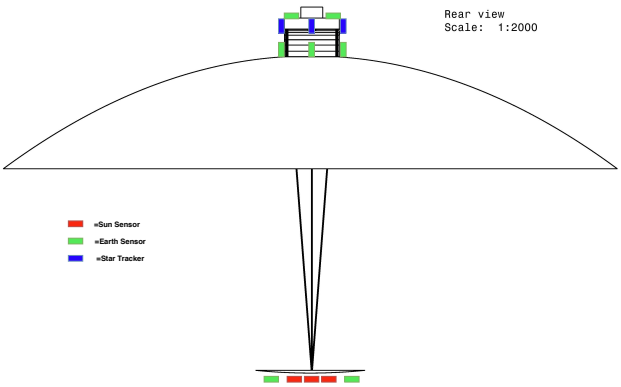

Figure 11.5: ADCS Sensor Positioning

Here, L is the angular momentum that needs to be stored, $\dot{\theta}$ is the required maximum slew rate of 0.1 °/s, I is the mass moment of inertia of the system, which is estimated at 50,000.0 kgm^2 (axis with highest inertia is used) and t is the time in which this slew needs to be completed, in this case it is expressed per seconds, so 1 second. This leads to a required momentum storage of 3490 Nms. The mass moment of inertia estimation was done based on data from the ISS [33].

For the momentum storage in a wheel, the following relation was used [83]:

$$L_{MOM} = \frac{T_D}{\theta_a} \cdot \frac{P}{4} \tag{11.10}$$

Here, T_D is the total maximum disturbance torque of 0.04555 Nm, θ_a is the allowable motion (the accuracy) of 1 ° and P is the orbital period of 86,164.0 seconds (length of a sidereal day). Entering these values in the equation leads to a required momentum storage of 37,220 Nms, which is significantly larger than the slew rate momentum storage.

To store this momentum, nine CMG's per spacecraft are required (one for redundancy). This means 180 CMG's are needed for the whole space segment. Another consideration is the lifetime of these actuators: they have been applied to the ISS in space but have a lifetime of 10 years. Also, two of the four CMG's failed before the end of their lifetime.

Considering this was twenty years ago, and the fact that equally powerful CMG's that have longer lives are under development it is not considered to be a problem for this system [87].

Sensors

In order to control the attitude of a spacecraft, first the attitude must be known. To know this attitude, sensors are used, both relative and absolute. There are multiple sensors available, which will now be shortly discussed. There are two types of relative sensors, which measure a change in attitude and acceleration compared to an initial position. The first is a gyroscope, the second is a Motion Reference Unit (MRU).

For absolute sensing, there are horizon sensors (also known as Earth sensors) which sense the IR radiation from the Earth's surface and there are sun sensors which use the sun to determine the orientation of the spacecraft. Another possibility is an orbital gyrocompas which use gyroscopic precession to determine a geometric direction [55]. There are also star trackers which use the position of stars and the last option are magnetometers which use the Earth magnetic field to determine the spacecraft attitude.

Since the goal of the ADCS is to point the system at the sun, a sun sensor is logical to determine the attitude around the pitch and yaw axis, which leaves one axis undetermined. For convenience, this second sensor will be mounted aft of the concentrator which means it will be eclipsed by them. This makes it ideal for horizon sensors and star trackers, which will be placed in a multitude to allow for rotation around the Earth and redundancy. The positioning of the sensors can be seen in Figure 11.5.

As can be seen, there are three sun sensors on the back of the secondary concentrator and one coarse sun sensor which can be used in safe mode to allow for rough attitude sensing. There are also two Earth sensors which will be used when the spacecraft is in eclipse. Aft of the concentrator part there are 4 Earth sensors which are positioned equally along the radius of the filter-photovoltaic complex. This is to allow for rotation around the Earth and redundancy. There are also 4 star trackers which can be used during eclipses. Finally, at the transmitter there are two more Earth sensors to allow for attitude sensing when the spacecraft is exactly between the sun and Earth.

11.2.3. Thermal Control System

This section presents the TCS, which has the function of keeping all components on the spacecraft within their allowable temperature limits. This is to ensure all **M-SY-P-THER-XXX** requirements are met. In SPECTRE, incoming sunlight is partially absorbed at each component it strikes, which generates a very large amount waste heat in the system, making the TCS one of the most critical subsystems in a SSPS design.

Contrary to heat flows in an atmosphere, heat can only be radiated or conducted in a vacuum. The TCS is based on those two heat flows. It has to ensure enough heat is radiated away from the system to keep it cool enough, and the conductances should be designed such a way that the different allowable temperature ranges of the components are all met. For all components and joints, the incoming and outgoing radiation as well as the conductance have been computed in order to understand how the heat flows in the spacecraft.

This section is split up into 4 parts. First the methods to determine the radiation and conductance coefficients will be explained. Afterwards, the full thermal model will be presented. This thermal model is then used to design the complete thermal control system.

Radiation
In space there is no air to convect heat, so all waste heat generated in the system has to be dissipated to the environment through radiation. Every surface with a temperature above 0K radiates IR radiation, but the amount of heat radiated depends the emissivity, area and temperature of the surface. In order to calculate the radiative heat transfer from one surface to another, the geometric view factor, which describes the percentage of radiation leaving one surface that hits the other surface, between the two surfaces is required as well. The view factors were calculated analytically, using several references to find the equations for the view factors between all thermal nodes [40][34][140][96][72]. The complete equation describing radiative heat transfer between two surfaces is shown in Equation 11.11 [83],

$$Q_r = \sigma_s \cdot \epsilon \cdot A_r \cdot F_r \cdot (T_1^4 - T_2^4) \tag{11.11}$$

where σ_s is the Stefan-Boltzmann constant, ϵ is the surface emissivity and F_r is the view factor from surface 1 to surface 2.

Conduction
Heat conduction occurs when two solid surfaces touch each other. The heat flux is related to the thermal conductance coefficient according to Equation 11.12.

$$Q_c = h_t \cdot A_c \cdot \Delta T \tag{11.12}$$

the total thermal conductance coefficient can be decomposed in contact conductance, radiative conductance, and gap conductance.

$$h_t = h_c + h_r + h_g \tag{11.13}$$

At microscopic level, surfaces are never perfectly smooth. This causes a reduction in the actual contact area between

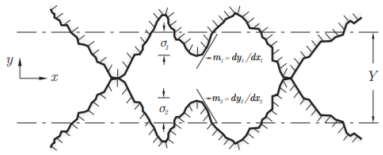

Figure 11.6: Microscopic interpretation of two surfaces in contact [25]

two surfaces, as is illustrated in Figure 11.6. The real contact area is typically only a few percent of the apparent contact area [126]. Heat conductance occurs at the actual contacting points, while gap and radiative conductance might occur through the gaps in between the contact points.

In a vacuum environment like space, there is no gas that occupies the gap's spaces. Therefore gap conductance is eliminated for this designed system. Furthermore, since the system is not likely to exceed temperatures over 900 K, the radiative conductance can be dismissed as well [25]. This leaves only the contact conductance. Equation 11.13 then becomes:

$$h_t = h_c \tag{11.14}$$

The goal of this section is to find the thermal conductance coefficients of all joints in order to find the total heat fluxes. To find those thermal conductance coefficients, the following assumptions are made.

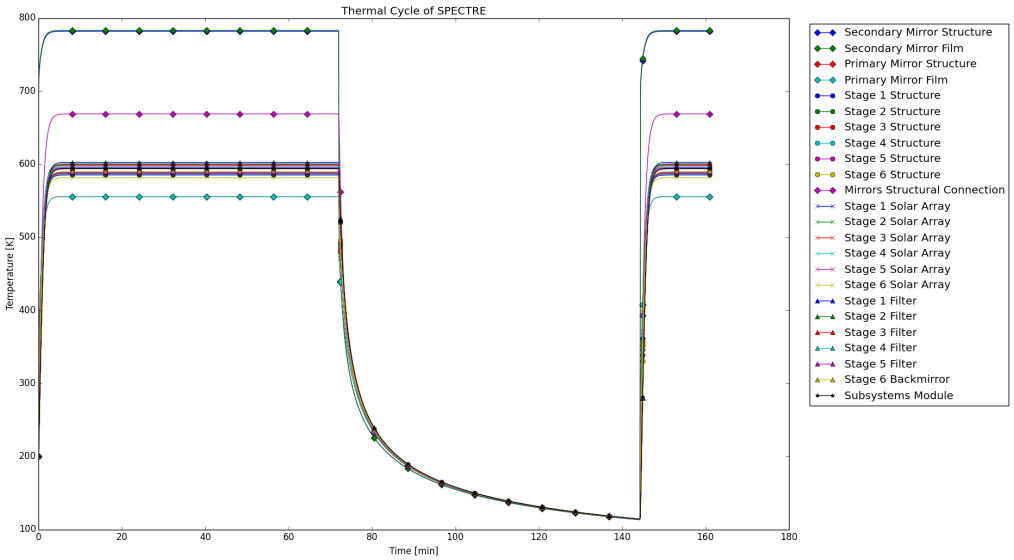

Figure 11.7: Simulation of component temperatures during system operation. The large temperature drop in the middle is caused by a simulated eclipse period.

- All contact surfaces are relatively smooth
- The deformations at the contact points are solely plastic, not elastic.
- The gaps between the contact points are vacuum
- Material properties are constant throughout a component and do not significantly differ with temperature.
- the bonding material between structures (adhesives, bolts, etc) has no influence on the conductance.
- The pressure is constant over the contact area.

In general, it is really hard to find this analytically since the contact area is nearly impossible to determine without large uncertainties. Therefore this is usually done experimentally. There have been many studies that estimate the thermal conductance coefficient, the analysis that is used in this section is from Mikic [92]. It is mathematically expressed in Equation 11.15

$$h_t = 1.13\left(\frac{k_e \tan\theta_e}{\sigma_e}\right)\left(\frac{P_c}{H_e}\right)^{0.95} \tag{11.15}$$

It is assumed that all joints have relatively smooth surfaces, hence for each component, θ is set at 0.03 rad, and σ at 0.1 μm. Those are typical values for smooth surfaces [92]. The pressure is assumed to be low, 0.1 MPa [85], between the space web and the thin film aluminium of the mirrors since those are lightweight and fragile components. Structures between mirrors are slightly tighter attached, 10 MPa, and joints that require high stiffness, like the joints at the filters need higher contact pressures. Those are set at 100 MPa to 1 GPA. The structure of the collector module are seen as separated components in the thermal model for computation convenience, but they are in fact one solid structure. Hence, to simulate this solid structure, the contact pressures between the structure stages have contact pressures of 100 GPa.

Thermal model

The conductance and radiative coefficients have been worked out and implemented in a thermal model. The temperatures for each component over time are determined in Equation 11.16,with H_c being the heat capacity of the node.

$$T = \frac{(Q + Q_{in})}{H_c}\, t \tag{11.16}$$

Where Q is the sum of the heat flows due to conduction and radiation.

$$Q = Q_r + Q_c \tag{11.17}$$

This is computed for 24 isothermal nodes that represent major components in our spacecraft in order to determine whether they are within their thermal limits. Furthermore an eclipse has been simulated to see the temperature fluctuations the system needs to sustain. The results are shown in Figure 11.7.

Identifying Critical Elements

Figure 11.7 shows the results of a thermal simulation of the system without any thermal design measures present. It is immediately clear there are several problem areas that have to be addressed by the thermal control subsystem. First

of all, two of the most critical parts of the system, the solar arrays and the subsystem module, reach an equilibrium temperature of 600K, which is almost twice as high than their maximum allowable temperature of 300K. The optical filters reach an equilibrium temperature of about 600K as well, with is 100K higher than their maximum allowable temperature of 500K. The extremely high temperature of the secondary mirror, which is close to 800K, might be a problem area as well.

Besides the high temperatures, it can be seen the simulated eclipse creates very high temperature gradients, since the spacecraft is still dissipating the same amount of heat as before the eclipse for a short time, with no heat entering the system. These high temperature gradients may cause a lot of problems at joints because of the different thermal expansion coefficients in different materials, as well as damage the filters that are made from several different thin-film layers, and are therefore an area of concern as well.

Thermal Control Design

The back side of the primary mirror has a very large surface area, as well as an almost continuous view to free space, so it automatically acts as a heat sink. The first design measure therefore was to apply a higher emissivity coating to the backside of the primary mirror to make it a more effective radiator. However, this coating is not enough to lower the Collector and Subsystems Module (C&SM) temperatures below an acceptable limit. It was estimated from the thermal model results that an additional 10MW per spacecraft had to be dissipated to keep the critical components within acceptable temperature ranges, which results in a very high required radiator area. It was therefore decided other methods of heat dissipation should be explored. A design option tree shown in Figure 11.8 was thus created to identify all approaches for dissipating this large amount of waste heat.

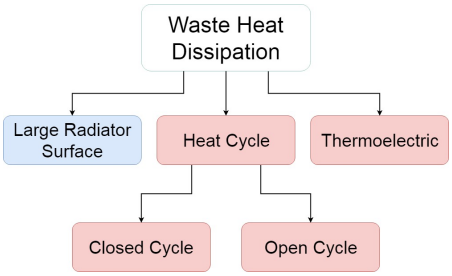

Figure 11.8: Design Option Tree for SPECTRE waste heat dissipation

Two options were discarded from the start, thermoelectric and open cycle heat dissipation. Thermoelectric heat dissipation is achieved by reverse operation of a thermoelectric generator like a Seebeck converter. The efficiencies of thermoelectric converters are still very low however (lower than 10% [44]), and therefore the electric power generated by a SPECTRE satellite will not be enough to use for cooling with thermoelectric converters. The second option is using a heat cycle to convert thermal energy to mechanical work to cool down the system. In a open cycle heat engine the working fluid or cryogen used to cool down the system is consumed and released into space. For the required mission duration of 30 years and the estimated waste heat levels, this will result in thousands to millions of tonnes of required cryogen, so this is obviously not feasible for the SPECTRE system. Closed cycle heat engines were considered, as these are capable of very high heat conversion rates. However, all heat engines are limited to the ideal Carnot efficiency, and therefore the amount of electric power necessary to dissipate the waste heat will always be higher than the amount of waste heat dissipated. Since the primary function of the SPECTRE system is to produce useful power, the power load required by closed cycle heat engines is not considered to be feasible either.

Having explored all other options, it is concluded a large radiator surface will be necessary after all. Due the high mass increase of adding large, additional radiator 'fins', another method of increasing the radiated heat had to be found. Using the developed thermal model, such a method was found by running a large amount of heat pipes from the C&SM to the backside of the primary mirror, effectively increasing the conduction from the thermal source to the thermal sink, increasing the effectiveness of the radiator surface.

Lastly, the extremely high temperature of the secondary mirror, caused by the incident concentrated sunlight, had to be decreased. It was decided large heat pipes will be running along the struts to increase the heat conduction between the secondary mirror (a heat source) and the primary mirror (a heat sink), in order to decrease the temperature of the secondary mirror.

With these added heat pipes the TCS will be able to keep the critical components below their maximum temperature range during the entire system operation. The result of this thermal control design is shown in Figure 11.10.

The additional weight of the above mentioned heat pipes is based on the total heat flow it conducts. This is determined by computing the difference in total heat flow, before and after the heat pipes have been simulated in the thermal model. This turned out to be 608988 W. Using an average heat transfer capacity of 100 W/m from ammonia

and a heat pipe density of 145 g/m [58], the total weight of the heat pipes is 883 kg. This is however not taking into account the distance the heat pipes have to travel between the components. Due to this, the total weight of the heat pipes is increased to 1000 kg.

Design for Eclipse
With the thermal control system sized for full-sun operation, the next step is to solve the problem of the high temperature gradients during eclipse transitions and the too low temperatures during eclipse. The first measure taken is to block heat pipe conduction between the C&SM and the primary mirror when the spacecraft goes into eclipse, so the heat in the C&SM is retained for longer. The longest eclipse duration the system will encounter is 72 minutes, and because of the large external surface this will still cause the C&SM to cool down too much. To limit this heat loss it is decided thermal energy storage will be needed.

Thermal energy storage has already been used on Earth on very large scales, but is still a very new concept in aerospace applications. The principle of thermal energy storage is based on using a Phase Change Material (PCM) to store heat. During hot operation, the PCM will undergo a phase change (either melting or evaporation) which stores heat as enthalpy, and the PCM will then be insulated from the rest of the system. In cold operation (during eclipse) the PCM will be reconnected to the rest of the system, so heat will be released again as the PCM returns to its original phase.

In order to size the thermal storage, an estimation of the required stored heat had to be made. The thermal model was used to sum the heat fluxes out of the C&SM components over the entire eclipse duration, in order to estimate the total lost thermal energy in those components. It was assumed this is the minimum amount of energy that will have to be stored. The resulting required thermal energy per spacecraft is approximately 500 MegaJoules. Different PCM materials were explored, but hydrated salts were determined to be most feasible for space applications with heat levels as high as in SPECTRE, especially because solid-liquid PCMs allow for lighter container design than liquid-gas PCMs. From [39], Lithium Chlorate Trihydrate (chemical formula: $LiClO_3 \cdot H_2O$) seems to be the best option, with a melting point of 8°C and a latent heat capacity of 253 kJ/kg. The minimum mass based on this PCM and the estimated required thermal energy storage is found to be approximately 2,000 kg.

At this point in the design, it is not yet possible to fully calculate the effect of the thermal energy storage. More research has to be performed on the implementation of the thermal energy storage into the SPECTRE system.

Finally, to smooth out the temperature gradients at the starts and ends of eclipses even more, the concentration of light on the secondary mirror and the rest of the spacecraft is reduced just before entering and after leaving eclipse. this is accomplished by adjusting the guy-wires of the mirrors. This results in a more gradual transition between the full sunlight phase and the eclipse phase in terms of temperature.

Complete Thermal Subsystem Design
At the start of the thermal control design process, 3 problems were indicated. The first problem was the very high temperature of the C&SM in full-sun operation, which was solved by connecting them with highly conductive heat pipes to the primary mirror. The second problem, the extremely high secondary mirror temperature, was solved by running large heat pipes along the supporting struts to the primary mirror. The third problem, the heat loss during eclipse, was solved by two design measures. Firstly, the conductance of the heat from the C&SM to the radiator (the primary mirror) will be stopped during eclipse to retain more heat. Secondly, a thermal energy storage container will be placed in each satellite to keep the spacecraft warm enough during eclipses.

Figure 11.9 shows the complete TCS architecture. The backside of the primary mirror will be covered in a Loop Heat Pipe (LHP) network that runs along the space web to make the mirror a very effective radiator. Due to the high temperature of the secondary mirror, the heat pipes between the two mirrors will use a different working fluid and their condenser ends will be connected to the primary mirror LHP through heat conductance strips. The C&SM will be covered with a LHP network to conduct heat to and from the components. During full-sun mode, this LHP network, which acts as heat source, will be connected to the primary mirror LHP network (the heat sink) through a conductance. When eclipse starts, the system will go in eclipse mode, which disconnects the C&SM LHPs from the primary mirror, and connects the thermal storage in the back of the spacecraft to the C&SM through a similar conductance, so it can act as heat source to keep the spacecraft warm. When the eclipse ends, the C&SM LHP network will be connected to the primary mirror again, and the thermal storage will be disconnected once it is heated up again. The result of the designed Thermal Control System is shown in Table 11.7.

Besides meeting all mandatory thermal requirements (**M-SY-P-THER-XXX**), this thermal control solution also makes sure the system meets requirements **D-SY-P-THER-000**, **D-SY-P-THER-001**, **D-SY-P-THER-002**. It does not yet meet requirement **D-SY-P-THER-003** however, because not enough is known about the toxicity of Lithium Chlorate Trihydrate to confirm whether or not it meets the requirement. The working fluid of most of the heat pipes, ammonia, is considered non-toxic as it has been used safely in the industry for a long time. The materials of heat pipes themselves

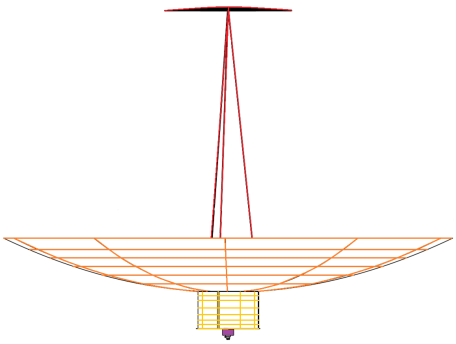

Figure 11.9: Overview of the complete Thermal Control System architecture. The mirror-to-mirror heat pipes are shown in red, the primary mirror LHP network is shown in orange and the C&SM LHPs are shown in yellow. The thermal energy storage container is located in the subsystem module (shown in purple).

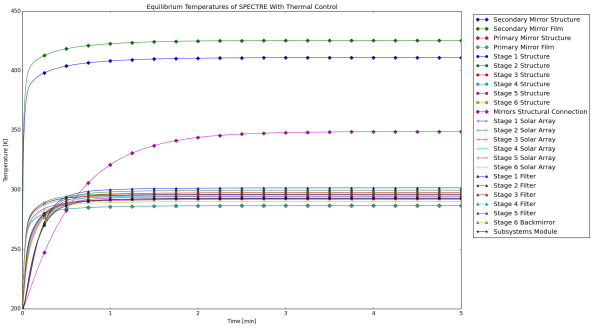

Figure 11.10: Simulation of component temperatures in full sunlight with thermal control

and the working fluid of the mirror-to-mirror heat pipes have yet to be chosen, so no conclusions can be drawn on their toxicity.

Table 11.7: The minimum and maximum allowable temperatures of all critical components compared to the estimated temperatures before and after thermal control implementation. The minimum temperatures with thermal control are expected values, because they cannot be accurately predicted by the current thermal model.

	Allowable Temperatures		**No Thermal Control**		**With Thermal Control**	
Critical Components	*Min T [K]*	*Max T [K]*	*Min T [K]*	*Max T [K]*	*Min T [K]*	*Max T [K]*
Solar cells	-	300	114	600	200	297.5
Filters	-	500	114	603	290	301.5
Subsystem module	250	300	114	594	273	293

11.2.4. Electric Power System

The electrical power system has to provide power to all the subsystems and deliver the electrical power from the solar cells to the power transmitter. It must operate nominally while maintaining a high power quality, implying low voltage ripples and transients in accordance with the requirements.

Electrical Power System Architecture

The system architecture should be optimised in such a way as to transport electrical power in the least mass, cost and most reliable manner possible. In order to achieve this some design options exist. These are summarised in Figure 11.11.

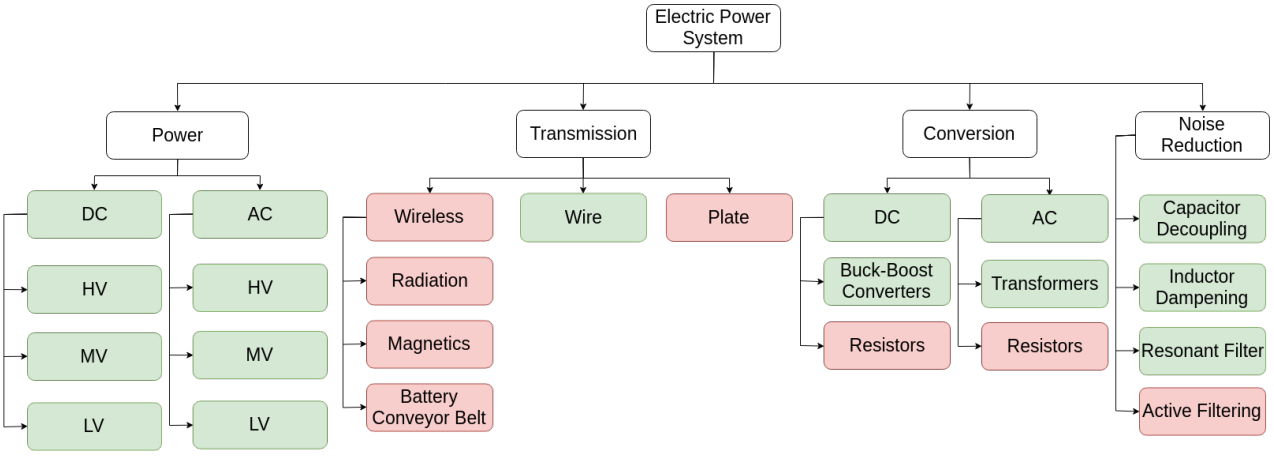

Figure 11.11: DOT for the EPS. Feasible options are shown in green and infeasible options are shown in red.

In order to ensure power quality, noise reduction in the power, voltage and current as well as sudden changes in amplitude should be smoothed out as much as possible. This has to be in accordance with **M-SY-P-EPSY-002** through

to **M-SY-P-EPSY-004**. For small electronics this can be done through active filtering, which is performed by an external control module. However, for these high power applications it is simply to risky and complex to perform these actions purely for the sake of noise. Hence the system should rely on more conventional methods through the use of passive filtering as done with capacitors and inductors.

Power conversion techniques are viable for both Direct Current (DC) and Alternating Current (AC) power are also depicted in Figure 11.11. Resistors for dropping power is wasteful and hence would violate the efficiency requirement **D-SY-P-EPSY-003**, as well as add to the thermal loads. Hence the power conversion through DC power converters or AC transformers should be considered.

Power transmission through the electric bus can only feasibly be performed through regular wires. The TRL and efficiency for wireless transmission makes this option unfeasible as well as the weight of the plate transmission would make it unattractive for space applications. Hence only wires/cables would meet requirements **D-SY-P-EPSY-001/003**, The higher TRL ensures compliance with **M-SY-P-EPSY-005** and **M-ST-S-ECON-001**. Hence these have been indicated in red in Figure 11.11.

As shown in Figure 11.11, for power engineering all options and configurations are possible. Hence these should all be considered in the creation of the concept.

DC power on first sight would be ideal, since the solar cells produce DC power and the subsystems require DC power. However, the voltage output from a solar cell is not high which causes losses over the transmission wire to be higher. This can be combated by increasing the radius of the indicator which increases the mass significantly, hence it is in risk of violating **D-SY-P-EPSY-000** and **D-SY-S-ECON-000**. The losses induced during the transmission of electrical power through a wire are proportional quadratically to the current through the resistance of the wire:

$$P_{wireloss} = R_{wire} {I_{trans}}^2 = R_{wire} \frac{{P_{trans}}^2}{{V_{trans}}^2} \tag{11.18}$$

As can be seen the wire losses are quadratically and inversely proportional to the voltage as a result. Hence stepping up the voltage and decreasing the resistance of the wire would increase the efficiency of the system. However transformation of power induces losses in the system, increases the need for heavy insulation and requires expensive and heavy machinery which can fail. This could lead to long periods of unavailability and hence violation of **D-SY-S-ECON-002** and **M-ST-OPER-000**. From research the power density of AC transformers is much higher (especially at high frequencies) than DC converters [122][70][73], and have very little reliability problems due to their long lasting use and TRL. However, AC power is not compatible with the other subsystems and laser transmitters. Also, AC power at high frequencies tends to have higher losses in the transformer due to hysteresis, eddy currents, conductor skin effect and flux leakage [135][32]. Furthermore, there are some concerns that the bus is not insulated effectively from the AC due to residual capacitances and isolating capacitors.

The DC voltage of the solar cells could be stepped up by placing them in series. However, should one of these "strings" of cells fail, a significant part of the power can be lost, as well as requiring more cells than there are available to make it competitive with AC power. This is all considering that the subsystems would require enormous DC converters, for a comparatively little amount of power [122][70]. This would reduce the chance of not meeting **M-SY-P-EPSY-005** and **M-ST-S-ECON-001**.

A combination of the 2 could imply a best of both worlds. These concepts include a DC to AC converter and then use a transformer to step up the voltage, and then converted back to DC again. Among the highest power density and efficient methods for this is the use of a series-parallel resonant converter [64][82]. In order to select the optimum concept, a trade-off was performed. The Quality Function Deployment (QFD) is displayed in Figure 11.12. The resulting trade-off weights are depicted in Table 11.8. The concepts for the electrical power were given a score as to their effectiveness resulting in Figure 11.13.

1: low, 5: high	Functional Characteristics (How)								
Weight	Customer Desires - (What)	Extra Mass	Reliability	Production	Risk for other subsystems	Safety systems	Ease of maintanance	Heat losses	Weighted Score
5	The system shall be profitable	6	3	6	4		3	7	145
4	The system shall be safe				9	9	2	5	100
3	The system shall be reliable		9	3	9	4	5	2	96
3	The system shall be opterational by 2030			7	6				39
3	The system shall opperate for 30 years		3		2	2	7		42
4	The system shall be mainainable		2				9		44
2	The system shall be efficient	5					2	9	32
5	The system shall cost less than 1.5 billion Euros	8		5					65
3	The system shall not be unavailible for more than 14 days per year		6		5	4	5		60
5	The system shall provide electrical power at the right current and voltage				9	7			80
	Technical importance score	80	77	85	167	101	114	79	703
	Importance %	11.38%	10.95%	12.09%	23.76%	14.37%	16.22%	11.24%	100.00%

Figure 11.12: Quality Function Deployment for the EPS Architecture

Table 11.8: Criteria and Weights for EPS Architecture Trade-Off

Identifier	Criterion	Weight
CR-EP-01	Extra Mass	0.11
CR-EP-02	Reliability	0.11
CR-EP-03	Production	0.12
CR-EP-04	Risk for other subsystems	0.24
CR-EP-05	Safety systems	0.14
CR-EP-06	Ease of maintanance	0.16
CR-EP-07	Heat losses	0.11

Identifier	CR-EP-01	CR-EP-02	CR-EP-03	CR-EP-04	CR-EP-05	CR-EP-06	CR-EP-07	Total
Direct Transmission	1	10	5	1	1	1	1	2.47
DC LV Buck-Boost converter system	2	8	4	10	10	7	1	6.65
DC LV-MV Buck-Boost converter system	3	6	4	6	8	6	5	5.59
DC LV-HV Buck-Boost converter system	1	3	4	4	6	6	10	4.83
AC LV system	5	8	3	5	10	6	1	5.52
AC LV-MV system	6	8	3	4	8	6	4	5.44
AC LV-HV system	7	8	3	2	6	6	7	5.13
DC LV-HV Series-Parallel resonant converter	7	7	5	2	7	6	10	5.75
DC LV Buck-Boost and LV-HV Series-Parallel resonant converter system	10	9	5	9	8	5	10	7.95

Figure 11.13: EPS Concept Trade-Off

The winner of the trade-off is an electrical power system with a Low Voltage (LV) DC bus for the subsystems supplied by a boost or buck converter and a High Voltage (HV) DC bus supplied from a Series-Parallel resonant converter.

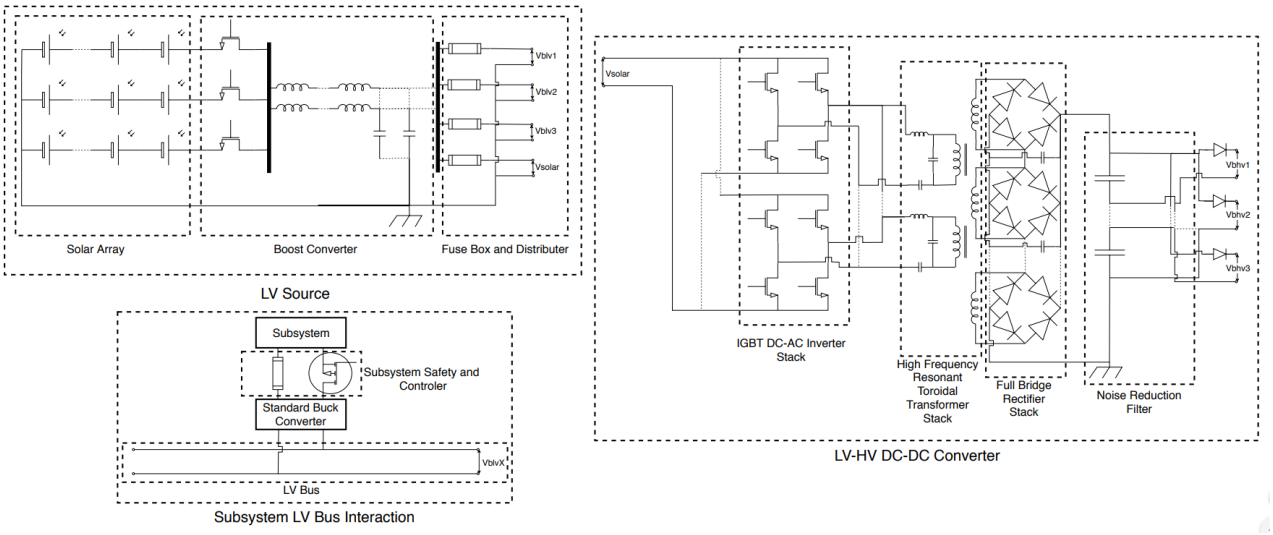

Figure 11.14: Detailed design of the Series-parallel resonant converter, LV Source and Subsystem LV Bus Interaction (LV=600V and HV=100,000V).

Power Flow and Detailed EPS Design

The solar cells will be placed in strings of 600V, each string will consist of a wide variety of different bandgap cells in different optimal configurations in order to maximise the reliability, efficiency and maximise the number of strings (which increases reliability). This is shown as the solar array in Figure 11.14 and Figure 11.15. The total number of strings is 30. These strings are placed in parallel, each with their own Insulated-Gate Bipolar Transistor (IGBT) safety and control switches. These are connected to a large Boost converter in order to maximise the total power from the solar arrays, and minimise noise in the system. The IGBTs will be controlled by a Max Power Point Tracker (MPPT), in order to operate the converter optimally. After the converter there is a fuse box and then the power is distributed to the LV busses and the LV-HV DC-DC converter which includes the transformer.

The LV-HV DC-DC Converter uses a IGBT DC-AC inverter stack to convert DC to AC. This is controlled by a second MPPT for optimum efficiency. The high frequency transformer stack will consist of smaller transformers, reducing skin losses, and will have micro laminations in its toroidal core of Silicon Steel reducing eddy currents, hysteresis and flux losses to almost 0 [134][73][122][64][41][82]. Finally, the AC power out of the secondary is rectified and noise reduced before splitting the output power into 3 HV busses.

The system will consist of 6 busses, of which 3 will be LV and 3 HV, each large enough to carry the maximum loads for reliability. The HV busses will only transport power to the power transmitter, and will do so at 100,000V in order

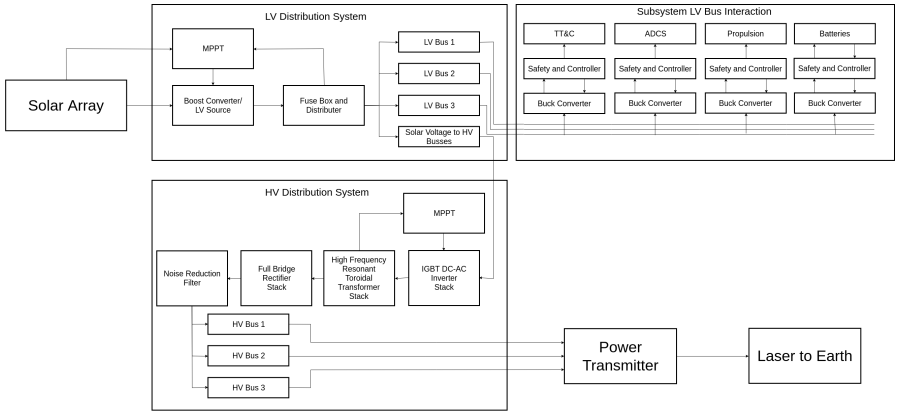

Figure 11.15: Block diagram showing the integration between different components of the EPS (LV=600V and HV=100,000V).

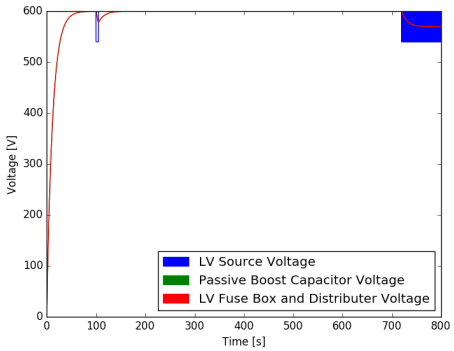

Figure 11.16: Low voltage side response to square pulse at 100 s for 5 seconds and white noise from 720 seconds

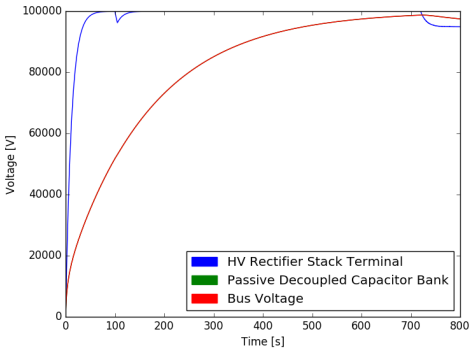

Figure 11.17: High voltage side response to square pulse at 100 s for 5 seconds and white noise from 720 seconds

to minimise the transmission losses. This was chosen since the power transmitter requires high voltage and to reduce the wire mass. The LV bus will remain at 600V and then be converted to the correct subsystem voltage, safety standard and noise level on site, meeting requirements **M-SY-P-EPSY-000**,**001** and **004**. This saves weight on DC-DC converters, allows for smaller batteries and safer operations. All in all it was found that using commercially available IGBTs and diodes with the high efficiency transformer of 97%, the converter can be made 96% efficient, with an additional 1% wire losses leads to an overall efficiency of 95% with peak power consumption[76][75]. It is however expected that this efficiency will be even higher in practice due to the conservative estimations made. Either way, requirements **D-SY-P-EPSY-001/002/003**. The predominantly DC system will hence also not have to deal with AC phase shifts, automatically meeting **M-SY-P-EPSY-006**.

The system has to meet the requirements **M-SY-P-EPSY-002** through to **M-SY-P-EPSY-004** for noise such as ripples and transients, and for safety reasons has to be able to handle this with the feedback loop for the active controller broken. Using a LV source capacitor bank with a capacitance of $0.05(10^{-6})$ Farad and a high voltage capacitor bank of $100(10^{-6})$ Farad, and simulating these scenarios, the resulting low and high voltages results in the response depicted in Figure 11.16 and Figure 11.17. These graphs depict the case of an unresponsive system, which has to maintain the voltages within the bounds set by the requirements. As can be seen, the noise does not register on both the high voltage and low voltage side. Sudden changes in generator voltage also results in smooth voltage changes within the bounds. Hence the system meets all the requirements. The output voltages are also as expected. Therefor this electric power conversion method works and meets all requirements for these high electrical loads, and is successfully maintaining a high efficiency and the correct voltages.

In conclusion, the use of a low voltage DC will result in too high wire masses in order to meet the weight requirements **M-SY-P-EPSY-005** and **M-ST-S-ECON-001**. As a result, high voltages should be used for the bulk power transfer and low voltages should be used for subsystem power. This will allow the subsystems to be dealt with separately with of the shelf and dedicated DC-DC converters. Hence meeting requirements **M-SY-P-EPSY-000**,**001** and **004**. The predominantly DC system will hence also not have to deal with AC phase shifts, automatically meeting **M-SY-P-EPSY-006**. The system is also capable of meeting the efficiency requirements in accordance with **D-SY-P-EPSY-001/002/003**. It is noted that any build up charge on the spacecraft can be grounded to space through the Ion engine. This is due to the fact that the engine emits ions which are recombined with the electrons after the exhaust.

Should some extra electrons be discharged or withheld then the overall system charge can be regulated. Effectively grounding to space.

Batteries
Some subsystems require constant power, even during ellipse and power failures. These subsystems where deemed to be the ADCS and TT&C. These have to be supplied with power for 72 minutes during the longest eclipse, as discussed in the astrodynamics part.

The life of and quality of the battery should also be maximised. Hence it was chosen to implement a 15% depth of discharge from the depth of charge [141]. This will also include all safety factors. The result is that the battery can sustain essential power for 12 hours and 1 hour when applying full thrust on the propulsion system. The total capacity amounts to 24 kWh, with a weight of 400kg. The charging requirements are also easily met due to lithium polymer technology. Hence all requirements are met. The batteries themselves where chosen to be Lithium-ion due to their high power density and predicted drop in price as well as degradation characteristics [83].

11.2.5. Command and Data Handling System

Every subsystem needs to communicate with the central On-Board Computer (OBC) and/or other subsystems to send/receive commands and processes housekeeping and mission data. The system is part of TT&C and is defined by one or more computing/processing units, controllers, memories and fail safe data busses. The general overview of data connections between subsystems is shown in Figure 11.18.

The diagram shows communication flow through the spacecraft and to and from its environment. It contains data rates for constant flows of mostly sensor data and a single upload data flow for ground commands. It also describes hardware characteristics and which data flows to and from different blocks.

Software on the OBC processes the data and handles the data flow to and from the different subsystems on board as well as the ground station. It can manage the subsystems in an autonomous manner. This communication goes through a low speed data link, for which a robust data bus architecture is needed. A separate high speed data link is necessary to send video feeds to the ground.

Low Speed Data Link
Many low speed data link busses are possible for this purpose. Because of the 30 year lifetime, high reliability is a must so only tried and true bus architectures should be considered. Many different interfaces are possible [90]. However, as reliability is of the highest importance, MIL-STD-1553B is chosen as bus interface as it is an often used interface with the longest lifetime of any of the busses considered [35][16]. It also has a high allowable cable length, which will be necessary considering the size of the spacecraft [11][36].

Because the spacecraft is large, a multiple-unit CDHS is chosen. Each subsystem will have its own controller with a direct connection to the OBC. From these controllers one or more serial connections will connect the sensors and actuators. These serial connections will be set up in a quadruple configuration to make it highly reliable.

High Speed Data Link
Commands and housekeeping data from the cameras can be transmitted through the aforementioned low speed data link. However, for the video feed itself, a direct high speed connection is necessary. Optical fibre is chosen for this. It will connect the cameras to solid state memory with which in turn is connected to the radios in order to send the feed to the ground station. The memory is there in case of short downtimes of the radios and 8 GB is estimated as a reasonable size for this storage. The separate connection is shown in purple in Figure 11.18.

On-Board Computer
The OBC can be seen as the brain of the system. It needs to work all the time in order for the system to keep working as it handles the closed-loop control software of the various subsystems. It is therefore crucial that it remains in working condition during the system's lifetime. For this purpose, processors are specially made radiation hardened so it can withstand high amounts of radiation. Two examples that have been proven in flight are the Intel 386 (rad-hard) and the BAE RAD6000, which are used on the International Space Station (ISS) and Mars Exploration Rovers respectively [35]. The latter is still being produced and has a reported price of $200k [15]. It has a clockspeed of 25 MHz and 32-bit register [8]. For redundancy purposes, two processors will be used per spacecraft. A watchdog timer will be used to monitor the computer health which will reset, interrupt or disable a processor when necessary [83]. When one processor stops to function, the other can take over.

Parameters
An estimate of the main parameters size, weight and power is made based on averages of other spacecraft and specifications of a MIL-STD-1553B cable manufacturer [83][9]. The estimated nominal power of the CDHS is 30 W. As the size of the spacecraft is large, long cables will have to be used which will attribute most to the size and weight. A size of 10,000 cm^3 and a mass of 30 kg is estimated.

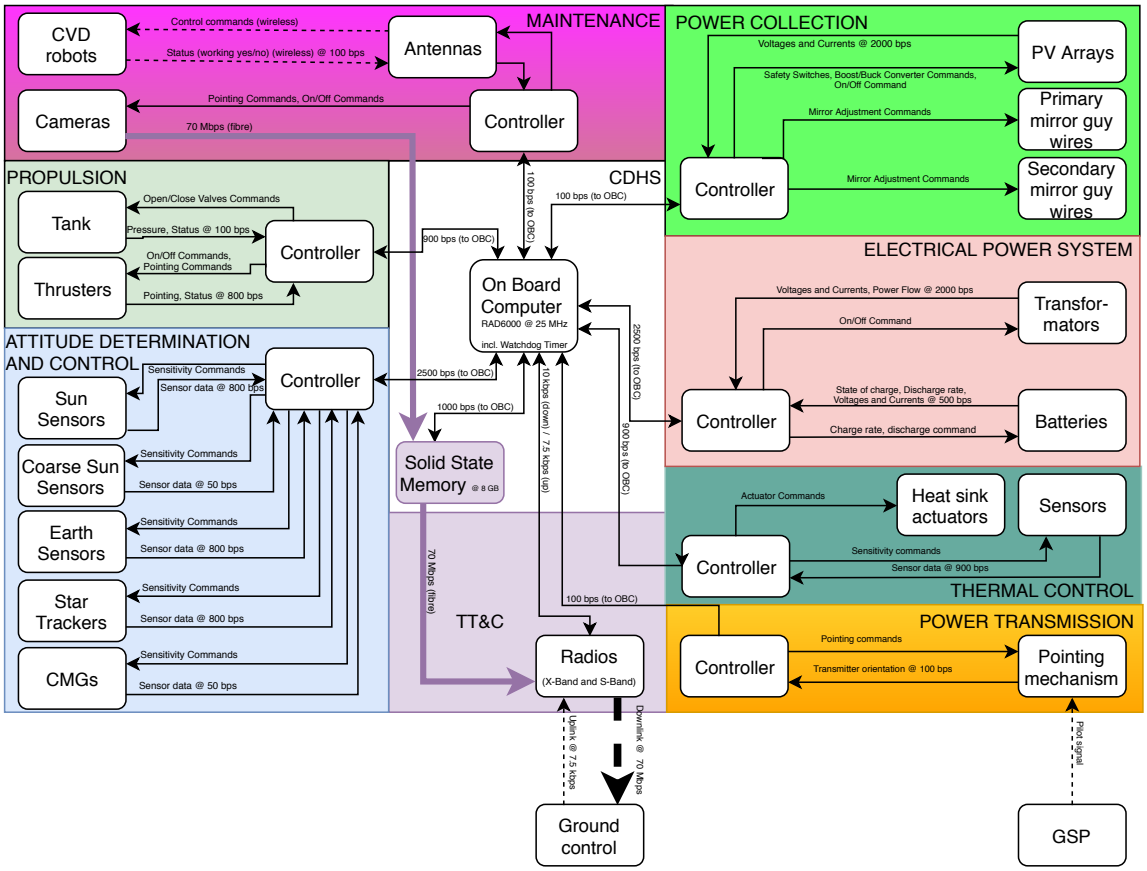

Figure 11.18: Data handling block diagram and communications flow diagram for one spacecraft

11.2.6. Telemetry, Tracking and Command System

Any spacecraft that is not autonomous needs to have contact with a ground station. This way, data can be transmitted to the ground (downlink) and operators can send commands to the spacecraft (uplink). In the case of SPECTRE, there is a special requirement on the downlink since a live video feed is required. Alongside this video, housekeeping data will also be sent down to the ground for further analysis.

Requirements

The driving requirements for this TT&C system are the data rates, which are 70 Mbps downlink and 7.5 kbps uplink (**M-SY-P-TT&C-001/006**), as well as the Bit Error Rate (BER). In this case it is required to be 10^{-5}, which means one in 100,000 bits are allowed to be wrong (**M-SY-P-TT&C-004/007**). Other requirements include a lifetime of 33 years and link availability of 99%, since in GEO it is possible to have contact with the ground at all times (**M-SY-P-TT&C-005** and **D-SY-P-TT&C-004**).

Architecture

The TT&C system architecture is shown very roughly in Figure 11.19, where a transmitter (Tx) can be seen which transmits a signal to an amplifier, where the signal is amplified and is then sent to the antenna. This antenna will broadcast the signal in the direction of the ground station, where the ground station antenna picks this up. The ground station then amplifies this signal again after which the receiver (Rx) gets the signal. This system works the other way around as well, so from ground station to spacecraft with only swapping the Tx and Rx. Both are present in the spacecraft and ground station.

The antennas are parabolic antennas with efficiency's η_{ant}= 55 % [83]. The spacecraft antenna is 1 m in diameter and the ground station antenna is assumed to be around 10 m as these ground stations already exist for X-Band.

Link Budget

The link budget shows where the signal gains and loses strength, and what the Signal-to-Noise Ratio (SNR) is at the receiver. The link budget should close to show that an X-band or S-band can be used (**M-SY-P-TT&C-002/003**) and that communication up to a distance of 40,000.0 km is possible (**M-SY-P-TT&C-000**). To close the link budget, the

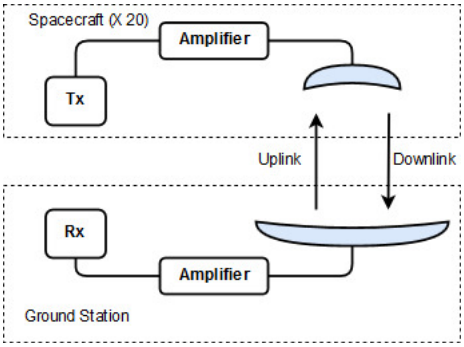

Figure 11.19: TT&C System Architecture

Table 11.9: Link Budget Input Data

Parameter	Value	Unit
Power	10	W
Tx Antenna Loss	0,8	-
Tx Antenna Gain	4262,805338	-
Path Losses	1,00693	-
Rx Antenna Loss	0,8	-
Rx Antenna Gain	426255,3899	
Space Losses	1,5881E+20	-
Downlink Data Rate	70000000	bps
System Noise Temperature	315	K
Frequency	8400000000	Hz
Light Velocity	299752458	m/s
Wavelength	0,035684816	m
Tx Antenna Efficiency	0,55	-
Tx Diameter Antenna	1	m
Rx Diameter Antenna	10	m
Rx Pointing Offset	0,025	deg
Half-Power Beamwidth Rx	0,25	deg
Tx Pointing Offset	1	deg
Half-Power Beamwidth Tx	2,5	deg
Boltzmann Constant	1,38E-23	J/K
Coding Type	BPSK	-
Coding Gain	4	dB

Table 11.10: Downlink Link Budget (X-Band)

Quantity	Value [dB]
Tx Power (RF Output)	10
Tx Antenna Loss	-0,96910013
Tx Gain	36,29695501
Path Losses	-0,3
Rx Antenna Loss	-0,96910013
Rx Antenna Gain	56,29669884
Space Loss	-202,0087911
Pointing Loss Tx	-1,92
Pointing Loss Rx	-0,12
Reception Feeder Loss	-0,96910013
Data Rate	-79,54242509
System Temperature	-24,98310554
Coding Gain	4
Boltzmann	228,6012091
SNR	**19,41324087**
Link Margin	**13,099532367**

SNR is required to be at least 3 dB larger than the required SNR, calculated based on the Shannon-Hartley Theorem:

$$C_c = B \cdot \log_2(1 - SNR) \tag{11.19}$$

Here, C is the required channel capacity or bitrate, B is the available bandwidth in Hz and SNR is the required SNR to achieve this bitrate with this bandwidth. For uplink this required SNR is 31 dB using S-Band (2.12 GHz) and a bandwidth of 1,500 Hz per spacecraft, so 30,000 Hz in total. This bandwidth is very small since the required data rate is very small as well.

For the downlink, this required SNR is found to be 10.31 dB using X-Band (8.4 GHz) and a bandwidth of 20 MHz per spacecraft, or 400 MHz in total which is common for X-Band transmissions [83]. To find out how much power is needed to be able to receive this signal on the ground, the input parameters seen in Table 11.9 were used. The antenna losses, path losses, efficiencies and system temperature were found from literature [83]. Gains, Space Losses, and wavelength were calculated using relations from [83]. Also, Binary Phase Shift Keying (BPSK) coding is used to achieve a gain of around 4 dB [42]. This leads to a link margin for the downlink budget of 13.1 dB, which is sufficient to receive the signal.

For the uplink, the procedure is the same except that the used frequency is S-Band uplink (2.12 GHz) and the transmitting and receiving antenna diameters are switched around. Also, the power can be increased to 500 W in this case but in principle (since it is Earth-bound) the power can be much larger. This leads to a link margin of 40.5 dB which is also more than sufficient.

Hardware
To achieve this, an X-Band transmitter needs to be found that has a lifetime of 33 years and is rated for space operations. However, current technology does not have this type of transmitter, so a transmitter will be used for around 5 years after which another transmitter will take over. This means each spacecraft will carry 8 transmitters (one for redundancy) which each have an efficiency of around 10%, hence requiring around 110 W of power input per spacecraft [93]. The required power was therefore determined to be 150 W average and 200 W peak power in **D-SY-P-TT&C-001/002**.

11.2.7. Spacecraft Structure

A spacecraft needs a structure to support all its physical parts. In essence, all the physical parts are structures, because they have mass and carry loads when undergoing an acceleration. This is no different for the structure of SPECTRE. Typically, structures are divided into different categories: the primary structure, the secondary structure and the tertiary structure. The primary structure can be seen as the backbone between the components and carries the major load path. The secondary structure includes support beams, trusses, antenna dishes and solar panels. The primary and secondary structures both carry shear, bending moments, axial loads and torsional loads. The tertiary structure consists of component housing, mounting brackets, cable-support brackets and connector panels. However, due to the large scale of this project and the conceptual nature of our design, the structural analysis in this report will not go into this level of detail.

Load case
In order to be able to design the structure necessary to support all the components of SPECTRE, firstly the forces which are exerted on the system should be inventoried. The following loading case is seen as critical in the structural design of SPECTRE. For mirror deployment reasons, SPECTRE is required to spin around its longitudinal axis (y-axis in figure Figure 11.20) at 0.5 rounds per minute, which is equal to 0.052 radians per second. Also, SPECTRE should be able to have a pitch rate of 0.0002 radians per second, in order to maintain its attitude. These angular velocities imply centripetal forces on the structure. At the same time, an ion thruster could be activated, exerting a 0.011 Newton force on the structure. The structure should be able to withstand all these forces without failure or excessive deformation. It should be noted more load cases should be analysed in future design phases to improve the structural design. These load cases could for example include fatigue loading, which was considered outside of the scope of the current design phase.

Required structures
SPECTRE consists of several individual physical parts, which should be connected in order to guarantee the correct functioning of the system. The primary and secondary mirror are connected with the mirror connecting structure, in order to maintain there relative position and therefore the correct guidance of light. The knikkerbaan, which houses the filters, solar cells, electric converters and subsystems module docking location, must be strong enough to support the relatively large masses of the components attached to it while spinning. The space web behind the primary and secondary mirror should be able to support the reflective film but also a web crawling robot applying the reflective film to the space web during the production.

Analysis Methods
In the structural analysis of SPECTRE, the mirror connecting structure and the space web structure will be analysed separately. First the analysis and design of the primary structure will be described. It will be analysed by the means of a Finite Element Method (FEM) model.

Secondly, the analysis and design of the space web will be described in the following way. The space web structure consists of concentric rings and 'clock hands'. The space web structure will be analysed and designed in the most critical situation, as if all the mass of a section of the thin reflective film and the production robot would be at the end of one single 'clock hand'. The space web will be designed in a way it can carry the tension which is present in the aforementioned situation. The space web will be designed for the worst case and the described load case can be solved analytically. This analysis will be described after the analysis of the primary structure.

Spacecraft Structure FEM Model
In Figure 11.20, the primary structure can be seen with the labelled point masses and distributed masses. The primary structure will be modelled with the aforementioned masses in FEM software (ANSYS).

One of the biggest challenges in structural analysis is boiling the structure down to a clean and simple model which is easy to analyse. In order to achieve this, assumptions have to be made. However, this should be done with great care as they can make or break your analysis. This modelling is performed in line with the thoughts on modelling satellite structures from Finite Element Analysis for Satellite Structures [65].

The model is created in ANSYS Workbench and contains the aforementioned masses, rotational velocities and the thruster force. The primary structure is modelled with line bodies, which are converted to beam elements by apply-

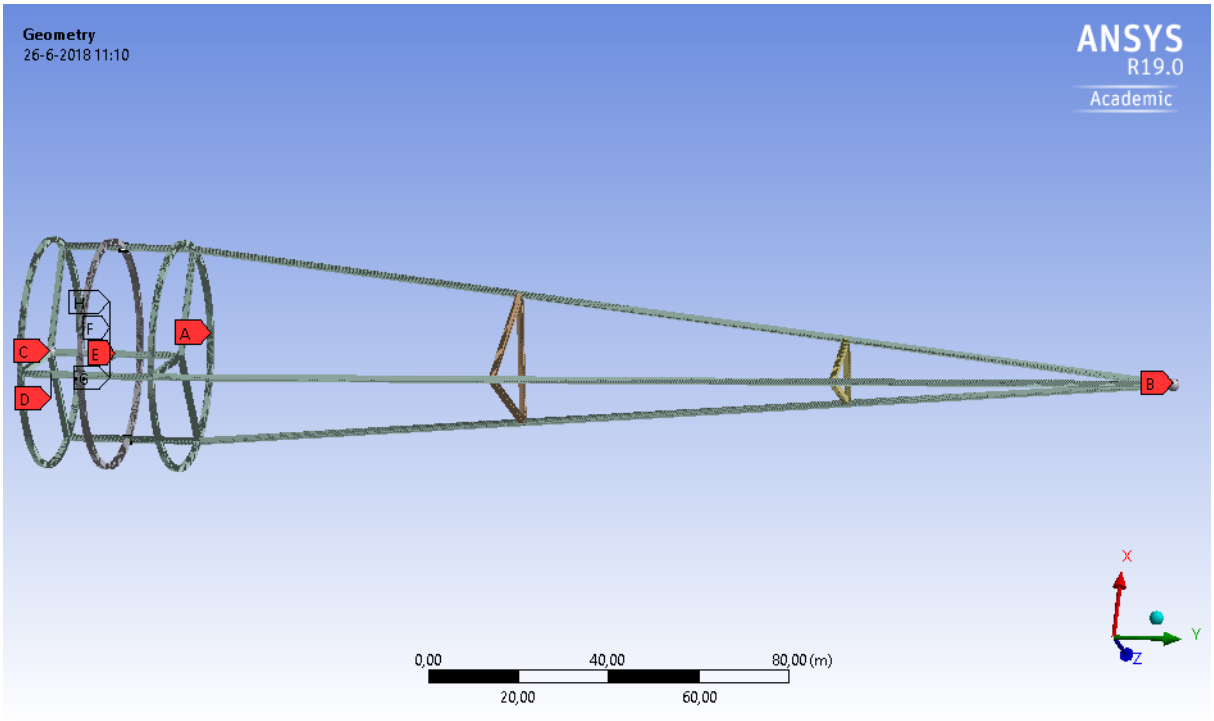

Figure 11.20: Spacecraft primary structure with point masses and distributed masses

Table 11.11: Modelled masses on structure

Label	Type of mass in model	Corresponding part	Mass	Remarks
A	Distributed mass	Primary Mirror (incl. web)	350 kg	This includes the mirror film itself (250 kg) plus the 100 kg for the space web. Because the centripetal forces will be point away from the axis of rotation (perpendicular on the ring structure), the mirror and space web may be modelled as a distributed load on the ring structure.
B	Point mass	Secondary mirror (incl. web)	58 kg	This includes the mirror film itself (50 kg) plus 8 kilograms for the web structure.
C	Point mass	Subsystems module	6500 kg	The point mass is located at the location where the subsystems module will dock onto the primary structure.
D	Distributed mass	Solar cells	911 kg	The total mass of 911 kilograms is divided over the three trusses that go from the first ring all the way to the third ring. The label is only placed at one of the beams.
E	Distributed mass	Filters	2000 kg	The filters are attached to a central truss inside the knikkerbaan.
F, G, H	Point masses	Electric converters	352 kg each	On each place where the three trusses of the knikkerbaan structure meet the middle ring structure, there is an electric converter attached to the structure.

ing a cross section onto them. Even though it is possible to simulate truss geometries in ANSYS, it is not possible within the time frame of the project to perform such an analysis with the accessible CPU power. The type of cross section used in the model and the way it corresponds with the actual truss structure, is explained further on in this section.

The centre of gravity is calculated to be at 7.5 meters up from the docking location on the primary structure. This is based on a simple calculation, only including the attached point and distributed masses that are present in the model, because these will predominantly define the centre of gravity location. The mass of the trusses is considered as negligible in comparison with the attached masses. In order to be able to perform an analysis on a FEM model, the model should have boundary conditions/constraints. In this model, the structure is assumed to be spinning around its own centre of gravity. Therefore, the model is fixed only at that location by the means of a fixed support.

The spacecraft structure will consist of truss elements, like the one in Figure 11.22, created by additive manufacturing as described in subsection 13.2.2. In the sizing and designing of the rectangular truss dimensions, the trusses will be simplified to four circular beams, one on every corner. However, the addition of mass by the struts to the structure has been taken into account.

The FEM model is created with a rectangular tube cross section. The sizing of the simplified trusses is based on the required area moment of inertia and has to be bigger than the area moment of inertia of the rectangular tube beam

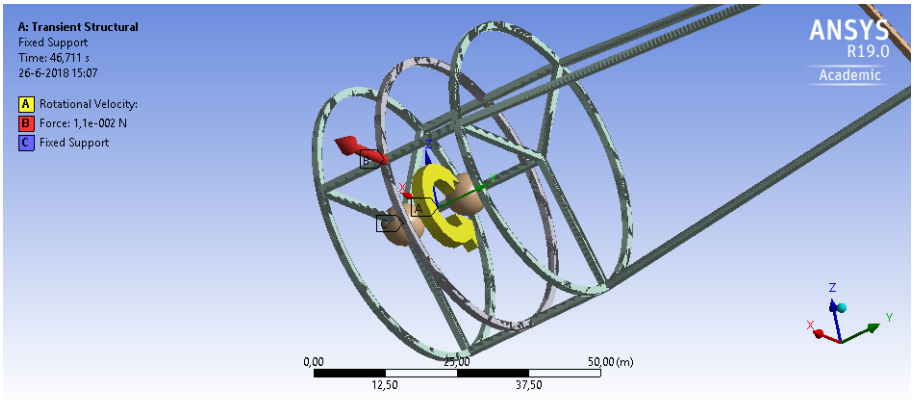

Figure 11.21: Structural analysis load case & supports

Figure 11.22: Truss element produced by the Trusselator from Figure 13.3

sections, in order to have a safety factor in this design step. Also, because the rectangular tube beams are considered less efficient (larger cross sectional area for the same area moment of inertia), the beams used in the model have a larger mass and therefore exert bigger forces when spun around. In reality, the centripetal forces on the structure will be lower than modelled in the FEM analysis. This is regarded as additional factor of safety.

Materials used in structural design
The truss elements will be made out of carbon reinforced PEEK, from which the properties can be seen in Table 13.2. As the material properties of this type of PEEK are not isotropic, the equivalent stress solver (based on Von-Mises stress calculation) of ANSYS Workbench can not be used.

The space web will be made of Zylon™ HM, of which the properties can be seen in Table 13.3.

The selected materials are a result of **M-ST-L-PROD-000**, which requires to use materials that are manipulatable by the machines available. For the Trusselator, this means it can produce PEEK type of materials, therefore the strongest PEEK, PEEK 90HMF40 is selected.

Design Iteration
By iteration, the structure and cross section have been sized so the structure does not fail and does not deform more than **D-SY-P-STRU-001** states, which means that the collection area shall not deflect more than 0.04 degrees.

Not all the iteration steps will be described in this report. However, a good example of such a step is the following. Before adding reinforcements to the three long beams that connect the primary and secondary mirror, the deformation was considered too large, resulting in not meeting **D-SY-P-STRU-001**. Therefore, reinforcements were added which resulted in a total deformation not bigger than 0.13 metre, which is the worst case situation. Considering the distance of 228 metres from the primary mirror to the secondary mirror, this deflection can be 0.03 degrees at the worst case, meeting **D-SY-P-STRU-001**.

The model beam section results will be analysed in order to size the trusses. During iteration, it became clear that the forces and moments that are exerted on the structure are not really driving the structural design as they became relatively small after only a few iterations, seen from the resulting stress point of view. However, the deformation of the structure could be seen as the biggest drive in the structural design, as the primary structure's deformation may not lead to large deflections (and therefore disrupting the power collection).

The iterations led to the following cross sections of the modelled beams and designed trusses.

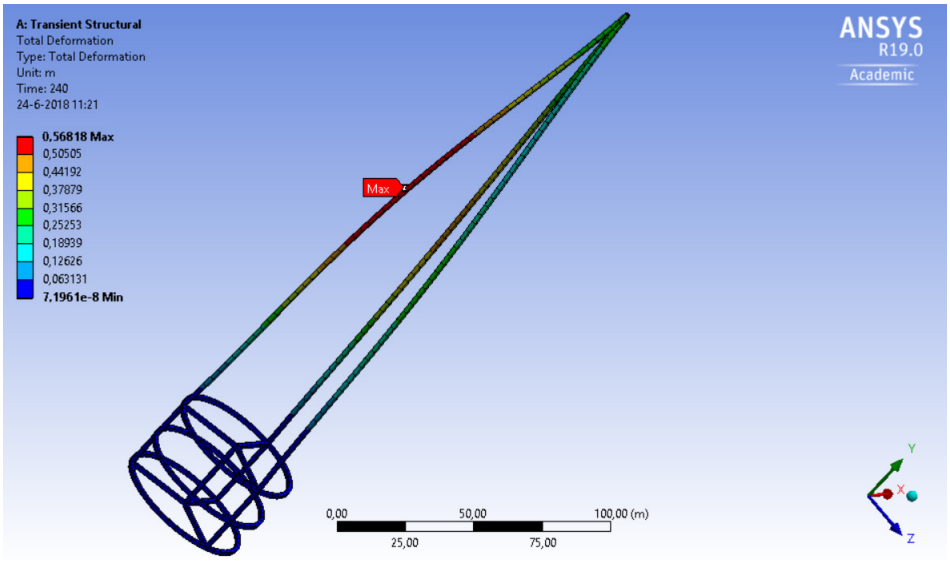

Figure 11.23: Deformation of the structure before iteration

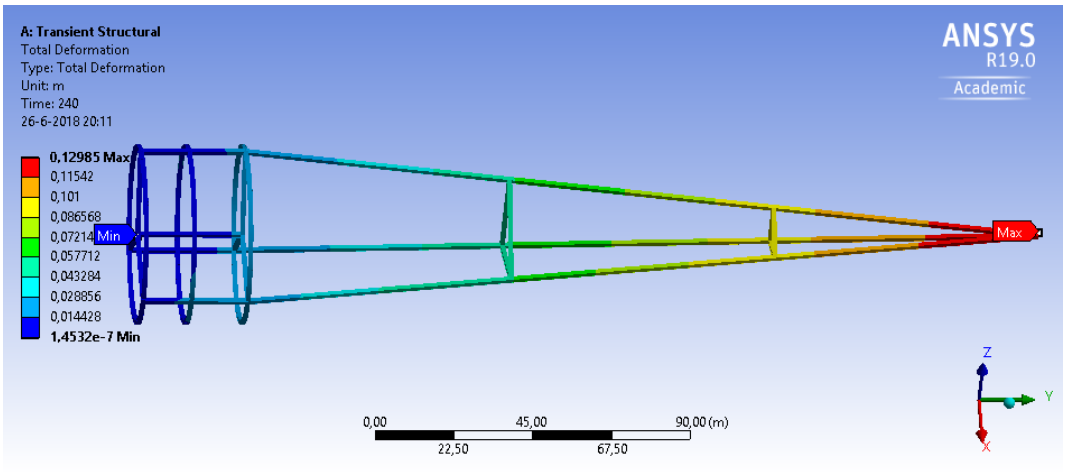

Figure 11.24: Deformation of the structure in the worst case loading scenario

The model in ANSYS consisted of square hollow tubes with an outer dimension of 1.3 metres, while being 0.0002 metres thick. This leads to an area moment of inertia of 0.00029 m^4. To match these properties, the truss structure cross section was designed so that the inertia was equal to or greater than the one utilised in the analysis. Next to this, the area of the square tube cross section is larger and therefore the modelled beams are heavier than the actual truss structures. Therefore, the forces on the structure due to the angular velocity are modelled greater than they would be in reality. This adds to the robustness of the analytical simulation.

The cross section geometry of the simplified truss can be seen in Figure 11.25. The resulting area moment of inertia is equal to 0.00031 m^4, while the resulting area is equal to 0.00031 m^2.

Considering the sum of all the truss lengths of 1559.43 metres, the density of PEEK of 1450 kg/m^3 from Table 13.2 and the aforementioned cross section area, the total mass of the simplified trusses comes down to 710.37 kilograms. However, while the struts are not considered in the structural analysis, their mass will be accounted for by the means of an estimated factor of 1.2. The total mass of the primary structure therefore boils down to 852.44 kilograms.

Analysis Results

The primary structure will be analysed for the beam results: the bending moments, torsional moments, axial forces and shear forces. According to **D-SY-P-STRU-002**, the stresses may not exceed the following strengths: a Design Tensile Strength of 73 MPa, a Design Flexural Strength of 117 MPa and a Design Compressive Strength of 83 MPa. The shear strength of the carbon reinforced PEEK is not widely available. However, the shear strength of unreinforced PEEK is 55.2 MPa [5]. Even if we use a safety factor of 10 (resulting in Design Shear Stress of 5.52 MPa), the condition would be met.

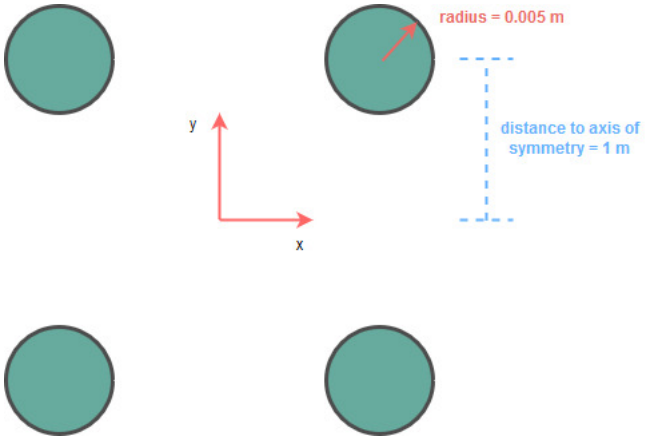

Figure 11.25: Simplified truss cross section

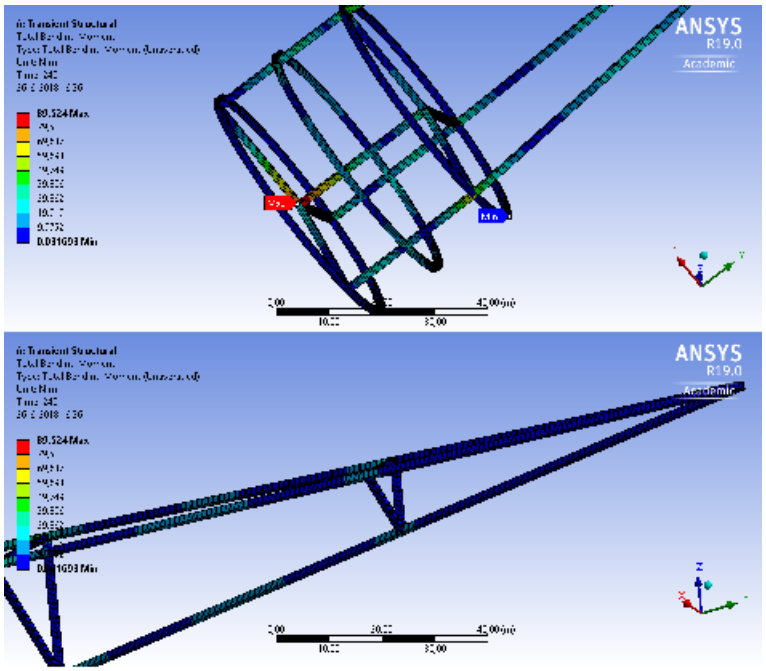

Figure 11.26: Bending forces in primary structure

The following safety factors have been taken into account during the analysis and design of the structures of SPECTRE. All the material strength properties have been divided by a safety factor of three to get the Design Strengths, which is inspired by the recommendation extracted from The Ultimate Factor of Safety of Aircraft and Spacecraft [2], where a 2.6 Factor of Safety was being advised for untested structures. Also, considering the effect of heat on the material properties, the expected temperature based on the thermal analysis is rounded up for selecting the strengths of PEEK 90HMF40 out of Table 13.2. The area moment of inertia of the trusses is 1.1 times bigger than the beams used in the model. The area of the cross section of the trusses are 3.3 times smaller than the beams used in the model. Therefore the beams in the model are heavier and exert larger forces onto the structure itself. The max design stress considered for the space web is the materials ultimate tensile strength divided by four. Also, the modelled point masses and distributed masses were always rounded up.

Based on the results, the maximum bending stress can be calculated to be 0.29 MPa. This is negligible considering the aforementioned design strengths. The normal stress is calculated to be 0.064 MPa, which is really low as well. The shear stress is calculated to be 0.05 MPa, also staying below the desired stress level. The shear stress due to torsion will be 0.017 MPa at max.

Space Web Analysis & Design

In order to fulfill **D-SY-P-STRU-003**, the space web consists of 3409 'clock hands' and 156 concentric rings. The space web will be made out of Zylon™ HM, from which the properties can be found in Table 13.3. Sizing the required cross section of the space web elements will be based on the worst case loading scenario, which can be seen in Figure 11.30.

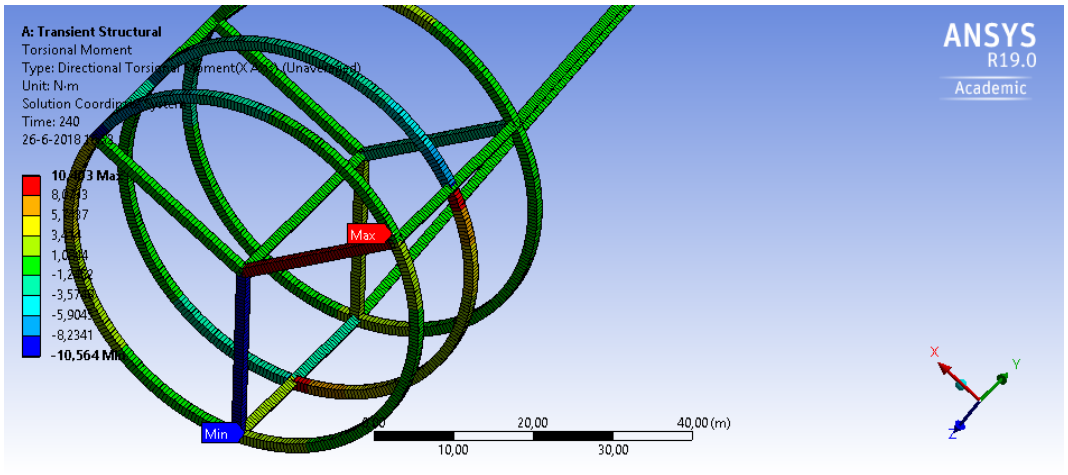

Figure 11.27: Torsional forces in primary structure

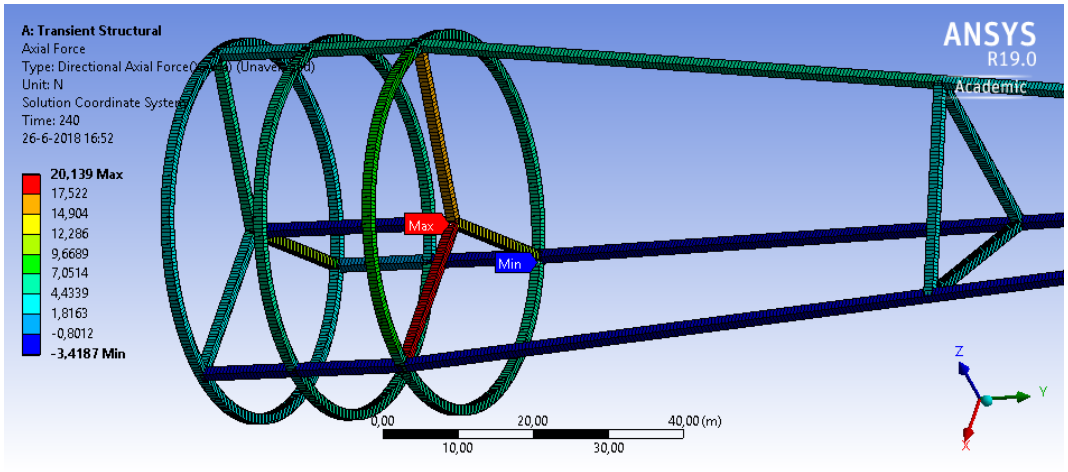

Figure 11.28: Axial forces in primary structure

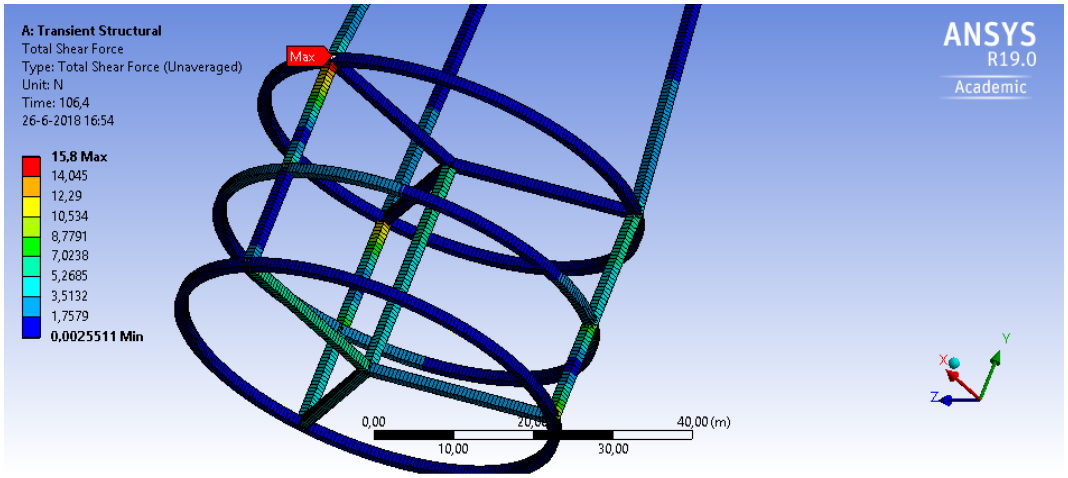

Figure 11.29: Shear forces in primary structure

A single 'clock hand' is assumed to carry 1/3409th part of the mirror mass (73.3 grams) plus an additional web crawler (of 180 kilogram). When having an angular velocity of 0.05 rad/s, and a radius of 180.801 metres, the centripetal force will be 128.53 N. Note that this actually a worst case situation because in reality, all the mass is not always entirely located at 180.801 metres away of the centre. Taking a safety factor of 4 into account and knowing the Ultimate Tensile Strength, the max tensile design strength is considered to be 1.450 GPa. In order to match the normal stress caused by tension in the single space web 'clock hand' element that is being analysed, the required area is 0.089 mm^2. Combining the area with the total length of all the space web elements (632731 metres) and knowing the density of 1560 kg/m^3, the total mass of the primary mirror space web is calculated to be 87.5 kilograms. In the same way, the mass of the secondary mirror space web is calculated to be 2.5 kilograms.

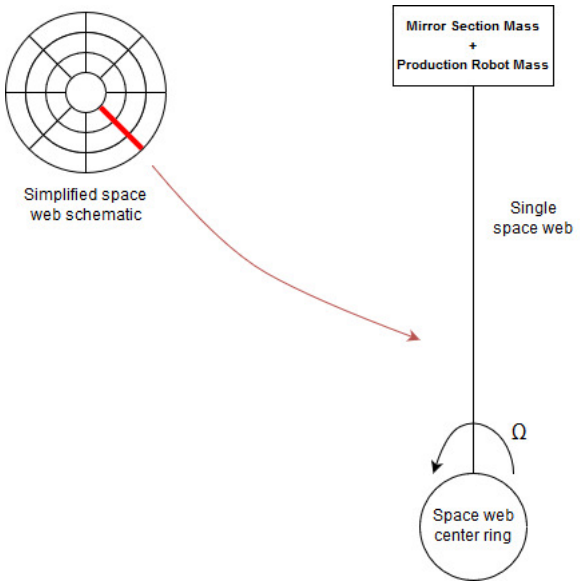

Figure 11.30: Analysis of single space web 'clock hand'

In order to make sure the space web, and therefore the mirrors, preserves its correct shape, a small piece of space web is analysed. The space web intersection points of the 'clock hands' and concentric rings (every one metre) are attached with guy-wires to the primary structure. The force exerted by the guy-wires onto the primary structure can be considered as negligible due to the relatively low weight of the mirror. However, the deflection of a one metre piece of space web was analysed in order to check if its deflection will disrupt the mirror shape. Therefore, a one metre piece of space web was supported by fixed supports at both ends (where the guy-wires support it) and was rotated around with the angular velocity for centrifugal deployment (0.05 rad/s). The maximum deflection of this piece of space web was analysed to be 4.07E-07 metre. The deflection can be considered as very small and therefore meets the **D-SY-P-STRU-001** requirement, as the maximum deflection angle of this piece of space web only is 4.7E-05 degrees. Attaching guy-wires to every intersection point at the space web and connecting them to the primary structure is therefore considered to be satisfactory.

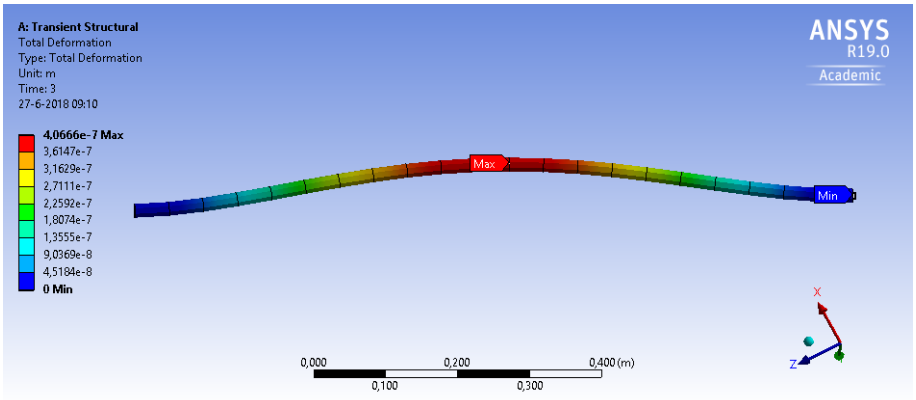

Figure 11.31: Analysis of piece of space web

Discussion
The combined mass of the primary structure and the two space webs comes down to 942.44 kilogram. The space web structure is designed in a way it can accommodate the web crawlers which will be attached to the space web during production but possibly also during repair. The forces and moments on the structure are maybe lower than one would expect. However, the forces on the structure are caused by the angular velocity, which is quite low, and the ion thruster, which also only exerts a 0.011 N force.

The structural components of SPECTRE therefore meet the requirement **D-SY-P-STRU-004**, which states that the mass of the structures shall not exceed 1500 kg per spacecraft. Therefore, one can conclude that all the structural requirements are met.

11.3. Subsystems Module Design

With all subsystem designs finalised, the next step is to determine where all the subsystem components will be located in the spacecraft. Since there is a large part of the subsystem components that will not be manufactured in orbit, it was decided to place as much of those components as possible together into one module. This module will be completely manufactured on Earth, it will be launched as one component, and after all in-orbit construction of a SPECTRE satellite is complete, the subsystems module will be docked to the rear end of the satellite and begin operation. In chapter 13 the production of the system is further elaborated upon.

First, a list was made of all subsystem components that will be placed inside the subsystem module, as can be seen in Table 11.12.

Table 11.12: List of all subsystem components located in the subsystems module

Subsystem Components	**Total Mass [kg]**	**Volume [m^3]**
Xenon propellant tank	1500	1.012
Thermal Energy Storage Container	2000	2
9 Control Moment Gyros	2448	1.125
8 Power Converters	13	1
3 Batteries	193	0.035
Electrical Wiring	13	0.18
8 Transmitters	10.4	0.000876
8 Receivers	10.4	0.000876
Flight Computer	4	0.016
Data Cables	2.5	0.001
Total Subsystem Module	6194.3	5.37

For the exact placement of all components in the module, it was assumed that the thermal requirements would be the most driving factor. One of the components in the subsystem module is the thermal energy storage container, which keeps the critical system components warm during eclipses. This component has to be insulated from the rest of the spacecraft for large periods of operation to prevent thermal energy leaking away. From all components in the module, the xenon propellant tank has the highest minimum allowable temperature and therefore should be placed closest to the thermal storage. To ensure sufficient thermal insulation, the thermal energy storage container will be placed on a truss support structure on top of the propellant tank.

The xenon propellant tank will be placed on the centre of a 3.5m diameter heat conducting base plate, with the other subsystem components placed in a ring around the propellant tank. The subsystems will be distributed in such a way that the centre of gravity of the module stays on the central axis. The base plate will ensure the components all stay within their allowable temperature ranges. To save space, the CMGs and some Electronic Power Converters will be stacked on top of each other. This basic subsystem module configuration is pictured in Figure 11.32.

The exact placement of the electrical wiring, data cables and heat pipes inside the subsystems module has yet to be decided. A structural analysis of the subsystem module will also have to be performed in order to make a more detailed mass estimate of the entire module.

11.4. External Subsystem Component Integration

Due to functional reasons, some of the subsystem components designed above will have to be placed outside of the subsystem module. There are two instances when components are outside of the subsystem module, they are either required to be on the power collecting structure, or on a non-rotating Earth pointing platform. These components will also have to be integrated with the subsystem module, and this will be discussed in the following 2 sections.

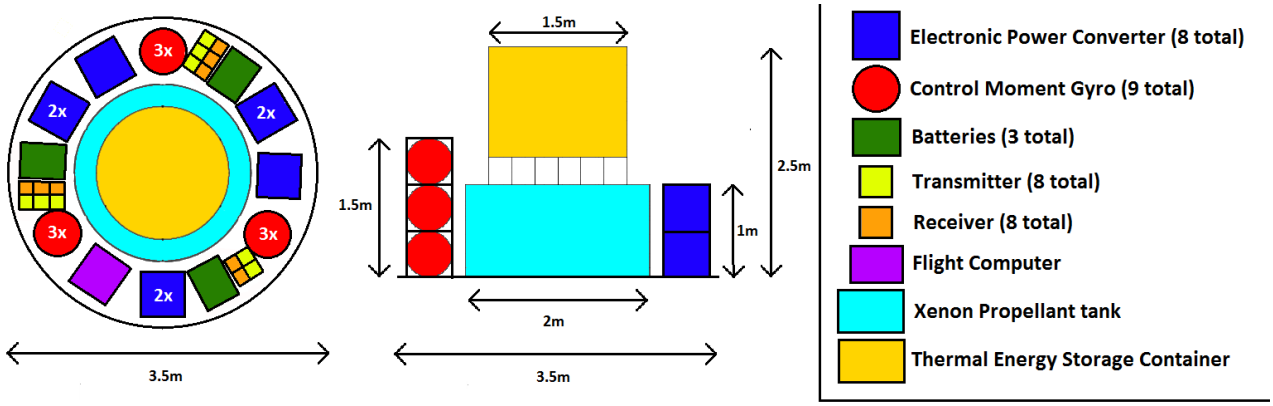

Figure 11.32: A basic drawing of the subsystem module configuration, with the location of all major components shown. A top view is shown on the left and a simplified side view is shown on the right.

11.4.1. Subsystem Components on a Earth Pointing Platform

Of course, some components will also be mounted onto the subsystem module and kept at an orientation such that communication and transmission to Earth is possible. Due to the constant rotation of the system for the deployment of the mirror, a separate non-rotating platform will be required for the communication and transmission system. This separate non-rotating platform will be just large enough to house the communications antenna and power transmitter. It will be connected to the subsystem module with bearings, to prevent itself from rotating along with the power collection system.

TT&C Components

For the communications subsystem, in order to communicate with the outside environment the antenna must be on the exterior of the module. It is also required to keep a consistent orientation towards the communicating ground station. Furthermore, it is deemed feasible to place the antenna in close proximity to the wireless power transmitter, since the operating frequencies of the laser and the radiowaves are extremely different. Therefore, it can be assumed that there is no, or minimal interference between the waves. The TT&C components will also be electrically integrated into the system by running wires from the electric bus. The TT&C components will also be connected to the CDHS to ensure they can forward the information from the ground station to the entire system, and vice versa.

Wireless Power Transmitter

Since the system will be generating power constantly when it is out of eclipse, the power transmitter should be able to point to the power ground station at all times. Therefore, it should also be located on the non-rotating platform outside of the subsystems module. The transmitter will be connected to the electric bus and CDHS of the system, in order to get sufficient power to transmit back to Earth and be able to communicate with the other systems. These connections will be done through data links and electrical wires.

11.4.2. Subsystem Components on the Power Collection System

Some of the subsystem components will also be located on the power collection system, either on the concentrator module, or the collector module. This is mainly required to maximise the performance and use of certain subsystems, such as the ADCS and TCS.

ADCS Sensors

First of all, in order to stay aware about the position of the system, ADCS sensors will be required around the system. Essentially, the system will require four earth sensors and 4 star trackers on the collector module. On the secondary mirror, it requires two earth sensors, three sun sensors and one coarse sun sensor for safe-mode operation. For the four earth sensors on the collector module, the power will be directly provided by the bus, while the earth sensors on the back of the secondary reflector will be incorporated with their own small array of solar cells. Note that the sun sensors do not require power to function. Furthermore, all of the sensors outside of the subsystem module will also have wired connections to the CDHS of the system.

EPS Components

Furthermore, the solar cells on the collector module would require some sort of connection with the electrical bus, found in the subsystem module. For this, electrical wires and converters will be placed along the outside of the collector module, which will lead the collected power to the bus.

Thrusters
The thrusters will have to be placed radially along the collector module, at the centre of gravity of every system. At this moment of the design phase, the exact centre of gravity cannot be determined, but due to the mass distribution of the system, it will be located somewhere along the collector module. At that location, an extra supporting structure will be required to sustain the loads from the thruster operation. This structure will be made from trusses, and will be a pentagon surrounding the thin film solar cells. These thrusters will be integrated with the propellant tank in the subsystem through pipes running along the collector modules exterior. The thrusters will of course also be connected with the CDHS.

Thermal Control
Most of the thermal control subsystem will be located outside of the subsystem module, as the majority of heat is generated at the collector and secondary mirror, and the heat is radiated away with the primary mirror. Therefore, heat pipes will be running between the two mirrors, throughout the C&SM and over the back side of the primary mirror. Essentially, the entire backside of the primary mirror was reserved for the radiator, and a coating will be applied to the back to make it more effective. The heat pipes will be continuous structures that will lead in and out of the subsystem module.

11.5. System Overview

In this section, an overview of the designed system will be given through the virtue of internal and external lay-outs, and block diagrams to show the flow of data and electricity. Afterwards, mass and power breakdowns of the system are also given.

11.5.1. Internal and External Lay-Outs

In order to provide a technical overview of the system several layouts have been developed, and will be presented in this section. The external layout of the system is presented in Figure 11.33a and Figure 11.33b. A side and top view are used with dimensions to illustrate the layout of the system. From this external view the two mirrors, the solar cells, the subsystem module and the connecting structures can be identified. In Figure 11.34 the same external layout is provided in two 3D views. In the right representation the filters in the middle of the collection system can also be identified.

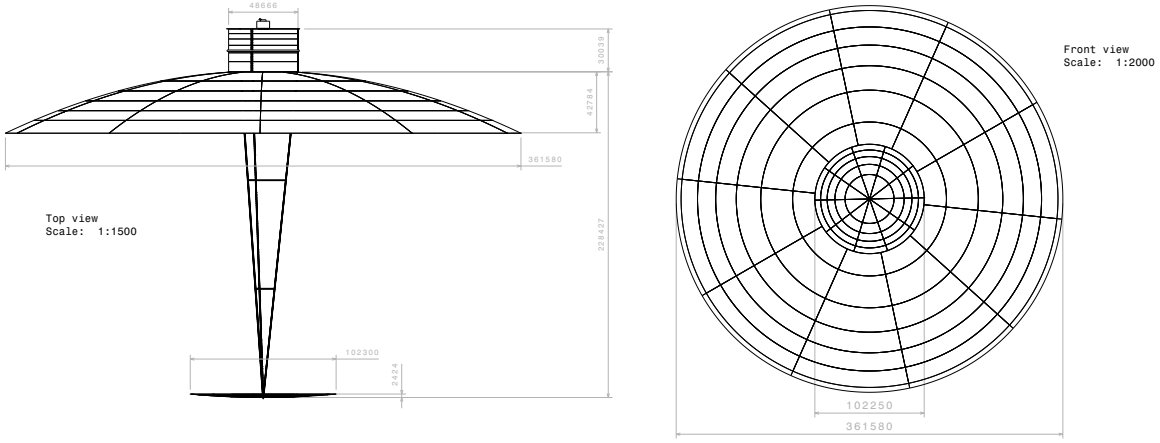

(a) Side view of the system

(b) Front view of the system

To illustrate the internal layout of the system two schematics have been made and presented in Figure 11.35a and Figure 11.35b. The first schematic shows the trusses supporting the entire spacecraft. These will start at the secondary mirror and extend all the way through the primary mirror and beyond up to the subsystems module. There are three struts that are spaced equally around the spinning axis.

In the second schematic the internal layout of the filters is shown from a side view. The converging radii can be identified and the dimensions of each filter are given. There are five filters present, the last stage on the right is the back mirror.

11.5.2. Product Tree

This section provides an overview of the components of SPECTRE's final design. The components are illustrated in a breakdown structure in Figure 11.36.

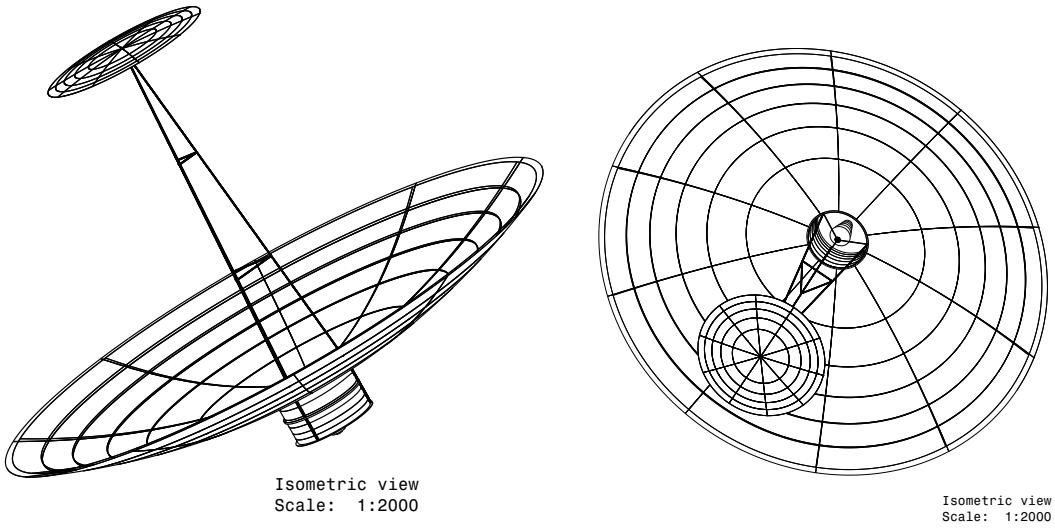

Figure 11.34: 3D views of the system

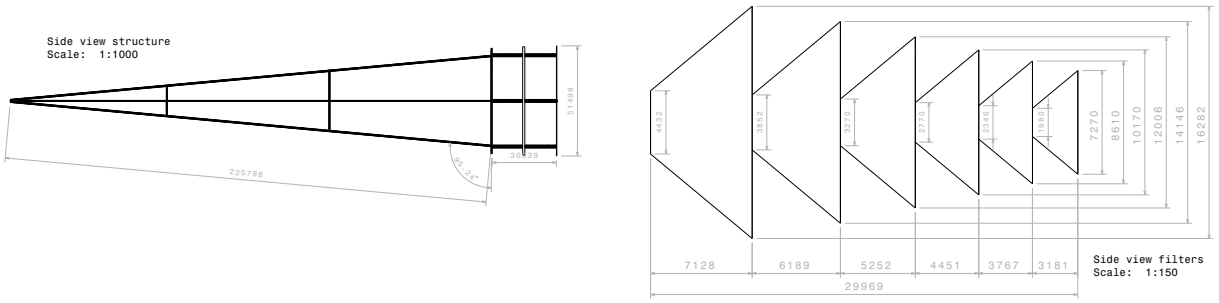

(a) Schematic of the Truss Structure

(b) Schematic of the Filter Layout

11.5.3. Hardware Block Diagram

Depicted in Figure 11.37 is the hardware block diagram. The system, once operational, consists of 9 subsystems. The arrow colours indicate the interaction medium across the interface. Optics/light is represented as orange, black is data/information, red are structural linkages, green is propellant, yellow is electricity and purple is heat/thermal exchanges. The arrow thickness indicates the concentration of light for optical relationships and the voltage level for the electrical power system.

As described above, the optics/power collection subsystem collects the light from the sun and filters it for the solar cell bandgaps. The cells then collect the light and send low voltage electrical power, preferably at 600V, and sends it into the EPS.

In order to maximise the power and reduce noise, a boost converter controlled by a MPPT is used that also feeds back into the collection subsystem in order to improve the shape of the mirrors through another MPPT.

Furthermore, the power collection system interfaces with the structural subsystem, in order to tension the guy-wires and generate a rigid structure holding the complete system in place.

The maintenance subsystem interface consists mostly of the repair and replacement of the mirrors. The only other interface is the structural maintenance data interface, which determines and performs maintenance.

The ADCS system has the function of pointing the primary mirror as accurately as possible to the sun. It does so by monitoring the output from the solar cells as well as the sun sensors.

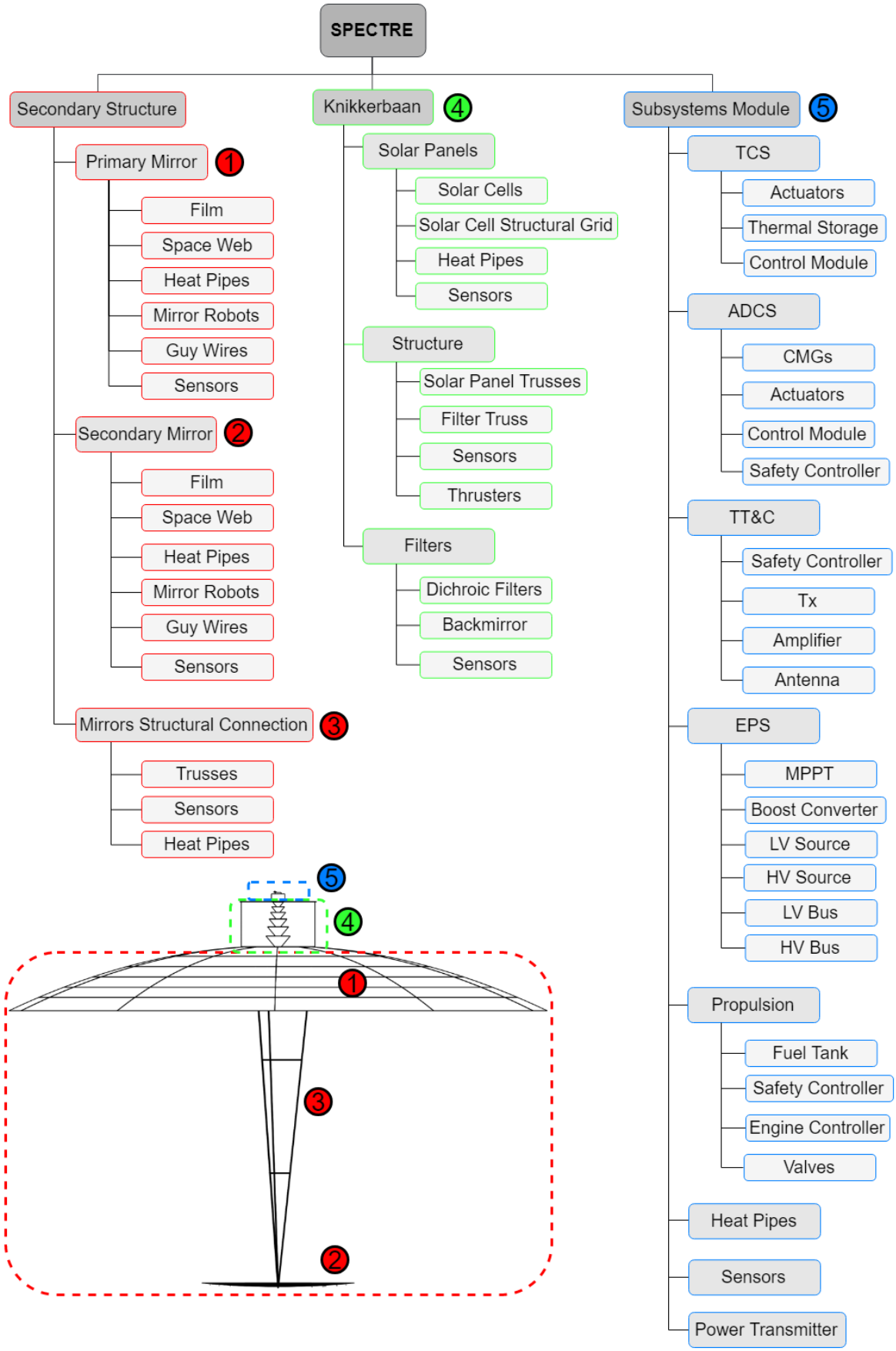

Figure 11.36: Component breakdown of SPECTRE

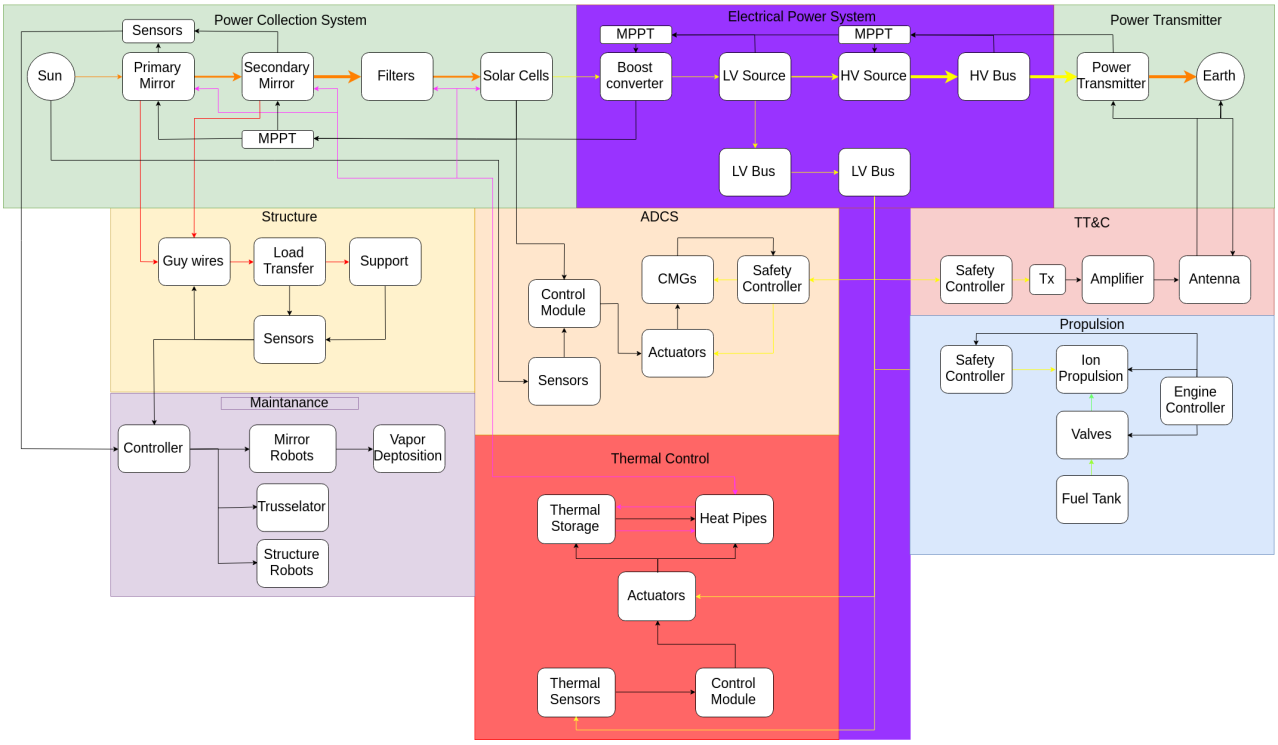

Figure 11.37: Hardware Block Diagram

Finally, the thermal subsystem interfaces with the power collection subsystem in order to cool it down and supply it with heat during the eclipses.

The electrical power system interacts with the ADCS, TCS, TT&C, propulsion and the power transmitter. The transmitter will determine the majority of the electrical power action. Its interface conists of 3 hefty HV cables which are supplied by the LV source through a series-parallel resonant transformer, powered by an MPPT. There is also a informatic feed back in order to regulate the power flow into the transmitter system.

The rest of the power is distributed among the subsystems in the LV bus. There is no data flow since they handle their own power quality and safety.

TT&C mainly interacts with the software flow, and hence has a less pronounced section of the hardware block diagram. It only amplifies and transmits/receives signals from Earth.

Propulsion interfaces only with the EPS, and internally mostly concerns powering and controlling the ion engine as well as fuel flow.

11.5.4. Software Block Diagram

To identify the required software that will have to be written in the later design phases, a software block diagram was created. For each of the subsystems the necessary actions were evaluated and their required interactions identified. These are presented in the software flow diagrams in Figure 11.38. For the ADCS subsystem extra detail was implemented in order to reflect the constant actions required to keep the spacecraft orientated correctly. The required steps of the ADCS algorithm were taken from [52]. For the other subsystems a more general approach was taken, which can be developed more in depth when the algorithms will be written.

11.5.5. Complete System Breakdown

The system breakdown includes the mass and power breakdown of the system. This gives an overview of the mass and power usages of the different subsystems.

Mass Breakdown

The mass breakdown includes the subsystem masses per spacecraft, for the total system and in percentages. This breakdown can be found in Table 11.13. As can be seen, the mass distribution is not that of a classic spacecraft. Large portions of mass are distributed to the propulsion system (12%), the ADCS (17%), the TCS (21%) and the power collection system (22%).

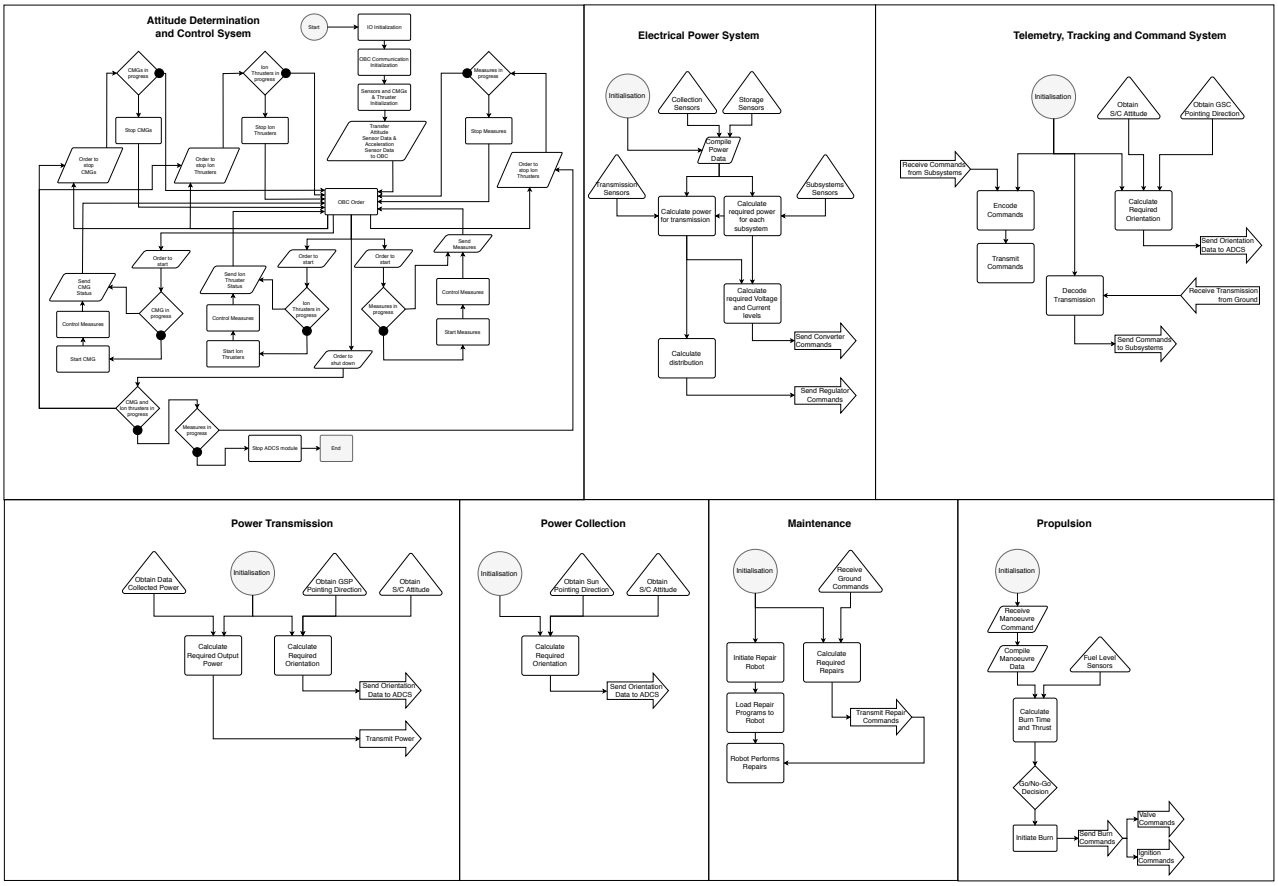

Figure 11.38: Software Diagram

The power collection system is the "useful" part of the space segment, so it follows that the mass should be largest. However, concentrating large portions of energy inevitably brings large temperatures and temperature differences with it, creating the need for a large thermal control system, with a large allocated mass in the mass breakdown.

Due to the scale of the system, the overall mass is very large. This directly effects propulsion as the Tsiolkovski equation shows, leading to a large propellant mass. The ADCS will become heavier as the system becomes heavier as well due to larger control forces and momentum storage required as the mass moment of inertia increases.

Amongst the lighter subsystems are the EPS, Maintenance and Structures. These have still scaled with the large overall mass of the system, but less so than the ADCS, Propulsion and the TCS. Especially the EPS has increased in mass due to the large amounts of power it needs to process when compared to regular spacecraft.

This mass has been the product of many iterations during the project. Contrary to the classic evolution of mass in an engineering project, the mass decreased instead of increased throughout the design as seen in Figure 11.39. This is due to the fact that the initial design was done using mature, off the shelf technologies. As the design phase

Table 11.13: SPECTRE Mass Breakdown in Tonnes

Subsystem	Total SPECTRE Mass Breakdown [tonnes]	Mass Breakdown per Spacecraft [tonnes]	Mass Breakdown (%)
Propulsion	35	1.8	12.11
ADCS	49	2.4	16.96
Thermal Control	60	3.0	20.76
TT&C	0.3	0.01	0.10
Power Collection	64	3.2	22.15
Power Storage	8	0.4	2.77
EPSY	26	1.3	9.00
Maintenance	20	1.0	6.92
Structure	26	1.3	9.00
Total	**289**	**14.4**	**100.0**

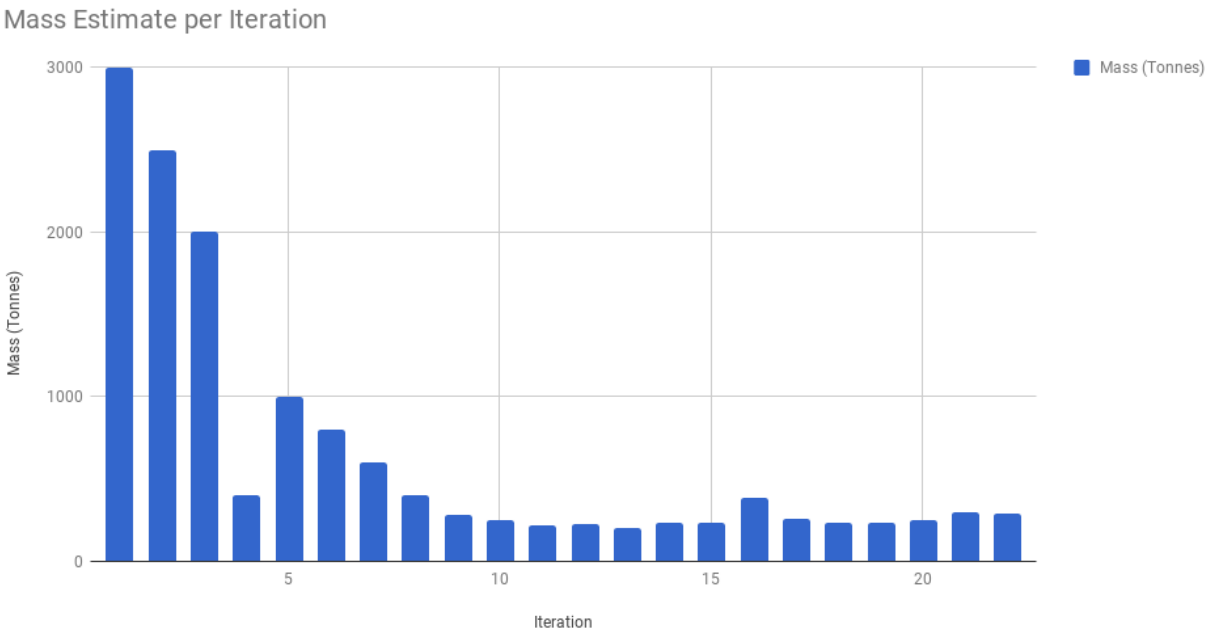

Figure 11.39: SPECTRE Design Mass Evolution per Design Iteration

Table 11.14: SPECTRE Power Breakdown at BOL in Megawatts

Subsystem	Electric power distribution [%]	Per Spacecraft [MW]	Total [MW]
Propulsion	0.00	0.0019	0.037
ADCS	0.00	0.0018	0.036
Thermal Control	0.00	0	0
TT&C	0.00	0.001	0.002
Power Collection	0.00	0	0
Power Storage	0.00	0.003	0.060
EPSY	0.04	2.24	44.78
Maintenance	0.00	0	0
Structures	0.00	0	0
Power Transmission	0.96	58.93	1178.67
Total	**1.00**	**61.18**	**1223.58**

progressed, research was done into new technology and creative solutions were found, decreasing the overall mass of the system.

At the fifth iteration however, some discoveries were made which increased the mass of the design again. After this, it can be seen that slowly the team worked to decrease this mass again by optimising the design. A similar event happened around iteration 16, however it was mitigated much faster. Eventually the final mass of 289 Tonnes was achieved.

11.5.6. Power Breakdown

Another important aspect of a spacecraft is how much power it consumes. Usually it is important to know how much power should be supplied, however in this case the supplied power is in the range of Megawatts and is not an issue. The main consideration here is that the more power is used on board of the spacecraft, the less power is available to generate revenue on the ground. A power breakdown has been made to have an overview on this, and can be seen in Table 11.14.

As can be seen, most subsystems use small amounts of power, in the order of kilowatts. Only the EPS consumes megawatt order power due to the losses in the system, around 4%, which is already a very significant amount. The rest of the power is sent to the power transmission and is then sent to the GSP where it can be distributed.

12

RAMS Characteristics and System Robustness

Considering the overall complexity of the system, its reliability and availability can become questionable. This can directly result in a system that is not capable of conforming to the requirements and mission statement, but may also be deemed unsafe. Therefore, the system must be made reliable and sufficiently available. Due to the long lifetime of the mission, it can be useful to use maintenance to increase the reliability and availability. Furthermore, this chapter will also study the effects of production inaccuracies and design uncertainties on the overall system.

12.1. Monte Carlo Simulation: Reliability and Availability

In order to test the reliability and availability of the system, a Monte Carlo simulation of the system was run. For the simulation, a variety of failures, degradations and impacts were considered, along with the biannual equinox eclipses. This simulation, with the randomised failures and repair rates, could give an impression on how reliable a single satellite from the system is at producing 50MW 90% of the time. In order to get the most reliable results, the Monte Carlo simulation was run for 30 years, with a resolution of 1 minute (15,768,000 minutes in total).

12.1.1. Programme Structuring

For the randomised values, four different randomising functions (three normal distributions with varying means and standard deviations, and one logarithmic distribution) were used. The normal distributions were used to model failure rates, degradations and impacts of the failure, with the normal distributions with the highest standard deviations representing the failures with the most uncertainty. The logarithmic randomising function was used to model repair times, as this is the most realistic method of modelling repair times. In essence, the repairs will at least take a certain amount of time, but may take longer, while the failures and degradations could happen at any time, with a certain mean failure rate.

There were a large variety of inputs for the Monte Carlo simulation, many of which were randomised. First of all, standard information such as incoming solar radiation, solar array area, mirror frontal area, total mirror area, debris size and solar cell size was used without randomisation. This information was derived from this report, and reportedly, there is a 10^{-7} chance to come across a piece of debris larger than 1mm in diameter, in 1 cubic kilometre at GEO [71]. Using the normal distribution with the highest deviation, the debris sizes were randomised.

Firstly, and most importantly, solar cell failures were incorporated. The solar cells were assumed to have a designed mean-lifetime of 35 years, with random failures occurring from BOL onwards, following a normal distribution. Then, considering the average solar cell size is $0.001 m^2$, every solar cell failure would result in a power loss of the average solar cell size divided by the solar array area. These solar cells, due to their method of implementation into the system, cannot be maintained.

On top of these solar cell failures, ADCS failures were also considered. It was assumed that the sensors were redundant enough, and easily maintainable. However, only one redundant CMG was used, and in the past they have proven to be relatively unreliable. For this mission, specialised CMG's will have to be created with average lifetimes of 35 years. Considering a normal distribution along that point, with a standard deviation of approximately 5 years, these CMG failures could also be incorporated. The impact of every consecutive CMG failing, after the first redundant one fails, is an approximate 15% power loss. This is due to the fact that if two CMG's fail (the redundant one and an additional one), the spacecraft will not be able to store enough momentum in one angular direction, and will therefore at one point start drifting from its required attitude. Due to their importance to the system, maintenance of the CMG's will be possible (this is discussed in section 12.2).

Furthermore, the aforementioned debris impact losses were considered for both solar cells and mirrors. The impact rates were related to the aforementioned debris density, and the impact magnitude for solar cells was the entire solar cell (or multiple if the randomised debris size was larger), and for the mirrors the impact magnitude was the same as

the debris size. On top of this, partial failures were also incorporated. Two partial failures were considered, including mirror partial failures and random partial failure. The mirror partial failure referred to a tear in the web. This failure could only be assumed, and was assumed to happen on average every 15 years, with an impact distributed normally between 1% and 99% in power loss. This partial mirror failure could be repaired within an average of 240 days. The random partial failure, was a failure incorporated into the simulation due to the overall complexity and uncertainty in the design. Partial failures were modelled to happen on average once every two years, and resulted in an average power loss of 10%. The partial failures could be repaired on average within 10 days. Note that the large difference in repair times is due to the fact that for a partial mirror failure, complete new mirrors will have to be redeployed. While the other partial failures refer to failures related to the EPS for example, and can be maintained through the methods described in section 12.2.

A final random failure was incorporated on top of these failures, which was a complete satellite failure. However this was assumed to be so rare, that it is yet to occur in a Monte Carlo simulation. Finally, the degradations for the solar cells and mirror were also randomised per minute, and incorporated into the program. Due to the relatively certain value for the degradations, these randomisations were limited.

Note that the programme was continuously verified through unit tests. Firstly, the eclipses were verified, after which all of the randomised functions were implemented. These randomised functions, and the results of their failures, were verified analytically.

12.1.2. Simulation Results

In Figures 12.1-12.6, one can see a simulation of the power produced (in Watts) by one satellite through a 30 year period, in 5 year intervals. Every figure shows one of these intervals, with the lower graph representing the daily averaged power output, with all of the noise at the minute resolution removed. Note some interesting characteristics of the presented graphs. In the graphs with minute resolution, the large densities of noise are caused by eclipses, where for a period of about 46 days, there are 3-72 minute intervals of eclipse. In the averaged graphs, these eclipses are represented through triangular drops. This is because the eclipse durations gradually increase when approaching the equinox, until a maximum time of 72 minutes. The eclipse duration then gradually decreases again until there is no more eclipse. Large densities of noise are also caused by the failures, which in the averaged graphs have less noise.

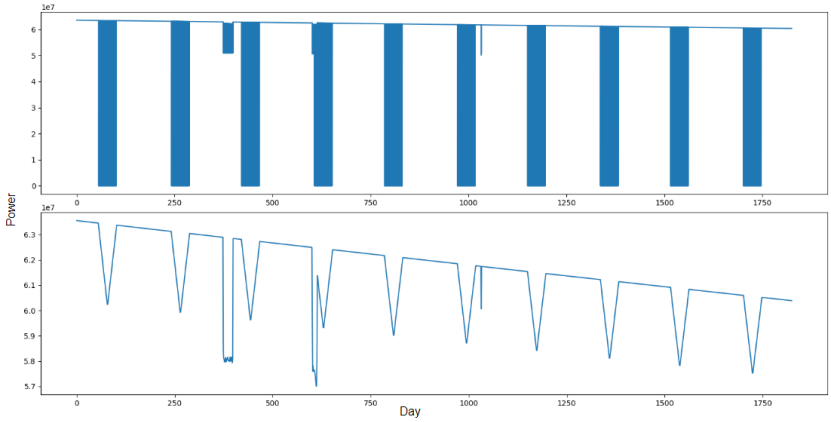

Figure 12.1: Monte Carlo Simulation for Years 0-5 of Operation

In the first five years, one can see the power decrease from a BOL power of almost 63MW per spacecraft, to about 60.5MW. During this time frame, three random partial failures have also occurred.

In the following five years, one can see the power decrease from just under 60.5MW, down to just above 57MW, which represents a random sudden decrease compared to the first year, possibly due to accelerated failures in the solar cells. Also, a partial mirror failure can also be seen to occur in the seventh year, with another partial failure happening in the tenth year.

Then, from years 10-15 of operation, the power generated decreases from above 57MW to above 54MW. During this period, one can interestingly see that the system operated without any failures for almost three and a half years. The only two failures that had happened were partial failures, and both happened within years 10 and 12.

In the next five years, the power dropped from 54MW to about 52MW. These five years were also affected by 3 partial failures, all of which were maintained or repaired very quickly.

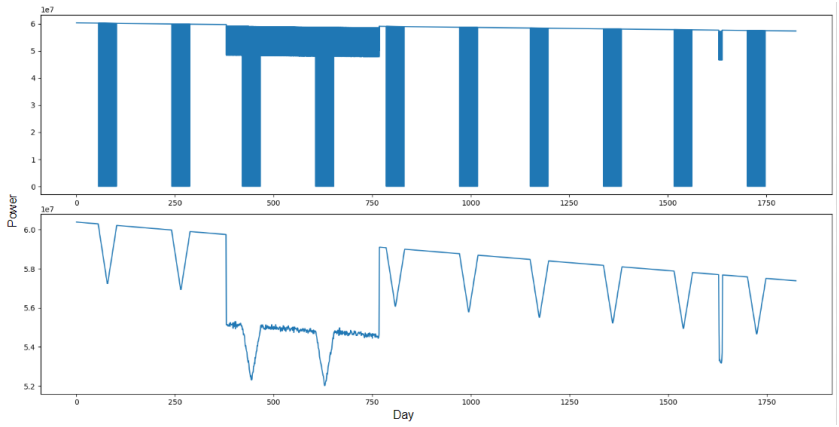

Figure 12.2: Monte Carlo Simulation for Years 5-10 of Operation

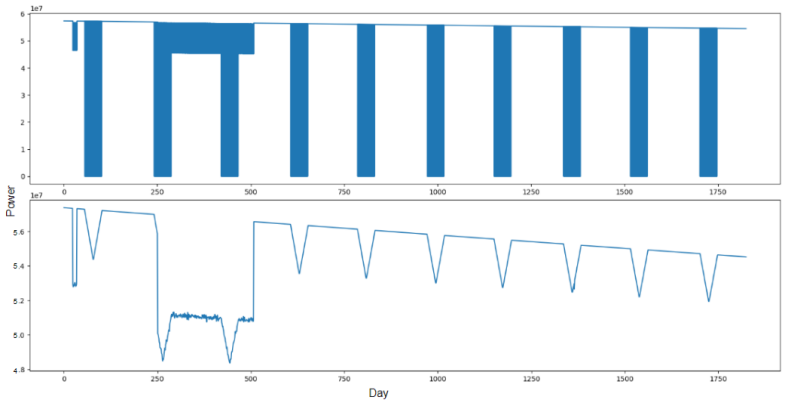

Figure 12.3: Monte Carlo Simulation for Years 10-15 of Operation

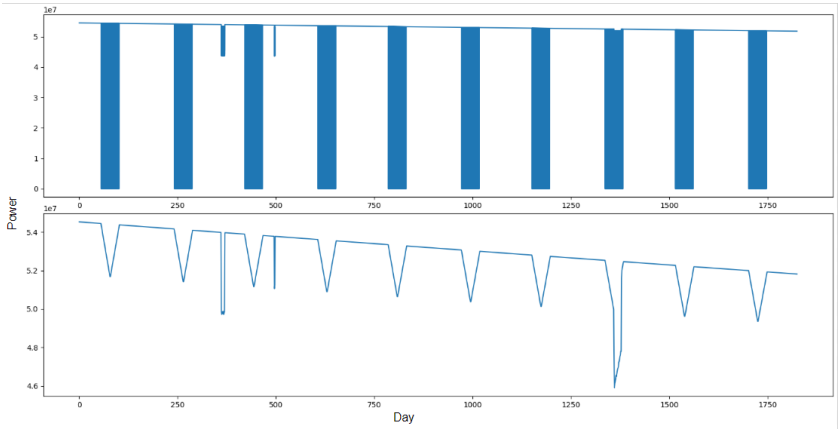

Figure 12.4: Monte Carlo Simulation for Years 15-20 of Operation

In the first half of the last third of the satellites lifetime, the power dropped from 52MW to just above 50MW. This period was also plagued by failures. First of all, three partial failures occurred, spread throughout the entire period. Between the last two years, one can also see an ADCS failure, which got repaired in about 100 days.

Above, the final five years of the required operational lifetime of the system are shown. Here, it can be seen that the generated power drops from 50MW to 48.5MW at the end of life. Furthermore, one can see that in this time period there was an abundance of failures once again. This can be justified by the gradual degradation of all the systems throughout the initial 25 years of operation. Essentially, four random partial failures occurred, and once again, an ADCS failure occurred.

The final power output of the satellite of 48.5MW, after 30 years of operation, still complies to the requirement for the system to generate 1GW at 90% availability, which means that this system can comply with the requirements throughout its entire lifetime. However, this simulation was run without the scheduled mirror maintenance, which

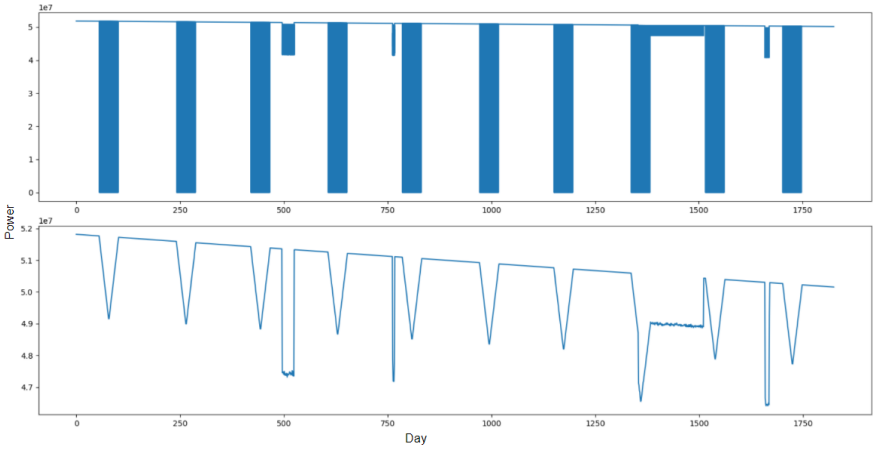

Figure 12.5: Monte Carlo Simulation for Years 20-25 of Operation

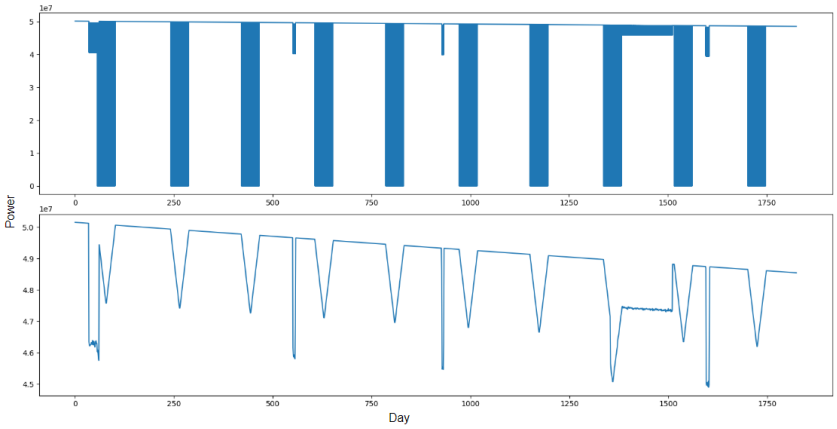

Figure 12.6: Monte Carlo Simulation for Years 25-30 of Operation

would directly increase the mirrors efficiency to produce over 50MW per spacecraft at EOL. Therefore, according to the outcome to the Monte Carlo Simulation, the solution model complies to requirements **M-SY-P-POCO-000** and **M-SY-P-POCO-001**. Furthermore, it is important to consider the handling of the power fluctuations by the EPS. However, analyses for this were performed, and the EPS perfectly handled the power fluctuations that occurred during the Monte Carlo simulation.

If one were to zoom in on one of the top graphs, to a time frame of 2 days, the noise due to a failure and the complete drops due to eclipses can be seen. This is shown in Figure 12.7. Note how once the failure is fixed, there is almost no more noise in the power production. The only noise that may occur outside of failures is due to randomised degradations and impacts. However, these have a minimal impact on the power output, and can therefore not be seen in the graph.

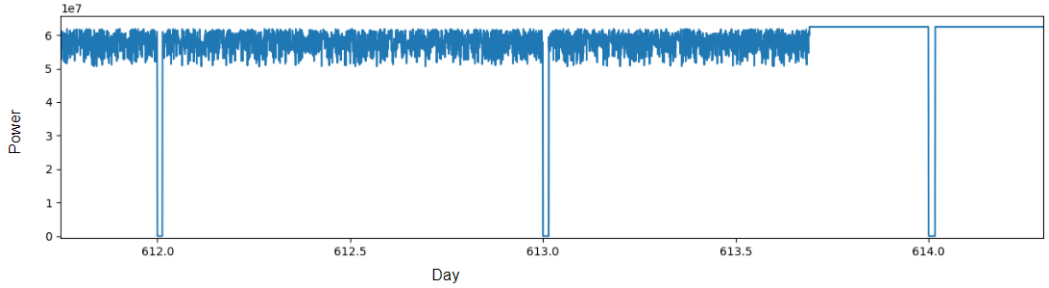

Figure 12.7: Zoom in on Simultaneous Eclipses and Failures

12.2. Maintainability

Due to the long life, the spacecraft will be exposed to a whole host of harsh environmental conditions, including, but not limited to, radiation and micrometeorites impacts. The maintenance will allow for less spare and backup systems to be installed, allowing for an overall lower mass, lower cost and therefore greater sustainability.

The mirror's major concerns are tears and holes in the mirror surface, which would decrease efficiency and structural integrity. A tear could propagate and completely destroy large sections. Hence, 2 of the robots producing the primary mirror and 1 for the secondary mirror surfaces shall remain on the system during the operation. These will perform scheduled maintenance's on the mirrors. The material for this is stored on the hub, and the robots shall come by to replenish when their on-board reservoir depletes.

Furthermore, the production modules with a large array of robotic and other maintenance capabilities with spare material will remain nearby the operational orbits of the SPECTRE satellites. These modules can be used to either completely replace a spacecraft or maintain and repair more completed systems. This will allow maintenance on the subsystem module, by letting it undock and then de-spin, after which the production module shall dock to it and start repair. While docked, the robotic arms can replace or adjust components such as a CMG, sensors, or electrical components. After it has been completed, the module can re-spin and dock to the spacecraft to resume normal operation.

For larger problems to the power collection subsystem, the entire craft can be de-spun. For this to be done however, the spacecraft should stop spinning and then allow the subsystem module to undock and the production module to dock. After which the maintenance shall take place. An example of such a repair job could concern the structure. Due to the light weight and slenderness of the design of the structure, it is possible that the structure could break during operation, which could potentially compromise the system. This procedure could allow the production robots to repair the system and allow it to enter back into normal operation.

Other subsystems such as the EPS and TCS, which are partially contained in the subsystem module and partially in the rest of the spacecraft, could also require replacement and maintenance of key components. This will hence require a combination of the 2 processes to maintain and repair.

Finally, should a system, such as the structural system, be beyond repair, then there shall be enough material to produce a replacement spacecraft. The subsystem modules, filters and any other component which can be recycled can be taken to be re-assembled in to a new spacecraft. This will replace the need to produce and launch complete spare spacecraft.

12.3. Safe Modes

Safe modes will be an integral part of the operations being performed throughout the lifetime of the system. Whenever a certain component or system fails, the system should be capable of continuing certain operations, such as communication with Earth, thermal control and attitude control. Therefore, certain measures have to be taken to ensure that these operations can continue in case of a failure. These measures, known as safe modes, will be discussed in this section. Essentially, one safe mode could ensure the proper future function of the system for most malfunctions, however, if the EPS or ADCS system malfunctions, separate safe modes are required. It is important to note that in order to decrease the operational costs of these manoeuvres, and due to the large amount of systems, the safe modes will mostly be performed autonomously. By applying various sensors in the subsystem that can track the function of all of the systems components, malfunctions can be detected automatically, and the procedures involved with the safe modes can be carried out autonomously, possibly with guidance from one supervisor for extra safety.

12.3.1. General safe mode

In general, if there will be a system malfunction that is not directly related to the EPS, ADCS or TT&C systems, the system will have a simple safe mode it can enter, until the issue is overcome or deemed beyond repair. This safe mode will be used for malfunctions in thermal control, solar cells, filters, mirrors, transmission, propulsion, command and data handling or structure.

This safe mode will essentially entail the need to cease all operations related to the transmission of power to earth, and therefore also for the collection of power. All of the solar cell switches will be turned off, or, if not possible, the attitude of the system will be changed to not face the sun. The system will then rely on the power stored in the battery, which can sustain the system for 12 hours on essential power. Furthermore, all other operations that are not essential for the systems function will be ceased. The essential systems, for which the battery power is given priority, are discussed in subsection 11.2.4.

12.3.2. ADCS or TT&C Malfunction safe mode Method

In case only the ADCS or TT&C malfunction, most of the safe mode operations will be identical to the general safe mode. However, this safe mode will be extremely critical due to the importance of the two subsystems, since both of these subsystems ensure that the ground station has control over the satellite. This will require the satellite to go into a safe mode where communication between the satellite and the production and material module is established as quickly as possible, and a docking and maintenance operation is ensued as soon as possible.

12.3.3. EPS Malfunction safe mode Method

In case of an EPS malfunction, it will be crucial to limit the load flow to the bus, such that the system can be turned off. Due to the large flows going through the system, a simple switch cannot be used since arcing may occur. To avoid arcing, the separation of wires at the switch would have to be at least 40 meters, which is not feasible. Therefore, another operation is required to ensure safety.

Below, a design option tree can be found on performing this safe mode. However, from an initial analysis into all of the feasible solutions, it was determined that none of the solutions could be used stand-alone. The only solution that would be quick enough, are the solar cell switches, however, being reliant on this could potentially ruin the solar cells, as turning off the switches for the solar cells would gradually heat them as well. Therefore, this can only be a temporary solution. So now, a trade-off will be performed on the last four options.

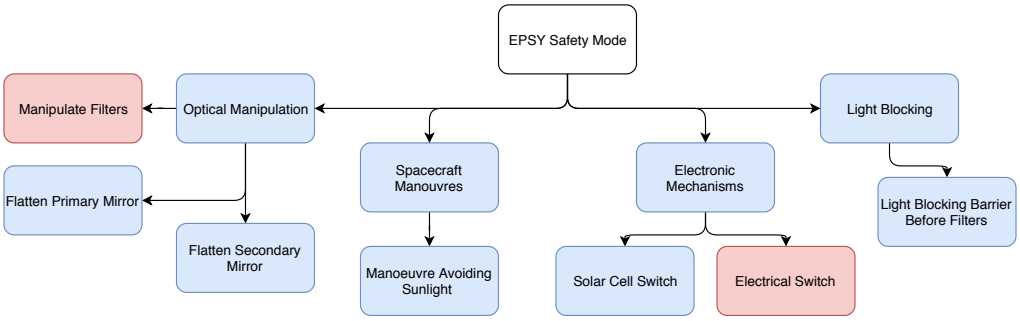

Figure 12.8: Design Option Tree for the EPS safe mode Method

Trade-off for EPS safe mode Method

For the EPS safe mode method trade-off, certain applicable criteria had to be defined. These criteria are the time to stop load flow, which is derived from the EPS requirement in case of malfunction. Note that since solar cell switches will be used either way, this criterion will now correspond to minimising the load flow on the solar cells. Furthermore, extra mass and reliability are derived from the stakeholder requirements, as the mass should be minimised, and the reliability maximised. The implementation into the system was mainly considered for the production of the system, and the risk on other systems was derived from the reliability, availability, maintainability and safety characteristics. These criteria can now be assigned weights using another QFD, and the following weights were established.

Table 12.1: Criteria and Weights for EPSY safe mode Method Trade-Off

Identifier	Criterion	Weight
CR-EP-01	Time to Stop Load Flow	0.28
CR-EP-02	Extra Mass	0.14
CR-EP-03	Reliability	0.26
CR-EP-04	Implementation	0.11
CR-EP-05	Risk on Other Subsystems and Components	0.20

With the criteria and weights defined, and an internal rubric created, the following trade-off results were acquired.

12.4. System Robustness

After designing the system, it is crucial to test the robustness of the design, and to identify how sensitive the system is to the variation of certain parameters. These parameters are either parameters that have a certain degree of uncertainty in their value, or parameters that are prone to variation due to production inaccuracies. The variation of these parameters has been tracked with respect to the mirror frontal area, total mass and total cost of the system. Note

Table 12.2: EPS safe mode Trade-Off Results

Identifier	CR-EP-01	CR-EP-02	CR-EP-03	CR-EP-04	CR-EP-05	Total
Flatten Primary Mirror	2	3	2	2	3	2.32
Flatten Secondary Mirror	2	3	2	1	3	2.21
Manoeuvre Avoiding	1	2	3	3	2	2.07
Light Blocking Barrier	3	1	1	1	1	1.55

that the number of launches was mainly optimised for packing efficiency rather than mass, such that although the system mass is 289 tonne, 15 launches with a capability of bringing up 675 tonne will be used. Therefore, the system costs will be less dependent on mass than expected.

12.4.1. Sensitivity Analysis on Design Uncertainties

First, a sensitivity analysis will be done into the parameters used in the design process. Essentially, there were five parameters that were used throughout the design, which have insufficient certainty. These were the TCS and EPS mass, the solar cell degradation and efficiency, and finally the solar cell area density.

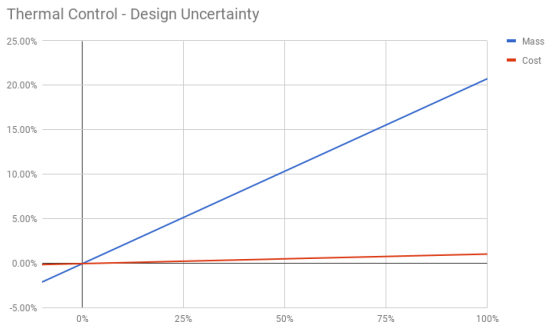

Figure 12.9: Sensitivity Analysis for Varying TCS Mass and Price

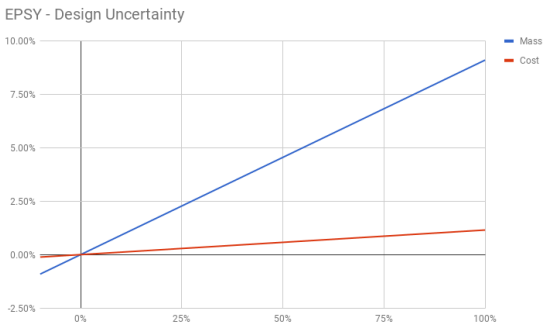

Figure 12.10: Sensitivity Analysis for Varying EPS Mass and Price

Above, the graphs for the sensitivity analyses of the TCS and EPS masses and prices are given. As one can see, compared to thermal control, the system cost is more sensitive when related to the electrical power system. However, in terms of the system mass, the system is a lot more sensitive to the mass of the thermal control system.

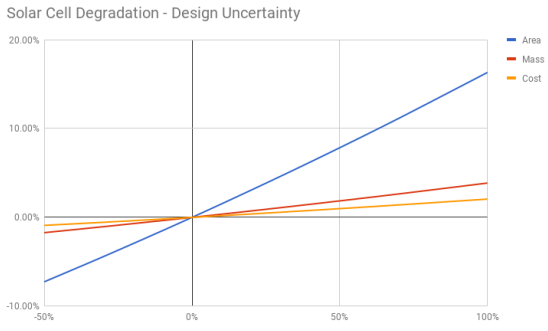

Figure 12.11: Sensitivity Analysis for Varying Solar Cell Degradation

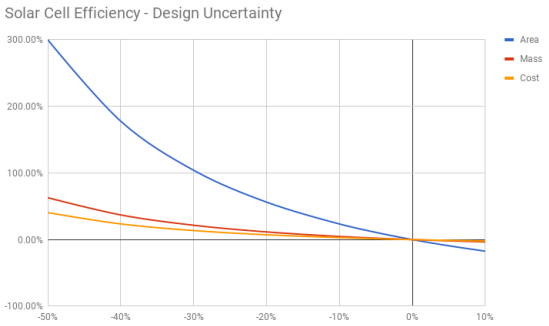

Figure 12.12: Sensitivity Analysis for Varying Solar Cell Efficiency

The sensitivity analyses for varying solar cell efficiency and degradation are given above. Once again, the area is clearly a very sensitive parameter, since compared to the variation in mass and cost, the variation in area is almost a magnitude larger. Interestingly, the systems mass, cost and area have an almost linear dependency on solar cell degradation, but a highly quadratic dependency on solar cell efficiency.

A final sensitivity analysis based on design uncertainties is given above. As one can see, the solar cell area density has an almost negligible effect on the total mass of the system. This is mainly due to the innovative use of light concentration.

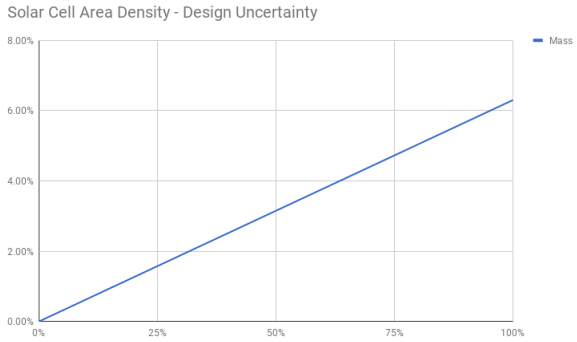

Figure 12.13: Sensitivity Analysis for Varying Solar Cell Area Density

12.4.2. Sensitivity Analysis on Production Inaccuracies

On top of the uncertain design parameters, production inaccuracies could also greatly decrease the performance of the system. The production inaccuracies that have been given priority in this analysis are the bus efficiency, mirror density, ADCS accuracy and mirror efficiency.

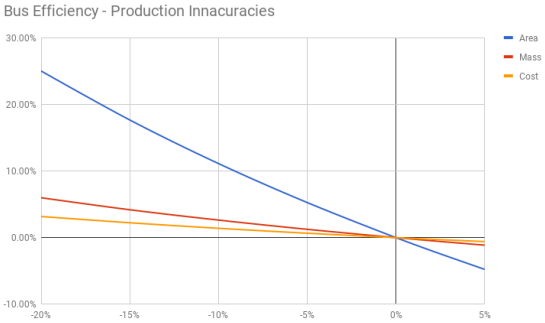

Figure 12.14: Sensitivity Analysis for Varying Bus Efficiency

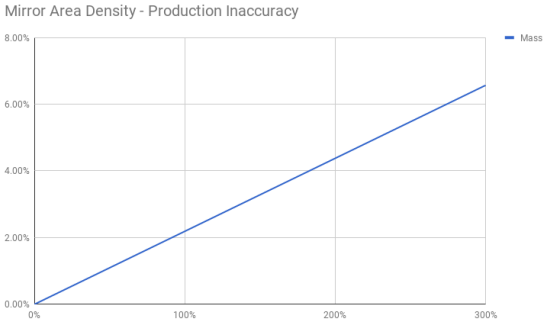

Figure 12.15: Sensitivity Analysis for Varying Mirror Density

The graph above to the left shows the systems mass, cost and area sensitivity with respect to the bus efficiency. Once again, area is the most sensitive parameter. Nevertheless, the relations of the mass, cost and area, to the bus efficiency, are logical. The graph to the right, for a variation in mirror area density, is very similar to the sensitivity analysis into varying solar cell area density.

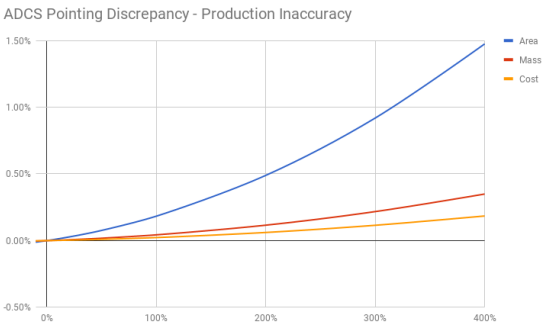

Figure 12.16: Sensitivity Analysis for Varying ADCS Accuracy

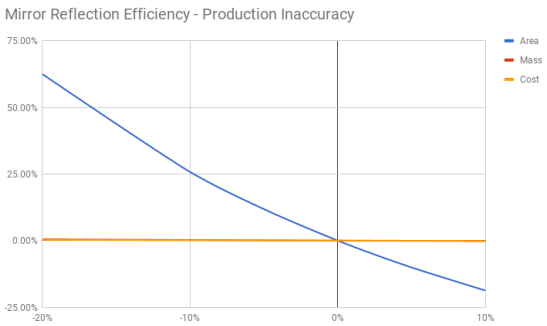

Figure 12.17: Sensitivity Analysis for Varying Mirror Efficiency

The sensitivity analysis for varying ADCS accuracy also has the most effect on the required surface area of the system. While mass is only slightly affected compared to the area, and cost even less so. For the reflection efficiency, one can see that due to the use of extremely thin mirrors, the mass and cost are practically unaffected. However, the area once again varies significantly.

12.4.3. Study into the most Sensitive Aspects

A study will now also be done into the most sensitive parameters that were studied above. These have essentially been chosen to be the solar cell efficiency, bus efficiency, mirror efficiency, and solar cell degradation.

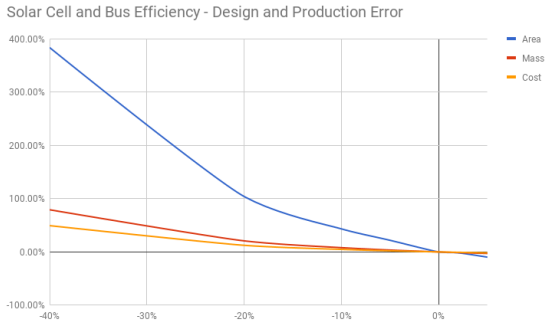

Figure 12.18: Sensitivity Analysis for Varying Solar Cell and Bus Efficiency

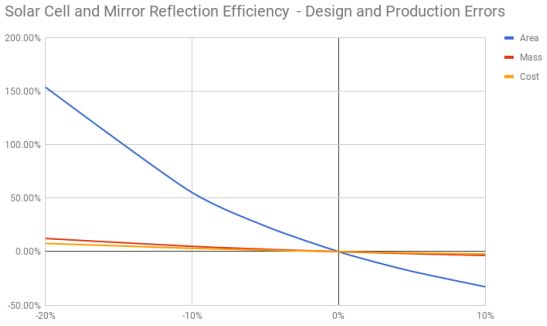

Figure 12.19: Sensitivity Analysis for Varying Solar Cell and Mirror Efficiency

Above to the left, and combined sensitivity analysis into solar cell and bus efficiency can be seen. This sensitivity analysis presents a very extreme case, where both efficiencies could be a lot lower than anticipated due to a design uncertainty and production inaccuracy. Clearly, this would result in an unsustainable system mass and cost. However, when considering solar cell and mirror reflection efficiencies, the effects on mass and cost are surprisingly sustainable. Therefore, a sudden drop in the solar cell or mirror reflection efficiency, would not result in a failed design.

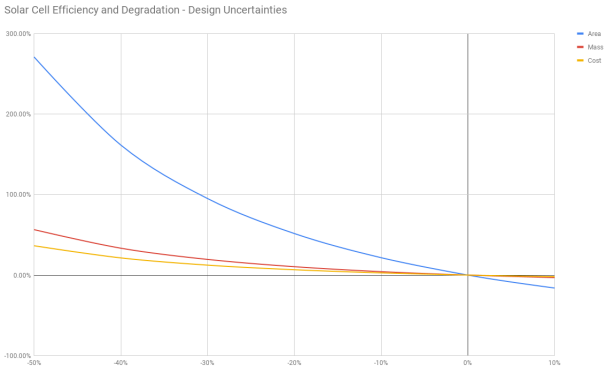

Figure 12.20: Sensitivity Analysis for Varying Solar Cell Efficiency and Degradation

Figure 12.20 shows the final sensitivity analysis, for varying solar cell efficiency and degradation. Varying these parameters results in conflicting effects to the system, since lower degradation would result in lower masses, costs and areas, but lower efficiency would instead increase those parameters. However, from the analysis above, one can see that the solar cell efficiency is the dominating factor in the design, when compared to the solar cell degradation.

13
Production Plan

Arriving at a large system in space involves a complex series of production activities. The Manufacturing, Assembly and Integration (MAI) or Production Plan presents a chronological outline of these activities required to construct the SPECTRE system from its basic parts, with a flow diagram at its core (section 13.5). However, to understand the reasoning behind this chronological outline, the selected production options and chosen concepts are to be discussed first (sections 13.1 and 13.2). Also a list of parts to be produced on Earth and some material characteristics are presented, in sections 13.3 and 13.4 respectively. The chapter concludes with further recommendations w.r.t. production of the proposed SPECTRE system in section 13.6.

13.1. Production Design Options

In this section the importance of in-orbit production is discussed first in subsection 13.1.1 and the in-orbit production design option tree is discussed in subsection 13.1.2. While this report can be read stand-alone, for a more extensive read on the subjects discussed here the reader is kindly referred to the relevant chapters from the Baseline and Midterm report [19][20].

13.1.1. On-Earth vs. In-Orbit

Using a launcher to reach orbit entails limits on volume and mass available for payload per launch. Due to this, large space systems unavoidably bring about some form of in-orbit production, be it either the joining of modules to construct a space station or the actual in-orbit manufacturing and assembling of parts. Also, because a structure built in space does not have to survive launch loads it can be significantly lighter than one built on Earth - or larger. On the flip side, extensive in-orbit production techniques are still very much in the infancy phase and thus expensive to develop while also introducing risk into the project. Therefore, when deciding on the (level of) in-orbit production processes, complexity is to be limited as much as possible [20]. Please take note that throughout this chapter focus will be on in-orbit operations, as these were found to be far more technically challenging when compared to the operations on Earth and will thus drive the design.

13.1.2. In-Orbit Design Option Tree

The design option tree related to in-orbit production means can be found in figure 13.1. As was stated before, this tree is to be treated more as a toolbox: because of the wide variety of processes to be completed, the final integral production concept will unavoidably end up as a combination of the presented options (DOT-PR-1.6) making a classic trade-off not applicable. Instead a practical option has to be decided upon for every operation, with the limitation of in-orbit production complexity as the main selection criterion. In this sense the repeated use of one production concept is preferred over the use of many different options, and for delicate high-accuracy operations on-Earth production is preferred over in-orbit.

Before moving on to the selected concepts in section 13.2 it is important to note that the production plan as presented in this chapter and the engineering design from chapter 11 are closely interrelated: it is the designed system that has to be produced, but the system also has to be designed for production. This is especially true for large space systems and therefore production complexity has been an important design consideration right from the start of the design process, as illustrated in previous reports [19][20].

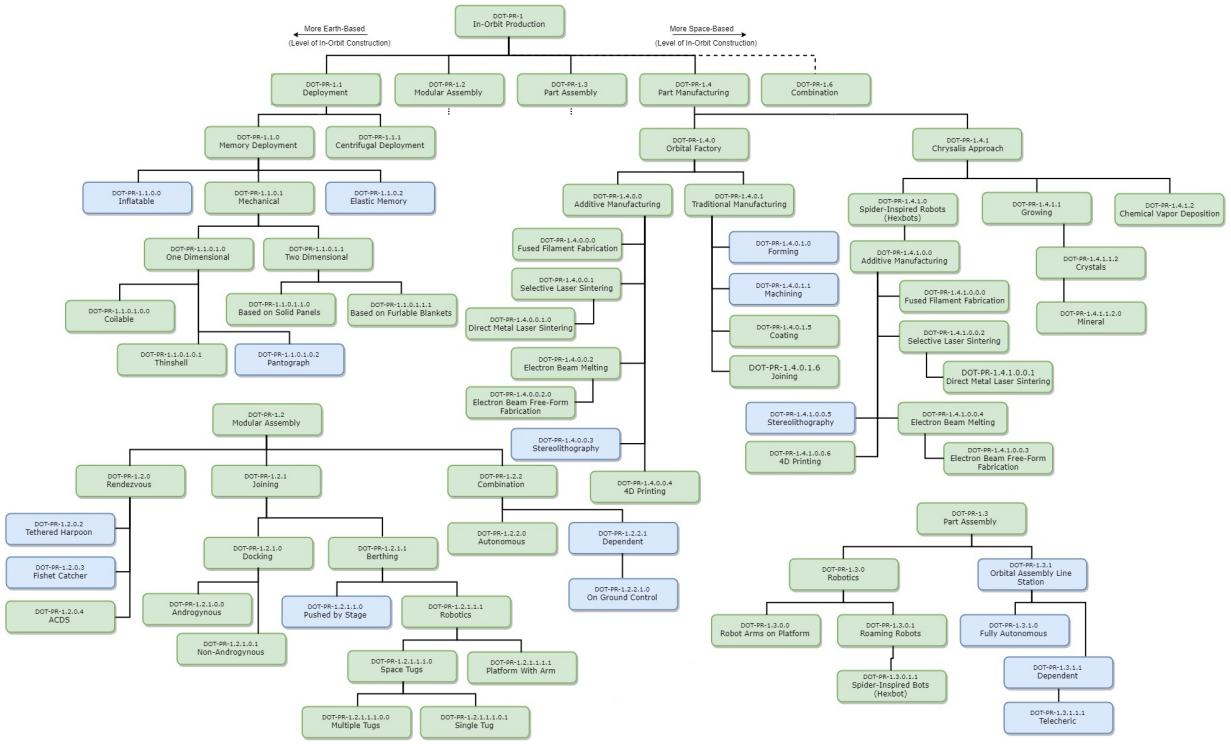

Figure 13.1: In-orbit production DOT. Please not that some branches are detached in light of packing efficiency.

13.2. Selected In-Orbit Production Concepts

In this section the selected production options from fig. 13.1 are elaborated upon. To enable a smooth discussion, these options have been assembled into four production concepts: modular production (subsection 13.2.1), additive manufacturing of trusses (subsection 13.2.2), robotic assembly (subsection 13.2.3) and the production of large mirrors (subsection 13.2.4). Also the filters and photovoltaics are briefly addressed (subsection 13.2.5). For the chronological integration into the actual MAI Plan, please refer to section 13.5. Also figure 13.8 can be found there, which illustrates the integration of below concepts through renders.

13.2.1. Modular Production

The production design will use a modular approach (DOT-PR-1.2). Three types of modules will be launched: five production modules, ten materials modules and twenty subsystem modules. A production module contains all the robots and other tools required to produce SPECTRE spacecraft, while also supplying the required power, control and communication for production. Each of the materials modules contain all the raw materials and basic parts required to produce two SPECTRE spacecraft. In its final configuration, the subsystems module will be docked to the SPECTRE structure to complete a SPECTRE spacecraft and will house all the subsystems that do not need to be on the SPECTRE structure itself.

First, the active production module will deploy and will use its robotic arm to berth (DOT-PR-1.2.1.1.1.1) with a materials module. At this point an orbital factory (DOT-PR-1.4.0) has been created and the production can start. When the SPECTRE structure is complete and ready for spin up and centrifugal deployment (see the following subsections), the production and materials modules will detach from the structure, after which point a subsystems module will dock with the structure to complete the SPECTRE configuration. This sequence is illustrated in figure 13.2.

This modular approach has a number of important advantages. Firstly, it allows the subsystems module (with a lot of different and complex parts) to be produced on Earth and launched whole. It also allows for the possibility for the subsystems module to be detached from the spinning SPECTRE spacecraft and de-spun for easy repairs, or replaced (important for requirement **D-ST-P-MAIN-000**). Additionally, it means that a complete set of production tools is not required for every spacecraft, which saves on launch mass. Finally, in the case of multiple production modules the modular approach provides redundancy: when (part of) a production module fails, the corresponding materials module can be docked to another production module such that the spacecraft is not lost (**M-ST-L-PROD-002**). Even after the production phase is over, the production modules can be kept in orbit to serve as maintenance platforms (**D-ST-P-MAIN-001**). The exact design of this production module, which is in effect a fully independent spacecraft,

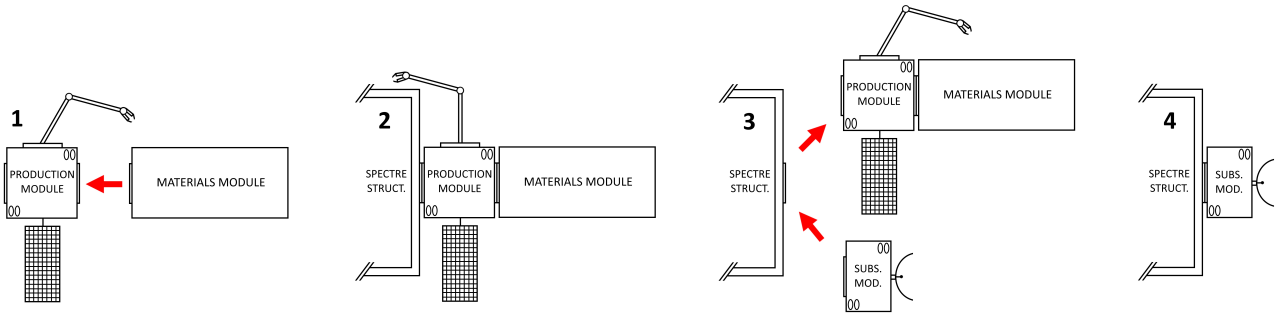

Figure 13.2: Modular production sequence. 1. Production module berths materials module; 2. This combination produces the SPECTRE structure; 3. The production and materials module detach (and go on to produce the next structure) and the subsystems module docks with its structure; 4. The operational combination ready for spin up.

was considered outside the scope of this DSE project. Please refer to section 13.6 for further recommendations w.r.t. production.

For this modular approach the use of a versatile docking interface is necessary. To accomplish this, the International Docking System Standard (IDSS) should be used [17]. This docking interface is androgynous and can be used for either docking and berthing. This makes it possible to use one type of interface for all three modules as well as the SPECTRE structure. As the IDSS will be a standard for spacecraft docking interfaces for many years to come, housing this universal adapter will make sure that future missions that want to benefit from the functionality of the SPECTRE structure or any of the modules can do so with relative ease (**O-ST-S-SOCI-000**). This also means that compliance with **D-ST-S-ENVI-004** is met, as with this approach every part of the system can be recycled.

13.2.2. Additive Manufacturing of Trusses

The structure of the SPECTRE system is built up out of trusses (for the exact structural design, please refer to chapter 11). It is especially true for these structural components that a high level of in-orbit production yields substantial weight savings, as an Earth produced structure would have to be designed to survive big launch loads. To comply with requirement **D-SY-S-ENVI-000** which limits production material scrap, additive manufacturing (DOT-PR-1.4.0.0) was a straightforward choice. Also deployable booms (DOT-PR-1.1.0.1) were considered, but even for the highest performing space deployables such as the ISS FAST Mast (33 metres length, stowed at 3 metres) a very large portion of the stowed volume is still empty [123]. Additive manufacturing promises higher packing efficiencies as the trusses are effectively launched as compact raw material. Additionally, large structures built in-orbit do not require the hinges, latches and other complex mechanisms of deployables, eliminating these parasitic masses.

Tethers Unlimited, Inc. (TUI) is currently developing in-orbit part manufacturing under a NASA Small Business Innovation Research program. One of the developed concepts is known as "the trusselator", which effectively combines Fused Filament Fabrication (FFF) (DOT-PR-1.4.0.0.0) with an automated composite layup mechanism to build continuous lengths of first order trusses from PEEK/carbon fibre composite material, which is fed to the machine from filament spools. The incorporation of pultrusion into the 3D printing process is particularly interesting, as it speeds up the FFF process and enables structural elements to be produced with high-modulus, high-tenacity fibres optimally aligned for the service loads. This method is now called the SpiderFab™ process. TUI's Trusselator mechanism as well as an Earth-based proof of concept can be seen in figure 13.3. The illustrated mechanism is designed as a 3U CubeSat-sized demonstrator [123][146].

For simplicity the SPECTRE spacecraft will be build up from one type of truss, with PEEK/carbon fibre composite material as the material of choice. The trusselator from figure 13.3 produces 5 cm of truss every minute [146]. Not one but two trusselators will be installed on the production module with redundancy as main concern, but this also speeds up the production process. Assuming a total truss length of 1559 metres, it will take two trusselators 11 full days to produce the trusses for one SPECTRE spacecraft (important for **D-SY-L-PROD-000**). Unfortunately, no trusselator mass or power budgets could be found in literature. For now, 200 kg (excluding raw truss material) and 800 W peak power were assumed per trusselator. For the manipulation and joining of the trusses, please refer to subsection 13.2.3.

13.2.3. Robotic Assembly

Robotics will form an important part of the production process. This section will discuss the robots launched with the production module. For the web crawling robots that produce and apply the reflective film on the space web, please refer to section 13.2.4.

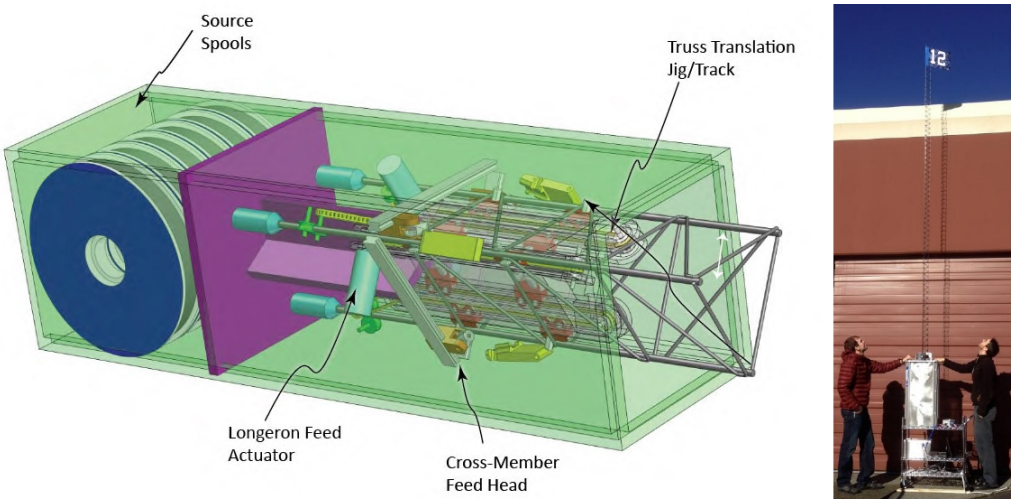

Figure 13.3: TUI's Trusselator. Left: CubeSat-scale mechanism. Right: successful proof of concept trusselator, producing a 1st order truss. Courtesy of Tethers Unlimited, Inc.

The robotics present on the production module must be able to move itself over the structure as it gets constructed, have access to power in situ, manipulate and join trusses and it needs the dexterity to install functional elements on the structure (refer to requirement **M-ST-L-PROD-000**). Furthermore, it must be able to reach all final functional element locations as well as the materials from the materials module, from the structure or module to which the robot is connected.

Considering the above requirements, the International Space Station's robotic system easily comes to mind: the Mobile Servicing System as developed by MacDonald, Dettwiler and Associates Ltd. for the Canadian Space Agency. It consists of three robots that can work together or independently:

- Canadarm2: a 17-metre long robotic arm with seven degrees of freedom used to assemble the ISS and move supplies, equipment and astronauts and to capture free-flying spacecraft to berth them to the station. It has two latching end effectors, one at each end, with which it can attach itself to data grapple fixtures along the station. By moving end-over-end in an inchworm like movement, it can relocate itself.
- Dextre: resembles a torso with two extremely agile 3.5 metre arms and several power tools. It can handle delicate assembly tasks for regular maintenance and repairs, which before its installation required astronaut extravehicular activity. It can attach to Canadarm2, the station or the Mobile Base System.
- Mobile Base System: a movable work platform and storage facility that slides on 108 metre rails along the length of the station. It can move Canadarm2, Dextre, supplies or even astronauts with a payload of up to 20,900 kg.

Due to the proven record of the above robotics and their versatility, these will serve as a baseline for the robotics present on the SPECTRE production module (DOT-PR-1.3.0.1). The specifications are summarised in table 13.1 [13]. It is assumed that by 2030, telemanipulators with these specifications will have the capabilities to perform the required in-orbit production tasks as outlined above, for example, that the Mobile Base System can be adapted to travel over the SPECTRE trusses. Combining the three systems we arrive at a peak power of 4825 W, average power of 2165 W and a mass of 4803 kg for the robotic system per production module. The production module will have to accommodate these machines in their power needs, as during production the SPECTRE system is not operational yet. Assuming an end of life solar array efficiency of 30%, an array of approximately 12 square metres will be required solely to power the robotics (at peak power) and per production module. This was considered well within the realms of feasibility.

A specific capability still missing from ISS' robotic system is the means to join different trusses together. In TUI's SpiderFab concept a Joiner Spinneret using thermoplastic bonding is proposed [123]. This specialized end effector can be fitted to a robotic arm and uses Fused Filament Fabrication techniques to print uniformally filleted joints around tubular truss elements to join them. As illustrated in figure 13.4, the print head is located on a finger with three independently cable-driven joints such that the spinneret can reach the required locations and angles, even through tight angles between two to-be-joined truss elements. One of these spinnerets will be fitted to the Dextre-like robot. PEEK was identified as an excellent material candidate, its properties can be found in table 13.2 in section 13.4.

Table 13.1: Specifications of the robotics present on the ISS.

	Canadarm2	**Dextre**	**Mobile Base System**
Length	17.6 m	3.5 m	-
Mass	1641 kg	1662 kg	1500 kg
Handling Capacity	116,000 kg	600 kg	20,900 kg
Degrees of Freedom	7	15	Fixed
Peak Power	2000 W	2000 W	825 W
Average Power	1200 W	600 W	365 W

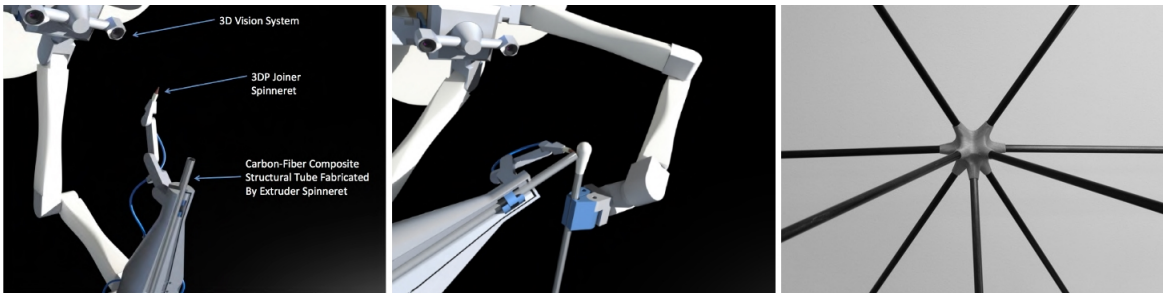

Figure 13.4: SpiderFab spinneret 3D-printing an optimized joint. Courtesy of Tethers Unlimited, Inc.

13.2.4. Production of Large Mirrors

The solar reflectors will form the largest part of SPECTRE system in terms of surface area. The production concept consists of four in-orbit operations: the centrifugal deployment of a space web (nr. 1), followed by tensioning of guy-wires to shape the mirror (nr. 2), a CVD process to produce reflective thin film (nr. 3), and finally the robotic attachment of this film to the web (nr. 4). The production of the solar reflectors is visualised in Figure 13.5.

1. Centrifugal Deployment of Space Web - The first in-orbit reflector production step is the centrifugal deployment (DOT-PR-1.1.1) and stabilising of an Earth-produced space web to effectively create a large structure that does not rely on hard parts for prestressing, but the stiffening effect of centrifugal forces. This is done by spinning a central hub, and after deployment, the whole assembly about a central axis. The result is a structure loaded mainly in tension, allowing for an extremely efficient design using fibrous Zylon™ material (important for **D-SY-S-ECON-000**, the structural design of the space web can be found in chapter 11) that can be stowed very compactly for launch. Also functional elements such as heat pipes (for the thermal subsystem design, see 11.2.3) will be integrated into the web during production on Earth, to be deployed together with the web.

Clever folding and deployment strategies are required to control and stabilise these flexible structures, which are subject to complex dynamics but have been demonstrated in space [138]. Spin control strategy is critical to prevent the web from collapsing on itself again after deployment. It was found in literature that uncontrolled, constant velocity or linearly increased velocity deployment do not yield stable results. Melnikov and Koshelev proposed the following control law for a stable deployment effect:

$$M = M_{\max}\left(1 - \frac{\omega_h}{\omega_{h0}}\right)$$

Where M is the applied torque around the spin axis, $M_{\max}$ is the maximum control torque (as determined by the ADCS thrusters that will be used for spin control), ω_h is the angular velocity of the hub and ω_{h0} is the initial angular velocity of the hub. L. Haitao et al. modelled different deployment strategies and found that this control law does indeed produce stable results [86].

2. Guy-Wired Shape Control - Next, guy-wires connected to the spinning space web and secondary structure will be tensioned to attain and maintain the exact parabolic shape of the individual webs (**D-ST-P-MAIN-001**). This is illustrated in nr. 5 in fig. 13.5. By increasing the amount of guy-wire connections, one can increase the resolution of control. Because the loads on the guy-wires will be relatively small (refer to chapter 11 for the structural analysis), light servomechanisms located on the secondary structure trusses can be used for actuation. These consist of a DC motor, a gearing set, a control circuit and a potentiometer. Determining the exact amount of required guy-wires and thus the resolution will involve an iterative process between the structural and power collection departments: increasing the resolution means that the final shape will show less deformation from the exact parabolic shape as designed in chapter 10. It is important to note that to maintain the shape and structural integrity of the mirrors, the SPECTRE structure needs to stay spinning at all times over its lifetime. This also means that the mirrors can be

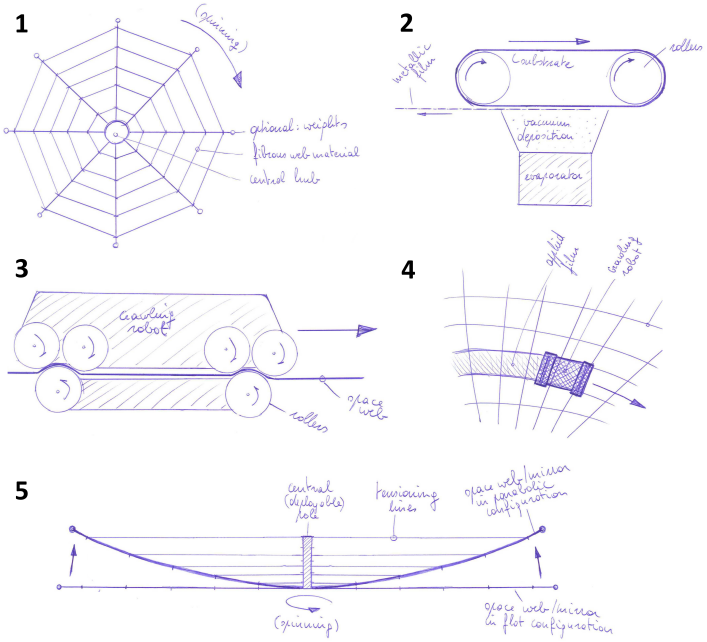

Figure 13.5: Strawman drawings of the proposed reflector production concept.
1. Centrifugally deployed Space Web; 2. CVD process; 3. Web crawling robot, 4. Attaching of the film; 5. Guy-wired shape control

defocused by slacking the guy-wires, which could prove helpful to ease thermal loads on the filters and photovoltaics in the knikkerbaan in case of an electrical power system failure.

3. CVD Process - A CVD process (DOT-PR-1.4.1.2) will be used to create a metallic thin film in the high vacuum of space. In this particular application the first step is the evaporation of aluminium from a supply in powder form, through electrical heating. The vapour then condenses on a substrate to form a reflective thin film. If a polymer film such as Kapton™, Mylar™ or Lexan™ is used as a substrate one would effectively end up with what in the industry is known as a "solar sail".

However, in literature Colin R. NcInnes [97] describes a setup in which the static substrate is replaced by a conveyor belt. Here the metallic thin film is deposited on the moving belt and separated from it again once cooled. This is what will be used for our in-orbit application, as the author indicates that the plastic substrate layer in a classic solar sail is only required to allow for handling and packing during manufacture and to ensure safe deployment without tearing. However, the thinnest sheets of Kapton™ commercially available have a thickness of 7,6 μm, which corresponds to a surface density of 10.8 g/m^2. Assuming an aluminium layer of 0.1 μm and 0.27 g/m^2, the Kapton™ substrate makes up 97.6 percent of the solar sail mass. Producing it in situ means that the plastic substrate layer can be omitted. Even when increasing the aluminium layer thickness with a factor ten to 1 μm for extra tear resistance, this still saves 80 percent on the surface density, or 22,200 kg for the entire SPECTRE system (important for **D-SY-S-ECON-000**). Furthermore, by altering the speed of rotation of the conveyor belt the thickness of the metal film can be varied to provide, for example, extra strength at the edges of the film.

Additionally, over its 30 years lifetime, the mirror surface will be exposed to micrometeorites, space debris, electromagnetic radiation from sunlight and occasional particles from solar flares which will degrade the optical performance, raising the need for maintenance of the surface. The production CVD process (and its equipment) can be used to regularly apply a fresh metallic layer to restore initial reflectivity (according to **D-ST-P-MAIN-001** and **M-SY-S-ECON-000**), by smoothing flaked areas and sintering together older foil surfaces that might have gone brittle over time. It is expected that this process will have to take place at least once every 10 years [88]. During initial production an aluminium layer of 0.5 μm will be applied, and layers of 0,25 μm at 10 and 20 years to arrive at an EOL thickness of 1 μm. Lithium and Silver were also considered as reflective surface material, but aluminium was found to be far superior when considering reflectivity, durability, density, cost and melting temperature as trade-off criteria.

To determine how much power is required to CVD the aluminium of one SPECTRE spacecraft within the determined time frame, one needs an estimate of how much energy it takes to vaporize 1 kg of aluminium powder. Its enthalpy of fusion is 10.9 kJ/mol and enthalpy of vaporisation 284 kJ/mol [54], or 404 J/g and $10.5*10^3$ J/g respectively using a molecular weight of 26.982 g/mol. Its specifc heat is 0.900 J/g°C. Therefore the energy required to heat up 1 kg of aluminium powder from 0 K to 2600 K (boiling point at 1 bar of atmospheric pressure) and then vaporise it is equal to $132*10^4$ J/kg. Please note that this is assuming the aluminium has to be heated up from 0 K and at atmospheric pressure. In reality the starting temperature will be higher and the pressure will be lower meaning that its boiling

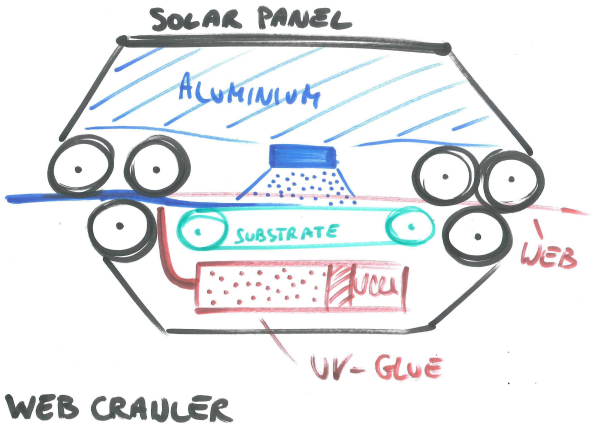

Figure 13.6: An initial straw man drawing of a web crawling robot.

temperature and enthalpy of vaporisation will be significantly lower. Hence it is not required to introduce another safety factor. Assuming an available time frame of 0.5 years for film application, the web crawling robots on the primary mirror will each have to deliver 6.2 W continuously to deposit the initial thin film, while the robot on the secondary mirror has to deliver 0.88 W. For the re-application at 10 and 20 years, these modest values can be halved as only a 0.00025 mm thick film will be applied compared to 0.0005 mm initially.

4. Web Crawling Robot - This CVD technology will be integrated in a web crawling robot (DOT-PR-1.3.0.1), which attaches the mirror thin film onto the space web using adhesives thus completing the mirrors. This robotic element is arguably the most advanced part of the mirror production concept, with the dynamic behaviour of the space web in combination with the robots as a particular concern. However, the web crawling concept has been demonstrated in the Japanese Furoshiki experiment including ESA's Roby Space robots [138] with the web deploying perfectly and at least one robot successfully crawling on it [136], demonstrating feasibility. 8

To assure symmetry around the spin axis, two robots will work in parallel on opposite sides of the primary mirror where the distances to the spin axis are large. For the secondary, smaller mirror, it is expected that one lighter robot will suffice. To limit web perturbations as much as possible, it is essential that the web crawlers travel at a slow constant speed. Assuming an application width of one metre and an application time frame of 0.5 years, the two robots on the primary mirror will have to travel 3.22 mm/s (millimetres per second), and the robot on the secondary mirror at 0.528 mm/s to cover the required surface area. To prevent the space web and applied thin film from stretching at different rates under the loading of the layers applied after and to the outside of it, the robots will apply this film starting from the outside perimeter of the web and work their way to the centre. In this way the space web at the production location is preloaded before film application. UV curing adhesives will be used to bond the film to the web, and a thermal emissive coating will be applied to the backside of the mirror surface. Because little is known about this coating at this point in the design, the application of this coating will have to be investigated at a later stage in the design process (for the thermal control design, please refer to subsection 11.2.3).

The web crawling robots will be loaded with a lifetime supply of aluminium and adhesive. The two crawlers on the primary mirror will start their mission with 147.6 kg of aluminium on board each, while the robot on the secondary mirror will carry 10.5 kg. As can be read above only modest power values are required for the deposition process (6.2 W for a primary crawler and 0.88 W for the secondary), but the robots will have to provide in their own power needs. When tripling these power values to arrive at assumed robot peak power requirements of 19 W for the primary crawlers and 2.6 W for the secondary, solar cells of 0.048 and 0.0066 m^2 will be required, respectively. This is assuming 30% solar cell efficiency at end of life. As the initial layer application will require more power than thinner the maintenance layers at 10 and 20 years, this was deemed feasible. An initial straw man drawing of such a web crawler can be found in figure 13.6.

13.2.5. Filters and Photovoltaics

As the filters and photovoltaics were deemed sensitive optical components, it was decided that these should be produced on Earth in an effort to limit in-orbit production complexity. In order to integrate the filters in the materials module that in turn needs to fit in SpaceX' BFR payload bay, the filters will be split up in parts simply because these have radii ranging from 8.1 to 3.6 metres, while the BFR is expected to have a diameter of only 9 metres [145]. Splitting them up into quarters allows the parts to fit into each other, allowing high packing efficiencies. Once in-orbit the robotic system of the production module will assemble these filter parts around a central truss.

Also for the photovoltaics, packing efficiency during launch is key. Luckily, the solar cells are of the thin-film type which allows them to be stored on rolls and integrated in the materials module. Once in-orbit the robotic system will unfurl these components and install them around the filters on the SPECTRE structure. This will be one of the last steps to be completed before spacecraft spin-up, as the installed photovoltaics obscure access to e.g. the filters.

13.3. On-Earth Produced Parts in the Materials Module

To enable the production concepts from above, apart from the production modules (incl. robotics and trusselator) and subsystems modules, the following parts will have to be produced on Earth and taken up into space in the materials modules:

- Cable harness (incl. connections)
- Web crawling robots
- Primary space web
- Secondary space web
- Docking interface
- Filter parts
- Furled photovoltaics
- Sensors and cameras
- Thrusters, fuel lines, valves, filters
- Heat pipes
- EPS parts (capacitors, inductors, controllers, switches etc.)
- Raw materials (PEEK/CF and PEEK filament, aluminium powder, adhesives)

13.4. Material Characteristics

This section contains the most important structural materials and their characteristics, as well as their locations within the system. For how these properties are integrated into the structural design, please refer to chapter 11.

13.4.1. PEEK (joints) and PEEK/CF Composite (trusses)

For the trusses of the primary structure, 40% carbon fibre reinforced PolyEtherEtherKetone or PEEK will be used, to be processed by the trusselators from section 13.2.2. The properties in table 13.2 correspond to Victrex™ PEEK 90HMF40 (40% carbon fibre reinforced) [3].

The optimised joints between the trusses of the primary structure will be 3D-printed using PEEK thermoplastic material (not reinforced, not a composite). The assumed properties correspond to Victrex™ PEEK 450FC30 [4] and can be found in table 13.2.

13.4.2. Zylon™ (space webs)

The Earth-produced and in-orbit centrifugally deployed space webs, which form the structures of the primary and secondary mirrors, will be build up from Zylon™ HM high performance fibres as developed by Toyobo Co., Ltd. [10]. The same material will be used for the guy-wires. These fibres were found to have excellent mechanical, thermal and creep properties, but will have to be coated to protect them from UV light before the mirror film is applied. Its properties can be found in table 13.3.

13.4.3. Aluminium (reflective thin film)

The reflective thin film is made up of aluminium. Pure aluminium will be used, as alloys are notoriously difficult to use for CVD (see section 13.2.4). The purest aluminium commercially available was found to be 1199-O [1], its properties can be found in table 13.4.

Table 13.2: Material properties of the PEEK/CF Composite (found in the trusses) and PEEK thermoplastic (found in the joints between trusses) materials.

	PEEK/CF composite (trusses)	**PEEK thermoplastic (joints)**
Type	Victrex™ PEEK 90HMF40 (40% carbon fibre)	Victrex™ PEEK 450FC30
Specific gravity	1.45 g/cm^3	1.45 g/cm^3
Hardness (shore D)	88.5	83
Tensile strength at break	85.0 MPa (@275 °C) 145 MPa (@180 °C) 220 MPa (@120 °C) 330 MPa (@23 °C)	35.0 MPa (@275 °C) 45.0 MPa (@225 °C) 55.0 MPa (@175 °C) 95.0 MPa (@125 °C) 150 MPa (@23 °C)
Elongation	1.2% (at yield)	2.3% (at break)
Tensile modulus	43.3 GPa	13.0 GPa
Flexural strength	120 MPa (@275 °C) 220 MPa (@180 °C) 350 MPa (@120 °C) 475 MPa (@23 °C)	45.0 MPa (@275 °C) 80.0 MPa (@175 °C) 160 MPa (@125 °C) 230 MPa (@23 °C)
Flexural modulus	37.0 GPa	11.5 GPa
Compressive strength	120 MPa (@200 °C) 250 MPa (@120 °C) 310 MPa (@23 °C)	45.0 MPa (@200 °C) 110 MPa (@120 °C) 170 MPa (@23 °C)
Thermal exp. coeff. (linear)	35.0 μm/m °C (below glass transition) 80.0 μm/m °C (above glass transition)	45.0 μm/m °C (below glass trans.) 115 μm/m °C (above glass trans.)
Thermal exp. coeff., (parallel to flow)	1.00 μm/m °C (above glass transition) 3.00 μm/m °C (below glass transition)	15.0 μm/m °C (above glass trans.) 20.0 μm/m °C (below glass trans.)
Thermal conductivity	2.00 W/m-K (average) 4.30 W/m-K (along flow)	0.850 W/m-K (average) 1.70 W/m-K (along flow)
Melting point	343 °C	343 °C
Glass transition temp.	143 °C	143 °C
Processing nozzle temp.	385 °C	385 °C
Specific heat	1390 Watt/kg-K	1390 Watt/kg-K
Emissivity	0.75	0.75

Table 13.3: Material properties of the Zylon™ HM high performance fibre material as found in the space webs and the guy-wires.

	Zylon™ high performance fibre (space webs)
Type	Toyobo Co., Ltd. Zylon™ HM PBO fibre
Specific gravity	1.56 g/cm^3
Tensile strength	37 cN/dtex 5.8 GPa 590 kg/mm^2
Tensile modulus	1720 cN/dtex 270 GPa 28000 kg/mm^2
Elongation at break	2.5%
Decomposition temp.	650 °C
Thermal exp. coeff.	$-6 * 10^{-6}$
Creep parameter (50% of breaking load)	$1.1 * 10^{-4}$
Thermal conductivity	42.9 W/m-K
Specific heat	1500 W/kg-K
Emissivity	0.8
Hardness	941 MPa

Table 13.4: Material properties for Aluminum 1199-O as found in the reflective thin film of the mirrors.

	Aluminium 1199-O (reflective thin film)
Specific gravity	2.70 g/cm^3
Hardness (Brinell)	12
Tensile strength (ulimate)	45.0 MPa
Tensile strength (yield)	10.0 MPa
Elongation at break	50%
Modulus of Elasticity	62.0 GPa
Poissons ratio	0.33
Shear modulus	25.0 GPa
Shear strength	34.0 MPa
Thermal exp. coeff. (linear)	21.8 μm/m °C (@-50 - 20 °C) 23.6 μm/m °C (@20 - 100 °C) 24.5 μm/m °C (@20 - 200 °C) 25.5 μm/m °C (@20 - 300 °C)
Specific heat	0.900 J/g-°C
Thermal conductivity	243 W/m-K
Melting point	660 °C
Reflection coeff.	0.9
Thermal conductivity	237 W/m-K
Emissivity	0.04

13.5. Manufacturing, Assembly and Integration Flow Diagram

At the core of the Production Plan is a flow diagram which illustrates the time-ordered outline of the activities required to construct the SPECTRE system from its basic parts. This MAI Flow Diagram can be found in fig. 13.7. PM stands for production module, MM for materials module. An *E* in the index identifies an Earth based step, while *O* indicates a step to be completed in-orbit. The in-orbit sequence is also illustrated through renders in figure 13.8.

To check compliance with requirement **D-SY-L-PROD-000** which states that construction of the system should be completed within two years from the first launch, we should evaluate the timeline associated with this flow diagram. Assuming 15 launches spaced one week apart and that two weeks from launch are required to reach GEO, it will take 17 weeks (**119 days**) from the first launch date for all the modules to reach operational orbit, where the production modules berth with the materials modules. Assuming five production modules, each production module has to produce four SPECTRE spacecraft. It takes two trusselators (present on each production module) 11 days to produce the required length of primary trusses and the robotics can join them into a SPECTRE structure simultaneously. It is assumed that twice this amount of days (22 days) will be required for the integration of functional parts, before the production module can detach to move on to the next SPECTRE structure to be produced. Following this logic, it will take **132 days** from in-orbit production start to deliver the last of the four structures. At this point the subsystems modules will dock, test the systems and spin up the spacecraft, which deploys the space webs. It is estimated that this process will not take longer than **3 days**. Lastly, for the production and application of the reflective thin film, half a year (**183 days**) was allocated. The summation gives **437** days from the first launch to arrive at a fully functional SPECTRE cluster in orbit. Considering the two year requirement (**D-SY-L-PROD-000**), this leaves plenty of time for intermediate steps and contingencies.

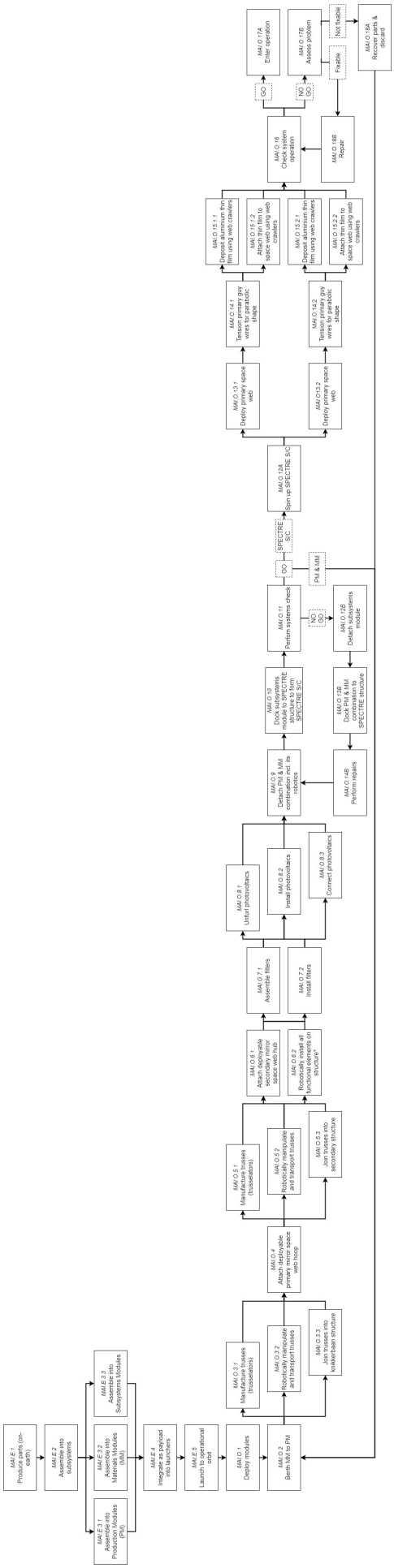

Figure 13.7: MAI Flow Diagram, a chronological outline of the steps required to construct the SPECTRE system.

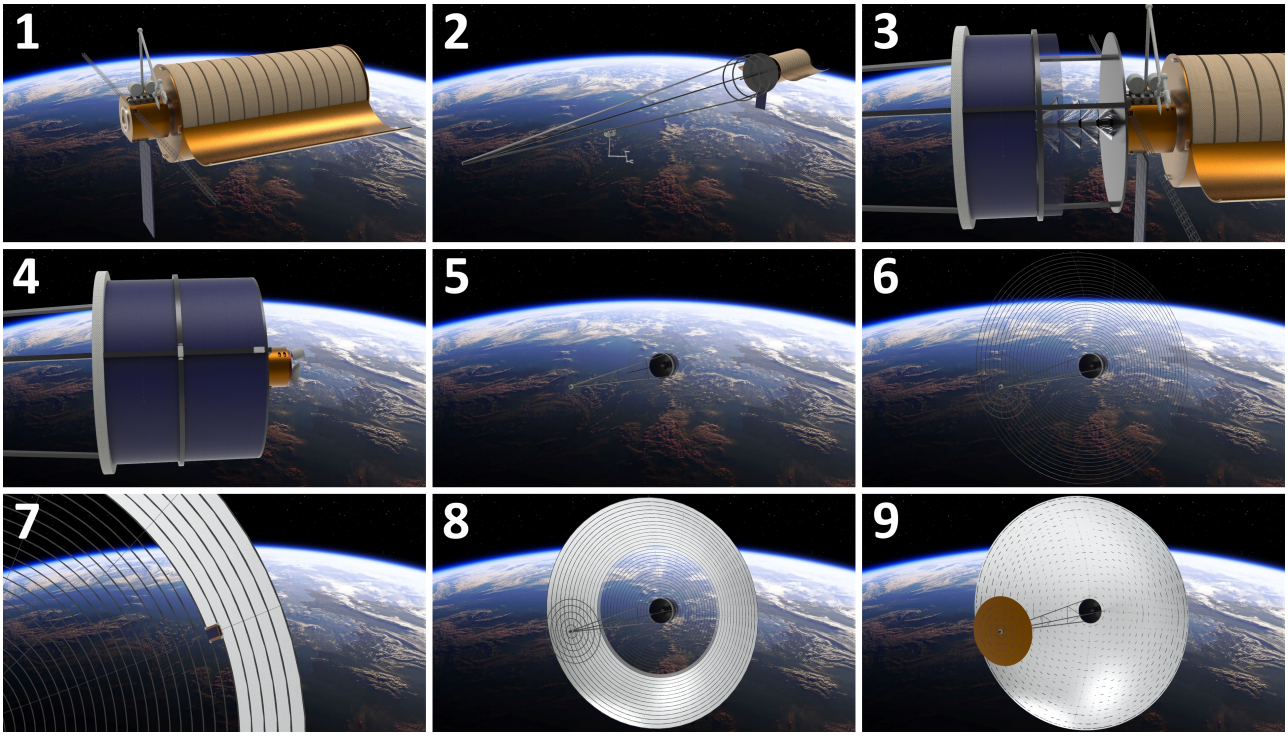

Figure 13.8: Illustration of the in-orbit production sequence as presented in the MAI Flow Diagram. From top left to bottom right: 1. Materials berthed to production module; 2. SPECTRE structure being completed by robot travelling over truss; 3. Integration of functional elements; 4. Subsystems module docked to SPECTRE structure; 5-6. Centrifugal deployment of space web; 7-8. Application of reflective thin film; 9. Completed SPECTRE spacecraft. Please note that the CAD models presented are not too scale.

13.6. Further Recommendations

In conclusion, a feasible in-orbit production plan has been established. It effectively combines modular production, additive manufacturing, robotic assembly, centrifugal deployment and a chemical vapour deposition process to arrive at the operational SPECTRE system in space while meeting important requirements from chapter 3 such as **D-SY-S-ENVI-000**, **D-ST-P-MAIN-001** and **D-SY-L-PROD-000** which correspond to a 1% scrap limit, a requirement on self-maintenance and an in-orbit production time frame of 2 years respectively. However, there is still a lot to investigate during future efforts. The following recommendations are made w.r.t. production:

- The production and materials modules should be sized in detail in order to determine a launch configuration.
- The combined centrifugal deployment of the space webs needs to be modelled in detail.
- The interaction between the web crawlers and the space webs needs to be analysed.
- The (on-Earth) production of large thin film filters needs to be developed.
- Controlling of the novel in-orbit CVD process needs to be developed and validated in space.
- The feasibility of a low earth orbit production pilot should be examined for overall production process validation.

14

Verification and Validation

Design of the system should be accompanied by proof that the system meets the requirements imposed on it. Likewise, it is essential that all numerical and computer models used during the conceptual and detailed design are proven to comply with the laws of physics and describe the real world as accurately as necessary. Therefore, verification and validation will have to be incorporated into the design process consistently.

The first section of this chapter describes requirement validation. The second section describes model verification, which shows that the calculations done by numerical and computer models make sense. Since the engineering design was essentially based on the requirements, in the third section of this chapter a requirements compliance matrix is provided. The next section describes product verification and validation, it shows how proof will be obtained that (part of) the system complies to system requirements and that the system does what it is meant to do. The last section will give an overview of what verification and validation methods are most applicable to each of the requirements.

14.1. Requirement validation

The first validation that was performed for this mission was the validation of the requirements. This validation ensures that the requirements are VALID, essentially meaning that they are verifiable, achievable, logical, integral and definitive. The incorporation of verification and validation procedures makes sure that these requirements on the system can be met.

14.2. Model Verification

The two parts of model verification are code verification and calculation verification. Verifying the code was done while writing it. The code that is used to design the system has been verified in a variety of ways, including unit tests. Unit tests incorporate the selection of a small piece of code, and checking whether or not that piece of code functions properly as a standalone script. Furthermore, code can also be verified by solving the problem by hand, also known as analytically. The code will also be continuously verified by inspection, where all of the inputs and syntax will be inspected in order to ensure the code is written correctly.

Calculation verification is done to make sure that the calculations are done correctly by the code or programmes used. During all phases of the project, it should be ensured that the calculations being performed comply to the laws of physics. Despite doing calculations by hand or through a programme, the calculations should model realistic physics and be able to describe the system without the system actually being there. For the verification of calculations, some standard rules have been set to ensure that all calculations are properly verified. First of all, all written code and simulations are verified analytically by hand calculations, or vice versa. Furthermore, all assumptions that are used for calculations should be supported by an expert in the related field. This is to ensure that realistic estimates are made when designing, and that no system is over- or under-designed.

Table 14.1: Numerical models and their respective verification method

Model	**Verification Methods**	**Section**
Thermal Control Model	Inspection, Analytical Calculations and Unit Tests	subsection 11.2.3
Bandgap Selection	Analytical Calculations	section 10.1
Filter Shape Determination	Analytical Calculations and Unit Tests	subsection 10.3.2
Monte Carlo Simulation	Analytical Calculations and Unit Tests	section 12.1

A list of models that have been made and used during the DSE can be found in Table 14.1. It includes the specific verification methods used per model. A detailed explanation of the models can be found in their respective sections in the report.

Thermal Control Model
The thermal control model has been verified by inspection, analytical calculations and unit tests. Inspection mainly refers to the behaviour of the model due to different inputs. The model should react logically and needs to make sense. For instance, the initial temperature of the system should not have any effect on the equilibrium temperatures it reaches. By lowering emissivities of components, the total heat flow due to radiation should decrease, thereby increasing the equilibrium temperatures. Furthermore, by eliminating incoming solar radiation, the temperature of the system should drop to the temperature of free space.

Additionally, unit tests have been performed to make sure the code works accordingly. The model has been separated in 3 parts, the import of excel files and functions, the simulation, and the plotting part. The import part has been tested to see if the functions and excel files are rightly imported. The simulation part has been unit tested by analytical calculations of the first 3 iterations. Finally, the plots have been compared to the actual values of the simulation to observe their similarities.

Bandgap Selection
The model has to be verified for accuracy. The Shockley Queisser Limit for a single bandgap is roughly 32-34% [143]. For the first placed bandgap this is 38% efficiency. This can be expected due to the smaller atmospheric attenuation experienced in space. Furthermore, the program assumes a slightly less power full black body radiator than the sun is in reality. It was hence deemed close enough to the limit and hence the model is verified for maximising the power out of the spectrum. From literature it was found that the maximum efficiency of an infinite stack solar cell is 86% [142]. The program can therefore be verified for this value. When considering Figure 10.4, it indeed shows a trend to 86%, verifying the model.

Filter Shape Determination Programme
The determination of the filter shape was mainly verified through analytical calculations, as well as some unit tests. This problem was extremely geometrical and could be easily solved analytically. However, due to the need to optimise the filter, the number of computations would make it too time consuming to solve them analytically. Therefore, this programme was written, and to verify the results, the results were always recalculated analytically if a result was put out.

Monte Carlo Simulation
In order to verify the Monte Carlo simulation, the simulation was first of all run multiple times to ensure that the results would have some level of consistency. Furthermore, the simulation code and the results output from the simulation were heavily inspected in order to ensure that the simulation properly modelled what was going on in the system. All input values were also altered to make sure the simulated outcome was logical.

Moving on, a variety of unit tests were performed on the simulation. The integration of the eclipses into the simulation were verified first, and this was done by outputting the eclipse times calculated by the programme into a text file, and inspecting this text file with literature eclipse times. Furthermore, the degradations were verified analytically by comparing them to the overall degradation of the system after a simulated time of 30 years. The failures, repair times and debris impacts were verified through unit tests as well, to ensure that these occurred at the anticipated times (around the average time to failure or repair) and had the expected impacts.

14.3. Design Compliance with Requirements

The design of the systems is meant to meet the requirements set out in chapter 3. In order to make the design successful, the design should meet all mandatory requirements. Table 14.2 shows whether requirements are met or not.

As can be seen in Table 14.2, all requirements are met with the exception of **D-SY-P-THER-003**. The thermal system contains a thermal storage system which utilises the toxic substance called Lithium Chlorate Trihydrate as discussed in subsection 11.2.3, in order to meet the thermal requirements during eclipse. This requirement is desirable and not mandatory, hence the system design is still successful. Since the requirement is not met, special care has to be taken during launch, production and transportation on Earth. Furthermore, further research into nontoxic thermal storage substances should be performed, perhaps mitigating this issue.

Some requirements, such as those for the electrical and thermal subsystems, will not be fully verified and validated until the components requiring verification or validation are built. This is because of the theoretical nature of the designs, and the lack of their previous applications in space. Hence the verification and validation processes for the product should prove definitively if the design meets all the requirements.

The majority of the requirements set have been met and exceeded. This is due the fact that during the design process the requirements played a central and driving role in the design decisions.

Table 14.2: Requirements compliance table. ✓ and ✗ indicate that the corresponding requirement is respectively met and not met.

Index	Check	Reference
Sustainability		
M-ST-S-ENVI-000	✓	chapter 11
M-ST-S-ENVI-001	✓	chapter 11
D-ST-S-ENVI-003	✓	section 8.4
D-ST-S-ENVI-004	✓	subsection 13.2.1
M-ST-S-ECON-000	✓	section 6.1
M-ST-S-ECON-001	✓	chapter 11
D-ST-S-ECON-002	✓	subsection 6.2.6
O-ST-S-ECON-000	✓	subsection 6.2.6
M-ST-S-SOCI-000	✓	section 8.3
O-ST-S-SOCI-000	✓	subsection 13.2.1
D-SY-S-ENVI-000	✓	subsection 13.2.2
O-SY-S-ENVI-001	✓	section 8.4
M-SY-S-ECON-000	✓	chapter 11
D-SY-S-ECON-000	✓	subsection 11.5.5
D-SY-S-ECON-002	✓	section 11.1
Performance		
M-SY-P-PROP-001	✓	subsection 11.2.1
M-SY-P-PROP-003	✓	subsection 11.2.1
M-SY-P-PROP-004	✓	subsection 11.2.1
M-SY-P-PROP-005	✓	subsection 11.2.1
M-SY-P-PROP-006	✓	subsection 11.2.1
D-SY-P-PROP-000	✓	subsection 11.2.1
D-SY-P-PROP-001	✓	subsection 11.2.1
D-ST-P-PROP-000	✓	subsection 11.2.1
M-SY-P-ADCS-000	✓	subsection 11.2.2
M-SY-P-ADCS-001	✓	subsection 11.2.2
M-SY-P-ADCS-002	✓	subsection 11.2.2
M-SY-P-ADCS-003	✓	subsection 11.2.2
M-SY-P-ADCS-004	✓	subsection 11.2.2
M-SY-P-ADCS-005	✓	subsection 11.2.2
M-SY-P-ADCS-006	✓	subsection 11.2.2
M-SY-P-ADCS-007	✓	subsection 11.2.2
M-SY-P-ADCS-008	✓	subsection 11.2.2
M-SY-P-ADCS-009	✓	subsection 11.2.2
M-SY-P-ADCS-010	✓	subsection 11.2.2
D-SY-P-ADCS-000	✓	subsection 11.2.2
D-SY-P-ADCS-001	✓	subsection 11.2.2
D-SY-P-ADCS-002	✓	subsection 11.2.2
M-SY-P-THER-000	✓	subsection 11.2.3
M-SY-P-THER-001	✓	subsection 11.2.3
M-SY-P-THER-002	✓	subsection 11.2.3
M-SY-P-THER-003	✓	subsection 11.2.3
M-SY-P-THER-004	✓	subsection 11.2.3
M-SY-P-THER-005	✓	subsection 11.2.3
M-SY-P-THER-006	✓	subsection 11.2.3
M-SY-P-THER-007	✓	subsection 11.2.3
M-SY-P-THER-008	✓	subsection 11.2.3
M-SY-P-THER-009	✓	subsection 11.2.3
M-SY-P-THER-010	✓	subsection 11.2.3
M-SY-P-THER-011	✓	subsection 11.2.3
M-SY-P-THER-012	✓	subsection 11.2.3
M-SY-P-THER-013	✓	subsection 11.2.3
M-SY-P-THER-014	✓	subsection 11.2.3
D-SY-P-THER-000	✓	subsection 11.2.3
D-SY-P-THER-001	✓	subsection 11.2.3
D-SY-P-THER-002	✓	subsection 11.2.3
D-SY-P-THER-003	✗	subsection 11.2.3
M-SY-P-TT&C-000	✓	subsection 11.2.6
M-SY-P-TT&C-001	✓	subsection 11.2.6
M-SY-P-TT&C-002	✓	subsection 11.2.6
M-SY-P-TT&C-003	✓	subsection 11.2.6
M-SY-P-TT&C-004	✓	subsection 11.2.6
M-SY-P-TT&C-005	✓	subsection 11.2.6
M-SY-P-TT&C-006	✓	subsection 11.2.6
M-SY-P-TT&C-007	✓	subsection 11.2.6
D-SY-P-TT&C-000	✓	subsection 11.2.6
D-SY-P-TT&C-001	✓	subsection 11.2.6
D-SY-P-TT&C-002	✓	subsection 11.2.6
D-SY-P-TT&C-003	✓	subsection 11.2.6
D-SY-P-TT&C-004	✓	subsection 11.2.6
M-SY-P-POCO-000	✓	chapter 10
M-SY-P-POCO-001	✓	chapter 10
M-SY-P-POCO-002	✓	chapter 10
D-SY-P-POCO-000	✓	chapter 10
D-SY-P-POCO-001	✓	chapter 10
M-SY-P-EPSY-000	✓	subsection 11.2.4
M-SY-P-EPSY-001	✓	subsection 11.2.4
M-SY-P-EPSY-002	✓	subsection 11.2.4
M-SY-P-EPSY-003	✓	subsection 11.2.4
M-SY-P-EPSY-004	✓	subsection 11.2.4
M-SY-P-EPSY-005	✓	subsection 11.2.4
M-SY-P-EPSY-006	✓	subsection 11.2.4
D-SY-P-EPSY-000	✓	subsection 11.2.4
D-SY-P-EPSY-001	✓	subsection 11.2.4
D-SY-P-EPSY-002	✓	subsection 11.2.4
D-SY-P-EPSY-003	✓	subsection 11.2.4
M-SY-P-POTR-000	✓	subsection 11.2.4
M-SY-P-POTR-002	✓	subsection 11.2.4
M-SY-P-POTR-003	✓	subsection 11.2.4
M-SY-P-POTR-005	✓	subsection 11.2.4
D-SY-P-POTR-001	✓	subsection 11.2.4
M-SY-P-POST-000	✓	subsection 11.2.4
M-SY-P-POST-001	✓	subsection 11.2.4
D-SY-P-POST-000	✓	subsection 11.2.4
D-SY-P-POST-001	✓	subsection 11.2.4
O-SY-P-POST-001	✓	subsection 11.2.4
O-SY-P-POST-002	✓	subsection 11.2.4
D-ST-P-MAIN-000	✓	section 12.2
D-ST-P-MAIN-001	✓	section 12.2
D-ST-P-MAIN-002	✓	section 12.2
O-ST-P-MAIN-003	✓	section 12.2
M-SY-P-STRU-000	✓	subsection 11.2.7
D-SY-P-STRU-001	✓	subsection 11.2.7
D-SY-P-STRU-002	✓	subsection 11.2.7
D-SY-P-STRU-003	✓	subsection 11.2.7
D-SY-P-STRU-004	✓	subsection 11.2.7
Logistics/Life		
M-ST-L-PROD-000	✓	chapter 13
M-ST-L-PROD-001	✓	chapter 13
M-ST-L-PROD-002	✓	chapter 13
D-SY-L-PROD-000	✓	chapter 13
D-SY-L-PROD-001	✓	chapter 13
O-ST-L-PROD-000	✓	chapter 13
M-ST-L-OPER-000	✓	chapter 11
D-ST-L-OPER-000	✓	chapter 5
D-ST-L-OPER-001	✓	chapter 5
D-ST-L-OPER-002	✓	chapter 11
D-ST-L-OPER-003	✓	subsection 11.2.1
O-ST-L-DISP-000	✓	subsection 13.2.1

14.4. Product Verification and Validation

Outside of the verification of the calculations being performed, verification will also have to be done to verify that (a component of) the system meets its required specifications. For this, in the early phases of a project, a plan should be made by analysing the products to be verified. There are three parameters that can define a verification programme, which are the verification method, the verification level, and the applicability. A combination of parameters should be selected that provides sufficient certainty that the product conforms to the requirements imposed on it and costs the least [81]. In order to set up a verification plan, standards of the European Cooperation for Space Standardisation (ECSS) for verification and testing are used [14][12]. These standards establish the requirements for the verification of a space system product and address the requirements for performing verification by testing of space systems.

14.4.1. Product Verification Methods

Before assembling and integrating the system, most, if not all, analyses should have been performed. The same can be said about performing verification on models. The different verification methods are test, analysis, review of design and inspection.

- **Inspection and review of design:** These are the cheapest methods, as it limits to reviewing design documentation of parts and inspecting the masses and dimensions of the product itself.
- **Analysis:** This is moderately expensive, as it takes up time to make mathematical or other analytical techniques that are suitable for the products. It also might need testing itself to verify that the model used describes the product sufficiently, as making models with wrong assumptions might lead to unpredictable effects.
- **Test:** The most expensive approach of product verification is testing, which can be further divided into testing under representative conditions and demonstration. With demonstration, compliance with the requirement is established by operation, adjustment or reconsideration of a test article. Producing this test article carries a large cost and takes up a lot of time. With verification by test, this is taken to the next level, as it is a test of (a model of) the product's compliance with requirement under representative conditions. These representative conditions can either be simulated in a test facility (e.g. vibration beds and vacuum chambers) or a test model

of the system can be put into orbit [113]. Any test methods that will be used should be included in an Assembly, Integration and Test Plan (AITP).

Below there is a collection of verification methods that could be applied to models or components of subsystems. Of course, the masses and dimensions of all of these systems can be verified through inspection and review of the design can provide a lot of other specifications, but these details have been discarded below.

Propulsion System

- Analysis - In order to verify the long lifetime of the propulsion system, simulations could be used to find out weaknesses in the propulsion system architecture. This includes the feed lines that go from the tank to each of the thrusters and the valves. Mounting and alignment analyses can also be performed for the thrusters.
- Test - Parts of the propulsion system can be tested on Earth. The tanks can be tested for its MEOP and the thrusters should be tested on their thrust and power consumption before assembly. Other parts that can be tested are the valves and the feed lines.

Attitude Determination and Control System

- Analysis - The ADCS can be verified by making a simulation on its operation in space, and stress test it by applying variable perturbations and analysing its response.
- Test - The ADCS can also be tested, various prototypes can be sent as payload on other spacecraft, and used to verify its use in space. It can also partially be tested on Earth, since for the CMG functionality, three-axis motion tests should be performed.

Thermal Control System

- Analysis - A simulation of the system in a GEO environment could be created to test the reaction of the thermal control to a certain irregular influx of energy or heat, in order to verify its functionality.
- Test - The thermal control system can also be verified partially by performing equilibrium tests on various parts of the system in a vacuum chamber. This should be performed on the heat pipes after filling. The heat pipes should be tested for leaks, contamination and if the wick design gives the desired results [112].

Command and Data Handling System

- Analysis - Before the CDHS is assembled, simulated hardware can be used to verify that the software performs how it should.
- Test - When integrating the software onto the OBC a hardware-software integration test should be performed to show compatibility.

Telemetry, Tracking and Command System

- Analysis - If the system is currently operational on other spacecraft, producers of the other spacecraft can be consulted for their verification on the TT&C system. Then, through the consultation and an analysis, the TT&C system can be verified. Simulations can be created in Python in order to verify the TT&C function throughout the entire orbit, and ensure no random propagation in functionality.
- Test - The TT&C system can be tested on Earth, although the conditions will be essentially impossible to replicate. The on-Earth functioning can therefore be verified, and certain aspects of TT&C. The system should be tested on the radio frequencies that will be used.

Power Collection System

- Analysis - The degradation of the cells, mirrors and filters can be verified through an analysis by simulating the conditions at GEO in a model. An analysis can also be used to verify the operational times of the power collection system with a simulation of the system operating coupled with a simulation of the orbit. Therefore, this will give an indication of the operational times based on the night time and start-up times of the collection system.
- Test - The spectral splitter can be verified through tests using a sun-photometer. The sun-photometer can measure the incoming solar flux at a certain specified bandgap. By testing this on Earth, the operation of the system in GEO can be modelled. This model can then be verified and validated separately. Of course, a vacuum can also be simulated to help conduct this verification. The function of the solar cells can be tested on Earth and the conducted analysis can then be modelled for the space environment. Of course, a vacuum can be simulated to help conduct this verification.

Electrical Power System

- Analysis - As the electrical flow through the system is critical for mission performance and the amount of power is higher than any spacecraft has ever had to handle, so a lot of resources should be put into EPS verification. Electrical analyses can be performed to simulate the electrical power flow through the system. These simulations can run for a simulated period of 30 years as part of RAMS analyses to show the predicted electrical performance and show flaws or weak spots in the design.
- Test - Every part of the EPS should be tested on its performance separately. The function of the EPS components can be tested on Earth with the application of 1GW (cumulatively) on the same amount of EPS that will be used for the solution. Stress testing can also be performed on the EPS components, where considerably higher voltages and currents can be applied. This will be necessary to check its ability to handle deviations from its nominal working conditions, essentially showing how robust it is as a system.

Power Transmission System

- Analysis - The transmission system will have to function constantly apart from eclipses. When functioning it is very important that pointing of the lasers is precise and accurate at all times. A functional performance analysis should be performed on this.
- Test - The transmission system can also be tested on the Earth to conduct specific tests into its pointing accuracy, internal efficiencies, functionality and robustness. For a more viable verification of the overall efficiency and function of the transmission system, a prototype of the transmission system can be sent to space and tested.

Power Storage System

- Analysis - The power storage system is there for use in an emergency. An operational analysis can be used that shows its performance during 30 years of operation to ensure the batteries are fail safe.
- Test - The capabilities of the batteries should also be tested separately on Earth, testing them for their robustness.

In-Orbit Maintenance and Production

- Analysis - As the in-orbit production and maintenance can not be tested completely on Earth, extensive analysis using simulations should be performed. RAMS analyses can be used to show the maintainability of the system. The separate software of both the web crawling robots and the production module should be tested in a simulation as well.
- Test - The best tool to verify the equipment and the methods that will be used for maintenance and production is to simply demonstrate the operations of the equipment and methods. This starts with hardware-software integration tests for the web crawling robots and the production module. Tests can also be conducted onto the equipment, in order to verify its functional and technical limits. The functioning of the robot arms should be tested using a flat floor test. The trusselators should be tested on operating in a vacuum chamber. The web crawling robots can be tested in a reduced gravity aircraft or drop test facility on its capability to perform CVD in microgravity.

Structures

- Analysis - Due to the long lifetime of the mission, it should be considered to make a simulation in order to analyse the long-term behaviour of the structure under variable loads. Particular focus should be on the trusses and web structure as the trusses will be produced and assembled in orbit whereas the web structure will be deployed in orbit and can not be tested to full extent on Earth.
- Test - The material's tensile and shear strength being used for the structure can be verified through testing. Loads can be applied to various models of the structure that is going to be used, and the effects can be documented. Furthermore, fatigue/stress testing could also be useful due to the long lifetime of the mission. In later stages of verification, the structure will be verified for launch loads.

Astrodynamics

- Analysis - Furthermore, simulations should be created in order to study the launching trajectory, applying certain perturbations and measuring the required operations to correct for the perturbations.
- Test - Testing the astrodynamics can only be done in the in-orbit verification stage.

14.4.2. Validation Methods

Validation will be the integral part of the design where the team will conduct assessments in order to determine whether or not the system does what it is meant to do. Hereby, it will be determined whether or not the mission is a success and if the mission objective was met. The different methods are experience, analysis and comparison [59]:

- **Experience:** Validation by experience is done by consulting an expert on application of similar models in similar circumstances.
- **Analysis:** Validation by analysis is showing that the elements of the model are of necessity correct and are correctly integrated.
- **Comparison:** Validation by comparison is done with test cases in the form of independent models of proven validity or actual test data.

Validation usually occurs after the production of every individual component, as the component can then be compared and analysed. Below, a variety of validation methods are given for different subsystems of the solution.

Attitude Determination and Control System

- Comparison - The ADCS can be validated by comparing to existing and similar ADCS systems found on spacecraft with similar control and pointing accuracy requirements.
- Analysis - Furthermore, the function of the ADCS can be tracked during operation, and its function can be analysed and validated with the requirements.

Thermal Control System

- Analysis - In order to validate the function of the TCS, an analysis will have to be performed when it is functional in GEO.
- Experience - Consultation with experts can also validate the feasibility of the TCS.

Telemetry, Tracking and Command

- Comparison - The TT&C can be validated through currently operational and similar (preferably identical) TT&C components on other spacecraft. The way the system receives and transmits data can be analysed from existing systems, thereby validating the chosen and designed TT&C system.

Electrical Power System

- Analysis - The EPS system cannot be validated through comparison or experience, mainly due to the novelty of the system. Therefore, analysis will have to be conducted into the function of the EPS during operation, to validate its proper and required function.

Power Collection System

- Comparison/Experience - The power collection could partially be validated through experience and comparison, by consulting specialists who have designed and worked with solar energy and spectral splitting.
- Analysis - Furthermore, an analysis would have to be conducted into the proper validation of the system. For example, the overall efficiency and collected power (1GW) could be analysed to see if the requirements are met.

Power Transmission System

- Comparison - The power transmission system can be validated through comparison of other space agencies testing laser and microwave power transmission to Earth.
- Analysis - The power transmission can be validated by analysing its function in the system, and determining its efficiency, the pointing accuracy, the amount of noise, and finally the amount of transmitted power.

In-Orbit Maintenance and Production

- Analysis - Comparison or experience cannot be used to validate this, due to the novelty of the system. Therefore the maintenance and production will have to be analysed during operation, and validated through the acquired analysis.

Structures

- Experience - The structure can be validated by experience of certain experts. Their knowledge could be sufficient to validate the structural integrity of the system.
- Analysis - Furthermore, the structure can be validated further by analysing the loads exerted on the structure during the orbit, and any structural components during launch that are produced on Earth. This will require the placement of strain gauges on the structure.

Astrodynamics

- Comparison - The orbit can be validated by comparing to other systems in a very similar or identical orbit. Their yearly ΔV budget can be analysed to determine whether or not the calculated propellant mass would be sufficient.
- Comparison - The main method to validate the launching of the system would include looking at the success rate of the launcher being chosen, and looking at their performance when launching with a similar payload mass.
- Analysis - During the launching and orbiting of the system, the astrodynamics can be validated by analysing its function.

14.4.3. Verification Level

Verification can be done at each level of the design process and should be done on the lowest level (e.g. smallest part or component) possible. Hereby, mistakes in the design can be found early on in the process and the verification of smaller parts means it remains relatively cheap and simple. It is however hard to account for integration of different parts on this lower level. To check if different components of a subsystem work together, some verification will have to be repeated on a higher level as well. The same can be said for subsystems that have interfaces.

The different levels on which this system will be verified are equipment, subsystem, segment and overall system level. On component level, separate parts of each subsystem will be verified before assembly. Next up is subsystem level, to verify the interface of different subsystems. The highest level is system level, where the compatibility between subsystems can be verified and validated. For this, a fully functional subsystems module can be built on which the OBC can operate with (partly simulated) inputs and outputs. In order to verify the in-orbit production and operation, a fully functional spacecraft could be tested in LEO. Although such verification will cost a lot and will take up a lot of time, it could be a serious consideration.

14.4.4. Applicability

In order to use different methods on different levels, models of a part of the system can be designed and produced. This way, critical parameters can be verified in an early stage of the design process. In this case, the size of one spacecraft is too big to conduct otherwise standard tests that would be done with a complete model on Earth. The costs for facilities on this scale would exceed the costs of launching a prototype to LEO and producing it there. Due to the size of the mission, testing a fully functional prototype in LEO would be reasonable before putting 20 spacecraft in GEO. The system will depend a lot on the space environment. For instance, the lightweight structure would not withstand loads on Earth, the production methods rely on a vacuum, the EPS is made for a vacuum environment as well, the heat pipes of the TCS are made for operation in microgravity, a complete thermal balance test is only possible in space, and the transmission method will need in orbit tests. The main focus of such a test would be to prove that construction of the complete system will work.

Before conducting a test on this scale, a mixture of models and verification objectives will have to be selected [81]. In-orbit mechanical loads can be simulated with structural tests. A thermal vacuum test can show that components still work in the predicted temperature ranges. The production and assembly of trusses could be tested on Earth. These and more tests will be necessary in order to provide a proof of concept before launch and operation will be performed.

14.4.5. Verification Stages

There are five verification stages possible. In chronological order these are qualification, acceptance, pre-launch, in-orbit (including commissioning), and post-landing [12]. Verification should always be done in the earliest phase possible, considering cost. Below a short summary of each stage is given. As the qualification stage and in-orbit phase are more extensive, they will be described in more detail after the summary of each stage. After this, the consideration of prototype testing in LEO will be discussed.

- **Qualification:** Verification shall demonstrate that the design meets the applicable requirements on hardware and software which is representative of the end item configuration in terms of design, materials, tooling and methods. In this stage, all products that will be assembled into the final product shall be subject to a qualification programme. Exceptions can be made for off-the-shelf products that have already been tested and used in the same way. On the flipside, newly designed and developed products should receive a full qualification programme. The qualification stage runs from the beginning of the design until manufacturing of the actual products that will be launched.
- **Acceptance:** After the final assembly and integration of the system, verification should demonstrate that the product is free of workmanship errors and is ready for subsequent operational use. When the qualification model has been verified, the acceptance stage can start. This should be done on the final hardware, so the actual assemblies that will be put into fairings as-is. These assemblies are the subsystems modules, production modules and material modules. It should be shown that everything put on these assemblies performs as well as the models on which qualification was performed.
- **Pre-launch:** Next, verification should demonstrate that the product is properly configured for launch activities and early operations and that it is capable of functioning as planned during launch and early operations. The three types of modules that will be put on the fairings should undergo vibration testing to show that they will survive launch loads.
- **In-orbit:** When the system is in-orbit, verification should ensure no degradation occurred during the launch, early orbit phase, at periodical intervals and before specific operational use. The verification should also supplement and/or confirm ground verification by providing operating conditions which could not be performed or accurately simulated on Earth. It should also be confirmed that the space and ground elements are compatible. Another verification that should be performed is calibration and tuning activities, such as testing the deflection of primary and secondary mirrors.
- **Post-landing:** This stage happens after the system lands and can be used to address the product integrity and performance. This will however not be the case for this mission.

14.4.6. Qualification Stage

This is the stage where the AITP comes in. Any off-the-shelf products that are implemented unmodified and have gone through qualification don't need new qualification. However, after producing novel products for this mission and after every assembly or integration step of on-Earth manufacturing (either in-house or 3rd party), qualification testing should take place. This can include any of the test methods listed before, but should also include integration tests and functional tests on a qualification model [81]. This qualification model is the closest a model will get to its intended configuration in-orbit, the only difference will be the exclusion of the primary and secondary mirror. Integration tests verify that all components of a system fit and work together. Functional tests verify that the combined components function as intended.

Integration tests should include:

- **Electrical integration tests:** As the main functions of the mission will be collecting and transmitting of large amounts of power, extra care should be taken into verifying the complete integration of the electrical power system of each spacecraft. All electrical signals, power interfaces, power consumption and grounding should be checked. The electrical model should include a power source that simulates the inputs that the solar arrays during operation would. The model should show that it can supply the correct amount of power to every subsystem as well as show a functional power transmission system.
- **Mechanical integration tests:** Every component should be put into place and mechanical interfaces and their alignment should be checked using a qualification model. The main mechanical integration test will be the subsystem module integration. This should also be done for materials and components that are not part of the subsystem module as the assembly of the spacecraft should be tested on Earth as much as possible. These tests include checking the docking interface of the different modules, assembly of the truss structure and subsequent assembly and integration of the thin film filters, solar arrays, harness, heat pipes, electrical power system, sensors and thrusters on this structure. A notable exception is the integration of the primary and secondary mirror webs and surfaces. These will be tested in a later stage.

Functional tests should include:

- **Hardware-software integration tests:** The qualification model used for mechanical integration testing can next be used for testing the interaction between operational software and the different subsystems.
- **Radio frequency tests:** Now that the TT&C is integrated into the qualification model, it should be tested that the downlink and uplink is transmitted correctly and that the system correctly reacts to ground commands.
- **Motion tests:** The mounted ADCS sensors and actuators as well as the thrusters should be motion tested.

- **Vacuum testing (including thermal):** To show the subsystems module will work in GEO conditions, a separate model of the module should be tested in a vacuum chamber that also simulates the thermal conditions. For this, the model should be fully functional but should exclude the connection to the EPS and the transmission system.

14.4.7. In-Orbit Stage

Once the system has been put into GEO the contents of the three modules should be checked for degradation issues that may have occurred during launch. The TT&C of the productions module should be tested to ensure a robust communication link during the in-orbit production phase. The robotic arm of the production module should be tested and next be used to attach the materials module to create an orbital factory. At this point, the functionality of the trusselators can be tested.

After this the in-orbit production phase will commence. This includes the assembly of the main truss structure and integration of subsystems into the structure using the robotic arm, the integration of the mirror webs and connecting the guy-wires to the mirrors and truss structure. The assembly and integration could not be tested in space conditions before, so this process will act as a supplement to on-Earth testing and simulation. The alignment of the power collection system, excluding the primary and secondary mirror, should now be checked. Once everything on the SPECTRE structure is assembled, the production and materials modules are disconnected and the subsystems module is docked.

Before operation starts, the system is spun up for the deployment of the primary and secondary mirrors after which the attachment of the mirror thin film by the web crawling robots can start. The alignment and shape control of the mirrors as well as the operation of the web crawling robots can at this point be tested. This process could only be simulated on Earth with the exception of testing the attachment of thin film on a small scale. This will therefore act as confirmation that those simulations were accurate.

All other subsystems should at this point have a ready check as part of the operation tests after which the operation itself can start. During operation, special attention should go to the performance of the power collection system, the EPS and the transmission system.

14.4.8. Separate Prototype Test in Low Earth Orbit

The in-orbit production is very extensive and not everything can be tested accurately on Earth. For the biggest part of in-orbit production processes the only way of verifying on Earth is analysis. The same can be said of the power collection, power flow and transmission of the spacecraft. Therefore, as a separate and more credible proof of concept, a prototype model could be launched to LEO where the production and operation can be validated by analysing its performance. Any flaws in the design that could not be foreseen with the test and analysis methods possible on Earth can as such be covered.

14.5. Verification and Validation with Respect to Requirements

To conclude, during the designing and production of the system, and once the system has been completed, the various components of the system will be verified and validated with respect to the requirements. In Table 14.3 a compilation of all the mandatory requirements are given, with the most effective method to verify and validate the requirement. Note that some of the verification and validation techniques listed below will be similar to the techniques listed in section 14.4.

Table 14.3: Compilation of Mandatory Requirements with the most Applicable Verification and Validation Method - The Respective Validation and Verification Methods are given to the right of the Requirement Index

Requirement	Verification	Validation	Requirement	Verification	Validation
M-ST-S-ENVI-000	Analysis	Analysis	M-SY-P-THER-011	Analysis/Test	Analysis
M-ST-S-ENVI-001	Analysis	Analysis	M-SY-P-THER-012	Analysis/Test	Analysis
M-ST-S-ECON-000	Inspection	Analysis	M-SY-P-THER-013	Analysis/Test	Analysis
M-ST-S-ECON-001	Inspection	Analysis	M-SY-P-THER-014	Analysis/Test	Analysis
M-ST-S-SOCI-000	Analysis	Experience	M-SY-P-TT&C-000	Analysis	Comparison
M-SY-S-ECON-000	Analysis	Analysis	M-SY-P-TT&C-001	Analysis	Comparison
M-SY-P-PROP-001	Analysis/Test	Analysis	M-SY-P-TT&C-002	Test	Comparison
M-SY-P-PROP-003	Analysis	Experience	M-SY-P-TT&C-003	Test	Comparison
M-SY-P-PROP-004	Analysis	Analysis	M-SY-P-TT&C-004	Analysis	Comparison
M-SY-P-PROP-005	Analysis	Analysis	M-SY-P-TT&C-005	Analysis	Comparison
M-SY-P-PROP-006	Test	Analysis	M-SY-P-TT&C-006	Analysis	Comparison
M-SY-P-ADCS-000	Test	Analysis	M-SY-P-TT&C-007	Analysis	Comparison
M-SY-P-ADCS-001	Test	Analysis	M-SY-P-POCO-000	Analysis	Analysis
M-SY-P-ADCS-002	Analysis	Comparison	M-SY-P-POCO-001	Analysis	Analysis
M-SY-P-ADCS-003	Test	Analysis	M-SY-P-POCO-002	Analysis	Analysis
M-SY-P-ADCS-004	Test	Analysis	M-SY-P-EPSY-000	Test	Analysis
M-SY-P-ADCS-005	Test	Analysis	M-SY-P-EPSY-001	Test	Analysis
M-SY-P-ADCS-006	Test	Analysis	M-SY-P-EPSY-002	Test	Analysis
M-SY-P-ADCS-007	Test	Analysis	M-SY-P-EPSY-003	Test	Analysis
M-SY-P-ADCS-008	Test	Analysis	M-SY-P-EPSY-004	Test	Analysis
M-SY-P-ADCS-009	Test	Analysis	M-SY-P-EPSY-005	Analysis	Analysis
M-SY-P-ADCS-010	Test	Analysis	M-SY-P-EPSY-006	Test	Analysis
M-SY-P-THER-000	Analysis/Test	Analysis	M-SY-P-POTR-000	Analysis	Analysis
M-SY-P-THER-001	Analysis/Test	Analysis	M-SY-P-POTR-002	Analysis	Analysis
M-SY-P-THER-002	Analysis/Test	Analysis	M-SY-P-POTR-003	Analysis	Analysis
M-SY-P-THER-003	Analysis/Test	Analysis	M-SY-P-POTR-005	Analysis	Analysis
M-SY-P-THER-004	Analysis/Test	Analysis	M-SY-P-POST-000	Analysis	Analysis
M-SY-P-THER-005	Analysis/Test	Analysis	M-SY-P-POST-001	Analysis/Test	Analysis
M-SY-P-THER-006	Analysis/Test	Analysis	M-SY-P-STRU-000	Test	Analysis
M-SY-P-THER-007	Analysis/Test	Analysis	M-ST-L-PROD-000	Test	Experience
M-SY-P-THER-008	Analysis/Test	Analysis	M-ST-L-PROD-001	Demonstration	Experience
M-SY-P-THER-009	Analysis/Test	Analysis	M-ST-L-PROD-002	Demonstration	Experience
M-SY-P-THER-010	Analysis/Test	Analysis	M-ST-L-OPER-000	Analysis	Analysis

15

Post DSE Activities

After the DSE, a variety of activities will still be required to realise the design discussed in this report. These activities will include further design, testing, marketing, verification and validation, qualification, and certification, essentially encompassing all operations before utilisation, except for launching, production and assembly. Of course, these are not the only activities that will have to be performed. Therefore, due to the large amount of activities that will still have to be completed, a proper design and development logic will have to be created. This design and development logic will first be presented in a Project Gantt Chart, and will be supported by a Project Design and Development Logic diagram for clarification. The Project Design and Development Logic, as well as the Project Gantt Chart, were based off of the ECSS-M-30A standardisation manual, and includes phases C and D.

15.1. Project Gantt Chart

In this section, the Project Gantt Chart is given. The Project Gantt Chart identifies the main logical flow of activities that will occur after the DSE, and also highlights some of the important milestones. These milestones include the Critical Design Review (CDR), Qualification Review (QR), and the Acceptance Review (AR). The CDR will occur once the design is finalised, and once everything in the system is properly defined. The QR will apply to the successful completion of verifying, qualifying and testing the system. Finally, the AR will happen when the first satellite is produced and operational in orbit.

15.2. Project Design and Development Logic

In this section, a block diagram will be used to discuss the post DSE activities in the most logical and efficient flow. As one can see, a detailed definition must first be completed, and after a successful CDR, the components and subsystems must be verified and validated. After successful verification and validation, integrated ground testing and qualification can start, which is followed by the QR. Finally, after successful marketing and production, the AR can occur.

Leading up to the CDR, the design team will have a Preliminary Design Review (PDR), from which the team will have to consider the given feedback, and implement it. Afterwards, the design of the solution, as well as communication with partners (related to power transmission and ground operations), can be done in parallel. Following these two tasks, the design has to be completed for production initiation, and a start-up production master file has to be created. The production master file is a file that will define all of the components that have to be produced, the materials and tools that their production requires and the amount of each component that has to be produced. While that is being done, the test, qualification and set-up conditions can also be confirmed.

After the CDR, the verification and validation means will have to be definitive, and prototypes will have to be created for verification and validation. In case these activities produce negative results in terms of requirement compliance, the system will have to be redesigned, and the activities related to verification and validation will have to be completed again.

Once the verification and validation of the individual components and subsystems is completed, integrated ground testing and qualification can commence, where the produced prototypes can be integrated into a small-scale product. Tests can then be performed on this integrated prototype, and the system can be qualified for the orbit and launch. This is where the launch readiness review will also occur. After this the QR is held, which will allow the team to start producing and marketing the product. Once the first product is produced, an AR can completed.

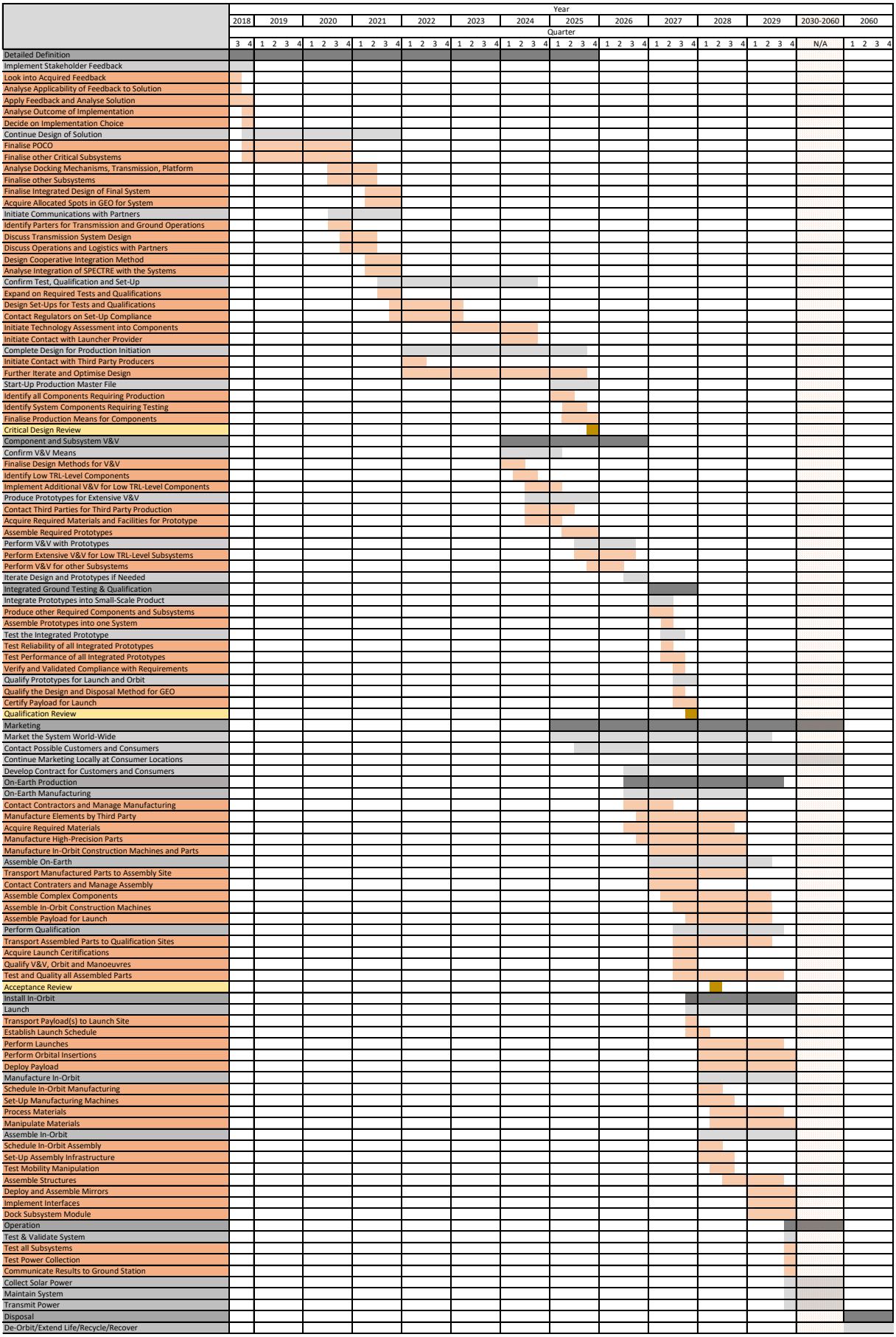

Figure 15.1: SPECTRE Project Gantt Chart

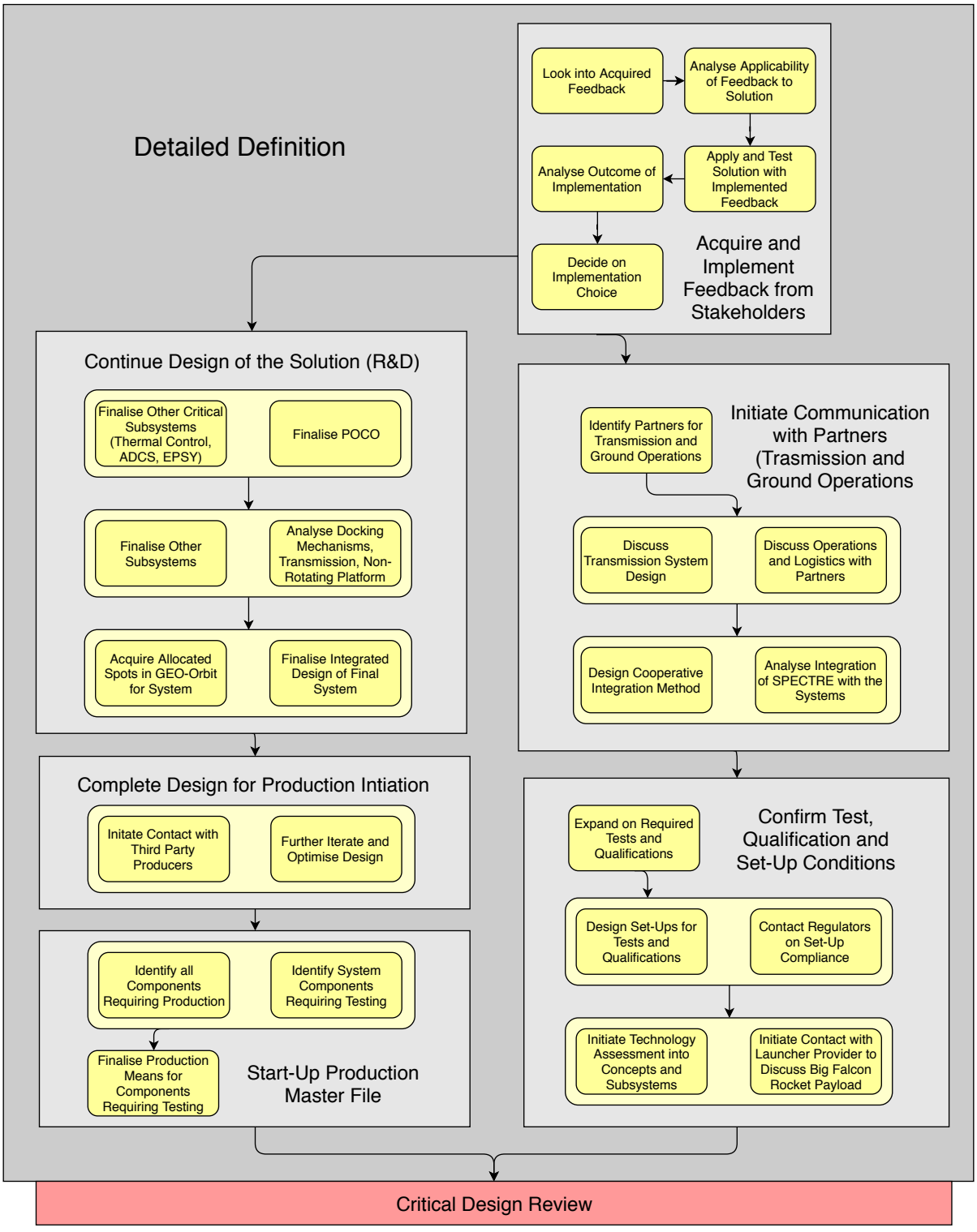

Figure 15.2: Post DSE Development and Design Flow Leading up to the Critical Design Review

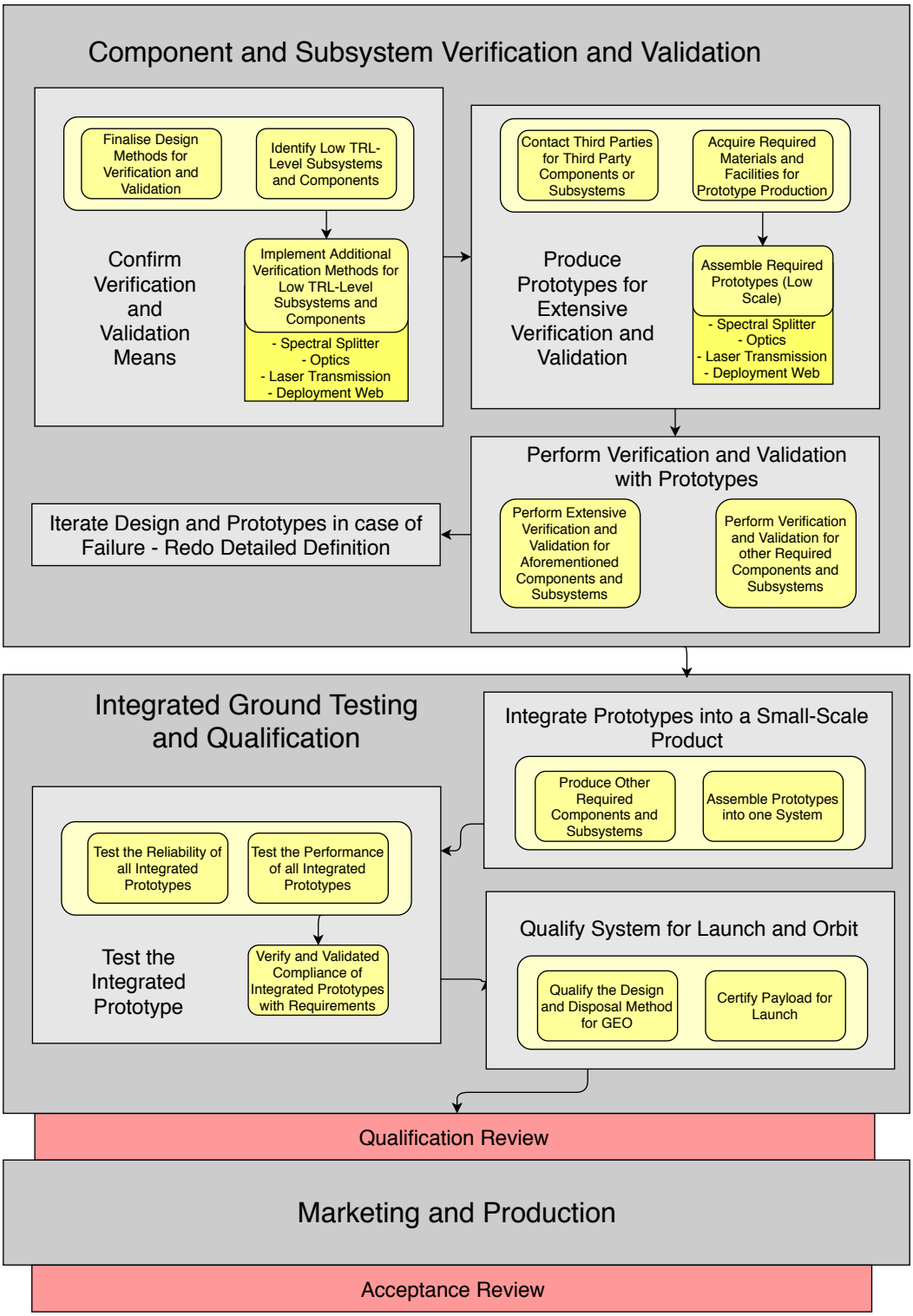

Figure 15.3: Post DSE Development and Design Flow After the CDR, Leading up to the Acceptance Review

16

Conclusion & Recommendations

The focus of this report was to expand on the final solution identified in chapter 2, laying a foundation to enter the detailed design stage for this solution. This was done by analysing various aspects of the solution, and deriving crucial design choices from these analyses. The solution refers to the SPECTRE system that will meet the following mission objective, *"Develop a concept with 9 students and within 11 weeks for a solar energy collecting system that can generate Gigawatt-range power in orbit by 2030 within the budget of one and a half billion Euros"*.

Initially, the origin of the solution designed in this report is given. This involves background information into what the solution is, and how it was chosen. Afterwards, the requirements related to the solution were re-identified and expanded where possible. These requirements were crucial in defining the system verbally, and giving a stronger foundation for the design. In order to compound this foundation, analyses were also done into the sustainability, market, risk, operations and logistic of the solution. From this foundation, the system and the production techniques could be designed to a sufficient level of detail to assess its compliance with the requirements.

16.1. Design Result

These analyses resulted in a design highlighted in section 11.5. The system will collect solar power through innovations including solar concentration, spectral splitting, and thin film solar arrays. A further innovation, which would also form an infrastructure for its further development, is the use of in-orbit production. These innovations also allow the system to meet all of the mandatory requirements set by the team. On top of this, the resulting design is more sustainable than its fossil fuel competitors and much more efficient that the European grid average.

By using parabolic mirrors, the solar energy can be concentrated onto a cascade of filters. These then reflect and diverge certain frequencies of light onto solar cells tailor-made to operate at those frequencies. This innovation allowed the solar cells to have an efficiency of 70%, and an overall system efficiency of 40%. This greatly outweighs the efficiencies of conventional photovoltaic power systems in space. Furthermore, not only is this overall system efficiency higher than conventional solar cells used in space, but the manner in which the system is configured allows for the use of thin aluminium mirrors, which weigh multiple factors less than solar cells. This allowed for the system to reduce its mass by hundreds of tonnes, and integrate the use of in-orbit production. In-orbit production further improved the design of the system by letting the design for certain components neglect the launch loads.

The integration of all the subsystems resulted in a system that can generate 1.3GW at BOL, and over 1GW at EOL. The total mass of the system amounts to 289 tonnes, with 68 tonnes allocated towards the power collection subsystem, 60 tonnes allocated towards the TCS and 49 tonnes towards the ADCS. These are the three heaviest subsystems, and make up over 60% of the system mass. Due to the innovative concepts implemented into this system, the costs of realising this system are only €1.34 billion, from a budget of €1.5 billion. Despite the large initial costs, the system is estimated to produce up to €3 billion in revenues. However, the costs for the transmission system, the ground segment and all operations will amount to €740 million, resulting in profits of almost €1 billion.

The system has been planned to require further designing, testing and qualification until 2028, with production starting before testing and qualification is completed halfway through 2026. In 2028, not only will the design, testing and qualifications be completed, but the first launches for the system will be initiated and the system will be produced in-orbit until its completion, during which on-Earth production will continue. From 2030 onward the system will operate until the end of its life in 2060.

16.2. Recommendation and Challenges

Due to the complex and innovative nature of this design, several recommendations and challenges must be highlighted for the future. These recommendations will have to be implemented in future design phases, and the challenges must be taken into consideration to avoid further issues and to minimise risks.

Firstly, the laser transmitter should be designed. This was considered to be outside the scope of this project, however, it is an essential part of the project. Seeing the design of the power collection system has dropped enormously in mass because of innovative new technologies that were identified, this will be assumed possible to do with the transmitter design for the given budget as well. Wireless transmission technology would have to undergo a radical transformation and improvement in order to achieve a high enough efficiency and power capacity. Therefore it would require significant investment between now (2018) and 2030. Moving on, as discussed in section 11.4 and section 10.6, the most logical placement of the laser transmitters is on a long boom with a gimbal on a non-rotating platform. However this boom will be required to be very large, and this length should preferably be minimised. Therefore it can be recommended that the laser transmitter could operate at frequencies that can efficiently transmit through the aluminium mirror. If this is not possible, considerations can be put into creating gaps in the mirror, such that the power can be transmitted through those gaps. This would require a slightly larger frontal area and diameter of the primary mirror, and would result in the unequal thermal loading of the secondary mirror, filters and solar cells. So this must also be further researched.

For thermal control, it is recommended that more research is done into thermal energy storage, as this is a technology that has barely been in used in aerospace applications yet. The optimal functioning of SPECTRE will depend on a developed thermal energy storage system. Although some work has already been put into this aspect of the design, more research will have to be done in order to ensure its feasibility. Thermal control will also require further research in heat pipe working fluids and material selection, due to the wide and high ranges of temperatures this system will be exposed to. This is especially true for the mirror-to-mirror heat pipes, which have a temperature range almost no working fluids can span as of yet.

The production methods that are currently available will not yet be capable of producing such a system. Hence, further research should be done into the robotics and methods in order to be able to produce this design. Sustainable production of the major materials should also be a priority. The sustainability of the system depends heavily on the sustainability of material production. This can therefore be enhanced quite significantly, should the current processes be cleaned up. Should this problem be solved, then the system could become comparable to geothermal methods.

A suggestion for the EPS is to use high frequency micro-laminated silicon steel toroidal cores. By using high frequencies, the system could use smaller cores, thereby decreasing its mass. Furthermore, by using toroidal cores instead of coils, the amount of flux losses can be decreased significantly. Also, micro-lamination decreases the amount of eddy currents occurring, thereby increasing the efficiency, and through the use of silicon steel, the hysteresis effects, that are seen with other materials such as iron, are minimised. Therefore, if more research could be put into these toroidal cores, the design of the EPS could significantly improve.

On top of this, extra research should be put into the production of filters. Currently, filter production requires precision in the order of nanometres and a heavy substrate composed of fused silicon. If nanotechnology can advance to become cheaper and more reliable, and a lighter substrate can be synthesised, the costs of producing filters and launching them to space could be lowered significantly. Additionally, a minor recommendation would be to improve the performance and reliability of CMGs, as well as their mass. This would significantly improve the design and its reliability.

If these challenges and recommendations are met, SPECTRE will be a sustainable energy source that can make some terrestrial energy sources obsolete. This system will lay the groundwork for a new future of sustainable power generation in a world where the increasing demand in power shows no signs of stopping.

Bibliography

[1] Aluminum 1199-o. http://www.matweb.com/search/DataSheet.aspx?bassnum=MA1199O.

[2] The ultimate factor of safety for aircraft and spacecraft–its history, application sand misconceptions. https://ntrs.nasa.gov/archive/nasa/casi.ntrs.nasa.gov/20150003482.pdf.

[3] Victrex™ peek 90hmf40 polyetheretherketone (peek), 40% carbon fiber reinforced. http://www.matweb.com/search/datasheet.aspx?matguid=759df769d1e14169bc4c739598bd26e1, .

[4] Victrex™ peek 450fc30 general purpose. http://www.matweb.com/search/datasheet.aspx?matguid=6cbf083a600a48cf908286f3508629d7, .

[5] Unreinforced peek datasheet. https://www.bearingworks.com/uploaded-assets/pdfs/retainers/peek-datasheet.pdf.

[6] How much does it cost to fill an ion thruster with xenon for a spacecraft propulsion system? https://space.stackexchange.com/questions/8698/how-much-does-it-cost-to-fill-an-ion-thuster-with-xenon-for-a-spacecraft-propuls.

[7] Energy gap values for ingaas at 300k. http://www.semiconductors.co.uk/eg(ingaas).htm, 2001.

[8] Rad6000 datasheet. https://www.digchip.com/datasheets/download_datasheet.php?id=809178&part-number=RAD6000, June 2002.

[9] Mil-std-1553 b databus harnesses. http://www.axon-cable.com/publications/SPACE_APPLICATION_Databus.pdf, 2004.

[10] Pbo fiber zylon™, technical information. http://www.toyobo-global.com/seihin/kc/pbo/zylon-p/bussei-p/technical.pdf, 2005.

[11] Standardized interface comparison. https://ams.aeroflex.com/pagesproduct/appnotes/SpWinterfaceComp.pdf, April 2008.

[12] *Space engineering - Verification (ECSS-E-ST-10-02C)*, March 2009.

[13] Mobile servicing system. http://www.asc-csa.gc.ca/eng/iss/mobile-base/overview.asp, 2010.

[14] *Space engineering - Testing (ECSS-E-ST-10-03C)*, June 2012.

[15] The cpus of spacecraft computers in space. http://www.cpushack.com/space-craft-cpu.html, August 2012.

[16] Review and rationale of mil-std-1553 a and b. http://www.milstd1553.com/wp-content/uploads/2012/12/MIL-STD-1553B.pdf, December 2012.

[17] *IDSS IDD Revision E*, October 2016.

[18] Lockheed martin to deliver world record-setting 60 kw laser to u.s. army. https://news.lockheedmartin.com/2017-03-16-Lockheed-Martin-to-Deliver-World-Record-Setting-60kW-Laser-to-U-S-Army, 2017.

[19] DSE Project Group 9. In orbit construction of a giant space solar energy collecting system, baseline report. TU Delft, 2018.

[20] DSE Project Group 9. Spectral photovoltaic energy collection & transmission to earth, midterm report. TU Delft, 2018.

[21] DSE Project Group 9. In-orbit construction of a giant space solar energy collecting system project plan, 2018.

[22] O. Isabella M. Zerman R. van Swaaij A. Smets, K. Jäger. *Solar Energy: The Physics and Engineering of Photovoltaic Conversion, Technologies and Systems*. UIT Cambridge, 2016.

[23] William Adkins. How to price for office cleaning. http://smallbusiness.chron.com/price-office-cleaning-13178.html.

[24] MT Aerospace. S-xta-60. https://www.mt-aerospace.de/files/mta/tankkatalog/Datenblatt_S-XTA-60.pdf, 2018.

[25] U. ESKIL NILSSON ALBIN K J. HASSELSTRÖM. Thermal contact conductance in bolted joints. http://publications.lib.chalmers.se/records/fulltext/159027.pdf, 2012.

[26] Alibaba. 1.5mm 2.5mm 4mm 6mm wire cable electrical cable copper cable price per meter. https://www.alibaba.com/product-detail/1-5mm-2-5mm-4mm-6mm_60673940840.html?spm=a2700.7724857.main07.19.1190620e4Q0YPE&s=p.

[27] World Aluminium. Primary aluminium production. http://www.world-aluminium.org/statistics/, 2018. Accessed on May 2018.

[28] AmBrSoft. Materials density table. http://www.ambrsoft.com/calcphysics/density/table_2.htm.

[29] Paul V. Anderson. Operational considerations of geo debris synchronization dynamics, 2015.

[30] Akihiro Hashimoto Akio Yamamoto Ashraful Ghani Bhuiyan, Kenichi Sugita. Ingan solar cells: Present state of the art and important challenges. *IEEE JOURNAL OF PHOTOVOLTAICS, VOL. 2, NO. 3*, July 2012.

[31] H. Pilz B. Brant. The impact of plastic packaging on life cycle energy consumption and greenhouse gas emissions in europe. http://denkstatt-group.com/files/the_impact_of_plastic_packaging_on_life_cycle_energy_consumption_and_greenhouse_gas_emissions_in_europe.pdf, 2011. Accessed on May 2018.

[32] A. Baggini. Power transformers - introduction to measurement of losses. http://www.intas-testing.eu/storage/app/media/INTAS_trasformers_descr.pdf.

[33] Hamilton Booz, Allen. On-orbit assembly, modeling and mass properties data book volume i: International space station program. 2008.

[34] D. E. Bornside and R. A. Brown. View factor between differing-diameter, coaxial disks blocked by a coaxial cylinder. *Journal of Thermophysics and Heat Transfer*, 4(3):414–416, 1990. doi: 10.2514/3.56245.

[35] Jasper Bouwmeester. Lecture notes - spacecraft technology (ae3534). https://ocw.tudelft.nl/wp-content/uploads/1.0-Command-and-Data-Handling-Lecture-Notes.pdf, 2017.

[36] W. G. Briscoe, Manuel Davila, and Brian Skinner. Bus length and loading limits of mil-std-1553 buses. *SAE Technical Paper Series*, Jan 1987. doi: 10.4271/872483.

[37] Busek. Ion thrusters. http://www.busek.com/technologies__ion.htm, 2018.

[38] R.E. Butler. The role of the itu in the use of the geostationary orbit. *Acta Astronautica Vol. 17, No. 6, pp. 607 10, 198*, 1987.

[39] L.f. Cabeza, A. Castell, C. Barreneche, A. De Gracia, and A.i. Fernández. Materials used as pcm in thermal energy storage in buildings: A review. *Renewable and Sustainable Energy Reviews*, 15(3):1675–1695, 2011. doi: 10.1016/j.rser.2010.11.018.

[40] Jose M. Cabeza-Lainez and Jesus A. Pulido-Arcas. New configuration factors for curved surfaces. *Journal of Quantitative Spectroscopy and Radiative Transfer*, 117:71–80, 2013. doi: 10.1016/j.jqsrt.2012.10.022.

[41] B.W. Carsten. The low leakage inductance of a planar transformers; fact or myth? https://ieeexplore.ieee.org/stamp/stamp.jsp?tp=&arnumber=912515.

[42] A. Cervone. Aerospace design & systems engineering elements ii, 2016.

[43] Scott Dickerson Stephen Didziulis Peter Frantz Charles Gurrisi, Raymond Seidel and Kevin Ferguson. Space station control moment gyroscope lessons learned. https://ntrs.nasa.gov/archive/nasa/casi.ntrs.nasa.gov/20100021932.pdf, 2018.

[44] Wei-Hsin Chen, Po-Hua Wu, Xiao-Dong Wang, and Yu-Li Lin. Power output and efficiency of a thermoelectric generator under temperature control. *Energy Conversion and Management*, 127:404–415, 2016. doi: 10.1016/j.enconman.2016.09.039.

[45] European Commission. Cement and lime. https://ec.europa.eu/growth/sectors/raw-materials/industries/non-metals/cement-lime_en, 2018. Accessed on May 2018.

[46] Inter-Agency Space Debris Coordination Committee. Report of the iadc activities on space debris mitigation measures. https://www.iadc-online.org/Documents/IADC-UNCOPUOS-final.pdf.

[47] TEM Electric Components. Infineon (irf) irfb7545pbf. https://www.tme.eu/nl/details/irfb7545pbf/tht-transistors-met-n-kanaal/infineon-irf/?brutto=1&gclid=CjwKCAjw9qfZBRA5EiwAiq0AbQ1I9QRMqzDPDDMXqKcRZdFbnE-iWWFeFLSFU5C9awFX1aSHS0aoOhoCWJsQAvD_BwE.

[48] Cubesatshop. Cubesatshop. https://www.cubesatshop.com/.

[49] Energy Department for Business and Industrial Strategy. Electricity generation costs. UK Government, 2016.

[50] JOSHUA M. PEARCE DIRK V.P. MCLAUGHLIN. Progress in indium gallium nitride materials for solar photovoltaic energy conversion. *The Minerals, Metals & Materials Society*, 2013. doi: 10.1007/s11661-013-1622-1.

[51] Rye Druzin. Spacex's south texas launch pad may get mars-sized boost. San Antonio Express News, 2018.

[52] ece3sat. Algorithm adcs main functioning. http://www.ece3sat.com/cubesatmodules/adcs/, 2018.

[53] Trading Economics. Trading economics. https://tradingeconomics.com, 2018.

[54] Justin Shorb Xavier Prat-Resina Tim Wendorff Adam Hahn Ed Vitz, John W. Moore. Enthalpy of fusion and enthalpy of vaporization. https://chem.libretexts.org/Textbook_Maps/General_Chemistry/Book%3A_

ChemPRIME_(Moore_et_al.)/10Solids%2C_Liquids_and_Solutions/10.09%3A_Enthalpy_of_Fusion_and_Enthalpy_of_Vaporization, 2017.

[55] Elliott-Laboratories. The anschutz gyro-compass and gyroscope engineering, 2003.

[56] Alternative Energy. Cost of solar panels. http://www.altenergy.org/renewables/solar/DIY/solar-panel-cost.html.

[57] Turan Erdogan. Construction of optical filters, 2011.

[58] Iber Espacio. Space thermal products. Iber Espacio.

[59] Wiley J. Larson et al. *Applied Space Systems Engineering*. Mcgraw-Hill Education - Europe, 2009.

[60] EuropeanCommission. Cermamics. https://ec.europa.eu/growth/sectors/raw-materials/industries/non-metals/ceramics_en, 2018. Accessed on May 2018.

[61] Eurostat. Energy balances. http://ec.europa.eu/eurostat/web/energy/data/energy-balances, 2016. Accessed on May 2018.

[62] Farnell. Semiconductors. http://nl.farnell.com/c/semiconductors-discretes/prl/resultaten?CMP=KNC-GNL-GEN-CMDTY-.

[63] FEVE. Eu container glass production growth shows industry resilience. http://feve.org/eu-container-glass-production-growth-shows-industry-resilience/, 2014. Accessed on May 2018.

[64] D. Bortis J.W. Kolar O. Apeldoorn G. Ortiz, H. Uemura. Modeling of soft-switching losses of igbts in high-power high-efficiency dual-active-bridge dc/dc converters. https://www.pes-publications.ee.ethz.ch/uploads/tx_ethpublications/10_Modeling_Switching_Ortiz_03.pdf.

[65] Ahmed H. Gad Gasser F. Abdelal, Nader Abuelfoutouh. *Finite Element Analysis for Satellite Structures*. Springer-Verlag London, 2013.

[66] Orin M Gould, Allen J. Linden. Estimating satellite insurance liabilities, 2000.

[67] Grainger. Safety switches. https://www.grainger.com/category/safety-switches/safety-switches-panel-and-door-disconnects/power-management-circuit-protection-and-distribution/electrical/ecatalog/N-rcy.

[68] International Copper Study Group. The world copper factbook 2017. http://www.icsg.org/index.php/component/jdownloads/finish/170/2462, 2017. Accessed on May 2018.

[69] Jian Guo. Project guide design synthesis excercise: In-orbit construction of a giant space solar energy collecting system, 2018.

[70] D. Maksimović R. Erickson Z. Cole B. Passmore K. Olejniczak W.A. Chree H. Kim, H. Chen. Sic-mosfet composite boost converter with 22 kw/l power density for electric vehicle. http://ecee.colorado.edu/~rwe/papers/APEC17.pdf.

[71] K.D. Bunte et al Holger Krag, J. Bemdisch. Introducing the esa-master 2001 space debris model. *Advances in the Astronautical Science*, 2002.

[72] John R. Howell. A catalog of radiation heat transfer configuration factors. URL http://www.thermalradiation.net/tablecon.html.

[73] G.J. Su I. Takahashi. A 500 hz power system - applications -. https://ieeexplore.ieee.org/stamp/stamp.jsp?tp=&arnumber=96764&tag=1.

[74] IEA. Key world energy statistics. https://www.iea.org/publications/freepublications/, 2016.

[75] Infineon. Fast switching diode. https://www.infineon.com/dgdl/Infineon-IDP18E120-DS-v02_03-en.pdf?fileId=db3a30432313ff5e01237a90bd2b7c24, .

[76] Infineon. Technicalinformation iff2400p17ae440989. https://www.infineon.com/dgdl/Infineon-IFF2400P17AE4-DS-v02_01-EN.pdf?fileId=5546d4625fe36784015fe9492b5c309a, .

[77] INSG. The ongoing economic crisis and nickel. http://www.insg.org/docs/INSG_Insight_08_Economic_Crisis.pdf, 2009. Accessed on May 2018.

[78] PV Insider. Us solar market boom cuts o&m costs years ahead of forecast. http://analysis.newenergyupdate.com/pv-insider/us-solar-market-boom-cuts-om-costs-years-ahead-forecast, 2016.

[79] European Copper Institute. Copper market: Demand and economic value. http://copperalliance.eu/industry/market, 2014. Accessed on May 2018.

[80] InvestmentMine. Alluminium prices and alluminium price charts. http://www.infomine.com/investment/metal-prices/aluminum/.

[81] prof. dr. ir. M.J.L. van Tooren ir. R.J. Hamann. Ae3-s01 systems engineering & technical management techniques - lecture notes, January 2006.

[82] Zhang R. Li L. Zhao X. Sun L. Wang B. Zeng J. Cheng Y. Wang J. Peng X. Song J. Su, X. An 8-gw long-pulse generator based on tesla transformer and pulse forming network. https://aip.scitation.org/doi/full/10.1063/1.4884341.

[83] J.J. Puschell J.R. Wertz, D.F. Everett. *Space Mission Engineering: The New SMAD*. Microcosm Press, 2011.

[84] Shahab Khoshmashrab. Power plant reliability. http://www.energy.ca.gov/2008publications/CEC-700-2008-013/FSA/32_Ivanpah%20Reliability.pdf, 2009.

[85] Kahoru Torii Koichi Nishino, Shigemasa Yamashita. Thermal contact conductance under low applied load in a vacuum environment. https://ac.els-cdn.com/089417779400091L/1-s2.0-089417779400091L-main.pdf?_tid=45161199-74df-4e08-aba2-5112f753225f&acdnat=1530623764_7f54cdafae74b7c753fdc319796c637f.

[86] L. Qi C. Hua L. Haitao, S. Xumin. Deployment dynamics and control of spinning space web. https://ieeexplore.ieee.org/document/8027530/, 2017.

[87] Lu Ming Lai lin Tian Xing Li Gang, Wu Dengyun and Zhang Jiyang. Research on high accuracy, long life, and high reliability technique of control moment gyroscope. 2016 International IEEE Conference, 2016.

[88] Noam Lior. Mirrors in the sky: Status, sustainability, and some supporting materials experiments. https://www.sciencedirect.com/science/article/pii/S1364032112005059, 2012.

[89] Air Liquide. Xenon gas physical properties. https://encyclopedia.airliquide.com/xenon, 2018.

[90] Birgitta Ljunggren. Spacecraft interface standards analysis and simple breadboarding. Master's thesis, Linköping University, 2005.

[91] M.A. Masius M. Planck. The thoery of heat radiation. https://ia601408.us.archive.org/17/items/theoryofheatradi00planrich/theoryofheatradi00planrich.pdf.

[92] Chakravarti V. Madhusudana. *Thermal Contact Conductance Second Edition*. Springer, 2014.

[93] Makesat. X-band high speed transmitter. https://makesat.com/en/products/x-band-high-speed-transmitter, 2018.

[94] John C. Mankins. A fresh look at space solar power: New architectures, concepts and technologies. *Acta Astronautica*, 41(4-10):347–359, 1997. doi: 10.1016/s0094-5765(98)00075-7.

[95] Jacob Marsh. Solar farms: what are they, and how do you start one? https://news.energysage.com/solar-farms-start-one/, 2017.

[96] Isidoro Martinez. Radiative view factors. URL http://webserver.dmt.upm.es/~isidoro/tc3/RadiationViewfactors.pdf.

[97] Colin R. McInnes. *Solar Sailing: Technology, Dynamics and Mission Applications*. Praxis Publishing Ltd, 1999.

[98] MIT. Technical success and economic failure. http://ardent.mit.edu/real_options/de%20Weck%20System%20Study/unit1_summary.pdf, 2003.

[99] NASA. Where do old satellites go when they die? https://spaceplace.nasa.gov/spacecraft-graveyard/en/, 2015.

[100] NASA. Green propellants. https://www.nasa.gov/centers/wstf/testing_and_analysis/propellants_and_aerospace_fulids/green_propellants.html, 2017.

[101] Y. Sokona K. Seyboth P. Matschoss S. Kadner T. Zwickel P. Eickemeier G. Hansen S. Schlömer C. Stechow O. Edenhofer, R. Pichs-Madruga. Renewable energy sources and climate change mitigation. https://www.ipcc.ch/pdf/special-reports/srren/SRREN_FD_SPM_final.pdf.

[102] Federation of Reinforced Plastics. The european grp market in 2016. https://www.materialstoday.com/composite-industry/comment/the-european-grp-market-in-2016/, 2016. Accessed on May 2018.

[103] Government of The Netherlands. Amount of the hourly minimum wage. https://www.government.nl/topics/minimum-wage/amount-of-the-hourly-minimum-wage.

[104] United States Government Accountability Office. Surplus missile motors sale price drives potential effects on dod and commercial launch providers. https://www.gao.gov/assets/690/686613.pdf, 2017. Accessed on May 2018.

[105] Premises & Facilities Management Online. Benchmarking maintenance. http://www.pfmonthenet.net/article/42806/Benchmarking-maintenance.aspx.

[106] Edmund Optics. Dichroic and color filters. https://www.edmundoptics.com/optics/optical-filters/color-dichroic-filters/.

[107] Edmund Optics. Edmund optics products, 2018.

[108] Sydney Owens. Athena laser weapon system prototype. https://www.lockheedmartin.com/en-us/products/athena.html, 2017.

[109] Payscale. Aerospace engineer salary. https://www.payscale.com/research/US/Job=Aerospace_Engineer/

Salary.

[110] PlasticsEurope. Plastics - the facts 2017. https://www.plasticseurope.org/application/files/5715/1717/4180/Plastics_the_facts_2017_FINAL_for_website_one_page.pdf, 2017. Accessed on May 2018.

[111] J.J. Pocha. An introduction to mission design for geostationary satellites. 1987.

[112] R. C. Prager, M. Nikitkin, and B. Cullimore. *14. Heat Pipes*, volume 1. The Aerospace Press, 2nd edition, 2002.

[113] prof. dr. Eberhard Gill. Ae3211-i systems engineering methods - lecture notes, February 2017.

[114] A. Marcu Dr.L. Schrefler Dr.G. Luchetta Dr.F. Simonelli Dr.F. Genoese Dr.D. Valiante F. Mustilli L. Colantoni F. Infelise W. Stoefs J. Teusch J. Timini J. Wieczorkiewicz Prof.Dr.J. Pelkmans, Prof.C. Egenhofer. Assessment of cumulative cost impact for the steel and the aluminium industry. http://ec.europa.eu/smart-regulation/evaluation/search/download.do?documentId=9438143, 2013. Accessed on May 2018.

[115] Space Launch Report. Angara data sheet. http://www.spacelaunchreport.com/angara.html, 2018. Accessed on May 2018.

[116] Space Launch Report. Ariane 5 data sheet. http://www.spacelaunchreport.com/ariane5.html, 2018. Accessed on May 2018.

[117] Space Launch Report. Atlas 5 iv data sheet. http://www.spacelaunchreport.com/atlas5.html, 2018. Accessed on May 2018.

[118] Space Launch Report. Delta iv data sheet. http://www.spacelaunchreport.com/delta4.html, 2018. Accessed on May 2018.

[119] Space Launch Report. Spacex falcon heavy. http://www.spacelaunchreport.com/falconH.html, 2018. Accessed on May 2018.

[120] Space Launch Report. Proton data sheet. http://www.spacelaunchreport.com/proton.html, 2018. Accessed on May 2018.

[121] Space Launch Report. Zenit data sheet. http://www.spacelaunchreport.com/zenit.html, 2018. Accessed on May 2018.

[122] T. Lim S.C. Kim O.B. Lee S.K. Park R.L. Provost, R.P. Marek. High power density transformers for improved performance. https://ieeexplore.ieee.org/stamp/stamp.jsp?tp=&arnumber=1177731.

[123] Jeffrey Slostad Robert Hoyt, Jesse Cushing. Spiderfab™: Process for on-orbit construction of kilometer scale apertures. http://www.tethers.com/papers/SPACE2013_SpiderFab.pdf, 2013.

[124] Fisher Scientific. Lithium perchlorate trihydrate, 99%, extra pure, acros organics™. https://www.fishersci.com/shop/products/lithium-perchlorate-trihydrate-99-extra-pure-acros-organics-3/p-44341.

[125] Proff. A. Smets. Sustainable energy technologies. Brightspace, 2017.

[126] E. Leonardi S.M.S. Wahid, C.V. Madhusudana. Solid spot conductance at low contact pressure. https://ac.els-cdn.com/S0894177703001158/1-s2.0-S0894177703001158-main.pdf?_tid=c57244f0-041d-4696-a418-be649782444d&acdnat=1528722492_a4fbe4bb5d3b23ceff46e6dfd3264459, 2004.

[127] E. M. Soop. Handbook of geostationary orbits, 1994.

[128] J. Spaander. Sustainability calculator. https://docs.google.com/spreadsheets/d/1y-BhgSXSiqZ1_qHDNbsv05uP8MDkoedZ8XTHUMGy6SQ/edit?usp=sharing, 2018.

[129] SpaceX. Making life multiplanetary. http://www.spacex.com/sites/spacex/files/making_life_multiplanetary_transcript_2017.pdf.

[130] SpaceX. Capabilities & services. http://www.spacex.com/about/capabilities, 2018. Accessed on May 2018.

[131] Statista. Average cost per square meter of internal area in the united kingdom (uk) for constructing an industrial building in 2016, by region in gbp. https://www.statista.com/statistics/601846/industrial-building-cost-uk-2016/, .

[132] Statista. Average price per square meter per year of prime office space in selected european cities in the 1st quarter 2017 (in euros). https://www.statista.com/statistics/792026/prime-office-rent-costs-europe/, .

[133] Leopold Summerer and Oisin Purcell. Concepts for wireless energy transmission via laser. URL https://www.esa.int/gsp/ACT/doc/POW/ACT-RPR-NRG-2009-SPS-ICSOS-concepts-for-laser-WPT.pdf.

[134] S. Takehiro T. Toshito, H. Kazuhiro. Recent development of grain-oriented electrical steel in jfe steel. http://www.jfe-steel.co.jp/en/research/report/021/pdf/021-02.pdf.

[135] A.G. Kladas A.T. Souflaris D.G. Paparigas T.D. Kefalas, P.S. Georgilakis. Multiple grade lamination wound core: A novel technique for transformer iron loss minimization using simulated annealing with restarts and an anisotropy model. http://citeseerx.ist.psu.edu/viewdoc/download?doi=10.1.1.711.9576&rep=rep1&type=pdf.

[136] ESA Advanced Concepts Team. Furoshiki & robyspace. https://www.esa.int/gsp/ACT/nrg/projects/Furoshiki.

html.

[137] Thumbtack. How much does a security guard cost? https://www.thumbtack.com/p/security-guards-cost.

[138] Gunnar Tibert and Mattias Gärdsback. Space webs final report. https://www.esa.int/gsp/ACT/doc/ARI/ARI%20Study%20Report/ACT-RPT-MAD-ARI-05-4109a-SpaceWebs-KTH.pdf.

[139] The Engineering Toolbox. Densities of common solids. https://www.engineeringtoolbox.com/density-solids-d_1265.html.

[140] C. P. Tso and S. P. Mahulikar. View factor for ring elements on coaxial cylinders. *Journal of Thermophysics and Heat Transfer*, 13(1):155–158, 1999. doi: 10.2514/2.6415.

[141] Battery University. Bu-808: How to prolong lithium-based batteries. http://batteryuniversity.com/learn/article/how_to_prolong_lithium_based_batteries.

[142] A. De Vos. Detailed balance limit of the efficiency of tandem solar cells. http://iopscience.iop.org/article/10.1088/0022-3727/13/5/018/pdf.

[143] H.J. Queisser W. Shockley. Detailed balance limit of efficiency of p-n junction solar cells. http://metronu.ulb.ac.be/npauly/art_2014_2015/shockley_1961.pdf.

[144] B. Wan. Energy density of methane. https://hypertextbook.com/facts/2004/BillyWan.shtml.

[145] Brian Wang. Spacex bfr to be lower cost than falcon 1 at $7 million per launch. https://www.nextbigfuture.com/2017/10/spacex-bfr-to-be-lower-cost-than-falcon-1-at-7-million-per-launch.html, 2017.

[146] Brian Wang. Building lighter and huge in the low gravity of space. https://www.nextbigfuture.com/2018/02/building-lighter-and-huge-in-the-low-gravity-of-space.html, 2018.

[147] D.G. Rethwisch W.D. Callister. *Materials Science and Engineering*. Wiley, 2015.

[148] Brian Weeden. Dealing with galaxy 15: Zombiesats and on-orbit servicing. http://thespacereview.com/article/1634/1, 2010.

[149] A. Zak. Angara-5 to replace proton. http://www.russianspaceweb.com/angara5.html, 2017. Accessed on May 2018.

Appendix

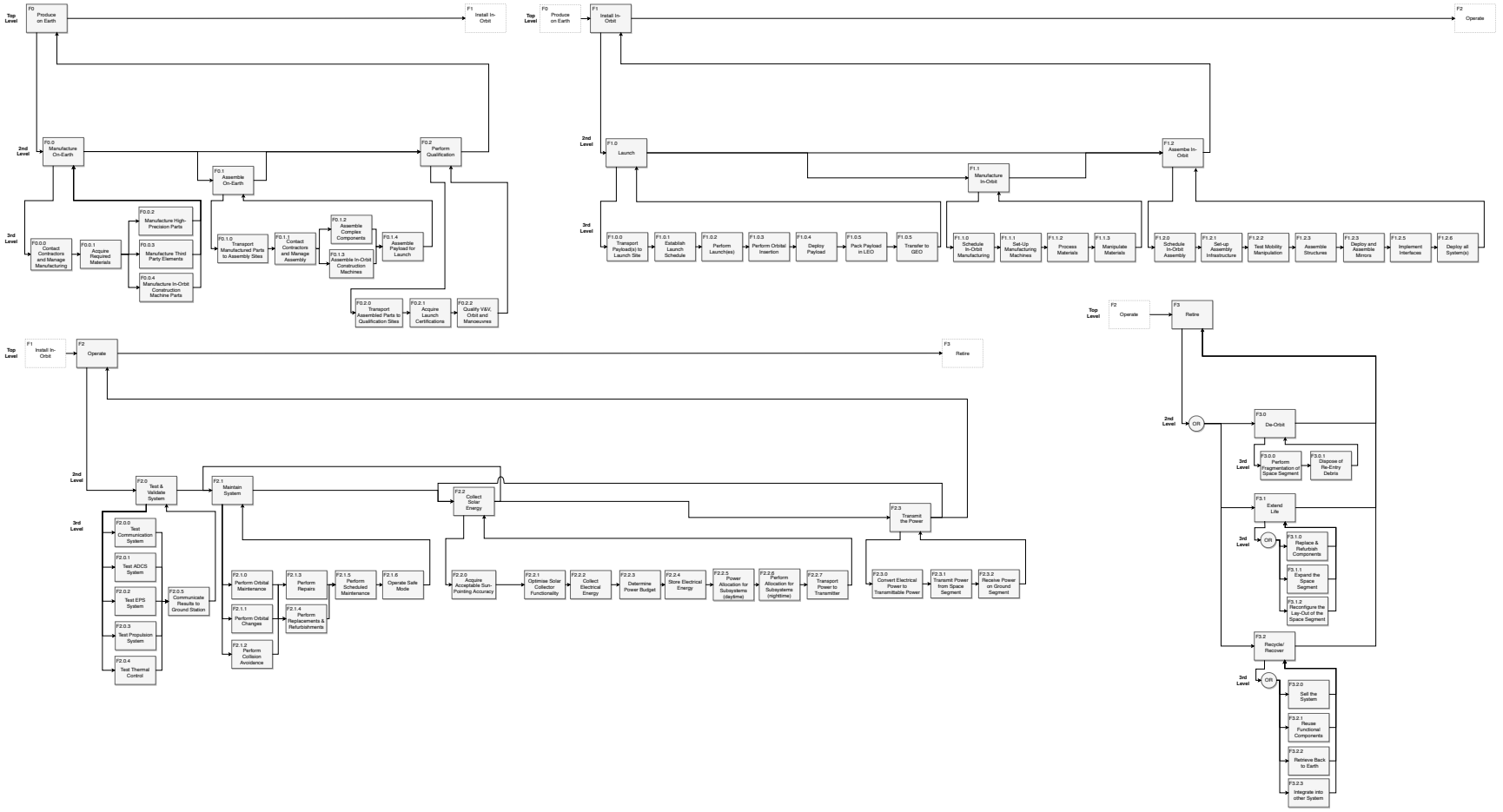

Figure A.1: Functional Flow Diagram

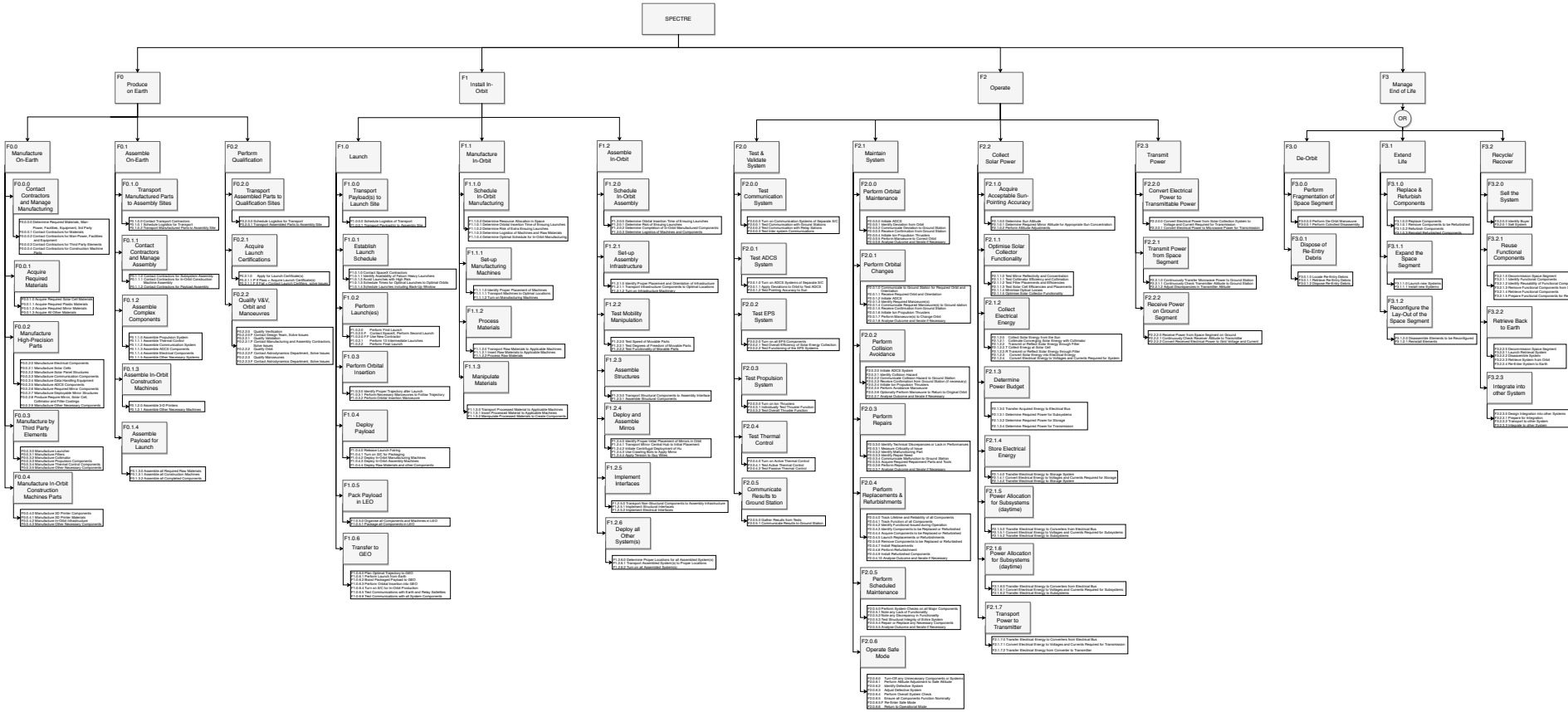

Figure A.2: Functional Breakdown Diagram

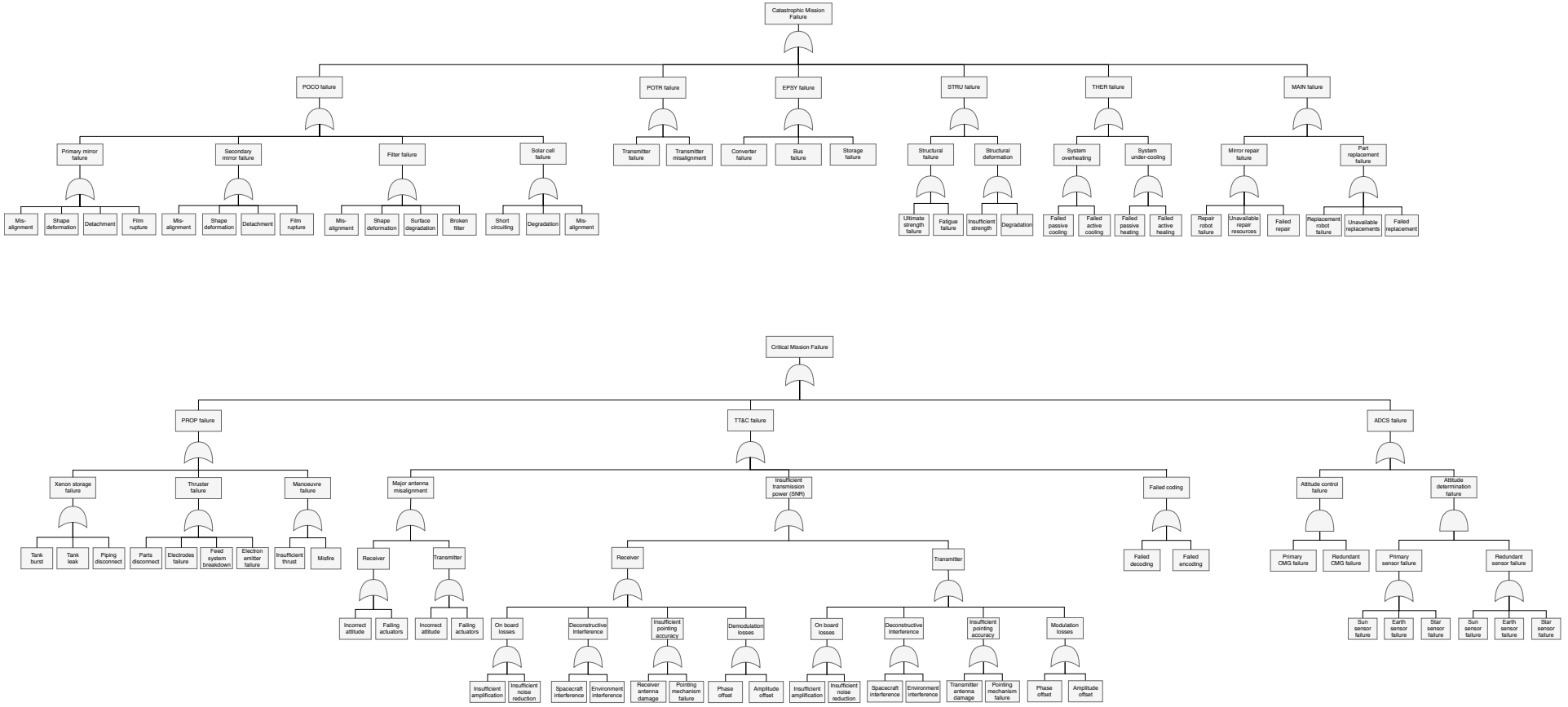

Figure A.3: Fault Tree Analysis